INFORMATION TO USERS

EXPERIMENTAL INVESTIGATIONS INTO THE PATHOPHYSIOLOGY OF HUNTINGTON'S DISEASE

by

Matthew Olding Hebb

Submitted in partial fulfillment of the requirements
for the degree of Doctor of Philosophy

at

Dalhousie University
Halifax, Nova Scotia
July, 1998

0-612-36584-0

Canada

DALHOUSIE UNIVERSITY

FACULTY OF GRADUATE STUDIES

The undersigned hereby certify that they have read and recommend to the Faculty of

Graduate Studies for acceptance a thesis entitled "Experimental Investigations into the

Pathophysiology of Huntington's Disease"

by   Matthew Olding Hebb

in partial fulfillment of the requirements for the degree of Doctor of Philosophy.

Dated: _____ August 12, 1998 _____

External Examiner

Research Supervisor

Examining Committee

ii
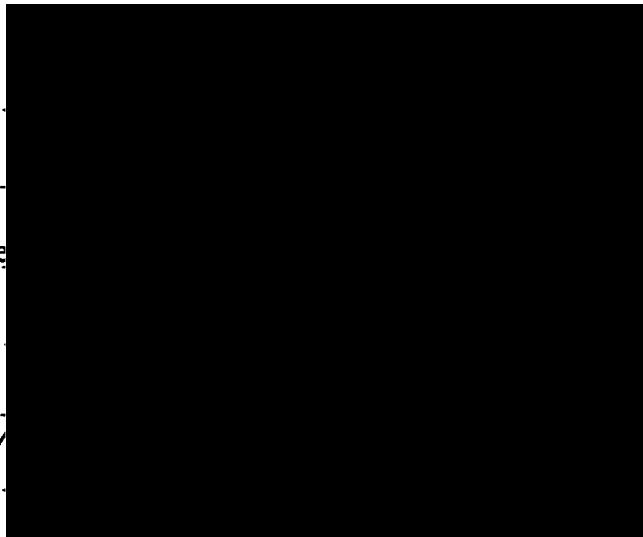
DALHOUSIE UNIVERSITY

DATE: 12 August 1998
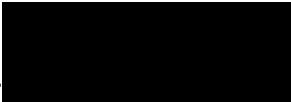
AUTHOR: Matthew Olding Hebb

TITLE: Experimental Investigations into the Pathophysiology of Huntington's

Disease.

DEPARTMENT OR SCHOOL: Department of Pharmacology

DEGREE: Doctor of Philosophy CONVOCATION: October 17 YEAR: 1998

Permission is herewith granted to Dalhousie University to circulate and to have

copied for non-commercial purposes, at its discretion, the above title upon request of

individuals or institutions.

Signature of Author

DEDICATION

I would like to take this opportunity to acknowledge and thank my beautiful partner in life, Shelley Keirs Hunter. At times when work became so focused that life outside the lab seemed to fade into grayness, she was always there to boost my sense of reality and encourage me to step back and enjoy life. How do you thank someone for years of unwavering support, assurance and love? A truly wonderful person. I love you.

TABLE OF CONTENTS

LIST OF FIGURES

x

LIST OF TABLES

ABSTRACT

Planning and initiation of movement is dependent upon efficient processing of cortical and subcortical information through the basal ganglia. Pathology of the basal ganglia or its associated nuclei results in impairment of motor control. Parkinson's and Huntington's diseases are prominent neurodegenerative conditions that have principle pathologies in the substantia nigra and striatum, respectively. The etiology of Huntington's disease has been traced to a trinucleotide expansion at the 5'-terminal of the *IT15* gene. This expansion is translated into a polyglutamine region on the protein product of this gene, huntingtin. The connection between the genetic mutation and the pathology of Huntington's disease is unknown and even the role of the normal form of huntingtin in the brain remains speculative. The striatum is a principle region of degeneration in Huntington's disease, and the loss of efferent transmission from this nucleus is thought to be responsible for the motor impairments in this condition.

We describe the application of antisense technology to the study of basal ganglia function and, particularly, the effects of striatal dysfunction on motor behavior and alterations in the functional activation of other motor-associated, subcortical regions. Unilateral suppression of stimulant-induced immediate early gene expression in the striatum produced robust rotational behavior and changes in the activation of several brain regions. In particular, the globus pallidus was disinhibited and was found to produce marked suppression of the observed motor asymmetry in these animals. Another prominent region that was affected by these conditions was the superior colliculus. The intermediate layers of this structure had different responses to a reduction in striatal and/or pallidal activity. These findings are in accord with clinical reports of motor symptomatology of Huntington's disease. A systematic comparison of subcortical changes in metabolic activation was performed between animals with unilateral antisense-mediated striatal suppression, which we suggest provides a novel animal model of Huntington's disease, and subjects that had unilateral depletion of mesencephalic dopamine (Parkinson's disease model). These alterations and their clinical relevance are discussed.

In an alternate study, we provide a novel description of the regulation of the *Hdh* gene (rat homologue of *IT15*) in the hypothalamus. The expression of huntingtin mRNA and protein was found to be significantly elevated ($\sim$7-fold) in the arcuate nucleus of lactating females when compared to naive female or male animals. This expression was localized to astrocytes that appeared to form intimate contacts with the neurons of this region. Also, in the same animals, cells of the subependymal region of the third ventricle, directly overlying the arcuate nucleus, were found to have a dramatic induction of huntingtin expression. These findings suggest that alterations in neuroendocrine structure and function that have been previously described by others, may involve recruitment and differentiation of glia to regulate the metabolic activity in the hypothalamus. Furthermore, the association of huntingtin with such processes provides novel clues into the role of this protein in the normal brain. Future investigations into this phenomena may ultimately reveal cellular systems through which the mutated huntingtin protein mediates its pathological effects

LIST OF ABBREVIATIONS

6-OHDA	6-hydroxydopamine
cAMP	cyclic adenosine monophosphate
DA	dopamine
EPN	entopeduncular nucleus
GABA	γ-aminobutyric acid
GAD	glutamic acid decarboxylase
GPe	globus pallidus, external segment
GPi	globus pallidus, internal segment
HD	Huntington's disease
htt	huntingtin
IEG	immediate early gene
ODN	oligodeoxynucleotide
PD	Parkinson's disease
RPO	oral pontine reticular formation
SC	superior colliculus
SNC	substantia nigra pars compacta
SNR	substantia nigra pars reticulata
STN	subthalamic nucleus
TH	tyrosine hydroxylase
VMT	ventromedial thalamus

ACKNOWLEDGMENTS

GENERAL INTRODUCTION

.

The discovery and isolation of the human *IT15* gene that encodes the huntingtin

protein (htt) (The Huntington's Disease Collaborative Research Group, 1993), has

assigned a putative origin for the development of genetic and cellular-based therapeutic

strategies designed to attenuate the progression of Huntington's Disease (HD). The

murine homologue of *IT15* (called *Hdh*) has also been isolated and studies have shown

that mice that were heterozygous for a neomycin-substituted *Hdh* loci were physically

indistinguishable from their wild-type counterparts. However, embryos that were

homozygous for the neomycin substitution (and, therefore, had no functional *Hdh* loci)

died *in utero* (Duyao *et al.*, 1995; Nasir *et al.*, 1995; Zeitlin *et al.*, 1995). In humans,

however, there is no significant difference in the severity of pathology or age of onset

between individuals that are heterozygous or homozygous for the HD mutation.

Together, these data suggest that 1. htt is essential for embryonic development and 2.

the mutation that produces HD does not significantly interfere with the normal role of

this gene. This second implication is the basis of the widespread view that the HD

mutation produces a protein that has a novel gain-of-function (see chapter 1).

The question remains: what is the normal function of htt in the adult CNS, and

is that function of such significance that elimination or reduction of this protein will

lead to mental or physical incapacitation of an animal? Basic understanding of the

normal function of htt is fundamental to establishing treatments which effectively

antagonize the cellular or molecular actions of this protein. In particular, as anti-gene

therapy for genetic diseases is becoming a promising therapeutic avenue, one cannot

justify the application of such treatments against a gene with unknown function. The

determination of the normal role of htt in the brain would be particularly beneficial for two reasons: 1. it would provide insight into the cellular processes that involve htt, establishing specific inter- and intra- cellular systems as potential mediators of cell death in HD; 2. it would provide support for, or refute, the development of antisense or anti-gene therapies for HD, depending upon the significance of htt in the mature CNS.

Antisense oligodeoxynucleotides (ODNs) are becoming increasingly popular as a tool with which to selectively suppress gene expression in the CNS. However, this technology has yet to be thoroughly explored as a potential means to investigate the role of the *IT15 (Hdh)* gene in the brain, although one group has reported an unsuccessful attempt (Haque and Isacson, 1996). We were interested in developing antisense ODNs that would effectively suppress the expression of the *Hdh* gene in the rat CNS in order to examine pathological changes that may be induced by this suppression.

Our laboratory has much experience using antisense ODNs to suppress the expression of immediate early genes (IEGs) in the CNS (reviewed in Chiasson *et al.*, 1994, 1997). Most of the previous studies used phosphorothioate derivatives (sulfur-for-oxygen substitution at phosphate linkage groups) of phosphodiester ODNs to increase the nuclease resistance of these molecules *in vivo* (see chapters 3 and 9). These thioate-substituted ODNs were very effective at suppressing IEG expression in the rat brain, but their repeated application produced marked cellular toxicity (Chiasson *et al.*, 1997). As many IEGs (i.e. c-*fos*) do not have high constitutive expression in the

brain, single-dose applications of ODNs were effective at preventing the production of stimulant-induced expression of these genes. However, to effectively apply this technology to reduce the constitutive expression of htt, it was necessary to develop ODNs that could be chronically or repeatedly infused into the brain without producing cellular damage. Initially, therefore, we sought to determine the ability of ODNs that had reduced sulfur content (end-capped ODNs) to suppress gene expression *in vivo*, in the CNS. Before attempting to suppress htt expression, we investigated the efficacy of end-capped ODNs that targeted IEG mRNA by infusing these molecules into the striatum of rats (chapter 3). This allowed us to compare the effects of end-capped ODNs with those of fully substituted ODNs, in terms of their ability to suppress IEG expression and potential toxic effects of these molecules.

Early in the course of this research, I became interested in the etiology of the locomotor alterations that are produced by unilateral IEG knockdown in the striatum. As the caudate-putamen is a primary region of pathology in HD, we were interested in determining if this striatal suppression paradigm could be used as a novel, rodent model of HD. Previously reported correlation between antisense knockdown of c-*fos* and alterations in locomotor activity suggested that the induction of IEGs in the striatum was important for the functional role of this nucleus in motor regulation (Sommer *et al.*,1993; Hooper *et al.*,1994). To examine the precise mechanisms that underlie these motor aberrations, end-capped ODN derivatives were used to investigate 1. the role of the IEGs, c-*fos* and *ngfi*-a, in the striatum in relation to motor function and 2. the downstream effects of striatal dysfunction on other basal ganglia and

brainstem nuclei. The role of several subcortical regions have been investigated for their contribution to the locomotor abnormalities observed in animals with striatal IEG inhibition. We present evidence that suggests that inhibition of striatal IEG expression, using antisense ODNs, provides a reversible, non-toxic method to specifically suppress the activity of the output neurons of this region. We suggest that ODN-mediated suppression of striatal IEG expression represents a novel animal model of end-stage HD. We further describe a systematic comparison between subcortical alterations that occur in motor nuclei in animal models of PD and HD. The clinical relevance of such alterations to the human diseases is discussed.

As previously discussed, an initial goal of this research was the development of antisense ODNs that could effectively suppress the expression of the *Hdh* gene. However, while performing preliminary examinations of htt expression, some very fortuitous discoveries were made. We felt that these findings were extremely important and warranted a divergence from our initial plan in order to perform a thorough investigation of this phenomena. While this study did not use antisense technology, per se, it provided novel clues to the role of htt in the CNS. The results presented in chapter 10 support the notion that htt is intricately involved in cellular processes in the adult CNS and that its induction may be delimited by specific chemotactic or neurotrophic stimuli.

CHAPTER 1

Huntington's Disease

1.1. Introduction and Background

Huntington's disease (HD) is a hereditary, neurodegenerative disorder with an autosomal dominant pattern of transmission and complete penetrance. It is characterized by cognitive, motor and psychiatric manifestations that cause progressive deterioration of an individual's quality of life, culminating in death 10-15 years after the onset of symptomatology (Folstein, 1989). Onset of HD typically occurs in mid-life, but there is a juvenile form of the disease which strikes before the age of 20. The prevalence of HD varies among regions but studies have estimated that it occurs 5.15/100 000 (1987) and 8.4/100 000 (1975) in the United States and Canada, respectively (Shokeir, 1975; Folstein et al.,1987).

In 1872, a family physician named George Huntington of Pomeroy, Ohio published an article describing what had been previously called 'that disorder' in a Philadelphia journal entitled, *The Medical and Surgical Reporter* (Huntington, 1872). Huntington's publication and description of this condition was a compilation of his own clinical observations as well as those of his father and grandfather, both of whom were also physicians. Huntington's article in 1872 was remarkable in its accuracy and brevity of its description of this disease, which was eventually called *Huntington's chorea*, and later *Huntington's disease*. While others had partially described this disease prior to 1872, Huntington was the first to give a complete account, with accurate records of case studies for verification. Following 1872, the knowledge of HD spread rapidly and numerous reports and case studies were published from several countries (cited in Harper and Morris, 1996). Today, HD is widely recognized as a

distinct disease and research into its etiology has identified a genetic mutation which produces this condition.

1.2. Symptomatology of HD

1.2.1. Motor Abnormalities   The motor abnormality that is most commonly associated with HD is chorea. The involuntary muscle contractions are frequently observed in adult-onset HD, but rarely in the juvenile form, and typically involve the limb, trunk and facial muscles. The severity of chorea can vary from imperceptible twitching or fidgeting of the fingers to violent, uncontrollable flailing of the limbs. Often the patient may suppress initial choreiform activity, but as the disease progresses the motor abnormalities worsen and become uncontrollable. In addition to trunk and peripheral limb muscles, those of the pharynx may also be affected and result in speech difficulties (dysarthria) and the production of grunting or clucking sounds from forced air from the respiratory tract being pushed against a partially closed glottis (Harper and Morris, 1996).

As the course of the disease progresses, the chorea observed in early stages of adult-onset HD is often replaced, or masked, by rigidity and bradykinesia. Both of these symptoms are also characteristic of juvenile HD. Bradykinesia may also occur concurrently with chorea in early-stage adult HD, although infrequently (Curran, 1930). Another motor abnormality frequently seen in advanced HD is dystonia. This may produce contortions of the face, limbs or trunk into characteristic postures. Additionally, irregularities in gait are frequently observed in HD patients. Individuals will often walk with a wide-based, staggering gait, which may be misinterpreted as

intoxication (Koller and Trimble, 1985). Patients with HD also often have difficulties performing normal eye movements. These symptoms may occur early in the disease and worsen as the pathology progresses. Typical ocular problems include saccade initiation (Leigh *et al.*,1983), decrease in saccade velocity (Lasker *et al.*,1987) and accuracy (Leigh *et al.*,1983; Bollen *et al.*,1986) and gaze fixation (Lasker *et al.*,1987). Other motor problems that occur less frequently in adult-onset HD, but are common in juvenile HD include cerebellar dysfunction, upper motor neuron abnormalities, epilepsy and myoclonus (Harper and Morris, 1996).

1.2.2. Cognitive and Psychiatric Abnormalities Cognitive and psychiatric abnormalities are common among HD patients. Symptoms include dementia, depression, paranoia, schizophrenia and personality disorders. There also tends to be a high rate of suicide or attempted suicide in this population (Farrer, 1986; DiMaio *et al.*,1993). The diversity and apparently non-specific mental problems that may arise in HD facilitate misdiagnosis of early stage HD, prior to the onset of motor abnormalities. Although several reports indicate that psychiatric symptoms occur prior to the onset of chorea or other motor abnormalities, there have also been reports of them occurring after the onset of motor symptoms (reviewed in Harper and Morris, 1996). However, because of the wide range of psychiatric problems produced by HD, it can be difficult to determine whether the mental symptoms began after the onset of motor symptoms or if they were present initially but went undetected. For example, the personality changes that occur in HD may be subtle in regards to linking them to neurological

disease and may consist of increased degrees of antisocial (psychopathic) behavior, irritability, or aggression.

Dementia is a fundamental characteristic associated with HD and has been defined as '...the global deterioration of the individual's intellectual, emotional and cognitive faculties in a state of unimpaired consciousness' (Roth, 1980). Thus, it has been suggested that dementia encompasses at least three primary elements: 1. it is an acquired condition; cognitive and behavioral alterations that persist from childhood are usually regarded as mental handicap; 2. the cognitive deficits are global and are not restricted to a subset of mental functions; 3. this condition occurs in the absence of impaired consciousness. Unfortunately, early studies that evaluated the prevalence of dementia in HD did not use standardized psychometric testing to access intellectual functions. As a result the statistics vary considerably, but still indicate that a significant proportion of HD patients exhibit signs of dementia. For example, three separate studies indicated that 78/82 (Heathfield, 1967), 234/334 (Bolt, 1970) and 15/100 (Oliver, 1970) patients with HD suffered from some form of dementia.

One particular facet of cognitive function that has been under intensive investigation in HD is the ability to recognize facial expressions of emotion. As this recognition ability is fundamental to social interactions, it has become of interest to determine to what extent this ability is impaired in neurodegenerative diseases such as HD. In particular, it appears that recognition of both fear and disgust involve the amygdala and cortico-striato-thalamic circuits (Phillips et al.,1997). As these regions of the brain are particularly susceptible to HD pathology, the degree to which these

recognition abilities are impaired in HD patients have been studied. Two recent reports describe the impairment of the recognition of disgust, but not fear, in HD patients relative to normal control individuals (Gray *et al.*,1997; Halligan, 1998). The deficit in recognition of disgust but apparently normal fear recognition may result from the specific regions that are affected by HD pathology, or may simply reflect differing degrees of neuropathology and alterations of cerebral circuitry in these patients.

A connection between HD and schizophrenia has been hypothesized for many years. Indeed, several reports have described the misdiagnosis of schizophrenia in patients that were later found to have HD (Bolt, 1970; Dewhurst, 1970; Folstein, 1989). The prevalence of schizophrenia in HD patients has been assessed by several investigators. Unfortunately, standardized diagnostic criteria were not used in most of the early studies. However, three later studies using standardized criteria for diagnosing schizophrenia reported the co-occurrence of HD and schizophrenia in 3/88 (3%) (Folstein, 1989), 9/86 (10%) (Pflanz *et al.*,1991) and 8/64 (12%) (Watt and Seller, 1993) patients. The etiology of schizophrenia in HD patients remains unclear. There are conflicting opinions as to whether this condition is a result of the HD gene mutation or neuropathology or if patients with HD simply have an increased susceptibility to mental disorders.

1.3. Pharmacotherapy for HD

Therapeutic management of HD is currently symptom-based and includes drug therapy as well as psychological and social strategies to improve a patient's quality of life. Drug therapy for ameliorating chorea has generally involved the dopaminergic,

GABAergic and cholinergic systems of the basal forebrain. Neuroleptics or antipsychotics are agents that block dopaminergic transmission in the forebrain. These drugs, including haloperidol and fluphenazine, have been successfully used to treat chorea in HD patients (Barr et al.,1988). These drugs are administered with caution, however, as they have been shown to induce both acute and chronic tardive dyskinesia as well as Parkinson-like symptoms (Marsden and Jenner, 1980). Reserpine and tetrabenazine are dopamine-depleting agents that decrease the presynaptic stores of dopamine and lower dopaminergic transmission in the brain. While the sedative effects of these agents decrease choreiform movements, they also produce many undesirable side effects, such as depression and dysphagia, which limit their therapeutic value.

An alternate strategy for treating chorea is to increase the GABAergic activity in the brain. Unfortunately, both direct (muscimol, baclofen) and indirect (isoniazid) GABAergic agents have been relatively ineffective at treating chorea in HD (Fisher et al.,1974; Barr et al.,1978; Shoulson et al.,1978,1989; McLean, 1982). It has been hypothesized that the overall reduction in GABAergic neurons (and, therefore, GABA receptors) is responsible for this lack of effect. Consistent with this, benzodiazepines have also been shown to produce limited effects in HD patients (Peiris et al.,1976; Stewart, 1988).

There is a reduction in the amount of choline acetyltransferase (ChAT) in the brains of HD patients (Spokes, 1980). Therefore, a third strategy of HD therapy is to increase the cholinergic transmission by administering either acetylcholine precursors (choline) or cholinomimetics (Arecoline). However, both these classes of drugs have

been shown to be ineffective or even exacerbated the choreic movements (Aquilonius and Eckernas, 1977; Nutt *et al.*,1978). Also, the beneficial effects of the cholinesterase inhibitor, physostigmine, remains controversial. Other potential anti-choreic agents that include NMDA glutamate receptor antagonists, such as MK801 and remacemide, are currently being investigated. A recent controlled study of remacemide suggested that this class of drug may have therapeutic potential in treating symptoms of HD (Kieburtz, 1996).

Rigidity often occurs in later stages of adult-onset HD or in juvenile HD. Anti-parkinsonian drugs (i.e. levodopa, amantidine, bromocriptine, anticholinergics) are typically used to treat this symptom. Depression is often treated with conventional anti-depressants, i.e. tricyclics, selective serotonin reuptake inhibitors, monamine oxidase inhibitors. Fluoxetine is commonly administered to treat depression in HD. Unfortunately, there are currently no drugs that improve cognitive impairment in HD.

1.4. Relationship Between HD Pathology and Symptomatology

The most prominent clinical symptom of HD is the development of dyskinesia. Two forms of dyskinesia, chorea and bradykinesia/rigidity, follow in succession as the disease progresses from early to late stages (Bruyn, 1968; Hayden, 1981; Phillips *et al.*,1996). Although the basis of chorea remains unclear, currently recognized circuitry of the basal ganglia may explain its development. The caudate-putamen receives massive input from cortical and subcortical regions and processes information primarily through efferent projections to the external segment of the globus pallidus (GPe), the internal segment of the globus pallidus (GPi) or the substantia nigra pars reticulata

(SNR) and the dopaminergic cells of the substantia nigra pars compacta (SNC) (Graybiel, 1990, 1995). While the cytoarchitecture of the striatum is complex, neurons may be categorized into two main striatal components: patch (striosome) and matrix. These two components represent neurochemically distinct populations of cells, and may be easily distinguished on the basis of their immunochemical staining for cellular markers such as acetylcholinesterase (AChE) or calbindin. Striosomal neurons project to the SNC where they inhibit dopaminergic nigrostriatal neurons. Matrical neurons may be divided into those that project to the SNR/GPi or the GPe. The SNR and GPi projections directly inhibit the thalamus and the superior colliculus (SC). Striatal projections to the GPe comprise the initial segment of the 'indirect pathway', which increases inhibitory SNR/GPi output via the GPe and subthalamic nucleus (STN) (Graybiel, 1990, 1995).

It has been proposed that the chorea produced in early stages of HD results from a preferential loss of striatopallidal neurons of the indirect pathway, as these neurons are particularly vulnerable to the effects of HD (Crossman *et al.*,1988; Albin *et al.*,1990; Storey and Beal, 1993; Richfield *et al.*,1995). Loss of this circuit disinhibits pallido-subthalamic neurons, ultimately reducing the nigral outflow and, hence, increasing thalamocortical and tectal stimulation. The idea that chorea results from reduced striatopallidal neurotransmission has been supported by numerous studies. In particular, Crossman and colleagues (1988) have demonstrated that infusing GABA antagonists into the GP, thus mimicking a reduction in striatopallidal transmission, produces contralateral choreiform activity in primates. Also, Young's

group reported that, while rigid/akinetic HD patients had a significant loss of striatal neurons projecting to the GPe, GPi and the SNR, choreic patients had relative preservation of neurons projecting to the GPi (Albin *et al.*,1990). More recently, Storey and Beal (1993) reported greater losses of GABA in the GPe than in the GPi in choreic HD. Studies in our laboratory have conclusively shown that suppressing stimulant-induced striatal activity in rats produces sufficient stimulation of the ipsilateral GPe to induce massive changes in gene expression (chapter 4). Ablation of GPe activity in this model significantly reduced the motor influence of the ipsilateral hemisphere, supporting the notion that GPe activity markedly increases motor responses in these animals (chapter 5).

The psychiatric manifestations of HD have an unknown etiology. However, because many of these symptoms are responsive to conventional neuroleptic therapy, it is thought that they are also caused by the altered striatal physiology (Harper and Morris, 1996). Cognitive decline likely results from both basal ganglia and cortical pathology.

1.5. Etiology and Neuropathology of HD

In 1993, the genetic mutation that produces HD was identified (The Huntington's Disease Collaborative Research Group, 1993). A novel gene, termed *Interesting Transcript 15* *(IT15)* was determined to contain an abnormally expanded terminal trinucleotide (CAG) repeat in patients with HD. This polymorphic region of *IT15* lies within the coding region of the gene and translates into a polyglutamine tract at the amino-terminal of the protein product, huntingtin (htt). Huntingtin is

ubiquitously expressed throughout the majority of brain regions and in peripheral tissues (Li *et al.*,1993; Strong *et al.*,1993; DeRooij *et al.*,1995; Gutekunst *et al.*,1995; Jou and Myers, 1995; Sharp *et al.*,1995; Bhide *et al.*,1996; Wood *et al.*,1996). In unaffected individuals, the *IT15* gene contains a stretch of 6-37 CAG repeats whereas in patients with HD it has been found to contain >37 repeats. Individuals who develop HD symptoms in mid-life generally have between 37-45 CAG repeats, whereas in the juvenile form of HD, patients tend to have greatly expanded repeat stretches, usually >50 CAG copies. Interestingly, CAG expansions (in different genes) are believed to be the cause of several other neurological disorders, including spino-bulbar muscular atrophy (SBMA), spinocerebellar ataxia type 1 (SCA1), dentatorubral-pallidoluysian atrophy (DRPLA) and Machado-Joseph disease (SCA3) (Koide *et al.*,1994; Housman, 1995; Monckton and Caskey, 1995; Trottier *et al.*,1995b; Aylward *et al.*,1997; Zhou *et al.*,1997). It is hypothesized that the expansion of the polyglutamine tract on htt confers abnormal binding properties to this protein and causes novel or altered protein-protein interactions that ultimately produce toxicity and cell death.

Transgenic mice have been produced that express markedly expanded CAG repeats by insertion of exon 1 of the human IT15 gene into the mouse genome (Mangiarini *et al.*,1996). These animals have been found to contain aggregates of htt-containing 'protein balls' in the nuclei of cerebral neurons and exhibited a progressive neurological phenotype. These aggregates have been termed neuronal intranuclear inclusions (NII) and have been previously reported in examinations of brain tissue from

HD patients (Davies *et al.*,1997). These inclusions were not found in either wild-type, control mice or in unaffected humans. A subsequent study showed, however, that insertion of a 146-unit CAG repeat into the mouse hypoxanthine phosphoribosyltransferase gene (Hprt), a so-called 'house-keeping' gene that has no association with any neurological disorders, produced a protein with an expanded polyglutamine region (Ordway *et al.*,1997). These animals also displayed a progressive neurological phenotype and, upon post-mortem examination, were found to contain NIIs. Furthermore, Igarashi and colleagues have shown that expression of DRPLA (dentatorubral-pallidoluysian atrophy) cDNAs with expanded CAG repeats in COS-7 cells produces NIIs and apoptosis (Igarashi *et al.*,1998). It is hypothesized that the expanded glutamine regions become substrates for cellular enzymes called transglutaminases, increasing the degradation of the original protein and producing fragmented, free polyglutamine peptides that are toxic to the cell. This notion has been supported the finding that transglutaminase inhibitors can reduce apoptosis in COS-7 cells that express expanded CAG repeat regions on the DRPLA gene (Igarashi *et al.*,1998). Together, these studies suggest that expansions of CAG trinucleotide stretches in the coding regions of genes and the subsequent translation of these mutations into elongated polyglutamine tracts, produces aggregates of peptides in the nuclei of neurons and ultimately induces apoptosis. This process appears to be independent of the gene containing the expanded CAG region. The mechanism of transnuclear transport of these aggregate components and whether specific-transmembrane proteins may be involved in this process remain unknown. Thus, while

these studies provide novel and exciting information regarding possible mechanisms of neuropathology in CAG repeat disorders, they do not help elucidate the etiology behind the regionally-specific cellular pathology seen in HD.

The cerebral pathology of HD is predominantly localized to the caudate-putamen, cerebral cortex and specific regions of the hypothalamus (Folstein, 1989). The regional selectivity of HD pathogenesis suggests that toxic interactions that occur in the caudate-putamen involve the mutant form of huntingtin and other unrecognized, region-specific cellular components. To date, four candidate proteins, huntingtin-associated protein (HAP-1), huntingtin-interacting protein (HIP-1), the glycolytic enzyme, GAPDH, and the human ubiquitin conjugating enzyme, hE2-25K (also called HIP-2), have been identified as possible interactive species, based on their increased binding efficacy to the huntingtin protein expressing an extended polyglutamine tract (except hE2-25K) (Li et al.,1995,1996; Burke et al.,1996; Kalchman et al.,1996; Wanker et al.,1997). Evidence also suggests that abnormal huntingtin may interact with well-characterized substrates such as calmodulin and the epidermal growth factor receptor (Bao et al.,1996; Liu et al.,1997). It remains unclear, however, whether any of the above protein interactions are involved in the pathogenesis of HD. Interestingly, neurons in the caudate-putamen that contain NADPH, a marker for nitric oxide synthase (NOS), appear to be relatively spared from HD pathology (Ferrante et al.,1985,1987). Choi and colleagues have also demonstrated the relative resistance of NADPH-positive neurons to various NMDA agonists, but their apparent increased susceptibility to excitotoxic damage by other glutamate agonists (Koh et

al.,1988a,1988b). Determination of the cellular components that confer protection in these neurons may provide valuable insight into cytotoxic mechanisms of HD and also identify possible therapeutic targets. Because the huntingtin protein is expressed in many neuronal subtypes, the protein interactions which lead to cell death in affected regions must involve cell-specific expression of huntingtin-associated proteins. Identification of differentially expressed genes in these neuronal populations could provide valuable information about the mechanism of the cytotoxic interactions involving huntingtin which lead to HD.

1.6. Hypothesized Functions of htt

Huntingtin is a large (350 kDa), cytoplasmic protein with no known homology to other recognized proteins. The expression of htt has been localized to the cytoplasm and, while it has been suggested that htt participates in vesicular transport and release, its normal cellular function remains unknown. Studies using gene knockout technology have shown that animals that have a homozygous deletion of the htt gene die *in utero*. Animals with a heterozygous deletion, however, develop normally and are relatively indistinguishable from wild-type controls (Duyao *et al.*,1995; Nasir *et al.*,1995; Zeitlin *et al.*,1995). The survival of HD patients with homozygous mutations, and the similarity of disease progression between individuals with heterozygous and homozygous mutations, supports the notion that, in HD, the normal function of htt is conserved and the pathology results from novel interactions of the mutated htt. However, while there is growing evidence to suggest that the elongation of the polyglutamine tract of the htt protein produces NIIs and contributes to cell death, the

specificity of HD pathology remains to be explained. The distinct regions of damage produced by different CAG-repeat diseases suggests that the mutation of the particular gene may also contribute to the specificity of pathology. While elongated polyglutamine tracts appear to produce non-specific NIIs, it is possible that the regional pathology of HD results from the interruption or alterations of the normal htt function. Although evidence suggests that the HD mutation produces a novel 'gain-of-function', there is no evidence to discount the possibility that this mutation alters or dampens specific cellular processes of htt. For example, if this protein participates in a specific cellular signaling cascade that is associated with trophic responses and development of neural circuitries, it is possible that the mutation of htt may not have as dramatic effects in the dynamic, trophic-factor rich environment of a developing brain as it would in the adult brain. Thus, functional htt processes may be elicited by the intense trophic stimulation that occurs during development, but not by that in the adult brain. In order to fully understand the processes behind HD, it is necessary to determine the functional role of htt in the brain.

A recent study investigated the possible association of htt with various signaling molecules involved in the epidermal growth factor receptor (EGFR) signaling cascade (Liu et al.,1997). The presence of multiple proline-rich motifs in the huntingtin sequence led this group to investigate the possibility that huntingtin would associate with signaling modules through binding of src homology 3 (SH3) domains. Experiments demonstrated that huntingtin associates with the EGFR signaling complex through binding of SH3 domains on growth factor receptor-binding protein (Grb2) and

Ras-GTPase-activating protein (RasGAP). These associations were highly dependent upon EGFR activation and autophosphorylation (Liu *et al.*,1997). Interestingly, huntingtin immunoprecipitates were found to contain Grb2, but not the Ras guanine nucleotide releasing factor, Sos. In contrast, Grb2 immunoprecipitates were found to contain Sos. As Sos is the normal associative molecule which complexes with the SH3 domains on Grb2, the authors suggested that huntingtin may be a competitive inhibitor of Sos-Grb2 binding and transduction of Ras-dependent signaling. The nature of the huntingtin-RasGAP association remains unclear.

Recent studies in our laboratory have shown that the expression of htt is dramatically elevated in the arcuate nucleus (AN) of the hypothalamus in lactating female rats that are suckling young (chapter 10). This increase in expression occurred in astrocytes of the AN. Previous neuroendocrine studies have shown that the AN is essential for lactation and there is increasing evidence to suggest that major physiological changes occur in the AN in postpartum females. These changes are believed to be mediated by astrocytic regulation of neuronal activity (Moore, 1987; Tranque *et al.*,1987; Olmos *et al.*,1989; Torres-Aleman *et al.*,1992; Ma *et al.*,1994,1997). Our results implicate htt in the cellular mechanisms that mediate hormone-induced transcriptional and morphological changes in the hypothalamus. The role of huntingtin as a regulator of receptor tyrosine kinase signaling and modulator of cellular plasticity would account for the widespread expression of this protein and offer an explanation for the embryonic mortality observed in mutant mice that are nullzygous for the huntingtin gene (Duyao, 1995; Nasir *et al.*,1995; Zeitlin *et al.*,1995). As the

expression of this protein is constitutive in neurons throughout most brain regions, it is conceivable that huntingtin may not only be involved in EGFR signaling, but may also be a component of other receptor kinase signaling cascades. However, the importance of htt in these cellular processes remains to be confirmed.

1.7. Summary and Future Directions

Major research efforts are currently in progress to determine the pathological mechanisms by which HD produces cellular toxicity. Once these processes are elucidated, therapies may be developed to specifically target relevant cellular mediators and attenuate disease progression. Also, intrastriatal transplantation of neural tissue offers potential for regeneration and repair of circuits lost to HD pathology.

CHAPTER 2

Immediate Early Genes and c-*fos* in the CNS

2.1. c-fos Function, Regulation and Induction

The central nervous system (CNS) is remarkable in its ability to adapt and alter synaptic connections that exist within it. A crucial aspect of this plasticity is stimulus-transcription coupling, a process which refers to alterations in transcriptional activity that occur as a cellular response to external stimuli (i.e. receptor activation) (Berridge, 1986; Goelet et al.,1986; Curran and Morgan, 1987,1991). Ligand-induced activation of membrane receptors produces a cascade of second messengers (i.e. cyclic adenosine monophosphate (cAMP), protein kinases) that can transiently alter (i.e. by phosphorylation) constitutively expressed cellular proteins. These proteins may then enter the nucleus and bind to specific DNA motifs, or activate other cellular components that bind DNA, to induce or suppress the transcription of specific genes. Repeated stimulation of neural circuits is thought to induce long-term changes in cellular phenotype that facilitate this transmission (Hebb, 1949). This is the basis of current theories of memory storage (Berridge, 1986; Goelet et al.,1986), learning (Kaczmarek, 1993b) and addiction (Nestler et al.,1993).

Upon stimulation of a cell, the first round of transcriptional activity involves immediate early gene (IEG) induction. Among the IEGs are a class of inducible transcription factors (TFs) that are thought to physiologically link transient changes in second messenger systems with long-term changes in the cell (Morgan and Curran, 1991,1995; Robertson, 1992; Hughes and Dragunow, 1995; Chiasson et al.,1997). Thus, the IEG TFs provide a means by which activity at the cell membrane can induce or suppress transcriptional processes in the nucleus. IEG TFs are a large family of

genes, which include c-*fos* (Curran,1988), *fos-related antigen*-1 (*fra*-1) (Cohen and Curran, 1988), *fra*-2 (Nishina *et al.*,1990), *fos*-B (Zerial *et al.*,1989), c-*jun* (Maki *et al.*,1987), *jun*-B (Ryder *et al.*,1988), *jun*-D (Ryder *et al.*,1989), *krox*-20 and *krox*-24 (Lemaire *et al.*,1988) (also known as *zif* 268 (Christy *et al.*,1988), *ngfi*-a (Milbrandt, 1987) and *egr*-1 (Sukhatme *et al.*,1988)). While a few IEG TFs have relatively high constitutive expression in specific regions of the brain (i.e. *ngfi*-a, *jun* D), generally, these genes have minimal basal expression in the absence of external stimulation (Curran and Morgan, 1995). The Fos and Jun families of IEGs have been extensively studied. Fos and FRAs bind to members of the Jun family through a leucine zipper motif to form heterodimers called activator protein-1 (AP-1) complexes (Rauscher *et al.*,1988; Kouzarides and Ziff, 1989). The AP-1 complex recognizes and binds specific DNA sequences, including the AP-1/tetracycline-responsive element (TRE) in gene promoter regions, and can induce or inhibit transcription, depending on the genetic loci of the binding site and the composition of the AP-1 protein (Curran and Franza, 1988; Rauscher *et al.*,1988; Curran and Morgan, 1995).

The expression of c-*fos* is under the control of several regulatory elements that are located in the 5' untranslated region of the c-*fos* gene. These include the serum-response element (SRE) and the cAMP/calcium-responsive element (CRE/CaRE). Several proteins have been identified that bind to the SRE and this site is essential for the induction of c-*fos* by serum, growth factors and protein kinase C (PKC)-activators (Curran and Morgan, 1995). Elevation of intracellular calcium (Ca^{2+}) concentrations (i.e. by glutamate activation of *N*-methyl-*D*-aspartate receptors) or cAMP (i.e. by

dopamine (DA) activation of DA1 receptors) leads to activation of Ca^{2+}/calmodulin-dependent kinases and cAMP-dependent protein kinase A (PKA), respectively. These kinases activate the TF, cAMP-responsive element binding (CREB) protein, by phosphorylation of serine 133 (Gonzalez and Montminy, 1989; Sheng et al.,1990,1991). Phosphorylated CREB induces transcription of c-fos by binding to the CRE/CaRE site in the c-fos promoter region. The c-Fos protein can mediate autoinhibition by activating an AP-1 site in the promoter region of the c-fos gene and negatively regulating its expression (Sassone-Corsi et al.,1988).

The expression of c-fos is induced in the CNS by a vast array of pathological stimuli, including focal brain trauma, excitotoxicity, seizures and ischemia-hypoxia (Curran and Morgen, 1995), as well as by the addictive psychostimulant drugs, amphetamine and cocaine (Graybiel et al.,1990; Moratalla et al.,1993). However, this gene also has more positive associations with processes such as memory acquisition and learning (Kaczmarek, 1993a,1993b), trophic responses (Bartel et al., 1989), regulation of circadian rhythms (Rusak et al.,1990), sensory stimulation (Hunt et al.,1987) and locomotion (Berretta et al.,1992; Paul et al.,1992; Ruigrok et al.,1996). Thus, there is a growing body of evidence that suggests that c-fos is involved in stimulus-transcription coupling in the CNS and that its expression is essential for proper neuronal functioning.

2.2. c-fos and Cortical Functions

Transcription factor activation has been associated with the execution of tasks that require learning and memory. Several investigators have demonstrated an impairment

in learning and/or memory functions after antisense ODN administration. For example, c-*fos* antisense ODN treatment prevented long term memory retention in chicks that were trained in a passive avoidance task (Mileusnic *et al.*,1996) and reduced the success rates of rats trained in a brightness discrimination paradigm (Tischmeyer *et al.*,1994). As alterations in neural circuitry and function are thought to underlie mechanisms responsible for learning and memory, these results suggest that c-*fos* expression is necessary for synaptic plasticity in the brain and that antisense ODNs that suppress this expression can affect such processes.

2.3. Expression of c-fos in the Basal Ganglia

The basal ganglia is a term used to collectively describe a group of forebrain nuclei that includes the striatum, globus pallidus and the amygdala. These structures participate in sensorimotor integration, limbic and cognitive processes and motor-associated learning, but have been best characterized for their influence on motor control (Graybiel, 1990; Mink, 1996; Wichmann and DeLong, 1996). Although basal levels are minimal, expression of c-*fos* in the striatum is induced by systemic administration of amphetamine or cocaine (Graybiel *et al.*,1990). The association of c-*fos* with the psychostimulant effects of these drugs has led many investigators to believe that this IEG TF is involved in mediating long-term, cellular changes that produce addiction. In rats, the induction of c-*fos* by psychostimulants is mediated through activation of dopamine (DA) D1 receptors and is associated with increased locomotor activity and stereotypic behavior (i.e. focused sniffing, rearing) (Graybiel *et al.*,1990; Cole *et al.*,1992; Paul *et al.*,1992). The inducibility of this gene in the striatum and the

associated motor behavior have made this region an attractive locus in which to study the effects of c-*fos* antisense ODNs.

The expression of c-*fos* in the striatum appears to be integrally involved in the processes of stimulus-transcription coupling and in producing alterations in the expression of other genes. The establishment of a causal link between c-*fos* and its target genes, in distinct regions of the brain is complicated by the great diversity of neuronal and non-neuronal cell populations, their state of activity, and their connections with each other (microcircuits) and with neurons from other brain regions (macrocircuits). In theory, any of a vast number of genes containing AP-1 binding sites in their promoter regions could be influenced by changes in the expression of c-*fos*. These potential targets include genes that encode enzymes (i.e. tyrosine hydroxylase, glutamic acid decarboxylase) that are involved in the synthesis of neurotransmitters (i.e. norepinephrine, dopamine, gamma-aminobutyric acid), peptides (i.e. cholecystokinin, enkephalin, dynorphin, neurotensin), growth factors (i.e. nerve growth factor), transcription factors (i.e. *jun*B, *ngfi*-a) and others (Hughes and Dragunow, 1995). Two examples of c-*fos*-regulated genes in striatal neurons are those of the peptide precursors of neurotensin and substance P (Merchant, 1994; Robertson *et al.*,1995; Svenningsson *et al.*,1997). Although it is unknown whether the changes in peptide expression account for the behavioral effects produced by intrastriatal infusions of c-*fos* antisense ODNs, they provide evidence for biochemical disturbances produced by these agents. Increased levels of c-*fos*, *jun*B and *ngfi*-a mRNA have been reported in the striatum shortly (90 min) after intrastriatal infusions of c-*fos* antisense ODNs

(Sommer *et al.*,1996). These results suggest an inhibitory role of the Fos protein on the basal expression of these genes in the striatum. Such transcriptional influences between IEG TFs could explain the enormous variability in the composition of AP-1 and other transcription factor complexes. Furthermore, suppression of basal c-*fos* expression by antisense ODNs in striatal neurons significantly reduced the release of the neurotransmitter gamma-aminobutyric acid (GABA) in the substantia nigra, one major projection area of the striatum (Sommer *et al.*,1996).

Several behavioral and physiological consequences have been reported to result from suppression of striatal c-*fos* expression. For example, bilateral injections of c-*fos* antisense ODNs into either the nucleus accumbens or the neostriatum blocked the motor activation induced by cocaine and amphetamine, respectively (Heilig *et al.*,1993; Umekage *et al.*,1997). Also, animals that were stimulated with *d*-amphetamine, following an unilateral intrastriatal infusion of anti-c-*fos* ODNs, demonstrated postural and motor asymmetries that manifested as rotational behavior towards the side of suppression (Sommer *et al.*,1993; Hooper *et al.*,1994). This circling activity has been the behavioral response typically used to assess the effects of antisense ODNs targeting c-*fos* in the striatum.

2.4. Role of c-fos in the Amygdala

Kindling is an animal model of epileptogenesis where repeated subconvulsive electrical stimulation of 'seizure-responsive' regions of the brain (i.e. amygdala, hippocampus) eventually produce full generalized seizures (Goddard *et al.*,1969; Racine, 1972). A single kindling stimulus produces focal seizure activity or an afterdischarge (AD) that

is essential for kindling to occur (Curran and Morgan, 1995). A single AD in the amygdala results in IEG induction in the amydala, claustrum, piriform cortex and the perirhinal cortex (Dragunow and Robertson, 1987; Dragunow *et al.*,1992; Hughes *et al.*,1994; Chiasson *et al.*,1995). Experiments have shown that repeated infusions of antisense ODNs to c-*fos* into the amygdala can suppress the expression of this gene and significantly accelerate the rate of kindling in rats (Chiasson *et al.*,1997). This increase in kindling rate is possibly due to a reduction in GABAergic neurotransmission in this region. GABA is the primary inhibitory neurotransmitter in the CNS and a reduction in its release would facilitate excitatory transmission of seizure-producing neurons. These studies strongly implicate the involvement of c-*fos* in the kindling process and in the production of seizures elicited from the amygdala.

The amygdala is a limbic structure that has been associated with emotional integration of fear and anxiety. As numerous stressors have been shown to increase the expression of IEGs, including c-*fos*, in this region, it is thought that these genes play a role in mediating limbic responses (Honkaniemi, 1992; Honkaniemi *et al.*,1992). Moller *et al.* (1994) investigated the role of c-*fos* in anxiety disorders using a modified version of Vogel's drinking conflict test. They showed that administration of c-*fos* antisense ODNs into the amygdala attenuated c-*fos* expression and reduced the animals' anxiety to drink. Thus, this gene appears to be essential for mediating appropriate limbic functions in the amygdala.

2.5. c-fos and the Circadian Rhythm

The principle circadian pacemaker in mammals is the suprachiasmatic nucleus of the hypothalamus. Expression of Fos and Jun proteins is induced in this region by photic stimulation and is synchronous with the cyclicity of the circadian rhythm. Intracerebroventricular (ICV) administration of a cocktail of antisense ODNs to c-*fos* and *jun*B blocked the light-induced expression of these genes and inhibited the phase shift of the mammalian clock by the light pulse (Wollnik *et al.*,1995).

The preoptic hypothalamus is known to play a major role in the regulation of sleep. The expression of c-*fos* and other IEG-TFs is strongly modulated in this region both during the sleep-wake cycle and after sleep deprivation. Injections of c-*fos* antisense ODNs into the rat medial preoptic area blocked the expression of Fos protein. Rats that received infusions of c-*fos* antisense, but not sense, ODNs into the medial preoptic area showed a higher percentage of wakefulness the day after the injection (Cirelli *et al.*,1995). These studies indicate that blocking the expression of Fos protein in the hypothalamus may interfere with the homeostatic regulation of sleep and wakefulness.

2.6. c-fos and Central Blood Pressure Regulation

Increases in c-Fos immunoreactivity (IR) of several brain stem nuclei have been observed upon pharmacological activation of the pressor response and baroreceptor reflex. Local injection of c-*fos* antisense ODNs into the nucleus tractus solitarius reduced the increase in c-Fos IR in barosensitive neurons and reduced the inhibitory modulation of these neurons on the baroreflex control (Shih *et al.*,1996). In another study, the local blockade of c-*fos* in the rostroventral medulla attenuated the blood

pressure response to pharmacological disinhibition of these neurons and also reduced resting blood pressure (Suzuki *et al.*,1994). These results suggest that, in brain stem neurons associated with cardiovascular regulation, the c-*fos* gene has tonic functions and is important in the central regulation of blood pressure.

2.7. Role of c-fos in Nociceptive Transmission

Peripheral sensory stimulation induces c-*fos* expression in spinal dorsal horn neurons (Hunt *et al.*,1987). The pattern of Fos-LI is dependent upon the type and intensity of stimulus given. For example, the majority of Fos-LI is induced in superficial layers I and II of the dorsal horn (the termination zones of unmyelinated nociceptive fibres) following noxious heat or chemical stimulation (Wisden *et al.*,1990; Naranjo *et al.*,1991; Strassman and Vos, 1993). In contrast, gentle limb manipulation or hair brushing induced Fos-LI in layers II-IV, but rarely in layer I (Hunt *et al.*,1987). It appears, therefore, that the expression of Fos-LI is restricted to spinal neurons that transmit specific sensory information that is associated with the type of stimulus given (i.e. innocuous or noxious). While these data suggest that c-*fos* is induced by sensory-regulated release of neuropeptides (i.e. substance P) from axons of neurons that reside in the dorsal root ganglia, Lucas *et al.* (1993) have reported that, in spinal cord neurons, the 5-HT1A receptor is responsible for the induction of c-*fos* expression. This leads to some confusing interpretations regarding the function of this gene in sensory transmission. For example, induction of c-*fos* in response to sensory stimulation suggests that the Fos protein is involved in the regulation of genes that are associated with this transmission. However, regulation of this expression by 5-HT1A

receptor activation suggests that inhibitory, descending neurotransmission from central nociceptive centers (i.e. raphe nucleus) is responsible for c-*fos* expression and that this gene may be involved in the production of neuromodulators that decrease the amount of ascending sensory transmission. This latter hypothesis has been supported by evidence demonstrating that c-*fos* is a positive regulator of the endogenous opioid, preprodynorphin (Draisci and Iadarola, 1989; Noguchi *et al.*,1991). Intrathecal and systemic infusions of antisense ODNs to c-*fos* attenuated both the expression of c-*fos* and preprodynorphin, but had no effect on the expression of preproenkephalin (Lucas *et al.*,1993; Gillardon *et al.*,1994,1997; Hunter *et al.*,1995; Guo *et al.*,1996). Despite several reports of the ability of antisense ODNs to suppress c-*fos* expression in the spinal cord, the role of spinal c-*fos* expression remains unclear. For example, Hunter *et al.* (1995) reported an increase in nociceptive behavior in response to an attenuation of spinal c-*fos* expression. They attributed this behavior to a decrease in transactivation of the preprodynorphin gene and a reduction in spinal opioid activity. In contrast, Hou *et al.* (1997) reported a reduction in nociceptive behavior following a similar treatment and suggested that pharmacological blockade of c-*fos* may have potential in reducing nociceptive transmission. It is interesting that both groups used the same nociceptive model (formalin injection into the hindpaw) and reported their results as they occurred in the tonic phase of the experiments. Thus, while it is evident that c-*fos* plays a significant role in spinal nociceptive neurophysiology, determination of the function of this gene in these processes clearly needs further investigation.

CHAPTER 3

In vivo Suppression of Immediate Early Gene Expression Using End-Capped

Antisense Oligodeoxynucleotides [*]

3.1. Introduction

The application of antisense ODNs is rapidly becoming a popular method with which to suppress gene expression both *in vitro* and *in vivo* (Robertson *et al.*,1989; Chiasson *et al.*,1996,1997). However, most cellular environments contain endo- and exonucleases that rapidly degrade any endogenous or exogenous fragments of DNA, including synthetic ODNs (Stein and Cheng, 1993). Various modifications have been devised to alter and protect the structural integrity of the ODNs in attempt to endow them with nuclease resistance and attenuate their degradation. These include liposomal encapsulation (Zelphati *et al.*,1994), internal hairpin loop designs (Tang *et al.*,1993) and, more commonly, incorporation of sulfur atoms in the phosphate linkage groups of the ODN phosphodiester backbone (Stein and Cheng, 1993). These latter phosphorothioate derivatives have been used extensively *in vivo* for gene-specific suppression, particularly in the brain (Chiasson *et al.*,1992; Dragunow *et al.*,1993,1994; Hooper *et al.*,1994; Konradi *et al.*, 1994).

Phosphorothioate-modified antisense ODNs can be used to effectively suppress immediate-early gene (IEG) expression in the striatum and to assess behavioral and physiological alterations which are produced by such an inhibition (Chiasson *et al.*,1992,1994; Dragunow *et al.*,1993,1994; Hooper *et al.*,1994). A single application of phosphorothioate antisense ODNs effectively and specifically inhibit protein expression by virtue of their robust nuclease resistance and extended duration of action. However, inhibition of constitutively-expressed genes (i.e. those encoding membrane receptors) may not be achieved with short-term dosing and may require chronic or

repeated ODN infusions. Previous studies examining the effects of repeated intrastriatal administration of phosphorothioate antisense ODNs revealed extensive cellular toxicity and gliosis near the site of infusion which was attributed to non-specific interactions between the phosphorothioate molecules and cellular targets (Chiasson *et al.*,1994,1996).

Presently, we have used intrastriatal infusion of end-capped phosphorothioate antisense ODNs targeted to the IEGs c-*fos* and *ngfi*-a to assess the efficacy and viability of these molecules *in vivo*. We hypothesized that sulfur modifications solely between the terminal base pairs of the ODN would reduce toxicity (by minimizing sulfur content) while maintaining an adequate degree of nuclease resistance and effectively inhibiting gene expression. The results of this study indicated that, although their duration of action is much less than that of fully substituted molecules, these end-capped antisense oligodeoxynucleotides are capable of gene-specific suppression during their periods of peak efficacy.

3.2. Materials and Methods

3.2.1. Experimental Design Male Sprague-Dawley rats (250-350 g) were anesthetized with halothane until a surgical plane was reached and subsequently mounted on a Kopf stereotaxic apparatus in a flat skull position. Animals were supplemented with halothane (Fluothane) during the course of the surgery. Once mounted in the apparatus, the scalp was retracted and the skull exposed. Two burr holes were drilled in the skull and a 25-gauge cannula was guided into each striatum (from bregma: AP, 1.0 mm; DV, 6.0 mm; LAT, ± 3.0 mm). Solutions of oligodeoxynucleotides (1mM) or vehicle were then infused at a rate of 0.25 μl/min using a CMA 100 (Carnegie-Medicin) microinjection pump until a total volume of 2.0 μl (2.0 nmol) was reached. After the appropriate solution was infused, the cannulae were left in place for an additional two minutes to allow for diffusion away from the injection site. Following removal of the cannulae, the animals were sutured and placed in their home cage for a recovery period of 1, 2, 4 or 10 hours. Animals were subsequently injected with *d*-amphetamine (5 mg/kg, i.p.) and placed in a rotometer, where the number and direction of their rotations were recorded in 10 minute intervals for a period of two hours. After the rotation period, animals were deeply anesthetized with sodium pentobarbital (>100 mg/kg, i.p.) and sacrificed.

3.2.2. Immunohistochemistry   Animals were transcardially perfused initially with saline followed by 4% paraformaldehyde in a 0.1 M phosphate buffer solution (pH 7.4). Brains were subsequently removed and post-fixed at 4°C until further analysis. Brains were blocked and cut on a vibratome in 50 μm coronal

sections and were processed for c-Fos or NGFI-A immunohistochemistry. For this, the

tissue was washed for 10 minutes in 0.1M phosphate-buffered saline containing 0.1%

Triton-X (PBS-TX). This was followed by a 15 minute incubation in 1% hydrogen

peroxide to inactivate endogenous peroxidase activity and subsequent 3 X 10 minute

washes in PBS-TX at room temperature. The sections were then incubated in a 1:5000

dilution of polyclonal c-Fos antibody (Genosys) or 1:4000 dilution of polyclonal NGFI-

A antibody (Santa Cruz Biotechnology Inc.) for 16-24 hours at 4°C. Following

incubation with the primary antibody, the sections were washed 3 X 10 minutes in

PBS-TX and incubated in a 1:500 dilution of a corresponding biotinylated secondary

antibody (Vector Laboratories) for 1-2 hours at room temperature. Excess antibody

was removed by washing 3 X 10 minutes in PBS-TX and the bound secondary was

visualized using the avidin-biotin technique (ABC Elite; Vector Laboratories) using

diaminobenzidine (DAB; Sigma) as the chromogen. The sections were mounted on

gelatin-coated slides, air-dried, dehydrated in graded alcohols, delipidated in xylene

and coverslipped using Entellan adhesive (Merck). Selected sections were also stained

for visualization of Nissl substance. For this, 50 μm sections were mounted on gelatin-

coated slides, air-dried, dehydrated in graded alcohols and xylene, rehydrated and

stained with 0.1% cresyl violet.

3.2.3. Oligodeoxynucleotides

All oligodeoxynucleotides were purchased

from Genosys and had a single phosphorothioate modification between the first and last

nucleotide pairs (i.e. 'end-capped'). Standard phosphoramidite chemistry for

oligonucleotide synthesis was used with samples of each synthesis examined on

polyacrylamide gels to verify oligonucleotide quality. All oligonucleotides were extracted and precipitated by the manufacturer (to remove organics and salts) prior to lyophilization.

Oligodeoxynucleotides were reconstituted in ultrafiltered (millipore) distilled water at a concentration of 1 nmol/µl. The antisense oligodeoxynucleotide to *c-fos*, ASF, was a 15 base oligomer (15-mer) that had been previously used in both partially and completely phosphorothioate-modified form (Chiasson *et al.*,1992,1994; Dragunow *et al.*,1993; Heilig *et al.*,1993; Sommer *et al.*,1993,1996; Hooper *et al.*,1994). Its sequence was 5'-G$_s$AA-CAT-CAT-GGT-CG$_s$T-3', corresponding to bases 129-143 on the mRNA transcript (GenBank accession no. XO6769; the *s* indicates the sites of the sulfur modifications). The specificity of the ASF sequence in both partially and fully phosphorothioate ODN derivatives has been previously demonstrated using mismatch and sense controls (Chiasson *et al.*,1992; Heilig *et al.*,1993; Hooper *et al.*,1994; Sommer *et al.*,1996). The 18-mer antisense oligodeoxynucleotide to *ngfi-a*, ASN, corresponded to bases 348-365 of the mRNA transcript, with the sequence 5'-G$_s$GT-AGT-TGT-CCA-TGG-TG$_s$G-3' (GenBank accession no. M18416). Antisense oligodeoxynucleotides corresponded to regions that span the initiation codon on their respective mRNA transcripts. A random oligodeoxynucleotide, RAN, which had a randomly ordered, but identical base content to ASN, was used as a control. Its sequence was 5'-G$_s$TT-GGA-GTC-GGT-GGT-TC$_s$A-3'. All oligodeoxynucleotides used in this study were subjected to a BLASTN search on the National Center for Biotechnology Information BLAST server using the Genbank database (Altschul *et*

al.,1990). Antisense oligodeoxynucleotide sequences had positive matches only for their targeted mRNA sequences. The random sequence produced no positive matches.

3.2.4. Animal Groups   There were four groups: (1) ASF-treated (n=26), (2) ASN-treated (n=24), (3) RAN-treated (n=9) and (4) naive (n=8) animals. ASF and ASN groups were further divided into four subgroups that were given recovery periods of 1, 2, 4 or 10 hours following ODN infusion. The number of animals per group were as follows: ASF: 10 hours, n=4; 4 hours, n=4; 2 hours, n=6; 1 hour, n=12; ASN: 10 hours, n=4; 4 hours, n=4; 2 hours, n=9; 1 hour, n=7. All RAN-treated animals were given recovery periods of 2 hours.

3.2.5. Statistical Analysis   The number of ipsiversive and contraversive rotations were compared within a particular treatment group using a two-tailed, paired t-test. Significance was assumed when $p < 0.05$.

3.3. Results

3.3.1. Rotational Analysis

Animals with recovery periods of 4 and 10 hours, infused with either ASF or ASN showed no significant bias in their rotational behavior (Fig.3.1A,B). At 2 hours post-infusion, half of the animals in the ASF group demonstrated strong rotation towards the antisense-treated side (ipsiversive) whereas the other half did not demonstrate any rotational bias. In the ASF group with the 1 hour recovery period, 10/12 animals demonstrated significant ipsiversive rotation following ASF infusion and subsequent d-amphetamine challenge (285 ± 55 ipsiversive : 31 ± 12 contraversive; p= 0.00074; Fig.3.1A). Animals that received ASN demonstrated significant ipsiversive rotational behavior at 2 hours post-infusion (387 ± 103 ipsiversive : 42 ± 14 contraversive; p= 0.015) that was also evident in animals with 1 hour recovery periods. However, rotational differences at this time point were not statistically significant (Fig.3.1B). Naive animals and those that received unilateral infusions of RAN, showed no rotational bias when challenged with d-amphetamine (Fig.3.1C).

3.3.2. Effects of ASF on IEG Expression

Animals receiving ASF with recovery periods of 4 and 10 hours showed negligible suppression of Fos-like immunoreactivity (Fos-LI) between control and treated sides (data not shown). However, when recovery periods were reduced to 2 hours, 4 animals showed a slight to moderate decrease in Fos-LI in the ipsilateral striatum while the remaining 2 animals showed no evidence of Fos knockdown. All animals in the 1 hour recovery group treated with ASF and analysed for Fos-LI showed extensive reduction in the treated versus control striata

(Fig.3.2). None of the animals treated with ASF demonstrated any notable differences in NGFI-A expression.

3.3.3. Effects of ASN on IEG Expression Animals treated with ASN that had recovery periods of 4 and 10 hours showed no differences between control and treated striata, whereas all animals with 1 and 2 hour recovery periods demonstrated significant suppression of *d*-amphetamine-induced NGFI-A expression in the antisense-treated striatum, which was evident by the reduction in striosomal-like immunoreactivity (Fig.3.3A,B).

When ASN-treated animals were analysed for Fos-LI, those with recovery periods of 4 and 10 hours showed no difference in expression between control and treated striata. However, with recovery periods of only 1 and 2 hours, every animal demonstrated a marked reduction in *c-fos* expression in the ASN-treated striatum (Fig.3.3C,D).

3.3.4. Effects of RAN on IEG Expression Animals that received intrastriatal infusions of RAN had recovery periods of 2 hours. Immunohistochemistry revealed negligible differences in c-Fos or NGFI-A expression between control and treated striata (Fig.3.4).

3.3.5. Toxicity of ODNs Nissl staining of striatal sections from animals infused with ASF, ASN or RAN displayed continuous cellular integrity in all regions surrounding the infusion site, with the exception of the actual cannulae tracts (see Fig.5.1).

3.4. Discussion

Antisense ODNs have been used successfully *in vitro* (Shih *et al.*,1994; Duncan *et al.*,1996) and *in vivo* (Chiasson *et al.*,1992,1994; Dragunow *et al.*,1993,1994; Hooper *et al.*,1994; Bourson *et al.*,1995) to inhibit expression of specific proteins in various cellular systems. Studies have repeatedly demonstrated the ability of phosphorothioate antisense ODNs to specifically suppress IEG expression in the CNS (Chiasson *et al.*,1992,1994; Dragunow *et al.*,1993,1994; Hooper *et al.*,1994). In most of these studies, however, these molecules have only been used in acute dosing regimes.

Unmodified (phosphodiester) ODNs have been shown to be ineffective at suppressing gene expression *in vivo* (Hooper *et al.*,1994) as sulfur, or other, modifications along the backbone of these molecules is essential to their resistance against nuclease degradation (Campbell *et al.*,1990). Chronic administration of fully modified, phosphorothioate ODNs, however, has been shown to produce marked toxicity, which is thought to be conferred by the sulfur substitutions on the phosphate groups causing non-specific interactions between these molecules and cellular proteins (reviewed in Chiasson *et al.*,1994,1996). It was determined that, although marked cellular damage could be avoided if the ODN applications were separated by intervals of 2-3 days, this solution was not particularly feasible for chronic gene suppression given that their antisense effects had completely dissipated after approximately 24 hours.

In the present study, we have attempted to establish an *in vivo* model of striatal IEG suppression which utilizes partially modified, 'end-capped' antisense ODNs to

determine if sulfur substitution solely at 5' and 3' terminal phosphate groups would provide these molecules with sufficient nuclease resistance while minimizing their toxicity in the brain. By varying the lengths of the recovery periods following antisense ODN infusion and observing behavioral and, subsequently, immunohistochemical alterations in the animals, we were able to determine the efficacy and longevity of ODNs that targeted either c-fos (ASF) or ngfi-a (ASN) mRNA. As others have reported, we found that unilateral ASF administration into the striatum resulted in robust ipsiversive rotation following d-amphetamine challenge (Dragunow et al.,1993; Sommer et al.,1993; Hooper et al.,1994) and marked reduction in d-amphetamine-induced striatal c-fos expression in animals with 1, but not 2, 4 or 10 hour recovery periods, with no effect on NGFI-A expression. The antisense ODN to ngfi-a (ASN) had a similar profile, with rotational behavior maximal at recovery periods of 2 hours, and absent at periods greater than 4 hours. Immunohistochemistry revealed that ASN dramatically reduced both d-amphetamine-induced NGFI-A and c-Fos expression at 1 and 2 hours post-infusion, but had no effect at 4 or 10 hours (see chapter 4 for discussion of c-fos/ngfi-a interactions). Random ODNs had no effect on either rotational behavior or protein expression. Nissl staining revealed complete tissue viability in striata treated with ASF, ASN and RAN.

Together, these behavioral and immunohistochemical findings indicate that end-capped antisense ODNs are capable of suppressing protein expression in vivo with efficacy similar to that of their fully substituted, phosphorothioate counterparts. The sulfur modifications at terminal phosphate groups appear to endow these molecules

with sufficient nuclease resistance to permit protein suppression for approximately 1-2 hours post-infusion while minimizing the risk of sulfur-induced toxicity. The efficacy of these ODNs is further supported by the time-dependent rotational behavior observed in these animals; a finding which has been previously associated with unilateral suppression of striatal IEGs (Dragunow *et al.*,1993; Hooper *et al.*,1994). Because nuclease degradation is believed to occur primarily from the 3' end of the ODN (Tang *et al.*,1993), it may also be possible to employ single end-capped ODNs with similar results. With peak efficacy occurring between 1-2 hours post-infusion, their low potential for cellular toxicity makes phosphorothioate end-capped antisense ODNs prime candidates for *in vivo* application in chronic suppression models.

Figure 3.1 Temporal pattern of d-amphetamine-induced rotational behavior in ODN-infused and naive animals.
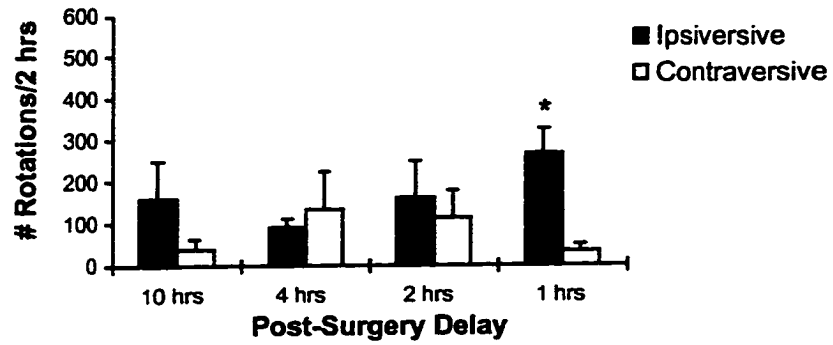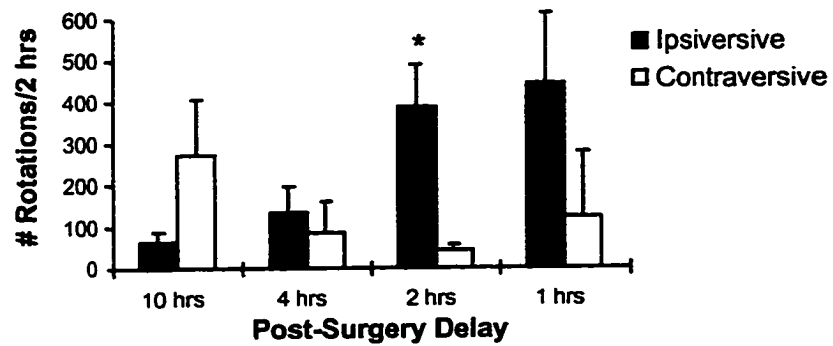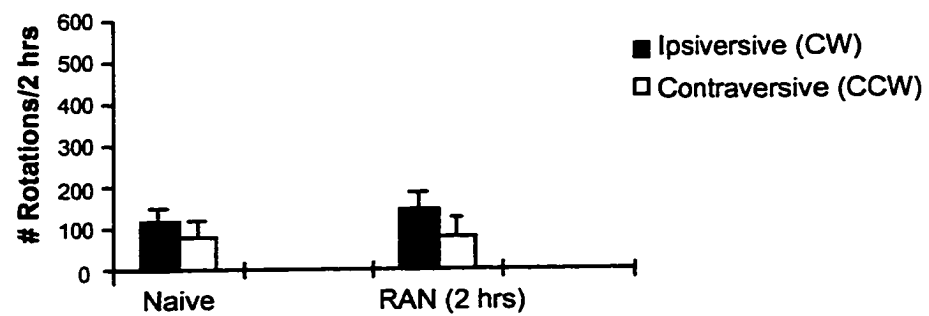
FIGURE 3.1

Figure 3.2 Effects of ASF on striatal *d*-amphetamine-induced c-Fos expression. A)

Control (vehicle-infused) striata displayed typical striosomal pattern of c-Fos induction

(arrows) whereas near total suppression of this induction was observed in ASF-treated

striata (B). Scale bar represents 100 μm.
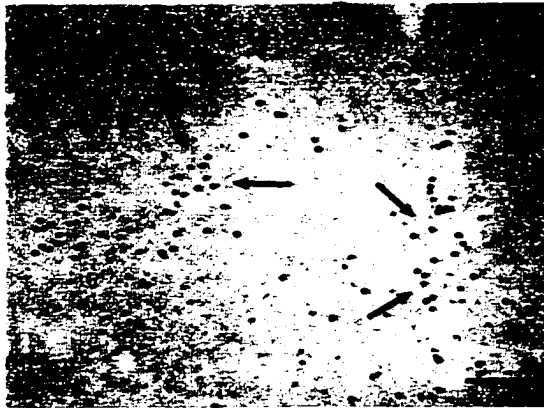
FIGURE 3.2

Figure 3.3 Effects of ASN on striatal *d*-amphetamine-induced NGFI-A (A,B) and c-Fos (C,D) expression. The striosomal IEG expression of the control (vehicle-infused) striata (A,C) was virtually abolished in the ASN-treated striata (B,D). After ASN infusion, only background expression of NGFI-A remained (B). Arrows in A) and C) indicate striosomal clusters of NGFI-A and c-Fos, respectively. Scale bar represents 100 μm.
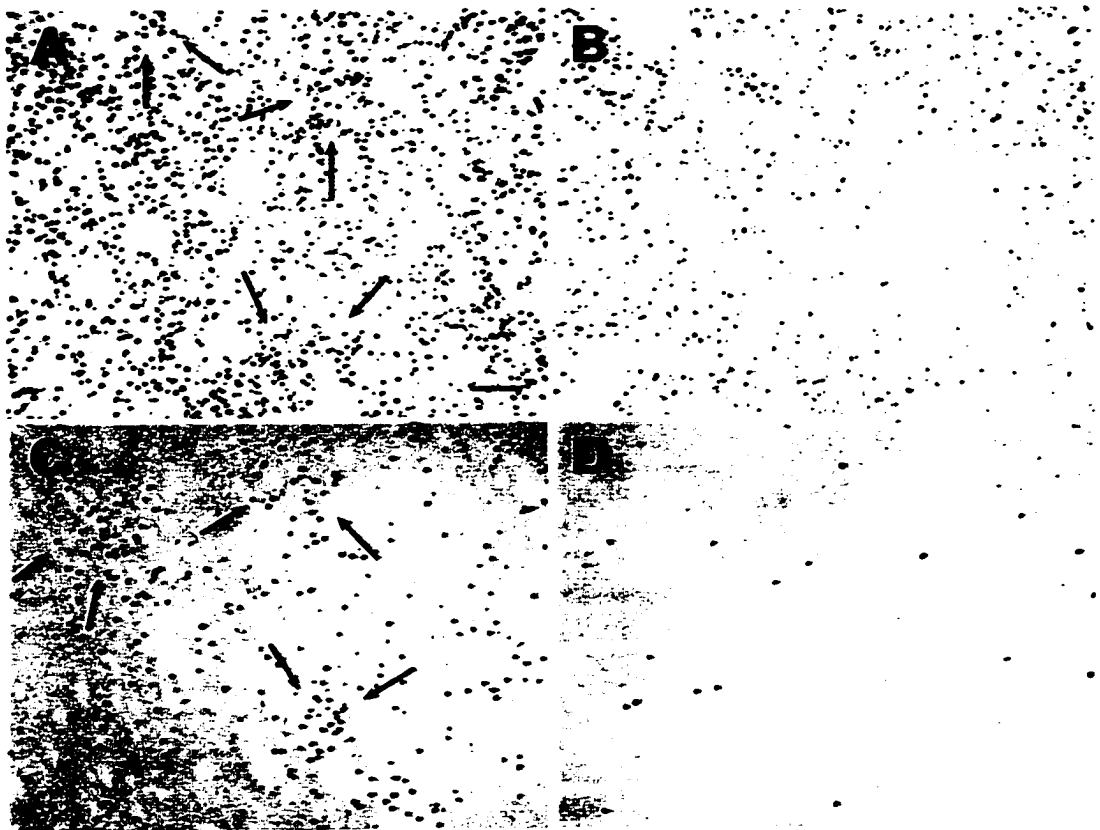
FIGURE 3.3

Figure 3.4   Effects of RAN on c-Fos (A,B) and NGFI-A (C,D) expression in the striatum. Protein expression in RAN-treated striata (B,D) appeared similar to that seen in control striata (A,C). Arrowheads indicate the tip of the cannulae tract. Arrows in C and D indicate individual striosomal clusters. Scale bar represents 100 μm.
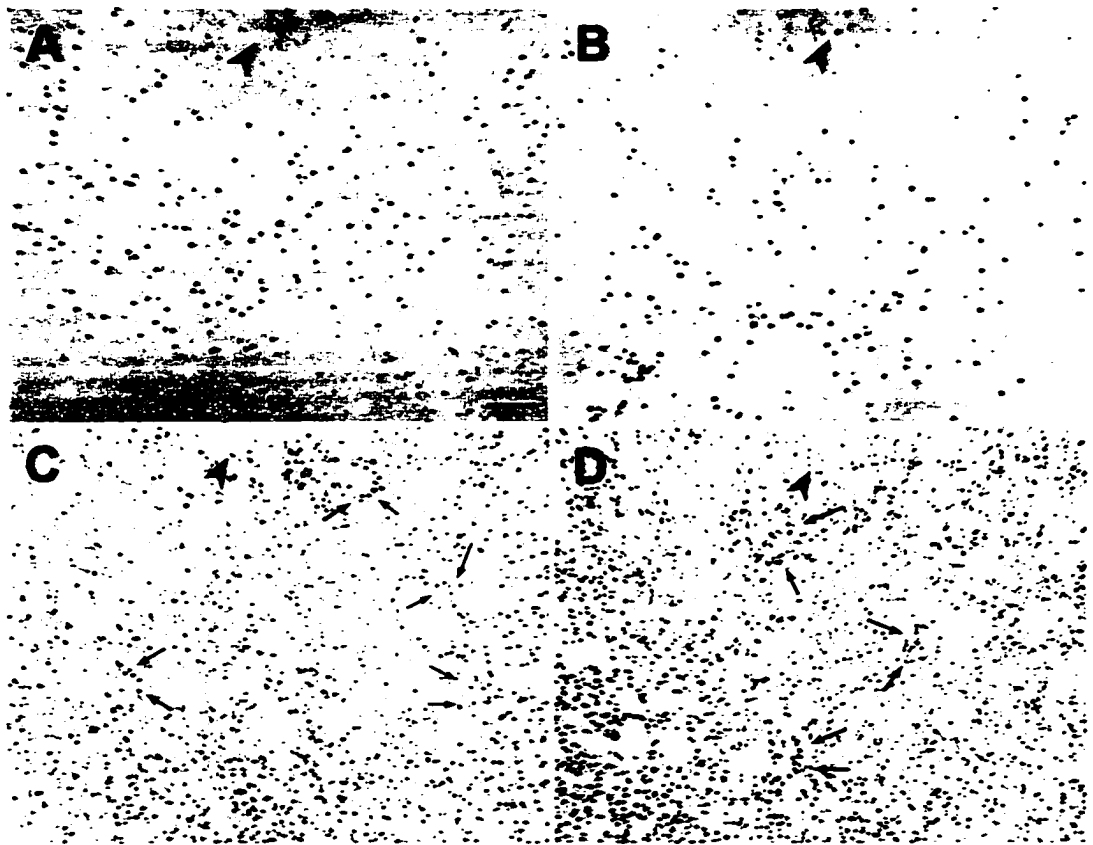
FIGURE 3.4

CHAPTER 4

Simultaneous Suppression of *ngfi*-a and c-*fos* in the Striatum Produces Asymmetric Motor Activation and Increased IEG Expression in the Globus Pallidus Following Stimulant Challenge[*]

4.1. Introduction

Despite intensive study, the precise function of immediate early genes (IEGs) in the CNS has yet to be determined. Because transcription of IEGs can be induced by a wide variety of stimuli which result in rapid, but transient upregulation of the protein product, it is thought that they may play a role in signal transduction (Morgan and Curran, 1989). By acting as transcription factors, it is possible that these proteins alter expression of late-effector genes, initiating long-term changes in the cell (Robertson, 1992). It has also been previously suggested that the expression of some IEGs may exert regulatory influences on that of others (Chiu et al.,1989; Graybiel, 1990). C-fos and ngfi-a (also called egr-1 (Sukhatme et al.,1988), krox-24 (Lemaire et al.,1988), and zif268 (Cole et al.,1992)) have nonconstitutive and constitutive expression in the neostriatum, respectively (Graybiel et al.,1990; Moratalla et al.,1992) and are frequently used as representatives of IEG proteins. Both are transiently upregulated in the neostriatum by various stimuli, including the indirect dopamine agonist, d-amphetamine (Graybiel et al.,1990; Moratalla et al.,1992). Previous studies have implicated D1, but not D2, dopamine receptor activation as mediating d-amphetamine-induced c-Fos expression, suggesting that the increase in cyclic adenosine monophosphate (cAMP) produced by D1 receptor activation may be involved in mediating c-fos transcription (Cole et al.,1992; Graybiel et al.,1990; Paul et al.,1992; Robertson et al.,1989). This is a plausible theory owing to the presence of at least one cAMP-responsive element (CRE) on the c-fos promotor sequence (Sheng et al.,1988,1990; Berkowitz et al.,1989). Furthermore, selective activation of D2

receptors in the neostriatum not only failed to induce c-Fos expression in this region (which is consistent with the cAMP theory as D2 receptor activation results in an inhibition of cAMP production) but also resulted in an increase in c-Fos expression in cells of the ipsilateral globus pallidus (Paul *et al.*,1992). More recently, evidence has been found to suggest that the CRE binding protein (CREB) may be involved in c-*fos* induction, further implicating the CRE as a trigger site for its transcription (Konradi *et al.*,1994).

It has been previously demonstrated that selective inhibition of *d*-amphetamine-induced c-Fos expression in the rat neostriatum could be achieved through intrastriatal infusion of phosphorothioated antisense oligodeoxynucleotides (ODNs) directed at a region of the c-*fos* mRNA (Chiasson *et al.*,1992; Hooper *et al.*,1994). Unilateral knockdown of c-Fos with these ODNs was associated with a strong ipsiversive rotational behavior (directed towards the antisense-treated side), the mechanism of which remains unclear (Sommer *et al.*,1993; Hooper *et al.*,1994).

We investigated the possibility that the simultaneous induction of c-*fos* and *ngfi-*a by stimulants such as *d*-amphetamine, may be the result of regulatory influences between these two IEGs. To examine this hypothesis, we employed end-capped phosphorothioated antisense ODNs to c-*fos* and *ngfi-*a mRNA to determine if inhibition of *d*-amphetamine-induced expression of either protein altered the induction of the other. End-capped (or chimeric) ODNs were used instead of fully phosphorothioated molecules solely to minimize their sulfur content and possible toxic effects (Chiasson *et al.*,1996). Our results indicate that, while inhibition of striatal c-Fos expression

appears to have no effect on that of NGFI-A, ODNs that specifically target *ngfi*-a

mRNA significantly reduce the expression of both proteins. Furthermore, extensive

inhibition of these striatal IEGs was associated with robust ipsiversive rotation and

marked IEG upregulation in the ipsilateral globus pallidus.

4.2. Materials and Methods

4.2.1. Experimental Design

Refer to section 3.2.1. for details of the animal surgery. Animals infused with oligonucleotides were given recovery periods of either one or two hours and were subsequently injected with d-amphetamine (5 mg/kg, i.p.) and placed in a rotometer, where the number and direction of their rotations were recorded for the next two hours. After the rotation period, animals were deeply anesthetized with sodium pentobarbital (> 100 mg/kg, i.p.) and sacrificed.

4.2.2. Immunohistochemistry

Animals were transcardially perfused with saline followed by 4% paraformaldehyde in a 0.1 M phosphate buffer solution (pH 7.4). Brains were then removed and post-fixed at 4°C until further analysis. Brains were blocked and cut coronally on a vibratome in 50 μm sections which were collected from a point rostral to the injection site, caudally to the globus pallidus and processed for c-Fos or NGFI-A immunohistochemistry and Nissl staining, as described in section 3.2.2.. Suppression of striatal IEGs was generally evident throughout >80% of coronal sections taken in proximity to the site of antisense ODN infusion, effectively producing an all-or-none pattern of expression between striata (i.e. control and treated). Likewise, pallidal IEG expression was compared between control GP, which expressed minimal immunoreactivity, and the GP ipsilateral to the antisense ODN infusion, which displayed abundant IEG immunoreactivity.

4.2.3. Electrophoresis and Western Blotting

Striata were bilaterally dissected following decapitation and brain excision. Right (treated) and left (control) striata were separately homogenized in a Potter-Elvehjem glass-teflon homogenizer

(~500 rpm; 5-6 strokes) in 1 ml of 0.32 M sucrose/ 3 mM $MgCl_2$ / 1 mM HEPES

solution (pH 6.8). Aliquots of homogenates equal to approximately 30 µg of protein,

as determined by Lowry protein assay, were diluted in sample buffer (10% glycerol,

5% 2-mercaptoethanol, 3% SDS, 12.5% Tris, in distilled water) and heat denatured for

2 minutes. Samples were then run on a SDS-PAGE with 4% stacking and 10%

separating gels. Gels were removed and protein transferred overnight onto

nitrocellulose membranes in an electrophoretic transfer system. After drying, blots

were incubated in a blocking solution (25g skim milk, 5g BSA, 0.165ml antifoam,

.0005g thimerosal mixed in a 1% phosphate buffer solution to 500ml) for 1 hour at

37°C and subsequently incubated overnight at 4°C in the same blocking solution

containing a primary antibody to Fos (Genosys; 1:2000 dilution). Membranes were

rinsed, then incubated in peroxidase-labeled secondary antibody followed by enhanced

chemiluminesence (ECL, Amersham) to visualize antigen.

4.2.4. Oligodeoxynucleotides

This study employed the ASF, ASN and

RAN oligodeoxynucleotides that were described in section 3.2.3.. Previous time

course analyses revealed that ASF demonstrated maximal efficacy at one hour post-

infusion, whereas ASN was optimal at two hours post-infusion, as determined by

rotational behavior and suppression of gene expression (see chapter 3). Therefore, to

elicit optimal gene suppression in the present studies, intra-striatal infusions of

antisense ODNs were followed by the appropriate recovery periods so as to elicit their

maximal effects (i.e. ASF-treated animals had a 1 hr recovery period, ASN-treated

animals had a 2 hr recovery period). As the relative specificity of the ASF sequence

has previously been demonstrated (Chiasson *et al.*,1992; Dragunow *et al.*,1993; Heilig *et al.*,1993; Sommer *et al.*,1993,1996; Hooper *et al.*,1994), the control animals receiving infusions of RAN were given the same recovery periods as those animals receiving the novel ASN. All oligodeoxynucleotides used in this study were subjected to a BLASTN search on the National Center for Biotechnology Information BLAST server using the Genbank database (Altschul *et al.*,1990). Antisense oligodeoxynucleotide sequences had positive matches only for their targeted mRNA sequences. The random oligodeoxynucleotide produced no positive matches.

4.2.5. Animal Groups   Animals were divided into three groups: (1) ASF-treated (n=12), (2) ASN-treated (n=16) and (3) Control animals. Group (3) consisted of three control subgroups: a) Naive, unstimulated animals (n=2) - used to determine basal levels of protein expression, b) *d*-amphetamine-only (surgery-free) animals (n=8) - used to determine the pattern of IEG induction in the striatum and globus pallidus and also to assess any innate rotational response to the stimulant and c) RAN-treated animals (n=9) - used to assess non-specific effects of oligodeoxynucleotides on IEG suppression and rotational behavior. All ODN solutions were infused into the right striatum, while the left striatum received vehicle infusion and was used as an internal control for each animal.

4.2.6. Statistical Analysis Comparisons between the number of ipsilateral and contralateral rotations within a particular treatment group was assessed using a paired t-test. Significance was assumed when p < 0.05.

4.3. Results

4.3.1. Rotational Analysis

Animals that received ASF demonstrated significant ipsiversive rotation with a group mean of 285 ± 55 : 31 ± 12 rotations/2 hours (ipsiversive : contraversive; group mean ± SEM; p=0.00074). Similarly, ASN-treated animals rotated 394 ± 80 : 69 ± 23 rotations/2 hours (ipsiversive : contraversive; p=0.004). Control animals receiving unilateral infusions of RAN showed no significant rotational bias when challenged with d-amphetamine at 2 hours post-surgery, nor did surgery-free animals receiving d-amphetamine only (Fig.4.1). Naive animals that did not receive d-amphetamine were not tested for rotational behavior.

4.3.2. Basal and d-amphetamine-Induced IEG Expression

Consistent with previous reports, we found that there was negligible c-Fos expression in the neostriatum of naive animals (Fig.4.2A), whereas administration of d-amphetamine produced a pattern of expression localized to distinct neuronal clusters (Fig.4.2B), presumeably striosomes (Graybiel et al.,1990). NGFI-A was found to have a constitutive homogeneous expression in the neostriatum (Fig.4.2C), a finding supported by previous reports of its mRNA distribution (Moratalla et al.,1992). After administration of d-amphetamine, however, there was strong enhancement of immunostaining in patchy clusters, which appeared similar to that seen with c-Fos expression (Fig.4.2D). Thus, ngfi-a and c-fos are dissimilar in their basal expression in the neostriatum but are both induced in striosomal-like clusters by d-amphetamine.

4.3.3. Effects of ASF on IEG Expression

All animals in the ASF group that were analyzed for Fos-like immunoreactivity (Fos-LI; n=5) showed a marked reduction in c-

Fos expression in the antisense-treated striata (Fig.4.3A,B). These immunohistochemical results were supported by a reduction in band thickness and intensity observed with Western blot analysis (Fig.4.6). ECL visualization confirmed labeling of a predominant band at approximately 65 kDa, indicating that the antibody labeled the authentic c-Fos protein. Interestingly, there was a significant upregulation in Fos-LI in the ipsilateral globus pallidus of these animals when compared to the scant staining seen in that of the control side (Fig.4.3C,D). None of the animals treated with ASF demonstrated any notable differences in striatal or pallidal NGFI-A expression.

4.3.4. Effects of ASN on IEG Expression

Because of the relatively high constitutive background of NGFI-A in the striatum, the effects of oligodeoxynucleotides on NGFI-A expression were invariably more subtle than those seen with c-Fos. Evaluation of the ability of ASN to suppress d-amphetamine-induced NGFI-A expression in the antisense-treated striatum was measured in terms of the reduction of striosomal-like expression of the protein. All animals infused with ASN demonstrated significant suppression of d-amphetamine-induced NGFI-A expression in the antisense-treated striatum (Fig.4.4A-D). Also, in 5/10 animals analyzed for NGFI-A immunoreactivity, the reduction in striatal expression was accompanied by a marked increase in that seen in the ipsilateral globus pallidus (Fig.4.4F). There was no increase in NGFI-A expression in the globus pallidus of the control side (Fig.4.4E).

When ASN-treated animals were analyzed for c-Fos, every animal (n=10 total) demonstrated a striking reduction in Fos-LI in the ASN-treated striatum (Fig.4.5A-D) that was accompanied by a marked increase in that of the ipsilateral globus pallidus

(Fig.4.5E,F). The reduction of c-Fos expression in the striatum was supported by Western blot analysis (Fig.4.6)

4.3.5. Effects of RAN on IEG Expression All animals that received intrastriatal infusions of RAN (n=9) revealed negligible immunohistochemical differences in c-Fos or NGFI-A expression between control and treated striata or their respective pallidal nuclei (see Fig.3.4 and 5.5). Western blot analysis also revealed no change in c-Fos expression between control and RAN-treated striata (Fig.4.6)

4.4. Discussion

Nuclear localization and the presence of AP-1-binding (Chiu *et al.*,1988; Rauscher *et al.*,1988) and zinc finger (Milbrandt *et al.*,1987; Christy *et al.*,1988; Swirnoff *et al.*,1995) motifs on c-Fos and NGFI-A, respectively, suggest that these IEG products function as transcription factors and influence the expression of late-effector genes. In the rat, c-Fos has negligible expression in the unstimulated striatum whereas NGFI-A is constitutively expressed. Although the distinction in basal expression of these two proteins suggests that NGFI-A is more likely to possess "housekeeping" functions than c-Fos, both of these IEGs can be induced (or upregulated) in the striatum by various stimuli, including trauma, excitotoxins (i.e. quinolinic acid) and stimulants such as cocaine and *d*-amphetamine (Graybiel *et al.*,1990; Aronin *et al.*,1991; Massieu *et al.*,1992; Honkaniemi *et al.*,1994,1995). In fact, *d*-amphetamine, which is thought to mediate its effects through D1 receptor activation induces similar patterns of expression of striatal c-Fos and NGFI-A, eliciting their transient upregulation in striosomes, as previously reported in mRNA studies and further supported here (Graybiel *et al.*,1990; Moratalla *et al.*,1992). Immunohistochemically, c-Fos induction is readily visualized in these distinct neuronal clusters whereas that of NGFI-A is more discrete owing to its background of constitutive staining. The similarity in the distribution of inducible expression suggests that while these two IEGs may differ in their functionality in quiescent neurons, they may have analogous or cooperative roles in neuronal responses to stimuli.

Immunohistochemistry revealed extensive suppression of striatal c-Fos following administration of ASF. Western blot analysis confirmed that the Fos-LI demonstrated with immunohistochemistry was that of the full 65 kDa c-Fos protein. A reduction in banding intensity also appeared evident in the samples from the ASF- (and ASN-) treated striata, supporting the immunohistochemical results. Further examination found no alterations in the d-amphetamine-stimulated induction of NGFI-A in response to this ODN. These results indicated that it is possible to suppress c-Fos expression without affecting that of NGFI-A, suggesting that if the c-*fos* transcript or protein wields any regulatory control over NGFI-A, this influence must be quite subtle and was not observed in this study.

Antisense ODNs targeted to *ngfi*-a transcripts also demonstrated impressive suppression capabilities. Immunostaining revealed that the extensive pattern of striosomal-like NGFI-A expression that is induced by d-amphetamine had virtually disappeared in the ASN-treated striata, leaving only the uniform background that is evident in naive animals. Unlike the specific suppression produced by ASF, however, further analyses revealed marked reduction of c-Fos in addition to NGFI-A following ASN administration. Table 4.1 summarizes the effects of ODN infusion on IEG expression. Because the reduction of c-Fos expression by ASN was so dramatic, the specificity of this ODN was initially met with skepticism. To control for non-specific effects of ASN (and ASF), a random ODN (RAN) was designed using the same base content as ASN, with the nucleotide bases ordered in a random sequence. We reasoned that if the effects of ASN on c-Fos were due to non-specific interactions, then RAN

should also produce similar effects; this was not the case. RAN had little effect on either c-Fos or NGFI-A expression in the striatum or the globus pallidus, nor did it produce the robust ipsiversive rotation seen with ASF or ASN. However, RAN did produce an insignificant tendency for the animals to rotate ipsilaterally, indicative of non-specific, ODN effects. To further validate our findings, we designed a second antisense ODN to *ngfi*-a (18-mer) whose target sequence was shifted seven bases upstream from that of ASN. Preliminary studies showed that this second ODN was also capable of suppressing both c-Fos and NGFI-A expression and eliciting ipsiversive rotation in the animals. Full characterization of this second anti-NGFI-A ODN was not performed, however.

Another possible explanation for the dual IEG suppression caused by ASN is cross-reactivity of this ODN with c-*fos* mRNA, as both ASN and ASF contained an identical stretch of six nucleotides (CATGGT) which may have permitted direct binding of ASN to c-*fos* mRNA, causing a reduction in its expression. However, if this particular stretch of nucleotides could confer effective antisense activity, one would also expect to see suppression of NGFI-A expression by ASF, but this was not the case. These control conditions indicated that it is unlikely that the effects of ASN were due to non-specific interactions and suggested that *ngfi*-a expression may be necessary for the induction of c-*fos*, at least in striosomal neurons. One argument against this theory is the lack of expression latency between these two proteins, which would support the independent induction hypothesis. However, given the high constitutive background of NGFI-A, it is conceivable that a stimulant-induced cellular response

may cause immediate effects which alter or utilize existing transcripts or protein to influence expression of other IEGs. In this situation, there may be no apparent difference between the induction rate of the initial IEG and that of its dependents. It is difficult to envision a similar process for IEGs that are not constitutively expressed (i.e. c-*fos*) in that there would be an initial latency period necessary, following stimulation, to permit induction of the regulatory gene.

Our findings contrast those of others (Dragunow *et al.*,1994) who report that intrastriatal application of phosphorothioated antisense ODNs to c-*fos* suppressed not only c-Fos, but also JunB and NGFI-A expression. It is possible that the greater sulfur content in their fully phosphorothioated ODNs conferred non-specific gene suppression and reduction of non-targeted protein expression. Furthermore, the number of control and experimental animals examined here suggest that our results are quite reproducible and provide a clear profile of the effects of the particular ODNs used in this study.

Previous reports have associated unilateral suppression of c-Fos with a *d*-amphetamine-induced rotational bias towards the side of the IEG knockdown (Sommer *et al.*,1993; Hooper *et al.*,1994). Our results further support these findings in that administration of antisense ODNs targeted to c-*fos* or *ngfi*-a mRNA elicited robust ipsiversive rotation in these animals. While the etiology of this locomotor bias remains unclear, it is possible that the inhibition of striatal IEGs somehow alters the inhibitory (GABAergic) output of the striatum, thus affecting the regulatory influence of the basal ganglia on motor function. In fact, further examination of ASF- and ASN-treated animals revealed a third common feature. In addition to the inhibition of stimulant-

induced NGFI-A and/or c-Fos expression and robust ipsiversive rotational behavior, the majority of these animals demonstrated marked enhancement of IEG immunoreactivity in the ipsilateral globus pallidus (Table 4.1).

Striatal projection neurons influence cortical motor output via direct (excitatory) and indirect (inhibitory) pathways (reviewed in DeLong, 1990). Neurons of the direct pathway project to the the internal segment of the globus pallidus (GPi) or the substantia nigra pars reticulata (SNR) and are negatively coupled to the neurons of these nuclei (Fig.4.7). Indirect striatal neurons inhibit those of the external segment of the globus pallidus (GPe) which further inhibit glutamatergic neurons of the subthalamic nuclei (STN) which are positively coupled to those of the GPi/SNR. These reciprocal innervations to the GPi/SNR, which represent the final output nuclei of the basal ganglia, permit fine modulation of cortical activity via the thalamic nuclei (Fig.4.7).

In the striatum, d-amphetamine mediates its stimulant effects through dopamine D1 receptor (D1R) activation, primarily in striosomal neurons projecting to the SNC and in matrical neurons projecting to the GPi and SNR. The majority of D1R-containing neurons comprise this direct pathway of the basal ganglia, with a smaller population of D1R-containing neurons projecting to the GPe, contributing to the initial segment of the indirect pathway (DeLong, 1990; Graybiel, 1990; Graybiel et al.,1990). Given the consistent pattern of IEG immunoreactivity in the basal ganglia of animals receiving ASF or ASN (i.e. striatal suppression / pallidal enhancement), it appears that suppression of striatal IEGs (c-Fos, NGFI-A) somehow inhibits the activity of

projection neurons to the GPe. This may occur through a disruption of the D1R-signaling cascade in the relatively few D1-activated striatopallidal neurons. Alternatively, the suppression of striatonigral activity to the dopaminergic neurons of the substantia nigra pars compacta (SNC) would increase the release of DA in the striatum. This elevation of DA would enhance the D2R-mediated suppression of striatopallidal neurons, and act synergistically with the antisense-mediated IEG suppression in these neurons. Regardless of the mechanism, the increased pallidal activity could effectively decrease the influence of the indirect pathway by reducing GPi/SNR excitation via subthalamic neurons, resulting in less opposition to the inhibitory striatopallidal/striatonigral neurons of the direct pathway (Fig.4.7). The final outcome of these alterations would be enhanced thalamic activation of cortical motor activity directed to the contralateral side of the animal, resulting in a rotational bias towards the IEG-depleted striatum. [While this is a plausible hypothesis, subsequent work has demonstrated that there is reduced, not enhanced, thalamic drive in ASF-treated animals and that the GP plays an important modulatory role in the motor asymmetry produced in these animals (see chapters 5 and 7)].

These theories imply that IEGs may actively function in signal transduction mechanisms in roles that are essential for normal cellular responses. While this notion is consistent with vast amounts of evidence linking IEGs to stimulus-response coupling in many neural systems (see chapter 2), our results are inconclusive as to whether this rotational behavior is mediated solely by c-Fos or through a general imbalance of striatal IEGs.

Figure 4.1 Rotational analyses for control and antisense-treated animals. Stars represent significant differences between ipsiversive and contraversive rotations ($p < 0.05$).
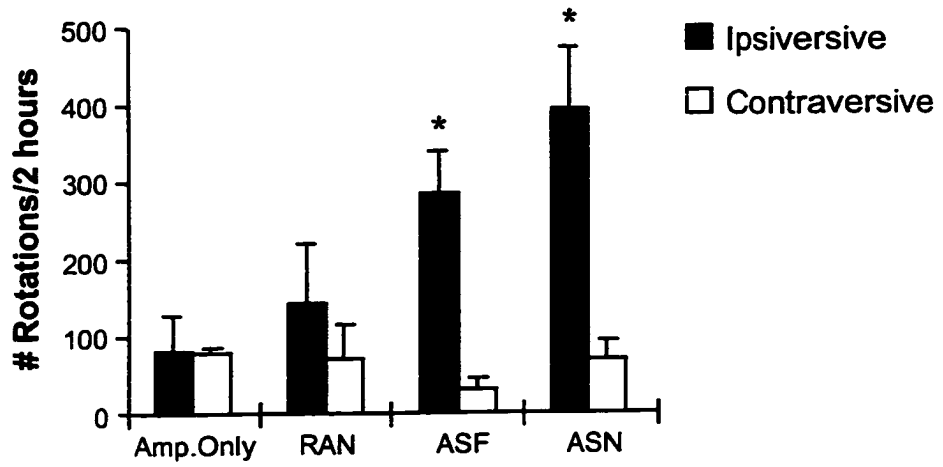
FIGURE 4.1

Figure 4.2   Striatal c-Fos (A,B) and NGFI-A (C,D) expression in a naive (A,C) and

amphetamine-treated (B,D) rat.   Arrows indicate striosomal-like clusters of D-

amphetamine-induced c-Fos (B) and NGFI-A (D). Scale bar = 100 μm.
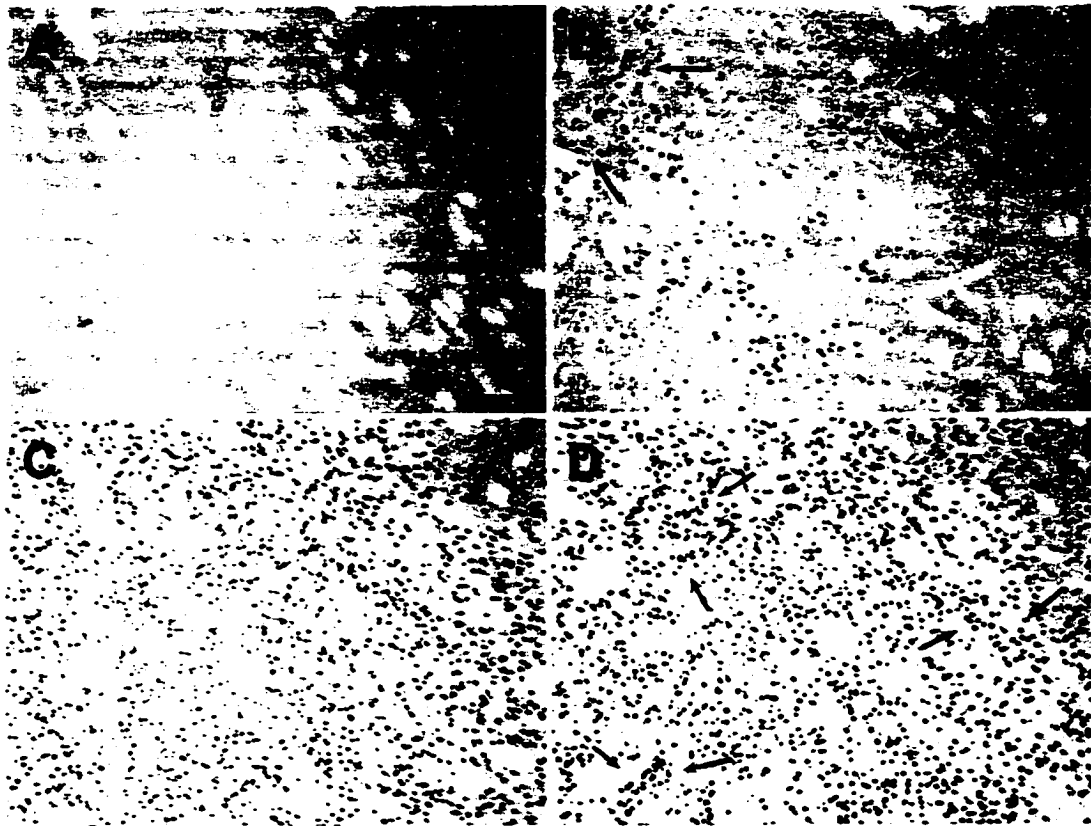
FIGURE 4.2

Figure 4.3 Effects of ASF on c-Fos expression: the clusters of d-amphetamine-induced c-Fos seen in the control striatum (A) were virtually abolished in the ASF-treated striatum (B). The control GP of the same animal (C) shows minimal expression whereas marked upregulation of c-Fos is seen in the GP of the antisense-treated side (D). Scale bar represents 100 μm.
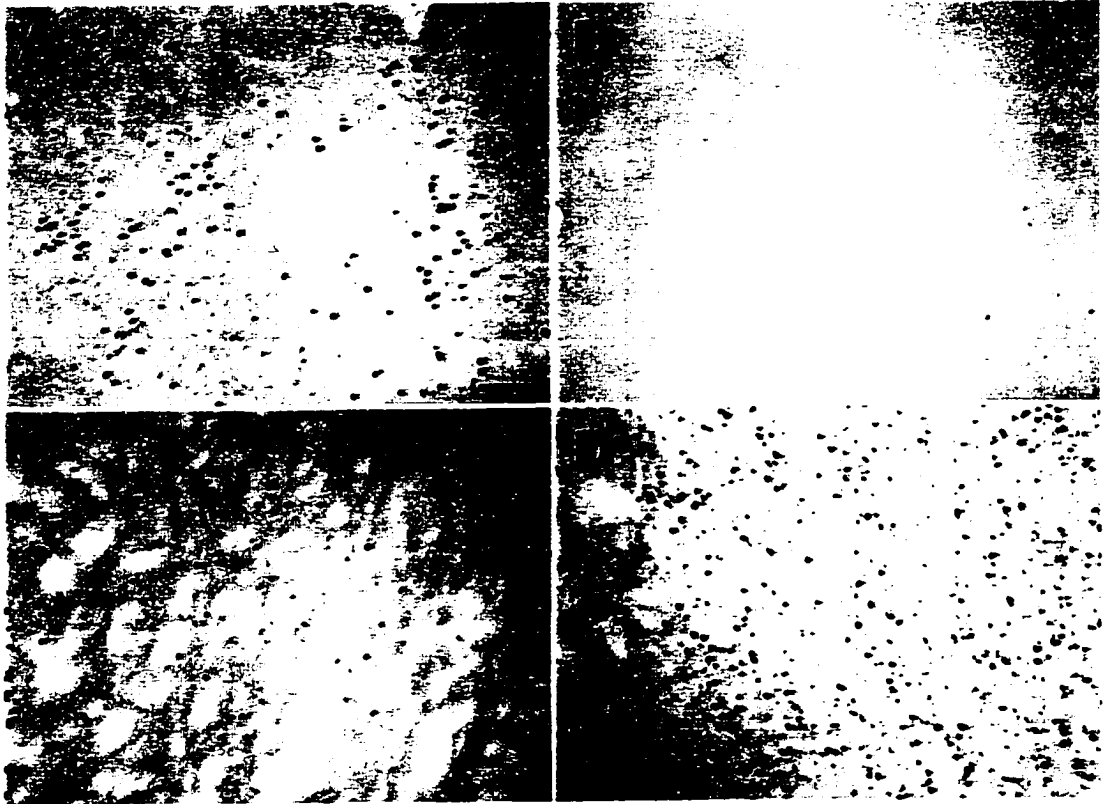
FIGURE 4.3

Figure 4.4 Effects of ASN on NGFI-A expression. At both low (A,B) and high (C,D) magnification it is evident that the clusters of d-amphetamine-induced NGFI-A seen in the control striata (A,C) are virtually abolished in the ASN-treated striata (B,D), leaving only background expression. Large arrowheads in (A) and (B) indicate the border between the striatum and the overlying corpus callosum. Small arrows indicate individual striosomal clusters. The control GP of the same animal (E) shows almost no expression whereas marked upregulation of NGFI-A is seen in the GP of the antisense-treated side (F). Arrowheads in (F) indicate the border of the overlying striatum. Scale bar in (A) indicates magnification for (A) and (B) and represents 1mm. Scale bar in (C) indicates magnification for (C)-(F) and represents 100 µm.
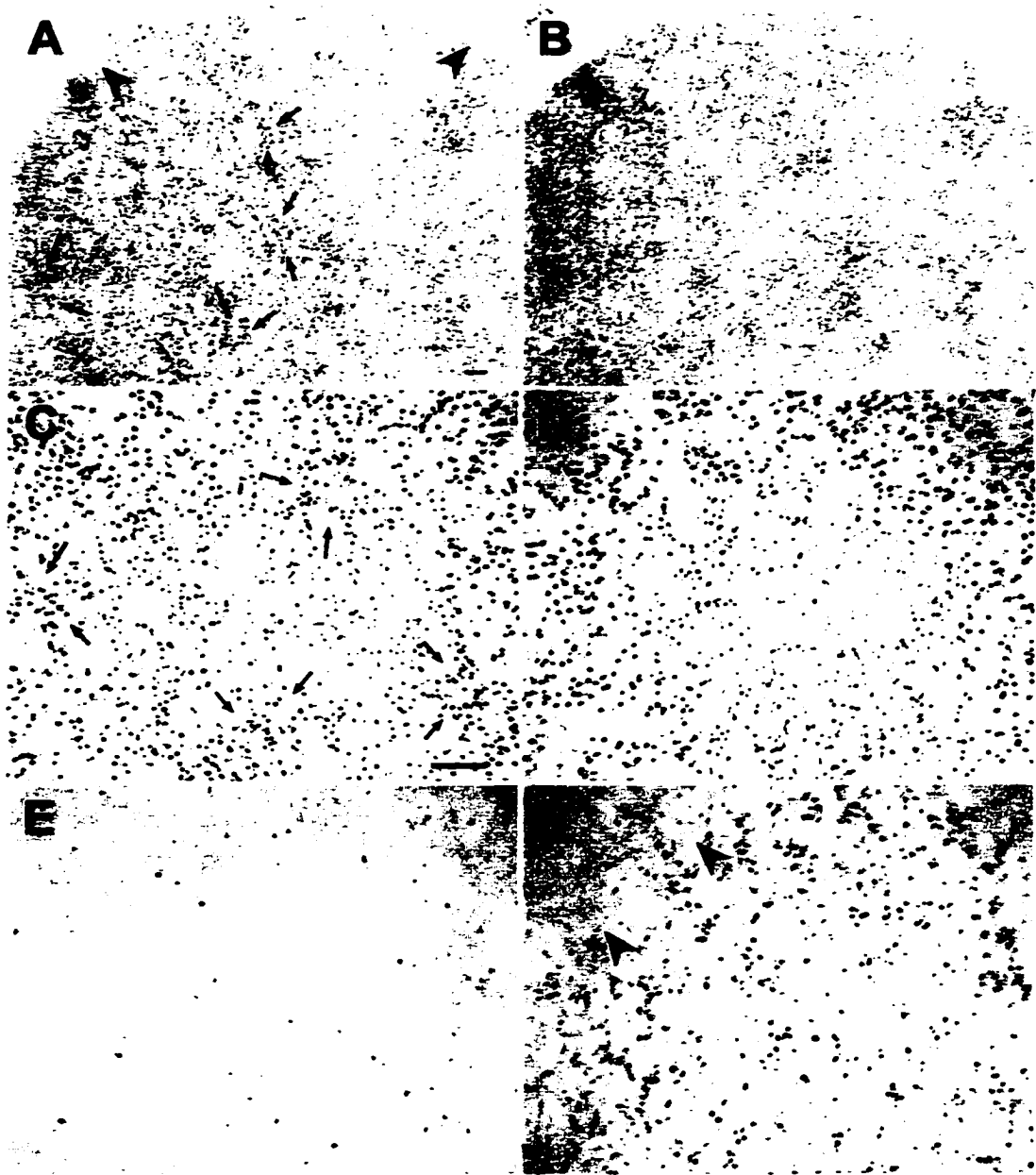
FIGURE 4.4

Figure 4.5 Effects of ASN on striatal c-Fos expression. Like ASF-treated striata, the clusters of d-amphetamine-induced c-Fos seen in the control striata (A,C) at both low (A,B) and high (C,D) magnification are markedly suppressed in the ASN-treated striata (B,D). Large arrowheads in (A) and (B) indicate the border between the striatum and the overlying corpus callosum. Small arrows point to individual striosomal clusters of c-Fos. The control GP of the same animal (E) shows little Fos-LI whereas extensive c-Fos expression is seen in the GP of the antisense-treated side (F). Arrowheads in (E) and (F) point to the border of the overlying striatum. Scale bar in (A) indicates magnification for (A) and (B) and represents 1mm. Scale bar in (C) indicates magnification for (C)-(F) and represents 100 μm.
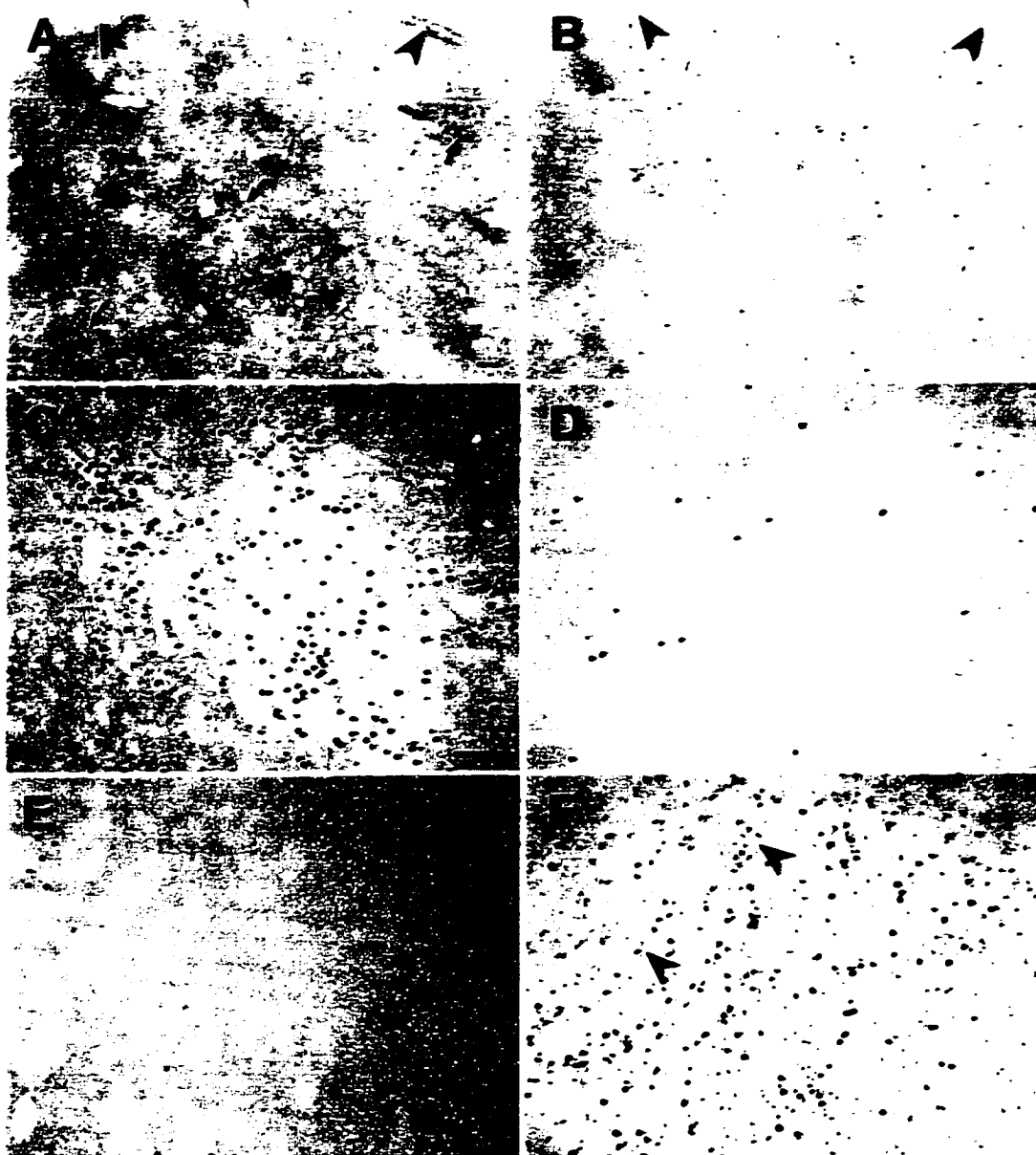
FIGURE 4.5

Figure 4.6 Western blot analysis of striatal c-Fos expression in animals that received unilateral infusions of RAN, ASF or ASN. Molecular weight markers on the left indicate 97, 50 and 35 kDa (from top to bottom). ECL revealed labeling of a prominent band at approximately 65 kDa (arrowhead). Consistent with immunohisotochemical results, there appeared to be a reduction of c-Fos in the treated striatum of ASF- and ASN-treated, but not RAN-treated, animals. C, control; T, treated.

RAN   ASF   ASN
C   T   C   T   C   T
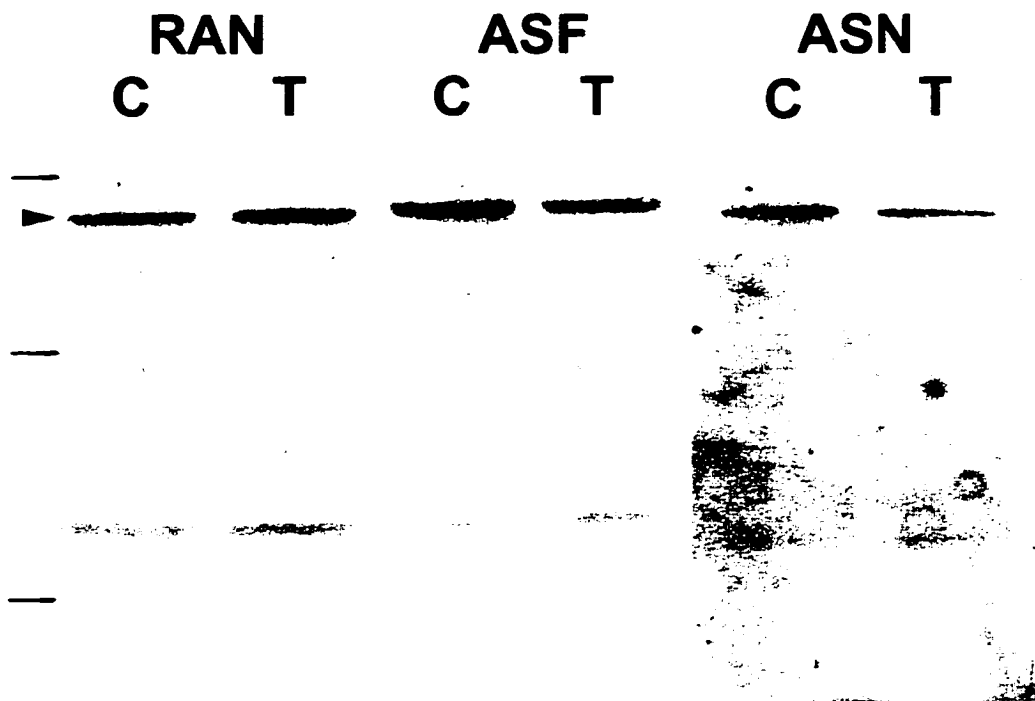
FIGURE 4.6

Figure 4.7 Basic circuitries of the basal ganglia showing direct and indirect pathways influencing motor function. Initial hypothesis of the etiology of antisense-induced locomotor effects: Suppression of striatal IEGs occurs in neurons projecting to the GPe (labeled A) causing a disinhibition and increased activity in GPe neurons projecting to STN (labeled B). This further results in a reduction of GPi/SNR activity directed towards the thalamus, producing less opposition to the excitatory (direct) pathway and enhancing thalamocortical activity to contralateral motor function causing ipsiversive rotation. While this theory was plausible when the experimental work was performed, further investigations revealed that the GP inhibited locomotor asymmetry (see chapter 5) and that the thalamus and other projection nuclei of the GPi/SNR were actually hypoactive under these conditions (see chapter 7). Arrow thickness corresponds to activity levels of neuronal circuits. GPe- globus pallidus (external segment); EPN- entopeduncular nucleus; MC- motor cortex; PMC- premotor cortex; SMA- supplementary motor area; SNR- substantia nigra pars reticulata; STN- subthalamic nucleus; STR- striatum; Th- thalamic nuclei. (Figure modified after DeLong,1990)
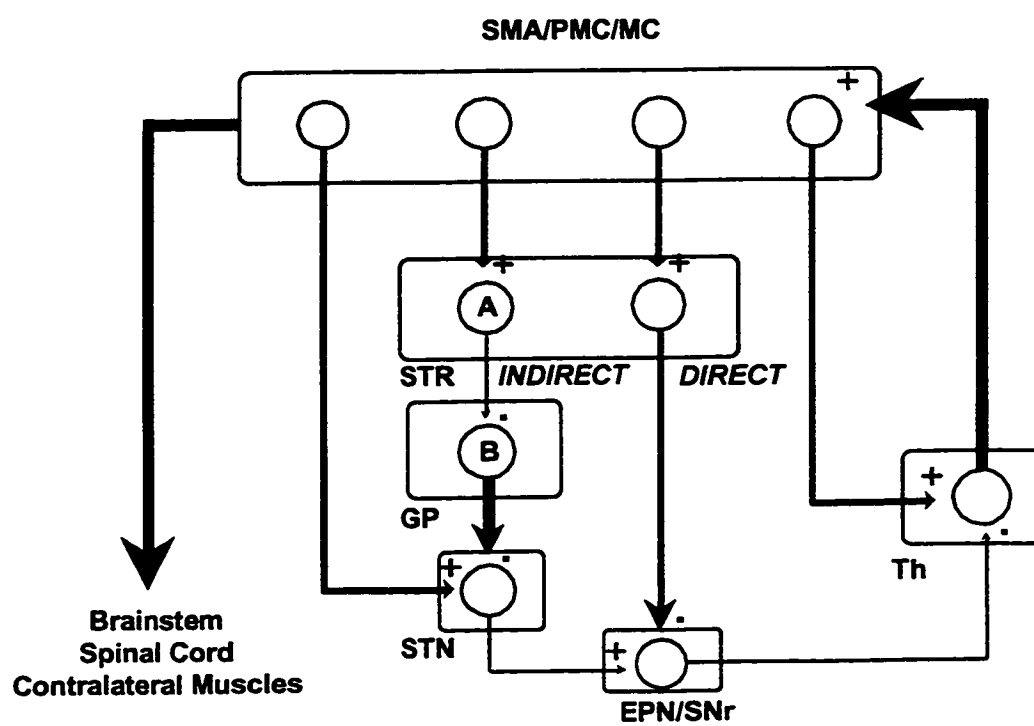
FIGURE 4.7

ODN Infused	Striatal Fos	Striatal NGFI-A	GP Fos	GP NGFI-A
ASF	decrease (5/5)	n/e (5/5)	increase (5/5)	n/e (5/5)
ASN	decrease (10/10)	decrease (10/10)	increase (10/10)	increase (5/10)
RAN	n/e (9/9)	n/e (9/9)	n/e (9/9)	n/e (9/9)

Table 4.1 Effects of ODN infusion on IEG expression in the striatum and the GP. The values in brackets show the number of individuals in a group that exhibited the indicated changes.

CHAPTER 5

Synergy Between the Postural and Locomotor Influences of the Striatum and Globus Pallidus[*]

[*] The results presented in this chapter are currently *in press* in *Neuroscience*.

5

5.1. Introduction

d-Amphetamine and cocaine are stimulant drugs which produce both acute psychomotor activation and long-term behavioral effects such as addiction and psychosis (Koob and Bloom, 1988). Systemic administration of these drugs produces robust and transient expression of immediate early genes (IEGs) such as c-fos and ngfi-a in cortical and subcortical regions (Graybiel et al.,1990; Robertson et al.,1991; Johansson et al.,1994; Wang et al.,1995; Curran et al.,1996; Lin et al.,1996). Although the association between IEG expression and elevation of neuronal activity has become widely accepted, the role these genes play in altering cellular physiology remains unclear (Sagar et al.,1988). The striatum, the primary input nucleus of the basal ganglia, is particularly responsive to indirect dopaminergic stimulation by d-amphetamine, as it is normally innervated by dopamine-containing afferents projecting from the substantia nigra pars compacta (SNC) (Graybiel,1990). Administration of this drug induces robust expression of c-fos, primarily in striosomal neurons which project to the SNC (Graybiel, 1990; Robertson et al.,1992).

Antisense oligodeoxynucleotides (ODNs) have been used to suppress stimulant-induced expression of striatal IEGs (Chiasson et al,1992,1994; Dragunow et al.,1993,1994; Sommer et al.,1993,1996; Hooper et al,1994; chapter 3 and 4). We have previously reported that end-capped, phosphorothioate ODNs targeted to c-fos or ngfi-a mRNA effectively and specifically suppress the d-amphetamine-induced expression of the respective protein products (c-Fos and NGFI-A) when administered intrastriatally to adult rats (chapters 3 and 4). Unilateral suppression of striatal c-fos

expression produces robust turning behavior, with the animals rotating towards the side of reduced IEG expression. This suggests that unilateral suppression of striatal c-*fos* expression leads to a motor asymmetry following *d*-amphetamine administration. Indeed, c-*fos* expression appears to play a role in striatal function in the absence of *d*-amphetamine challenge. Infusions of antisense oligonucleotides to c-*fos* into the striatum resulted in a rapid decrease in the levels of γ-aminobutyric acid (GABA) released in the substantia nigra (Sommer *et al.*,1996). The striatal IEG suppression and ipsiversive rotation observed in animals infused with ODNs targeted to c-*fos* or *ngfi*-a, was also associated with marked upregulation of IEGs in the ipsilateral globus pallidus (GP) (chapter 4). This novel IEG expression in the GP was only observed in animals with extensive striatal inhibition of IEG expression that had exhibited robust circling activity. While it is likely that the enhanced pallidal IEG expression resulted from suppression of inhibitory striatopallidal efferents, it is also conceivable that other stimulatory circuits contributed to this stimulation. It remained unclear what influence the neurons in the GP had on the rotational behavior observed in these animals. In the present study, we have investigated the role of the GP in producing the motor and postural asymmetry in animals with disruption of basal ganglia neurotransmission. We describe the effects of simultaneous infusions of antisense ODNs into the striatum and the GP and compare these results with those induced by excitotoxic lesioning of the GP.

5.2. Materials and Methods

5.2.1. Oligodeoxynucleotide Infusions   Male Sprague-Dawley rats (250-350g) were anesthetized with halothane until a surgical plane was reached and subsequently mounted on a Kopf stereotaxic apparatus in a flat skull position. Animals were supplemented with halothane (Fluothane) during the course of the surgery. Once the animal was mounted in the apparatus, the scalp was retracted and the skull exposed. Burr holes were drilled in the skull and a 25-gauge cannula was guided bilaterally into each striatum (from bregma: AP, +1.0 mm; DV, +6.0 mm; LAT, ± 3.0 mm), the striatum and the GP or the GP alone (from bregma: AP, -1.0 mm; DV, +2.8 mm; LAT, -6.5 mm). After the appropriate solutions were infused, the cannulae were left in place for an additional two minutes to allow for diffusion away from the injection site. Following removal of the cannulae, the wounds were sutured and the animals placed in their home cage for recovery periods of 1 hour, as this has been previously shown to be the period of maximal efficacy for the antisense ODN used (see chapter 3).

Animals receiving GP lesions had 2µl (50 nmoles) of a 25mM solution of ibotenic acid infused at the GP coordinates described above. The wounds were then sutured and the animals left to recover for 2-3 weeks, with free access to food and water. Some animals subsequently received infusions of antisense ODNs to c-*fos* into the ipsilateral striatum, as described above.

Following ODN infusion and recovery, animals were injected with *d*-amphetamine (5 mg/kg, i.p., a gift from SmithKline Beecham Pharma Inc.) and placed in a rotometer, where the number and direction of their rotations were recorded for the

next two hours. After the rotation period, animals were deeply anesthetized with sodium pentobarbital (>100 mg/kg, i.p.) and sacrificed. Cannulae and lesion placements were verified using Nissl stained sections. Only animals with lesions confined primarily to the GP were incorporated into the studies.

5.2.2. Immunohistochemistry   Animals were transcardially perfused, initially with saline, followed by 4% paraformaldehyde in a 0.1 M phosphate buffer solution (pH 7.4). Brains were subsequently removed and post-fixed at 4°C until further analysis. Brains were blocked and cut on a vibratome in 50 μm coronal sections and were processed for c-Fos immunoreactivity as described in section 3.2.2..

5.2.3. Oligodeoxynucleotides   Solutions of ODNs (right striatum / right GP) or vehicle (left striatum) were infused at a rate of 0.25 μl/min using a CMA 100 (Carnegie-Medicin) microinjection pump until a total volume of 2.0 μl (2.0 nmol) was reached. ODNs were used as described in section 3.2.3..

ODNs were reconstituted in ultrafiltered (millipore) distilled water at a concentration of 1 nmol/μl. The antisense ODN to c-*fos*, termed ASF, was a 15-base oligomer that had been previously used in its partially and complete phosphorothioate form (Chiasson *et al.*,1992,1994; Dragunow *et al.*,1993; Sommer *et al.*,1993,1996; Hooper *et al.*,1994; chapters 3 and 4). Its sequence, 5'-G$_s$AA-CAT-CAT-GGT-CG$_s$T-3', corresponded to bases 129-143 on the mRNA transcript (GenBank accession no. XO6769) and spanned the initiation codon (the subscript 's' denotes locations of the sulfur modifications). In these earlier studies we used a randomly-sequenced ODN, which we termed RAN, to control for non-specific ODN effects in the striatum. To

provide further confidence that the behavioral and immunohistochemical effects observed with ASF were specific and sequence-dependent, we have presently used a second random ODN, which we termed RANB. The sequence of RANB was 5'-C₅CC-TTA-TTT-ACT-ACT-TTC-G₅C-3'. ODNs used in this study were subjected to a BLASTN search on the National Center for Biotechnology Information BLAST server using the Genbank database (Altschul *et al.*,1990).

5.2.4. Animal Groups   There were a total of 8 animal groups: 1. *Naive* (n=8); these animals did not undergo any surgical procedures. As with the other groups, they received injections of 5 mg/kg *d*-amphetamine (i.p.) and were placed in the rotometer for 2 hours to measure intrinsic motor asymmetry. 2. *RANB* (n=4); these animals received an unilateral infusion of RANB (2 nmoles) into the right striatum with an equal volume of vehicle infused into the left striatum. 3. *ASF* (n=11); these animals received an unilateral infusion of ASF (2 nmoles) into the right striatum with an equal volume of vehicle infused into the left striatum. 4. *ASF/ASF* (n=6); these animals received simultaneous infusions of ASF (2 nmoles) into both the striatum and the GP of the animals' right side. 5. *ASF/RANB* (n=4); these animals received simultaneous infusions of ASF (2 nmoles) into the right striatum and RANB (2 nmoles) into the right GP. 6. *GP* (n=5); these animals received a single infusion of ASF (2 nmoles) into the right GP only. 7. *IBA* (n=8); these animals received unilateral GP lesions, as described above. For all lesioned animals, approximately 2 weeks elapsed before rotational testing. 8. *ASF/IBA* (n=6); these animals received unilateral GP

lesions (as described above) 2-3 weeks prior to a single infusion of ASF (2 nmoles) into the right striatum.

5.2.5. Statistical Analysis   To determine the animals' rotational bias towards the ODN-treated or lesioned hemisphere, the difference between ipsiversive and contraversive rotations was calculated for each animal and these values were compared between groups using an one-way ANOVA followed by Newman-Keuls posthoc analysis. Significance was assumed when $P < 0.05$. Values are expressed as group mean ± SEM.

5.3. Results

5.3.1. Assessment of Striatal and GP Cannulae Placement
The placement of cannulae used to infuse solutions into the striatum and the GP was confirmed using Nissl staining. Figure 5.2A illustrates the relative positions of striatal and pallidal infusion sites. In the IBA and ASF/IBA groups, only animals with lesions primarily confined to the GP were included in the studies (Fig.5.4C,D). Minimal tissue damage was evident surrounding the cannula tracts penetrating the striatum and GP following ODN infusions (Fig.5.1).

5.3.2. Antisense-Induced Striatal IEG Suppression
As previously reported, all animals that received intrastriatal infusions of ASF demonstrated marked reduction of striatal Fos-like immunoreactivity (Fos-LI) subsequent to d-amphetamine challenge (Fig.1B,C) (Sommer et al.,1993; Hooper et al.,1994; chapter 4). This striatal suppression frequently extended as caudally as the GP and was associated with marked upregulation of c-fos expression in the ipsilateral GP (Fig.5.2D,E). In contrast, animals that were infused with RANB had minimal IEG suppression which was primarily localized to regions surrounding the cannula tract (Fig.5.5A,B). These results are consistent with those previously reported for the effects of RAN on IEG expression (Fig.5.5C,D). Animals that received concomitant infusions of ODNs into the striatum and the GP did not show the atypical elevation of IEG expression in the ipsilateral GP (Fig.5.4A,B). This effect was observed in animals that had received either ASF or RANB into the GP.

5.3.3. Effects of GP Treatments on Rotational Response   Circling   behavior

was measured in all groups (Fig.5.3). Naive animals exhibited hyperactivity and

stereotypic behavior (focused sniffing, rearing), but no rotational tendencies, following

d-amphetamine challenge (117 ± 32 : 78 ± 37; clockwise (ipsiversive) :

counterclockwise (contraversive)). Consistent with the rotational behavior observed

following unilateral striatal infusion of RAN (chapters 3 and 4), animals infused with

RANB had a similar number of ipsiversive rotations as observed in naive animals (114

± 57.7 : 3.5 ± 2.5; ipsiversive : contraversive). The number of contraversive rotations

elicited in these animals was similar to that observed in other treatment groups.

Animals in the ASF group rotated 305 ± 53 : 22 ± 8, while those in the ASF/ASF

group demonstrated intense ipsiversive rotation, turning 1057 ± 204 : 13 ± 7.

To determine whether ASF infusions into the GP alone would produce a

rotational bias, we examined the behavior of the GP group. As anticipated, these

animals did not demonstrate an ipsiversive deviation in their direction of motion. In

fact, they had a tendency to turn in the contraversive direction (40 ± 13 : 140 ± 54).

These results suggest that the significant potentiation that was produced by

simultaneous infusion of ASF into both the striatum and the GP was dependent upon

the suppression of striatal efferent activity and was unlikely due to pallidal trauma.

Although we have demonstrated the specificity of ASF to suppress c-*fos* expression in

the striatum, we had not yet investigated the possibility of non-specific ODN effects in

the GP. Thus, we next infused ASF into the striatum concomitantly with RANB into

the ipsilateral GP to examine whether the behavioral potentiation could be produced by

the random ODN. Surprisingly, animals in the ASF/RANB group had mean rotations that were similar to those of the ASF/ASF group ($915 \pm 236.5 : 0.5 \pm 0.5$). Animals that received GP lesions (IBA group) also exhibited significant ipsiversive circling behavior following d-amphetamine challenge ($990 \pm 176 : 21 \pm 15$). Infusions of c-*fos* antisense ODNs into the striatum 2-3 weeks following GP lesions (ASF/IBA group) produced rotational behavior ($758 \pm 121 : 0$) that was similar to that of the ASF/ASF, ASF/RANB and IBA groups. When ipsiversive bias was compared between groups, animals in the ASF/ASF, ASF/RANB, IBA and ASF/IBA groups rotated significantly greater (approximately 2.5-3 fold) than those receiving striatal ASF alone ($P = 0.0015$, 0.0038, 0.0031 and 0.0140, respectively). However, there were no significant differences in rotational intensity among these four former groups.

5.4. Discussion

In this study, we have shown that the intensity of rotational behavior that is induced by infusion of antisense ODNs and suppression of IEG expression in the striatum is significantly potentiated by concurrent infusion of ODNs into the GP. Similar behavioral effects were also elicited by excitotoxic ablation of the GP, suggesting that reduction in pallidal transmission markedly influences the motor output of the basal ganglia. Antisense ODNs have been shown to inhibit the induction of IEGs by psychostimulant drugs when administered *in vivo* (Chiasson *et al.*,1992,1994; Dragunow *et al.*,1993,1994; Hooper *et al.*,1994; chapters 3 and 4). In particular, antisense ODNs targeted to c-*fos* or *ngfi*-a effectively suppress the induction of these IEGs in the striatum when administered into brain parenchyma of adult rats. Following unilateral striatal suppression of either c-*fos* or *ngfi*-a expression, animals showed marked upregulation of both of these IEGs in the ipsilateral GP, a phenomenon not typically observed following *d*-amphetamine challenge (Graybiel *et al.*,1990; chapter 4).

There are several possible explanations for the abnormal increase in GP Fos-like immunoreactivity (Fos-LI) produced by suppression of striatal c-*fos* expression. Amphetamine induces Fos-LI primarily in striosomal neurons of the (mid)rostral striatum which project to the SNC (Gerfen, 1984; Jimenez-Castellanas, 1989). However, c-*fos* expression in the caudal striatum becomes homogeneously distributed, suggesting that projection neurons to both the GP and the SN are activated by this stimulant (Robertson *et al.*,1991). Antisense ODNs to c-*fos* may impair stimulation of

some or all of the striatal efferent circuits, as ASF infusions into the rostral striatum generally produce a graded suppression of IEG expression throughout the entire striatal rostrocaudal axis. Thus, suppression of c-*fos* expression and neurotransmission in both types of projection neurons would result in disinhibition of both the GP and the SN. Alternatively, increased dopamine (DA) released into the striatum, via disinhibition of nigrostriatal projections, may enhance activity at striatopallidal DA receptors, which are thought to be primarily of the D2 type and whose stimulation reduces cyclic adenosine monophosphate (cAMP) and neuronal activity (Robertson, 1992; Robertson *et al.*,1992). This would lead to decreased firing of striatopallidal neurons and decreased inhibition of pallidal activity. Finally, it is possible that sparsely distributed nigropallidal efferents become hyperactive, releasing catecholamines at pallidal terminals and stimulating these neurons (Fig.5.6).

It has been reported that intrastriatal infusions of antisense ODNs targeted to c-*fos* reduced levels of γ-aminobutyric acid (GABA) in the SN pars reticulata (SNR), but not in the GP, of unstimulated animals (Sommer *et al.*,1996). These results support the notion that inhibition of c-*fos* expression in neurons prevents normal neurotransmission under both basal and stimulated conditions. The failure to observe a reduction in GABA in the GP may simply be the result of low basal release of this neurotransmitter by terminals of striatopallidal neurons, with relatively imperceptible alterations in GABA levels produced by striatal ASF in the absence of striatal stimulation. In fact, it has recently been shown, using *in situ* hybridization, that there is an increase in the hybridization signal for the IEGs, c-*fos* and *ngfi*-a, in the

ipsilateral GP following infusions of antisense ODNs to c-*fos* into the striatum in unstimulated animals (W. Sommer, personal communication). These results provide support for our previous immunohistochemical findings and suggest that the microdialysis method may not be sufficiently sensitive to detect the changes in the basal levels of GABA in this nucleus.

It has been previously demonstrated that unilateral suppression of striatal IEG induction produces a motor asymmetry where, following *d*-amphetamine challenge, the animals rotate towards the side of decreased protein expression (Sommer *et al.*, 1993; Hooper *et al.*, 1994; chapter 4). The upregulation of IEG expression in the GP ipsilateral to the striatal antisense ODN infusion prompted us to examine the role of pallidal activity in mediating the observed rotational behavior. We used the same antisense ODN (ASF) that had been previously infused into the striatum to manipulate the IEG response in the GP (chapters 3 and 4). The concomitant infusion of antisense ODNs to c-*fos* (ASF) into the striatum and the GP increased, by approximately threefold, the turning response produced by striatal infusions of ASF alone. It is possible that activation of GP neurons produces a motor influence which opposes the rotational response of the animals, probably through stimulation of pallido-subthalamo-nigral circuits (indirect pathway). The prevention of such activity with ASF would, therefore, permit unhindered control of the intact (contralateral), striatonigral efferents (direct pathway) and potentiation of the turning behavior (Fig.5.6). Alternatively, stimulation of GP neurons may be an inconsequential result of the striatal IEG inhibition and have no effect on rotational behavior. In this case, infusion of ASF into

the GP would be expected to have negligible effects on motor function and, thus, the potentiated response could be accredited to ODN diffusion and cumulative striatal IEG suppression.

To examine the possibility that GP-infused ASF had diffused into the overlying striatum and produced its effects through striatal inhibition of IEG expression, animals were infused with ASF into the GP without simultaneous striatal infusion, with motor behavior assessed following d-amphetamine stimulation. As d-amphetamine does not induce extensive c-fos expression in the GP, infusion of ASF into this region alone was hypothesized to have little effect on motor function (Graybiel et $al.$,1990; chapter 4). As expected, none of the animals in this group showed significant ipsiversive rotational responses to d-amphetamine challenge. These results suggest that, while it is possible that ODN diffusion into the striatum occurred, the action of ASF was predominantly confined to the GP.

We next attempted to reproduce the potentiation of circling behavior produced by concomitant infusions of ASF into both the striatum and the GP, by permanently ablating the GP with ibotenic acid (IBA). However, even without striatal IEG suppression, animals with large IBA lesions of the GP exhibited robust circling behavior when challenged with d-amphetamine. We postulated that additional suppression of striatal IEG expression would potentiate the alterations in basal ganglia output, creating a synergistic effect on the animals' rotational behavior. Although animals that received striatal ASF infusion and a GP lesion exhibited marked ipsiversive rotation, the intensity of this behavior was not significantly different from

that of animals with GP lesions alone. In fact, there was no difference in the rotational behavior produced by animals in the ASF/ASF, ASF/RANB, IBA or ASF/IBA groups, suggesting that concomitant suppression of striatal and pallidal activity, or complete ablation of the GP, induces changes which maximally alter the influence of the basal ganglia on locomotor function. The number of rotations produced by altering both striatal and pallidal activity with antisense ODNs was more than triple that produced by striatal changes alone, indicating that efferent pathways from both the striatum and the GP play crucial roles in modulating motor and postural function.

The specificity of a particular ODN is typically demonstrated by the absence of effect from the administration of theoretically non-hybridizing molecules such as sense or random ODNs. We have demonstrated the specificity of ASF in the striatum through the comparison of its suppressive actions with the effects of vehicle and two random ODNs (Fig.5.5). We and others have also demonstrated the specificity of the same ODN sequence in the striatum, in both partially and fully phosphorothioate forms, using mismatch and sense controls (Chiasson et al.,1992; Heilig et al.,1993; Hooper et al.,1994; Sommer et al.,1996). To date, however, there are no reports of the application of ASF to the GP. The potentiation of the behavioral response in the ASF/RANB animals suggests that the GP may be more susceptible to non-specific actions of ODNs than is the striatum. None of the animals that had striatal ASF infusions with simultaneous GP infusions of either ASF or RANB exhibited the elevation of Fos-LI that was observed in animals with striatal ASF infusion alone. While the reason for this apparently non-specific effect in the GP remains unclear, it is

possible that the GP requires a much lower dose of ODNs to exhibit sequence-specific action. This is a plausable theory owing to the large difference in tissue volume between the striatum and the GP. Thus, we are only able to infer from similarities in behavioral effects with the lesioning studies that the infusion of ODNs into the GP and ablation of this nucleus both produce their potentiating effects by suppressing pallidal activity. This inference is also supported by studies demonstrating a reduction in GABAergic transmission in projection nuclei following striatal ASF infusions (Sommer et al.,1996).

There are important differences between the effects of local ODN infusions and the excitotoxic ablation of neural tissue which may explain the failure of striatal ASF infusions to further potentiate the behavioral response produced by IBA lesioning of the GP. Presumably, ASF interferes with the induction of novel c-fos expression and, by an unknown mechanism, prevents the activation of neurons. Given the low basal expression of c-fos, the regions infused with ASF would not be expected to undergo massive alterations in basal activity. Simultaneous suppression of c-fos expression, therefore, in the striatum and the GP would prevent further stimulation of neurons in these regions but may not produce marked effects on intrinsic activity. Ablation of the GP, however, would not only prevent stimulation of pallidal neurons, but also reduce the tonic inhibition of the GP on the subthalamic nucleus (STN). It is possible that this disinhibition of the STN produces marked stimulation of output neurons in the SNR, through the indirect pathway, inducing maximal output from this system onto the thalamus and superior colliculus (SC). This notion is supported by a recent report of

massive alterations in SC activity that are positively correlated to the degree of postural

and locomotor bias observed in an animal (chapter 6). If nigral projections are firing at

their maximum capacity, inhibition of striatonigral circuits, through IEG suppression,

would not produce further SNR stimulation.

The results of this study suggest that neuronal activity becomes elevated in the

GP following disruption of striatal circuitry. This activity appears to compensate for

the reduction of ipsilateral striatonigral transmission and opposes the influence of the

contralateral striatonigral system in an effort to balance the basal ganglia output

between the two hemispheres. Although the mechanism remains unclear, it appears

that unilateral activation of pallidal circuits induces a motor influence directing the

animal towards the side opposite stimulation and, thus, serves as a balancing

mechanism in animals with unilaterally compromised striatal neurotransmission. This

suggests that unilateral activation of pallidal neurons, without striatal stimulation,

would result in a rotational deviation away from the side of stimulation. In fact, it has

been shown that animals with a unilateral 6-OHDA lesion of the medial forebrain

bundle, and were treated with the D2 agonist, quinpirole, exhibited little or no striatal

c-*fos* expression. However, this treatment induced Fos-LI in the GP, ipsilateral to the

lesion, and robust contralateral rotation (Paul *et al.*, 1992). Also, Schuller and

Marshall (1995) have shown that the AMPA-kainate antagonist, DNQX, produces both

contraversive rotation and an increase in Fos-LI in the ipsilateral GP when infused into

dopamine-depleted striata. Thus, the GP appears to function as a brake on the

rotational behavior elicited in animals with impaired striatal efferent systems as

compromising this structure markedly enhances circling intensity. We suggest that inhibition of striatal efferent circuitry, using antisense ODNs, provides an useful model in which to examine alterations in neural physiology and behavior produced by striatal dysfunction.

Figure 5.1 Typical pattern of Nissl staining surrounding ODN infusion sites. Coronal sections through the striatum (A,B) and globus pallidus (C-F) that have been stained for Nissl substance following ASF infusion. The micrograph in A) shows the ASF-infused striatum, whereas that in B) represents the vehicle-infused (contralateral) striatum. Tissue damage was minimal and primarily confined to the actual cannula tract and in the neuropil immediately adjacent its termination site. Low (C,D) and high (E,F) magnification micrographs through the globus pallidus following delivery of ASF (C,E) demonstrate the negligible toxicity induced by the ODN (compare to the intact, comtralateral globus pallidus in D and F). Arrowheads in C-F indicate the approximate border between the globus pallidus and the overlying striatum. Scale bars represent 1 mm.
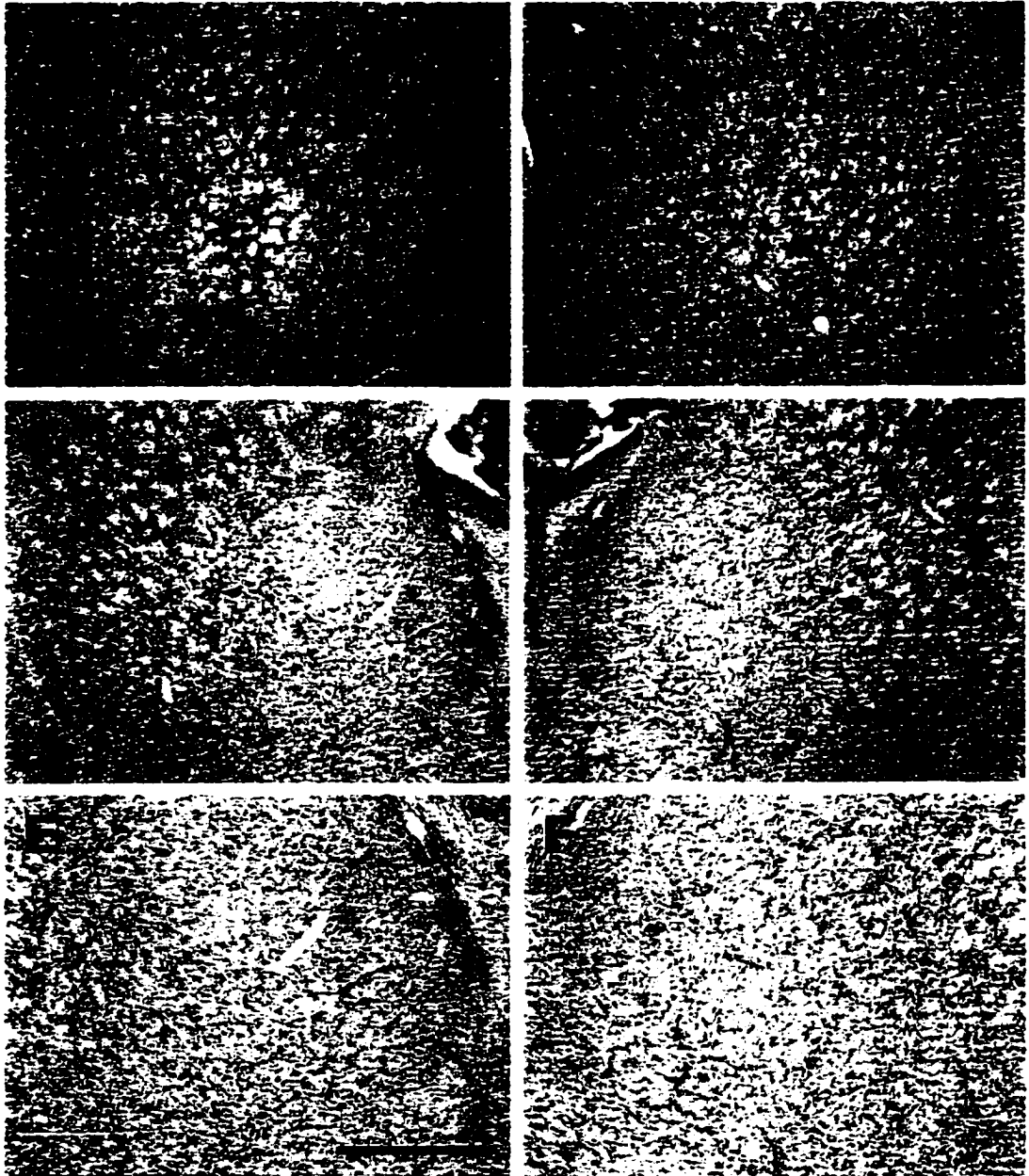
FIGURE 5.1

Figure 5.2 A) Schematic of a sagittal section through the rat brain showing the relative positions of striatal and pallidal infusion sites. Fos-LI-labeled coronal sections through the striatum of rats that had an unilateral, intrastriatal infusion of ASF (B), with vehicle infused into the opposite striatum (C) reveals the extensive reduction of IEG expression produced by ASF. D) and E) are sections showing Fos-LI at the level of the GP following ASF (D) or vehicle (E) infusion into the striatum. The dashed line in D) indicates the border between the striatum and the GP at the level shown in both D) and E). Note that the suppression of striatal Fos-LI extends as far caudally as the GP and that marked upregulation of this protein is seen in the ipsilateral GP (D). The contralateral striatum and GP in E) reveals the normal pattern of Fos-LI induced by *d*-amphetamine. Scale bar in B) represents 100 μm.
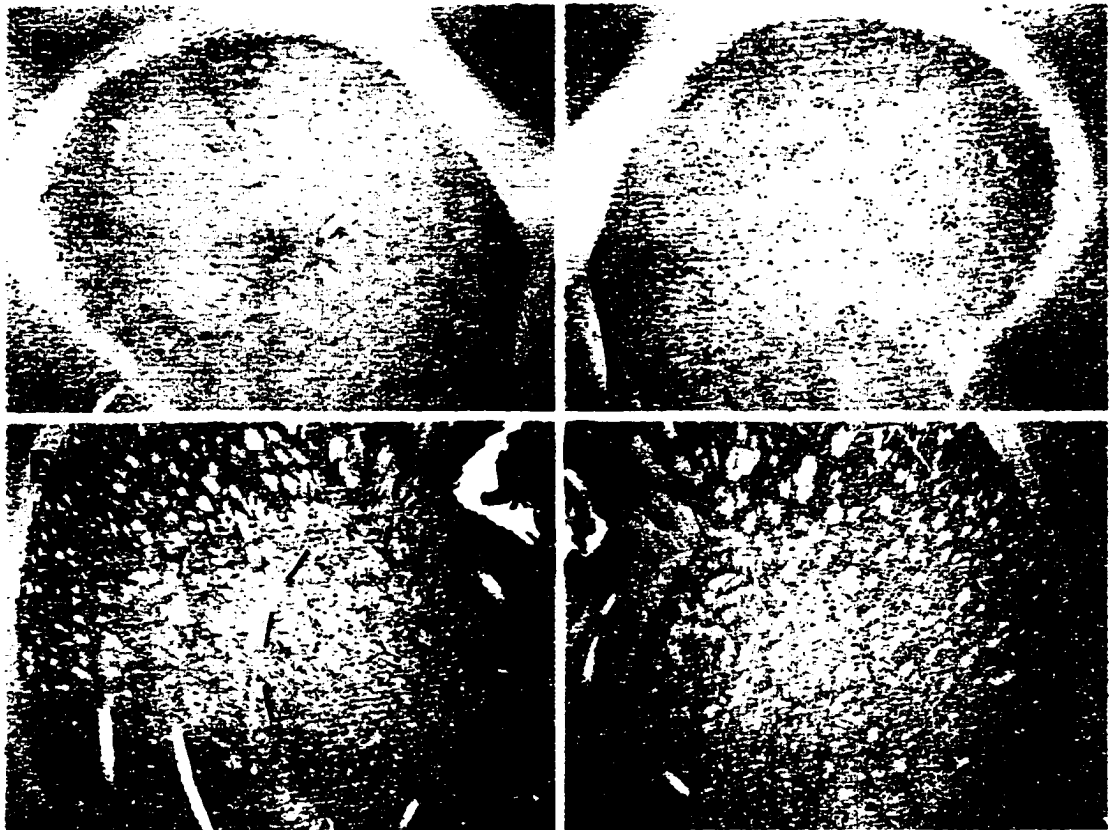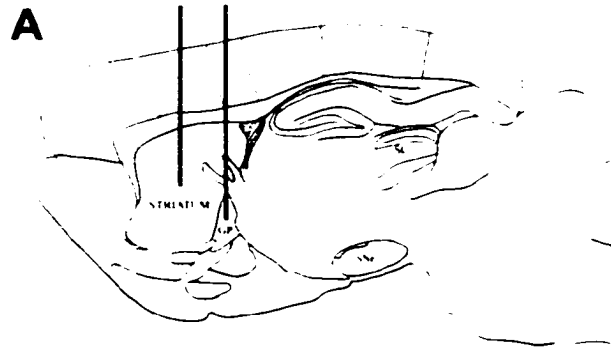
FIGURE 5.2

Figure 5.3   Rotational behavior observed in experimental groups. Animals in the naive, GP and RANB groups had negligible locomotor bias towards the ipsiversive (clockwise) direction. In contrast, animals of the ASF group demonstrated marked ipsiversive rotational behavior. Individuals of the ASF/ASF, ASF/RANB, IBA and ASF/IBA groups all had intense ipsiversive bias. The ipsiversive bias in all of these groups was significantly higher (~2.5-3 times) than that observed in the ASF group (indicated by asterisks). The numbers in parentheses indicate the number of animals per group. Positive values (black bars) correspond to ipsiversive turns; negative values (open bars) indicate contraversive turns. Significance at $P < 0.05$.
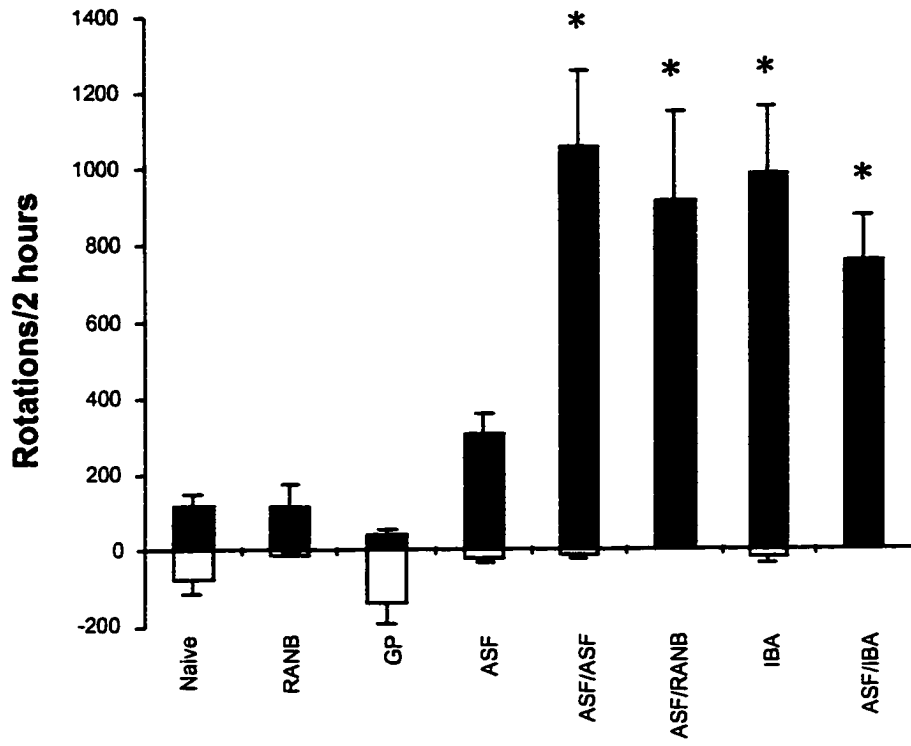
FIGURE 5.3

Figure 5.4 A) Coronal section through the GP showing Fos-LI in an animal which had received an intrapallidal infusion of ASF. The arrow indicates the approximate tip of the cannula tract. The ASF-infused GP appeared similar in Fos-LI to that of the contralateral side shown in (B). Striatal Fos-LI surrounding the GP was slightly less robust on the infused side, effects undoubtedly due to diffusion of ASF from the site of delivery. Animals in this group, however, did not exhibit significant ipsiversive circling, indicating that the extent of striatal suppression was not great enough to produce a behavioral effect. C) Nissl staining revealed the extent of IBA lesions in the GP. Note the extensive pyknosis, primarily confined to the GP of the lesioned hemisphere, as compared to the large, darkly stained neurons of the intact GP shown in (D). E), F) Fos-LI of the GP in the animal shown in C) and D), respectively. The arrow in E) indicates the tip of the cannula tract. Comparison of Fos-LI in the overlying striatum between lesioned (E) and intact (F) sides reveals similar expression, confirming the confinement of the lesion to the GP. Arrowheads mark the border between the GP and the overlying striatum. Scale bar represents 100 μm.
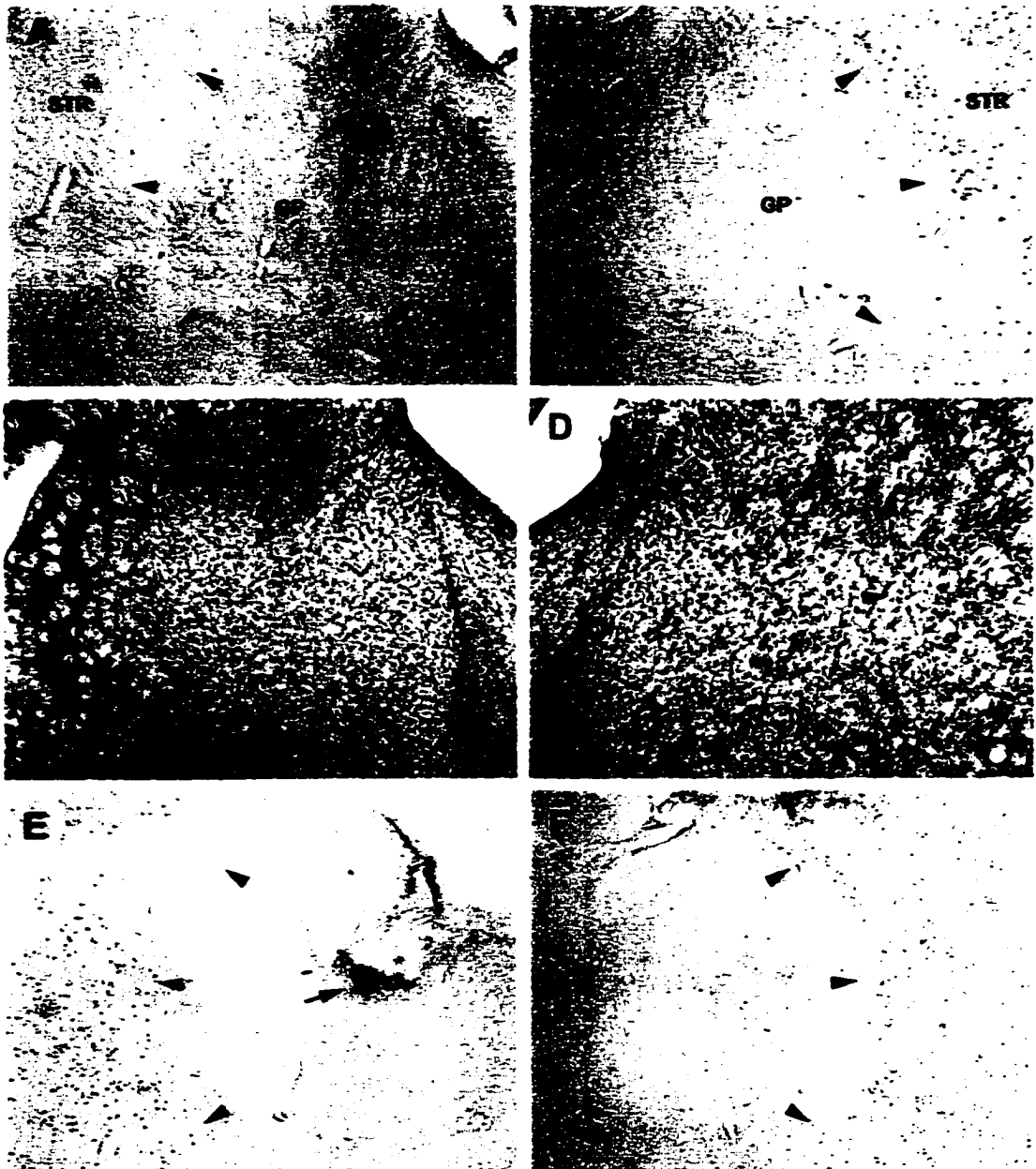
FIGURE 5.4

Figure 5.5   Fos-LI in the striatum of animals that had received unilateral infusions of

RANB (A,B) or RAN (C,D). Panels A and C represent ODN-infused striata whereas

panels B and D are the respective contralateral (vehicle-infused) striata. Animals that

received RANB were given a 1 hour recovery period following ODN infusion; those

that received RAN were given a 2 hour recovery period. While these ODNs had a

modest effect on *d*-amphetamine-induced Fos-LI, their suppression capabilities were

insignificant compared to those of ASF (compare with Fig.5.2B,C). Scale bar

represents 100 μm.
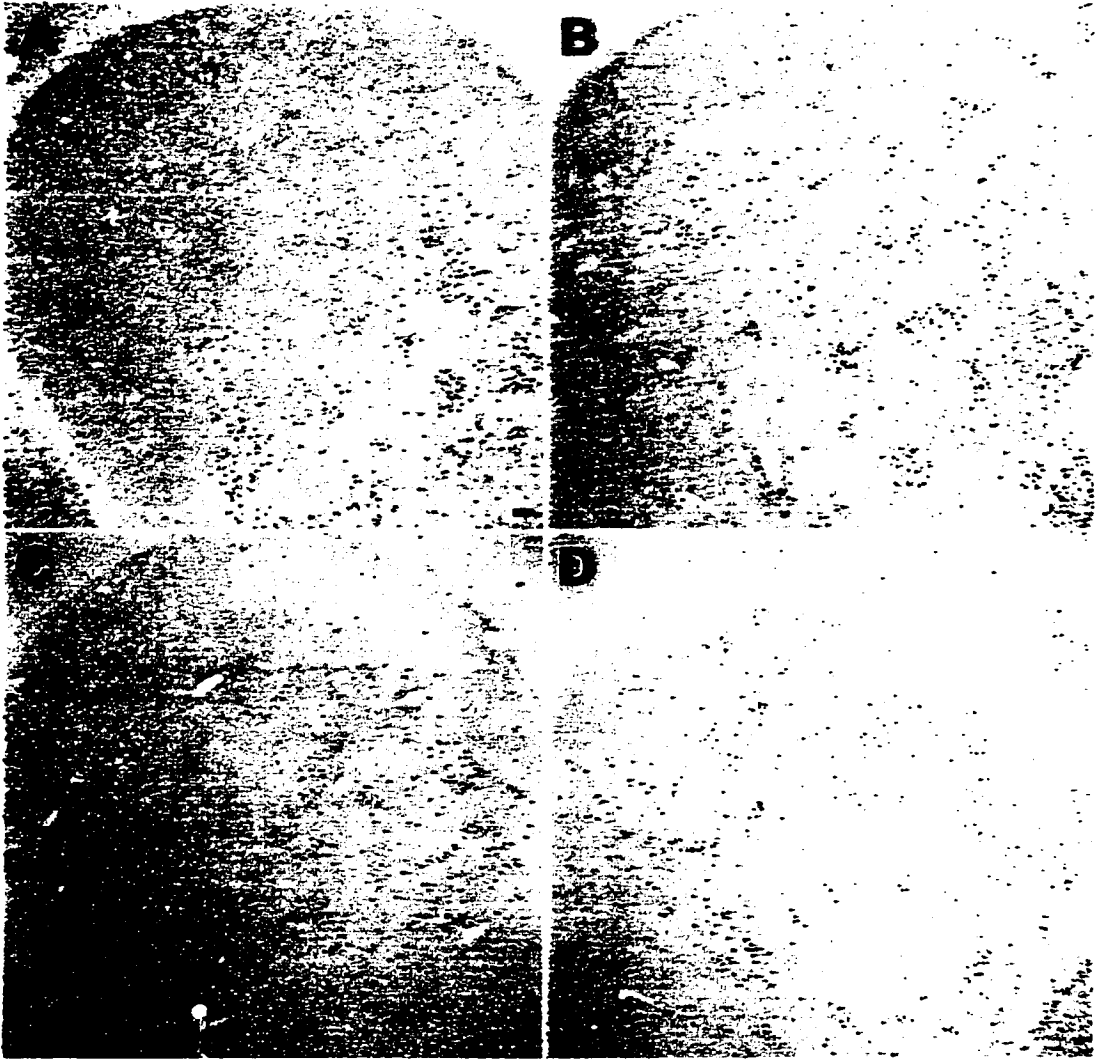
FIGURE 5.5

Figure 5.6 Schematic illustrating the hypothesized mechanism of behavioral potentiation induced by manipulation of GP activity. Panel A shows the alterations in basal ganglia circuitry following infusion of antisense ODNs into the striatum. Striatal IEG expression and efferent activity is suppressed and results in a disinhibition of neurons in the SNR and subsequent increase in nigrothalamic and nigrotectal inhibitory tone. Elevation of activity in the ipsilateral GP is also evident by the increase in Fos-LI in this nucleus following striatal IEG suppression. This activity counteracts the reduction in striatonigral transmission by reducing the stimulatory effect of the subthalamic nucleus on the SNR. As shown in panel B, concurrent suppression of striatal c-*fos* expression and suppression of GP activity with intrapallidal infusions of ODNs or IBA, reduces or eliminates the suppression of subthalamo-nigral stimulation and results in a potentiating effect on behavior through a further increase in SNR output. Open circles represent neurons whose activity is directly affected by either ODN infusions or IBA lesioning. The width of the arrows corresponds to the relative level of neuronal activity. GP-globus pallidus; SNC-substantia nigra pars compacta; SNR-substantia nigra pars reticulata; STN-subthalamic nucleus; STR-striatum.
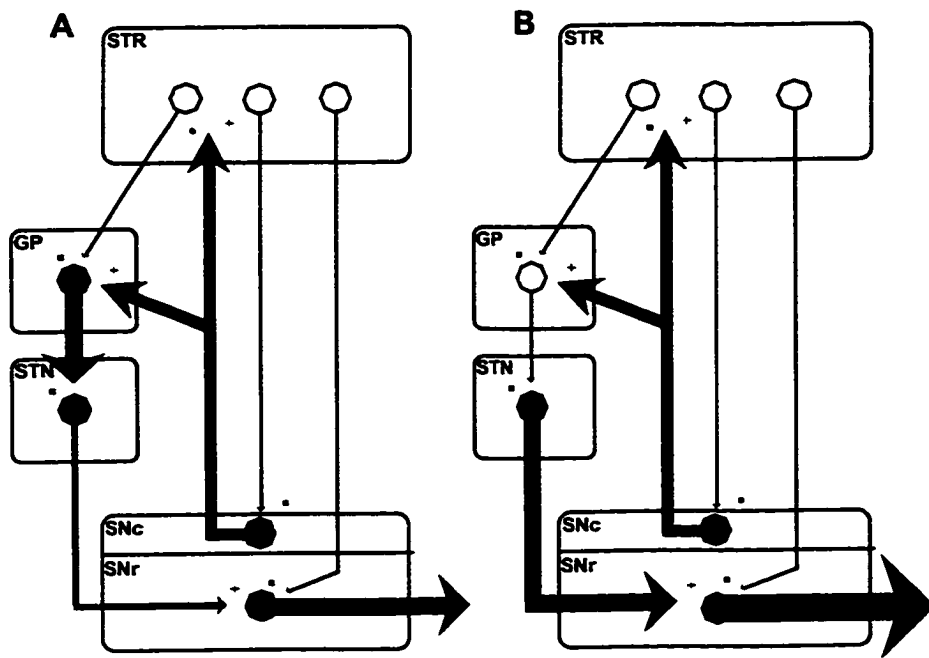
FIGURE 5.6

CHAPTER 6

Correlative Analysis of Rotational Behavior and Metabolic Alterations in the

Superior Colliculus[*]

6.1. Introduction

Rotational behavior in animals provides an accurate means of assessing locomotor and postural asymmetry arising from neural alterations in the basal ganglia and its associated motor nuclei. The primary input centre of the basal ganglia is the striatum, which receives massive afferent projections from cortical and subcortical regions (Parent, 1990). The output nuclei of the basal ganglia, the internal segment of the globus pallidus (GPi) and the substantia nigra pars reticulata (SNR), send extensive projections to both the thalamus and the superior colliculus (SC) (Anderson and Yoshida, 1977; Deniau et al.,1978; Guynet and Aghajanian, 1978; Bentivoglio et al.,1979; Wichmann and DeLong, 1996). Pharmacological and lesioning studies have implicated the ventromedial thalamus (VMT) in the production of rotational responses in animals (DiChiara et al.,1981; Kilpatrick et al.,1982), although this structure does not appear to be the sole mediator of this behavior (Reavill et al.,1981). It has been proposed that the induction of circling activity requires the participation of two motor components, locomotion and posture, which have been suggested to be controlled through nigrothalamic and nigrotectal circuits, respectively (DiChiara et al.,1981). Consistent with this notion, alterations in γ-aminobutyric acid (GABA) activity in the SC have been shown to produce tight postural asymmetry without actual rotation. Ipsiversive postural deviation may be produced by intracollicular infusion of GABA agonists, whereas tight contraversive contortions are elicited by GABA antagonists (DiChiara et al.,1981).

Presently, we have used a novel technique to study the effects of basal ganglia output on SC activity and motor and postural control. It has been previously shown that psychostimulant-induced expression of immediate early genes (IEGs), such as c-*fos* and *ngfi*-a, in the striatum may be suppressed using intracerebral infusions of antisense oligodeoxynucleotides (ODNs) (Chiasson *et al.*,1992,1994; Dragunow et al, 1993,1994; Heilig *et al.*,1993; Sommer *et al.*,1993,1996; Hooper *et al.*,1994; chapters 3 and 4). Following stimulation, animals with unilateral suppression of striatal c-*fos* or *ngfi*-a expression exhibited significant ipsiversive circling behavior, the intensity of which was inversely related to the length of time between antisense infusion and stimulant administration (chapter 3). Animals that were left to recover for between 1-2 hours following infusions generally exhibited robust circling behavior while those that were left for 4 hours had reduced ipsiversive bias which further decreased as the recovery period lengthened. Suppression of either c-*fos* or *ngfi*-a in the striatum was also accompanied by marked upregulation of IEG expression in the ipsilateral globus pallidus (GP) (chapter 4). Recent studies indicated that this GP activity was inhibiting full manifestation of the rotational response, as simultaneous infusion of antisense ODNs into the striatum and the GP tripled the rotational behavior elicited with striatal ODN infusions alone (chapter 5). Thus, using antisense ODNs to suppress IEG expression in the basal ganglia, we were able to generate animals that demonstrated graded degrees of locomotor and postural bias. We have used the expression of c-*fos* as an indicator of elevated neuronal activity (Sagar *et al.*,1988; Dragunow and Faull, 1989; Robertson, 1992; Curran and Morgan, 1994) and have analyzed Fos-like

immunohistochemistry (Fos-LI) in animals to investigate whether alterations in SC activity are related to the observed motor asymmetry. This report describes the correlation between changes that occur in the SC and the degree of postural and locomotor deviation observed in an animal.

6.2. Materials and Methods

6.2.1. Oligodeoxynucleotide Infusions

Animals were infused with antisense ODNs as previously described in chapter 3. Briefly, animals were anesthetized with halothane and received unilateral infusions of ODNs (2nmol in 2μl) into the striatum alone or into both the striatum and the ipsilateral globus pallidus (GP). Contralateral striata received equal volumes of vehicle infusions. After infusion, animals were placed in their home cage to recover for 1,2,4 or 10 hours. Animals with simultaneous infusions into the striatum and the GP had recovery periods of 1 hour.

Following recovery, animals were injected with d-amphetamine (5 mg/kg, i.p., a gift from SmithKline Beecham Pharma Inc.) and placed in a rotometer, where the number and direction of their rotations were recorded for the next two hours. After the rotation period, animals were deeply anesthetized with sodium pentobarbital (>100 mg/kg, i.p.) and sacrificed. Cannulae placements were verified using Nissl stained sections.

6.2.2. Immunohistochemistry

Animals were transcardially perfused, initially with saline, followed by 4% paraformaldehyde in a 0.1 M phosphate buffer solution (pH 7.4). Brains were subsequently removed and post-fixed at 4°C overnight, afterwhich they were transferred to a 0.12 M phosphate buffer solution containing sodium azide until further processing. Brains were blocked and cut on a vibratome in 50 μm coronal sections and were processed for c-Fos immunoreactivity as described in section 3.2.2.

6.2.3. Oligodeoxynucleotides   Oligodeoxynucleotides used in this study were described in section 3.2.3..

6.2.4. Animal Groups   Groups were selected from a primary pool of animals that had received intrastriatal infusions of ASF or ASN, with recovery periods of 1,2,4 or 10 hours (see chapter 3). Additional animals had received simultaneous infusions of ASF into both the right striatum and the globus pallidus, with recovery periods of 1 hour (see chapter 5). In general, animals with single striatal ODN infusions demonstrated intense behavioral responses to stimulant challenge following 1-2 hours recovery. However, as this recovery period was extended to 4 and 10 hours, the rotational behavior diminished dramatically (chapter 3). Animals that received simultaneous infusions of ASF into the striatum and GP demonstrated extreme postural deviation and rotational behavior, with a group mean of ipsiversive rotations approximately triple that of animals that had received striatal infusions alone (chapter 5). Animals were grouped (I-IV) according to the intensity of the d-amphetamine-evoked rotational behavior, regardless of which treatment protocol they had received. The difference between the number of ipsiversive and contraversive rotations was calculated to give a measure of an animal's ipsiversive bias (denoted $\Delta i\text{-}c$). For the purposes of this experiment, animals were selected and grouped accordingly: group I: $\Delta i\text{-}c < 50$ (n=5); group II: $\Delta i\text{-}c = 50\text{-}500$ (n=7); group III: $\Delta i\text{-}c = 500\text{-}1000$ (n=9); group IV: $\Delta i\text{-}c > 1000$ (n=4).

6.2.5. Quantification of Fos-positive nuclei   Following immunohistochemistry, sections were mounted on slides that were labeled in a non-descriptive manner. Fos-

positive nuclei in the stratum griseum intermediale (SGI) were counted with the investigator blind to the rotational status or group of the animal. As the most apparent alterations in Fos-LI were located in the (mid)rostral SC, all counts were performed in this region (approximately 6.3 mm posterior to bregma) (Paxinos and Watson, 1997).

6.2.6. Statistical Analysis

Rotational data was obtained and animals were grouped as described above. The raw values for ipsiversive and contraversive rotations were compared in each group using a two-tailed, paired t-test. To test our hypothesis that the SGI of the ipsilateral SC expressed relatively more nuclei labeled with Fos-LI than the contralateral side, we employed a one-tailed, paired t-test using the raw values of Fos-positive nuclei counted in this region. The Pearson Product Moment and linear regression was calculated using individual Δi-c values and number of Fos-positive nuclei in the ipsilateral SGI (expressed as % of contralateral). Normalization of the values for tectal Fos-positive nuclei was performed to remove the variation in total numbers which existed between animals. Significance was assumed when $P < 0.05$. Values are expressed as group mean $\pm$ SEM.

6.3. Results

6.3.1. Expression of Fos-LI in Non-Rotating Animals   Intraperitoneal

administration of *d*-amphetamine (5 mg/kg) induced abundant Fos-LI in the intermediate layers of the SC in non-rotating animals. This expression appeared diffuse and homogeneously distributed throughout the lateral portions of the stratum album intermediale (SAI) and SGI (Fig.6.1). The intensity and number of Fos-positive cells varied somewhat between animals but was symmetric between hemispheres in a particular animal. The thin, medially-projecting regions of these laminae had sparse Fos-LI, markedly less than the broad, lateral extensions (Fig.6.1).

6.3.2.Expression of Fos-LI in Rotating Animals   All   animals   in   groups   II-IV

expressed alterations in tectal Fos-LI relative to non-rotating animals from group I. Lateral regions of both the SAI and SGI ipsilateral to the ODN infusions and the direction of rotation appeared to have a marked reduction in the number of nuclei expressing Fos-LI (Fig.6.2, 6.3). As the intensity of rotational behavior increased, the reduction of Fos-LI in this region also increased, relative to the contralateral side (Fig.6.2, 6.3). Notably, animals that exhibited higher degrees of rotation also maintained a tighter radius of movement, with an apparent increase in contortional posture (data not shown).

While the lateral regions of the intermediate layers showed a marked reduction in Fos-LI, suggesting an increased inhibitory tone from the SNR, the medial zone of the ipsilateral SGI had an increase in expression. As the mean rotational bias for a

group increased, this medial band of the SGI increased in intensity and abundance of Fos-LI (Fig.6.2, 6.3). Moreover, as the circling activity became more intense, this band of SGI Fos-LI became increasingly well defined. Animals that exhibited the greatest rotational intensity had a marked banding pattern of Fos-LI in the ipsilateral SGI, an effect that was exaggerated by the concurrent reduction of expression in the underlying SAI and the lateral SGI (Fig.6.3).

6.3.3.Correlation of SGI Fos-LI and Rotational Behavior   Animals in groups I-IV expressed increasing degrees of ipsiversive bias in their rotational behavior, with the following Δi-c values (expressed as turns/2 hours): group I: 4.6 ± 14.8; group II: 317.7 ± 34.9; group III: 623.3 ± 30.9; group IV: 1343.3 ± 179.7. Analysis of raw rotational data confirmed that all groups, except group I, had significant ipsiversive bias (group I: P= 0.77; group II: P< 0.0001; group III: P< 0.0001; group IV: P= 0.0025). Calculation of Fos-positive nuclei in the SGI of coronal SC profiles produced the following group means (expressed as % of contralateral expression): group I: 131.0 ± 14.1; group II: 183.0 ± 17.2; group III: 227.0 ± 21.8; group IV: 307.0 ± 64.2. These data are illustrated in figure 4. All groups, including group I, had a significantly greater number of Fos-positive nuclei in the ipsilateral SGI, relative to the contralateral side (group I: P= 0.031 group II: P= 0.0014; group III: P< 0.0001; group IV: P= 0.027). Calculation of the Pearson product moment indicated a significant positive association between ipsiversive rotational bias and Fos-LI in the ipsilateral SGI (R= 0.652, P= 0.0004). Regression analysis revealed a linear relationship between these

two variables, corresponding to the function $y = 0.123x + 143.2$ (y = Fos-LI; x = Δi-c), as calculated using the above data (Fig.6.4B).

6.4. Discussion

The results of this study demonstrate that suppression of neuronal activity and IEG expression in the basal ganglia produce dramatic changes in Fos-LI in the SC. These changes include a decrease in Fos-LI in the SAI and a motor activity-dependent increase in the SGI. We have altered the output of the basal ganglia by interfering with the expression of IEGs in the striatum and the globus pallidus. Previous experiments have shown that the circling response that is induced by intrastriatal infusion of antisense ODNs to c-*fos* or *ngfi*-a is potentiated by simultaneous infusions into the globus pallidus (GP) (chapter 5). These results are consistent with the current knowledge of basal ganglia circuitry and suggest that inhibition of striatal and pallidal activity produces synergistic effects on the behavior of an animal by disrupting transmission through both direct and indirect basal ganglia pathways. It has also been shown that antisense ODNs that target either c-*fos* or *ngfi*-a mRNA produce increased IEG expression in the ipsilateral GP when infused into the striatum (chapter 4). This suggested that the suppression of striatal IEG expression, whether it was NGFI-A or c-Fos, produced a disruption of the inhibitory tone from the striatum to the GP. This was further supported by the report that c-*fos* antisense ODNs that were delivered to the striatum decreased the release of the neurotransmitter GABA in the projection nuclei (Sommer *et al.*,1996). Thus, we have presently used the intracerebral delivery of either ASF or ASN to disrupt basal ganglia circuitry and elicit rotational behavior in animals.

Animals that received intrastriatal ODN infusions but exhibited no difference between ipsiversive and contraversive turning (group I) had a diffuse, homogeneous expression of Fos-LI throughout the intermediate layers of the SC. However, as the degree of rotation increased, the extent of Fos-LI in the ipsilateral SAI and the lateral portion of the SGI appeared to decrease, consistent with an increased inhibitory tone elicited from hyperactive SNR projections. Animals exhibiting maximal degrees of rotation (Δi-c > 1000) had extreme definition of neuronal activation in the SC, with marked suppression of Fos-LI in the SAI and lateral SGI.

Animals that demonstrated moderate to high rotational intensity had a notable increase in Fos-LI in the thin, medial portion of the SGI. The expression of Fos-LI in this region produced a well-defined band of immunoreactivity in high-rotating animals, the intensity of which increased with the number of ipsiversive rotations. Correlation analysis revealed a significant, positive relationship between the number of immunopositive neurons and the number of ipsiversive rotations recorded from the animals. When the total number of Fos-positive nuclei was calculated in the medial portion of the SGI, all groups, including group I, were found to have a significant increase on the ipsilateral side. While the animals in group I did not exhibit significant rotational bias, the mean number of ipsilateral Fos-positive nuclei was 130% of the contralateral expression. It is important to note that these non-rotating animals had received the same ODN infusions as the other groups, but with recovery periods that were of sufficient length to allow for substantial ODN degradation and loss of suppressive effects (chapter 3). The tectal cell counts indicate that there may exist a

threshold of neuronal stimulation (and/or inhibition) which must be unilaterally achieved before any postural bias will be observed in the animal.

Saccadic eye movements are generated in the dorsal midbrain, in the SC, which receives afferent projections from the substantia nigra pars reticulata (SNR), visual cortex and retinal ganglion cells. The laminar structure of the SC suggests a function-dependent segregation of neurons. Wurtz and Albano (1980) have suggested that the superficial layers process visual information whereas the deeper layers facilitate the orientation of an animal's head, eyes and ears towards a stimulus. The superficial layers are the primary retinorecipient regions of the SC, whereas projections from the SNR terminate mainly in the intermediate strata. The anatomical connections between these structures lend opposition to the notion that the alterations in Fos-LI in the SC are the result of visual neglect or hemifield sight in these animals. Alternatively, basal ganglia activity has been shown to modulate the inhibitory nigrotectal efferents that project to the SAI and SGI (Hikosaka and Wurtz, 1983,1989; Kato et al.,1995). The SC sends primary efferent projections to the medial reticular formation (RF), particularly the paramedian pontine (PP) nuclei which further project to the medullary medial (MM) and mesencephalic reticular regions (Buttner-Ennever and Holstege, 1986; Dean and Redgrave, 1992). These premotor areas of the RF directly innervate contralateral motoneurons projecting to oculomotor muscles and postural muscles of the neck and trunk (Buttner-Ennever and Holstege, 1986).

The results of this study suggest that the neurons of the SGI and SAI are dissimilar in their activation and functional characteristics. Also, it should be noted

that animals that turned more vigorously generally maintained a tighter circle of rotation, such that high-rotators (>1000 turns/2 hours) had an extremely tight, head-to-tail conformation, whereas low-rotators turned in a much wider circle (Hebb and Robertson, unpublished observations). These observations support the dual-component hypothesis of circling behavior (i.e. posture and locomotion) and suggest that alterations in tectal activity are associated with increases in postural asymmetry.

Various cell types have been identified in the SC that are associated with the initiation and completion of saccadic eye movements, including burst, build-up and fixation cells (Wurtz, 1996). Unilateral, electrical stimulation of the SC results in contralaterally-directed saccades (Robinson, 1972; Schiller and Stryker, 1972; Sparks and Mays, 1976). In our model, the relative increase in neuronal activity in the contralateral SAI and lateral SGI (as indicated by Fos-LI) likely produced a postural deviation towards the ODN-infused side, eliciting ipsiversive rotations. In fact, as the rotational activity of the animal increased, the number and intensity of Fos-positive nuclei in the contralateral SAI also appeared to increase, likely a result of a reduction in intracollicular inhibition from neurons of the ipsilateral SC (compare Figs.6.1E, 6.2D,6.3D). Whether the Fos-positive neurons in the contralateral SAI and lateral SGI are characteristic of burst neurons remains unclear. However, because high-rotators displayed near total neglect of the contralateral visual field, it is also possible that the immunopositive cells in the SAI and lateral SGI are active fixation neurons. Electrophysiological methods are necessary to make this distinction.

The increase in activity in the medial portion of the ipsilateral SGI suggests that these neurons are functionally distinct from those of the underlying SAI and the lateral

portion of the SGI. This is consistent with the observation that infusions of picrotoxin into the lateral portion of the intermediate layers produced tight, contraversive circling whereas more medial injections produced no postural deviation but did evoke violent motor activity, characterized by seizures, vertical leaping and defensive behavior (Kilpatrick et al.,1982). Neurons of the intermediate layers of the SC may also be distinguished by their efferent projections. Projections from SGI neurons appear to primarily innervate the ipsilateral cuneiform area and dorsolateral pons whereas those from the SAI cross the midline to the contralateral medulla and spinal cord (Dean and Redgrave, 1992). Further distinctions in the neuronal subpopulations of the intermediate SC are evident from examination of the spatiotemporal expression of the cytosolic, calcium-binding protein, calbindin-28kD. Adult rats express this protein in a pattern that appears strikingly similar to that of the Fos-LI reported here, with strong immunoreactivity in the medial portion of the SGI and relatively low expression in the bulbous, lateral extension of this layer or the underlying SAI (Dreher et al.,1996). Thus, there appears to exist major functional and physiological differences between inter- and intralaminar subpopulations of SC neurons.

A subpopulation of nigrotectal neurons exists that are immunopositive for both tyrosine hydroxylase (TH) and glutamic acid decarboxylase (GAD), suggesting the co-localization of dopamine and GABA (Takada and Hattatori, 1988; Campbell et al.,1991). It is possible that certain subpopulations of collicular neurons are innervated by excitatory dopaminergic terminals, whereas others receive solely inhibitory GABAergic signals, thus producing opposing effects on SC activity (Fig.6.5A).

Alternatively, the increase in SGI activity may be the result of a reduction in inhibitory intracollicular neurotransmission. There is evidence to support the existence of GABAergic interneurons in the SC (Mize *et al.*,1981,1982; Mize, 1988). Activation of excitatory SAI neurons may stimulate, not only contralateral oculomotor systems, but also interneurons that inhibit activity of cells in adjacent layers. Increased inhibition of the SAI, through elevated nigral activity, would reduce the stimulation of the GABAergic interneurons and, thus, disinhibit the SGI neurons (Fig.6.5B).

The specific roles of ascending nigrothalamic and descending nigrotectal circuits in producing rotational behavior remain unclear. While previous studies have suggested that the thalamus mediates the rotational behavior produced by intranigral infusions of muscimol, transection of nigrothalamic circuits reduced circling but not postural asymmetry in these animals (Gale and Iadorola, 1980). However, posturing was reduced by collicular damage (Kilpatrick *et al.*,1982; Leigh *et al.*,1983; Scheel-Kruger, 1986). Thus, circling behavior appears to consist of locomotor and postural components, mediated through nigrothalamic and nigrotectal circuits, respectively. The results of this study provide support for the involvement of the SC in rotational behavior that is evoked by changes in basal ganglia neurotransmission. However, it remains unknown whether both the suppression and enhancement of neuronal activity in the SAI and SGI, respectively, are necessary to mediate the postural deviation in these animals.

Figure 6.1 Organization and Fos induction in the SC of non-rotating animals. A) Schematic representation of the SC, illustrating the laminar organization of this structure. Fos-LI was quantified in the medial SGI, represented by the filled region. The arrowheads in A) and B) point to approximately corresponding regions of the SGI. B)-E) Representative low (B,C) and high (D,E) magnification micrographs showing Fos-LI in the SC ipsilateral (B,D) and contralateral (C,E) to basal ganglia ODN infusions in animals of group I (Δi-c < 50). The boxed area in B) represents the corresponding regions magnified in D) and E). Examination of Fos-LI in these animals revealed a diffuse pattern of expression, with the majority of immunoreactivity in the lateral portions of the SGI and SAI. No apparent differences were noted between the Fos-LI of the ipsilateral SC and that of the contralateral side. Scale bar in B) represents magnification of B) and C) while that in D) indicates magnification of D) and E). Scale bars represent 100 μm. SZ: stratum zonale; SGS: stratum griseum superficiale; SO: stratum opticum; SGI: stratum griseum intermediale; SAI: stratum album intermediale; SGP: stratum griseum profundum; SAP: stratum album profundum; PAG: periaquaductal gray

A

SZ
SGS
SO
SGI
SAI
SGP
SAP   PAG

B

C

E
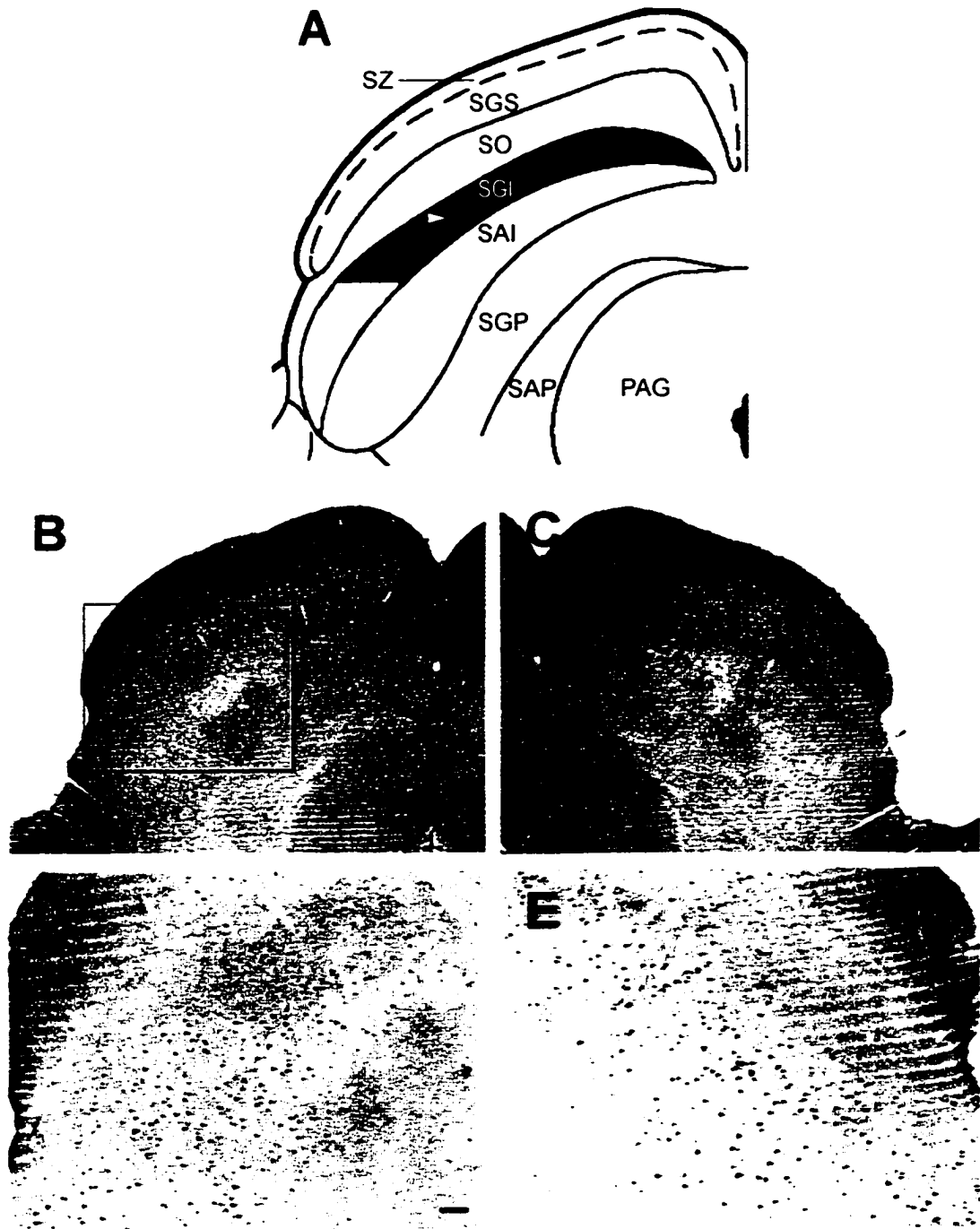
FIGURE 6.1

Figure 6.2 Fos-LI in the SC of group III animalsRepresentative low (A,B) and high (C,D) magnification micrographs of the SC ipsilateral (A,C) and contralateral (B,D) to basal ganglia ODN infusions in animals of group III (Δi-c= 500-1000). Note the apparent reduction of Fos-LI in the SAI of the ipsilateral SC relative to the abundant immunolabeling seen in the opposite side (see arrowheads in C and D). The medially-projecting band of the SGI is labeled with Fos-LI, which extends from the lateral to medial border of this lamina. The contralateral SGI (B,D) shows only sparse Fos-LI in this region. The boxed area in A) represents the corresponding regions magnified in C) and D). The animal in this figure rotated 788 : 38 turns in 2 hours (ipsiversive:contraversive). Scale bar in A) represents magnification of A) and B) while that in C) indicates magnification of C) and D). Scale bars represent 100 μm.
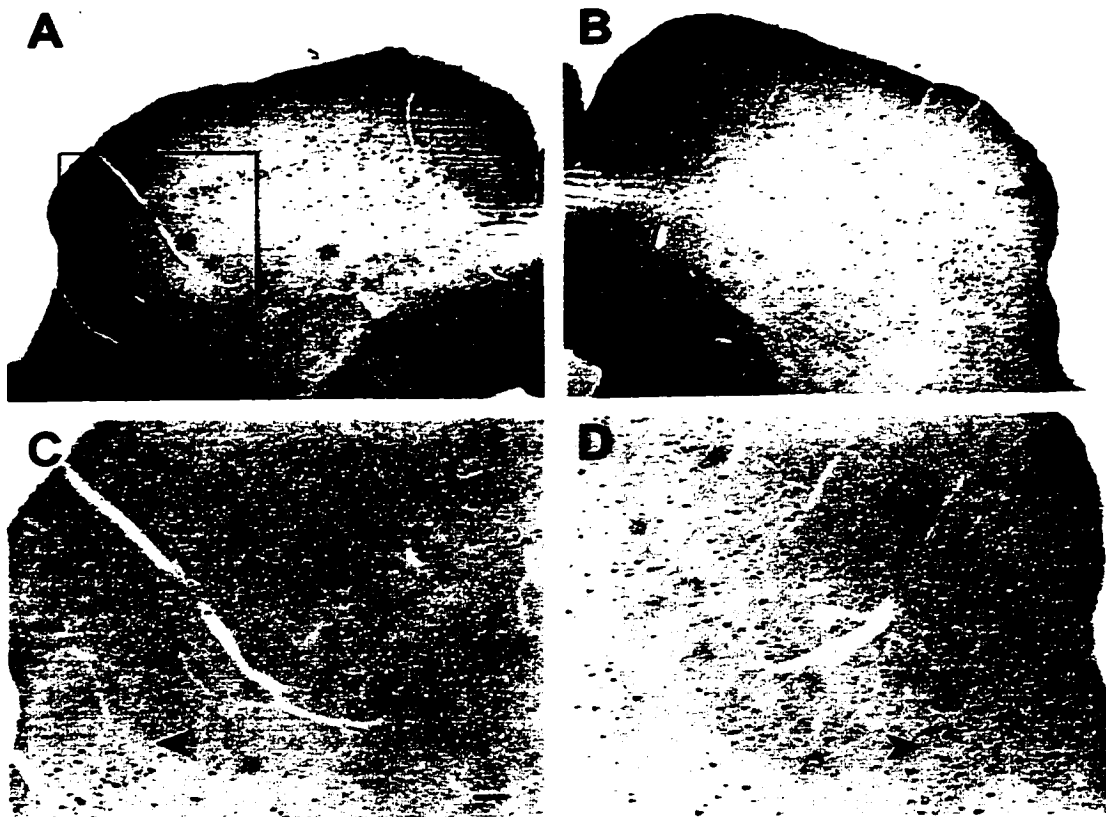
FIGURE 6.2

Figure 6.3   Fos-LI in the SC of group IV animals.Low (A,B) and high (C,D)

magnification micrographs of the ipsilateral (A,C) and contralateral (B,D) SC showing

typical Fos-LI in animals of group IV (Δi-c > 1000). Note the robust increase in Fos-

LI in the ipsilateral SGI that is associated with an extensive reduction in the underlying

SAI and the lateral portion of the SGI. This intense banding pattern is typical of the

ipsilateral SC in animals that demonstrated high degrees of rotation. While neurons of

SGI and SAI in the contralateral SC (B,D) express diffuse Fos-LI, those of the

ipsilateral SC have apparently undergone massive alterations in activation. The animal

in this figure rotated 1612 : 3 turns in 2 hours (ipsiversive:contraversive). The boxed

area in A) represents the corresponding regions magnified in C) and D). Scale bar in

A) represents magnification of A) and B) while that in C) represents magnification of

C) and D). Scale bars represent 100 µm.
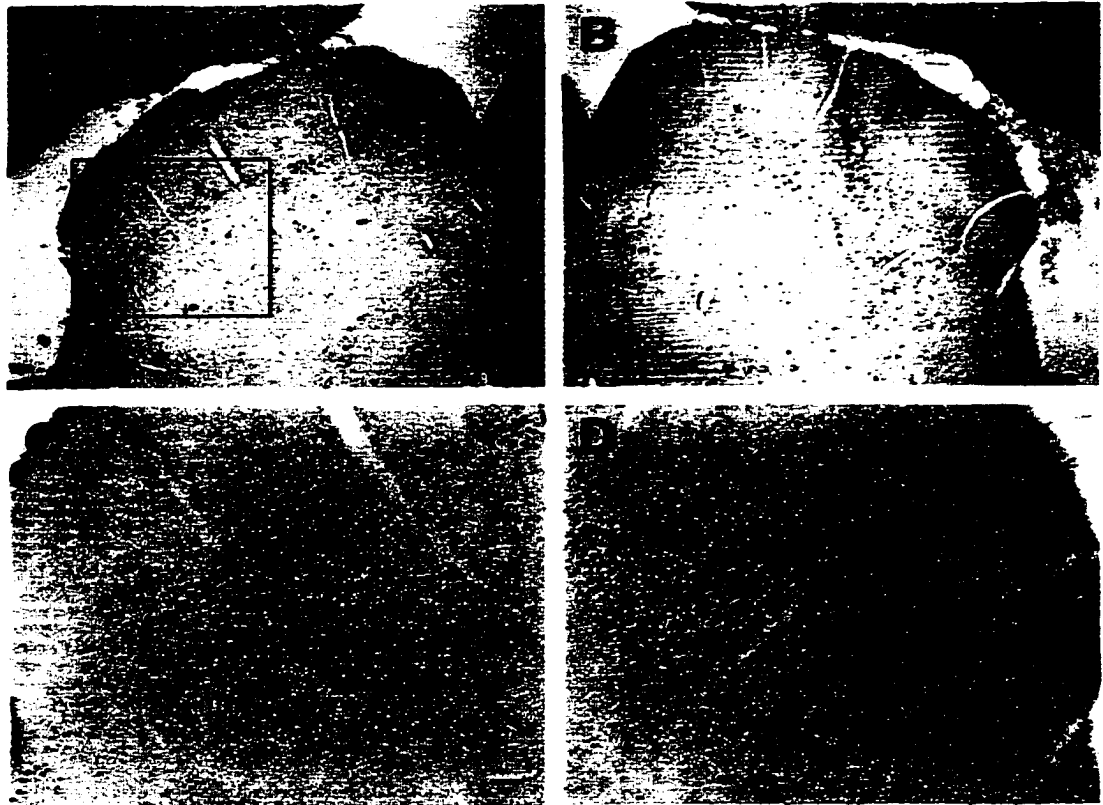
FIGURE 6.3

Figure 6.4   Correlation between rotational behavior and Fos-LI in the SC. A) Rotational and SGI Fos-LI data from groups I-IV. The ipsiversive rotational bias, represented by the histogram, indicates the progressive increase in ipsiversive rotations elicited among groups. This enhancement in rotation was paralleled by an increase in the number of Fos-positive nuclei in the ipsilateral SGI (line graph). * = significant ipsiversive rotation; # = significant increase in Fos-LI (relative to contralateral expression) B) Regression analysis revealed a significant, positive correlation between the number of Fos-positive nuclei and the intensity of ipsiversive rotation (R= 0.652, P= 0.0004). The relationship is represented by the linear function y= 0.123x + 143.2 (y = Fos-positive nuclei and x = Δi-c). The solid line represents the regression fit; dashed lines enclose the 95% confidence interval for the data.
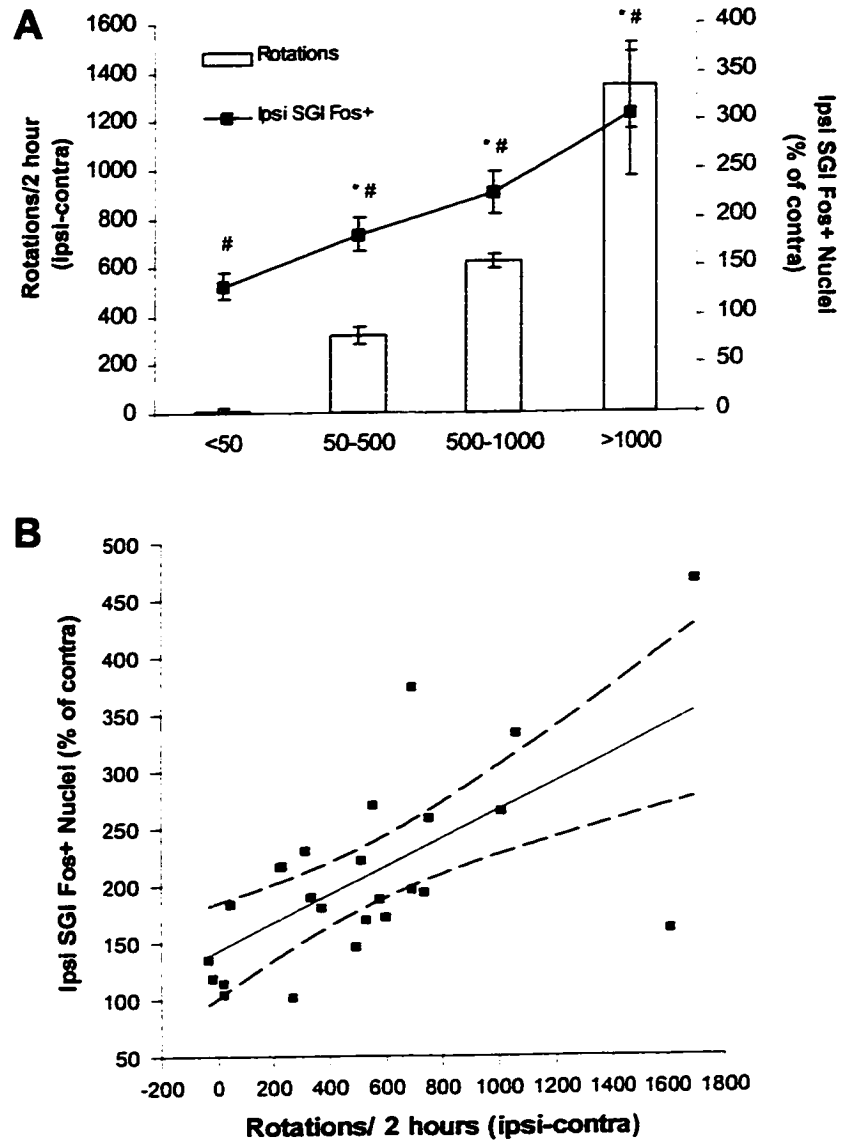
FIGURE 6.4

Figure 6.5 Two hypotheses that explain the reciprocal action of increased SNR activity on the SGI and SAI of the SC. A) Stimulation of the SNR may activate several distinct subpopulations of nigrotectal neurons. It is possible that efferent projections co-localizing both inhibitory and excitatory neurotransmitters (i.e. GABA and DA) innervate the medial portion of the ipsilateral SGI. Strong stimulation of such circuits may excite, rather than inhibit, post-synaptic terminals. Alternatively, disinhibition of pure GABAergic nigrotectal efferents to the SAI and lateral regions of the SGI would produce strong inhibition of neuronal activity in these areas. B) The nigrotectal efferents which become hyperactive in this model may be purely GABAergic and inhibit excitatory tectal projections which synapse onto inhibitory GABAergic interneurons in the SC. These interneurons are likely important mediators of intracollicular regulation. Thus, neurons of the SAI and lateral SGI may be responsible for inhibiting the cells of the medial SGI via stimulation of interneurons. Reducing the activity of the former cells would decrease the stimulation of GABAergic interneurons and, hence, disinhibit the target SGI neurons. SZ: stratum zonale; SGS: stratum griseum superficiale; SO: stratum opticum; SGI: stratum griseum intermediale; SAI: stratum album intermediale; SGP: stratum griseum profundum; SAP: stratum album profundum
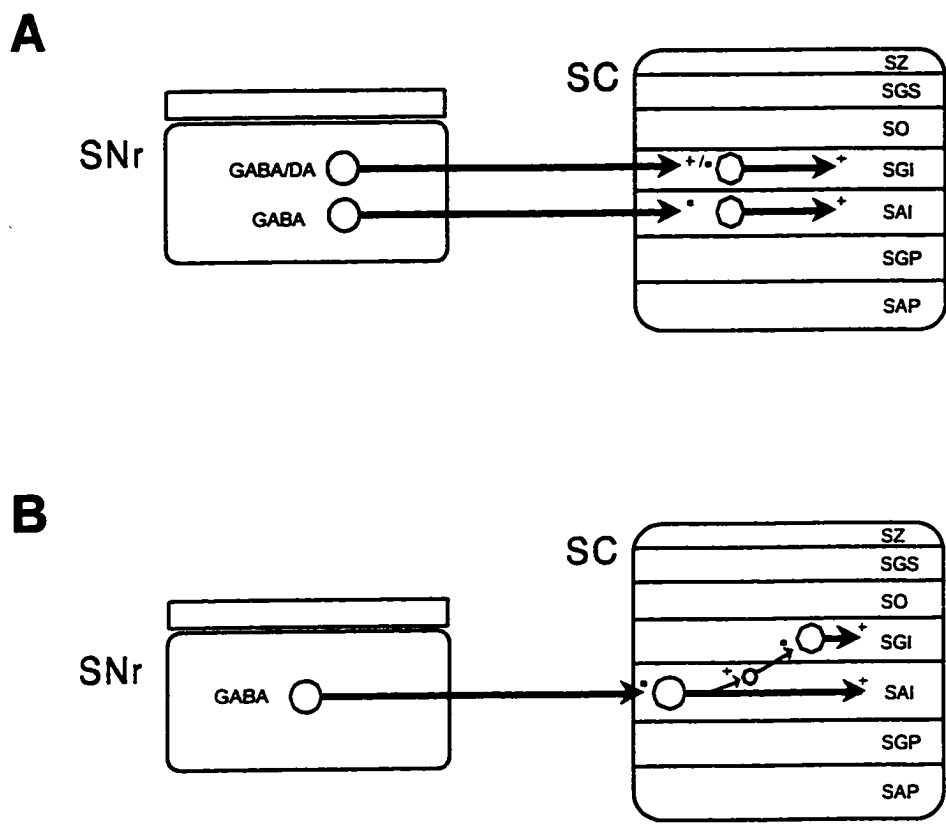
FIGURE 6.5

CHAPTER 7

A Comparative Study of Subcortical Alterations Between Rodent Models of Parkinson's and Huntington's Diseases[*]

[*] Results presented in this chapter have been submitted for publication.

7.1. Introduction

Parkinson's disease (PD) and Huntington's disease (HD) are progressive, neurodegenerative conditions of the basal ganglia that produce motor impairment. The pathology of PD involves the loss of nigrostriatal dopamine (DA) neurons in the substantia nigra pars compacta (SNC) and the development of rigidity and bradykinesia (Lee, 1987; Agid, 1991). HD produces marked atrophy of the striatum and neocortex and is characterized by choreiform movements and cognitive decline, with bradykinesia and rigidity often occurring in late-stage HD (Storey and Beal, 1993; Harper,1996). Different animal models have been developed to study the distinct pathophysiologies of the two diseases. While 6-hydroxydopamine (6-OHDA)-lesioning of the nigrostriatal DA system has become widely accepted as a model of PD in rats (Ungerstedt, 1968; Schwarting and Huston, 1996), animal models of HD have focused on the striatum as a general site of pathology, using lesioning techniques or other methods to suppress regional activity.

The etiology of the motor abnormalities produced in HD and PD remains unclear, but it is apparent that the distinct symptomatology produced by these conditions results from disease-specific alterations in motor circuits. However, the bradykinesia and rigidity produced in both PD and late-stage HD suggest that the pathological changes that are induced by these diseases eventually affect common regions or circuits in the brain. Although there have been numerous reports of changes in various cerebral nuclei in both PD and HD, there are currently no descriptions of a systematic comparison between the pathophysiologies of these conditions based on functional mapping of activity in the central nervous system.

Several groups have shown that intrastriatal infusions of antisense oligodeoxynucleotides (ODNs) that target the immediate early genes (IEGs), c-*fos* or *ngfi*-a, can effectively suppress protein expression and produce significant motor abnormalities and rotational behavior following stimulant challenge (Chiasson *et al.*,1992,1994; Dragunow *et al.*,1993,1994; Heilig *et al.*,1993; Sommer *et al.*,1993; Hooper *et al.*,1994; chapters 3 and 4). We have previously shown that suppression of IEG expression in the striatum produced an increase in IEG expression in the ipsilateral globus pallidus (GP) (chapter 4). Also, Sommer et al. (1996) have demonstrated that striatal infusions of antisense ODNs targeting c-*fos* mRNA significantly reduced the levels of neurotransmitter release in the substantia nigra (SN). Thus, suppression of IEG expression in the striatum inhibits the activity of the striatal projection neurons and directly affects both the gene expression and neurotransmitter release in effector nuclei, such as the GP and SN. Presently, we have used infusions of antisense ODNs targeting c-*fos* to create an animal model of the striatal dysfunction in HD.

In attempt to correlate motor impairment with alterations in cerebral activity using animal models of PD and HD, we have compared the changes in neuronal activation that result from 6-OHDA-lesioning of the nigrostriatal DA pathway with those produced by antisense ODN-induced suppression of striatal IEG expression. We report differential expression of stimulant-induced Fos-like immunoreactivity (Fos-LI) in the following motor-related nuclei: striatum, GP, substantia nigra pars reticulata (SNR), entopeduncular nucleus (EPN), ventromedial nucleus of the thalamus (VMT), superior colliculus (SC) and the oral pontine reticular formation (RPO).

7.2. Materials and Methods

7.2.1. Experimental Design The subjects were 29 adult Sprague-Dawley rats (28 male, 1 female) weighing 275-400 grams. Two groups of animals received an unilateral lesion of the nigrostriatal pathway using 6-OHDA (PD model) and were subsequently challenged with d-amphetamine (6-OHDAamp group; n=7) or apomorphine (6-OHDAapo group; n=11). A third group of animals received unilateral infusion of antisense ODNs targeting c-fos into the striatum (HD model), followed by administration of d-amphetamine (ASF group; n=11).

7.2.2. Surgical Procedures All surgeries were performed under halothane-induced anesthesia with the animals mounted in a Kopf stereotaxic apparatus. Both 6-OHDA and ODN infusions were performed by pressure injection using a CMA 100 (Carnegie-Medicin) microinjection pump with 25-gauge steel cannula. All stereotaxic coordinates are given according to Paxinos and Watson (1997). Animals that received 6-OHDA lesions were treated with desipramine (25 mg/kg, i.p.) 30 minutes prior to infusion of 6-OHDA (4 μl of 12 mM solution at 0.5 μl/min) into the right medial forebrain bundle (coordinates from bregma: AP -3.6mm, LAT 2.0 mm, DV -8.8 mm). After infusion, the cannula was left in place for an additional two minutes to allow for diffusion away from the injection site. Following surgery, the skin was sutured and animals were left to recovery for 21 days before behavioral testing.

Animals of the ASF group received bilateral placement of cannulae into the striata (coordinates from bregma: AP 1.0 mm; LAT ± 3.0 mm; DV -6.0 mm). The right striatum was infused with anti-c-fos ODNs (2 μl of 1 mM solution at 0.25 μl/min)

while the left striatum received an equal volume of vehicle. After infusion, the cannulae were left in place for an additional two minutes. The skin was then sutured and the animals were left to recover for 1 hour before behavioral testing. This post-operative latency had been previously established as the period of optimal suppressive effects of ASF (chapter 3).

Infusion of 6-OHDA or ODNs was performed unilaterally in order to produce motor asymmetry and to leave an intact, contralateral system with which to compare interhemispheric differences in neuronal activation. The expression of c-*fos* was used to map the functional (metabolic) activation of neural circuitry (Sagar *et al.*, 1988; Dragunow and Faull, 1989) by the psychostimulant drugs, *d*-amphetamine and apomorphine. In 6-OHDA-lesioned animals, administration of indirect (*d*-amphetamine) or direct (apomorphine) DA agonists stimulated opposing motor circuitry and induced rotational behavior in different directions, thus permitting comparison between the activation of specific nuclei and the direction of rotation. Administration of *d*-amphetamine induced ipsiversive rotational behavior in both 6-OHDAamp and ASF groups and allowed comparison of alterations in motor-related nuclei that were produced by either a loss of mesencephalic DA afferents or direct suppression of striatal efferent activity.

7.2.3. Behavioral and Immunohistochemical Analyses Following the appropriate recovery periods, animals were given intraperitoneal injections of either *d*-amphetamine (5 mg/kg; 6-OHDAamp and ASF groups) or apomorphine (0.5 mg/kg; 6-OHDAapo group) and placed in a rotometer where the number and direction of the rotations made

by the animal were recorded in 10 minute intervals for a period of 2 hours. After behavioral testing, animals were deeply anesthetized with sodium pentobarbital (>100 mg/kg) and transcardially perfused, initially with saline, followed by 4% paraformaldehyde in a 0.1 M phosphate buffer solution (pH 7.4). Brains were subsequently removed and post-fixed at 4°C until further analysis. Brains were blocked, cut on a Vibratome in 50 μm coronal sections, and processed for c-Fos immunoreactivity as previously described in section 3.2.2..

7.2.4. Oligodeoxynucleotides The antisense ODN to c-*fos*, called ASF, has been described in section 3.2.3.. We have previously demonstrated the specificity of end-capped ASF in the striatum through the comparison of its suppressive actions with the effects of vehicle infusions and two distinct random ODNs (chapters 3, 4 and 5). We, and others, have also demonstrated the specificity of the same ODN sequence in both partially and fully phosphorothioate forms, using mismatch and sense controls (Chiasson et al.,1992; Heilig et al.,1993; Hooper et al.,1994; Sommer et al.,1996). Unilateral infusions of control ODNs (random, sense, mismatch) or vehicle into the striatum produced negligible motor asymmetry and minimal suppression of stimulant-induced c-*fos* expression. Thus, the behavioral and neurophysiological effects described below in the ASF group have been attributed to the specific inhibition of c-*fos* expression and are not produced by non-specific ODN or vehicle infusions.

7.2.5. Quantification of Fos-LI and Statistical Analysis Sections were selected from each region at approximately the following anteroposterior coordinates (from bregma): striatum, +1.5mm; GP, -0.8mm; SNR, -5.8mm; EPN, -2.3mm; VMT, -2.8mm; SC, -

6.3mm; RPO, -7.3mm, and subsequently processed for Fos-LI. Because tissue from several animals was used in unrelated studies, the number of animals used to analyse a specific brain region may be less than that reported for the behavioral studies. The number of animals used in the analysis of each region is given in Figure 7.9. Specific areas were scanned and digitized using a CCD camera (JVC, Tokyo). Each region of interest was isolated, as indicated above, and the number of Fos-positive nuclei per area was calculated using NIH densitometry software.

Statistical analysis was performed using SigmaStat software. All groups of data were initially tested for normality and equal variance, with subsequent comparisons between ipsiversive and contraversive values made accordingly using either a Student's T-test or Mann-Whitney U-test. Multiple comparisons were made between groups using a one-way analysis of variance (ANOVA) followed by a post-hoc Newman-Keuls test. Significance was assumed at $P < 0.05$.

7.3. Results

7.3.1. Behavioral Analysis of 6-OHDA and ASF Animals

Animals of the 6-OHDAapo group exhibited contraversive circling that commenced within 5 minutes of apomorphine injection, with a peak intensity of 70 turns/10 minutes measured at 40 minutes after stimulant administration (Fig. 7.1A). The intensity of this behavior rapidly diminished and the animals were then sedentary and hypoactive by 90 minutes after drug administration. The total mean rotations for this group was significantly greater to the contralateral side: 3.2 ± 0.9 ipsiversive : 281.6 ± 38.2 contraversive ($P < 0.0001$; Fig. 7.1B). In contrast to the rapid onset and decline of apomorphine-induced behavior, d-amphetamine elicited ipsiversive circling in 6-OHDAamp animals that commenced approximately 10-20 minutes following drug delivery. The circling intensity peaked at 60 minutes post-administration, with an intensity of ~70 turns/10 minutes. The circling activity persisted throughout the 120 minute testing period and the animals continued to turn when removed from the rotometer until the anesthetic took effect. The total mean number of rotations elicited in the 6-OHDAamp group was significantly greater in the ipsiversive direction: 585.4 ± 100.5 ipsiversive : 2.3 ± 1.1 contraversive ($P = 0.0006$).

Amphetamine also induced ipsiversive circling in the ASF group. The peak circling intensity was less pronounced in this group in comparison to the 6-OHDAamp animals, peaking at approximately 30 minutes post-administration, with a maximum of 51 turns/10 minutes (Fig. 7.1A). As in the 6-OHDAamp group, the stimulant effects of d-amphetamine persisted throughout the testing period and the animals usually had

some degree of motor asymmetry remaining after 120 minutes. There was a significantly greater mean number of ipsiversive than contraversive rotations in the ASF group: 305.3 ± 53.0 : 21.5 ± 7.6 (P<0.0001; Fig. 7.1B). While the ipsiversive rotational behavior elicited by d-amphetamine in the 6-OHDAamp and ASF groups was similar in duration, the 6-OHDAamp animals appeared to have a heightened sensitivity to the stimulant, as reflected in the significantly greater number of turns elicited in this group. Comparison of absolute numbers of rotations among 6-OHDAamp (ipsiversive), 6-OHDAapo (contraversive) and ASF (ipsiversive) groups revealed that 6-OHDAamp animals turned significantly more than 6-OHDAapo (P=0.0045) or ASF (P=0.0033) animals. There was no difference in the absolute number of rotations produced between 6-OHDAapo and ASF groups (P=0.7856).

7.3.2. Expression of Fos-LI

7.3.2.1. Striatum. The dose of d-amphetamine used in these studies (5 mg/kg) was sufficient to induce robust Fos-LI in the striatum of naive animals (chapter 4). In contrast, the dose of apomorphine (0.5 mg/kg) produced negligible Fos-LI in naive animals, but robust expression in DA-depleted animals. In the ipsilateral striatum of 6-OHDAamp animals, there was significantly less Fos-positive nuclei than in the contralateral side (P=0.0045; Fig. 7.2A). This expression that was diffusely distributed, without preferential localization to striosomes. In the contralateral striatum, there was robust expression of Fos-LI in striosomal-like patches (Fig. 7.2B), as previously reported (Graybiel et al.,1990). In 6-OHDAapo animals, apomorphine induced intense, homogeneous Fos-LI in DA-depleted (ipsilateral) striata (Fig. 7.2C),

but negligible expression in contralateral, intact striata (Fig. 7.2D, P=0.0022, ipsilateral vs. contralateral expression).

Intrastriatal infusion of ASF resulted in a significant suppression (~65%) of *d*-amphetamine-induced Fos-LI (P<0.0001). This suppression was confined to the infused striatum and did not extend into the overlying cortex (not shown) or into the contralateral hemisphere (Fig. 7.2E,F). The greatest suppressive effects were observed near the cannula tract and extended in a graded fashion to the borders of the striatum. In the area of greatest suppression, there was a near total absence of Fos-LI.

7.3.2.2. Globus Pallidus. Administration of *d*-amphetamine produced scant, but distinct Fos-LI in the GP of naïve animals. We observed approximately 60 Fos-positive nuclei/coronal section. In the 6-OHDAamp group, however, this expression was significantly reduced in the ipsilateral GP (P=0.0314; Fig. 7.3A,B). A similar reduction of Fos-LI was observed in the contralateral GP of 6-OHDAapo animals (P=0.0079; Fig. 7.3C,D). In contrast, animals of the ASF group had a significant increase in the number of Fos-positive nuclei in the ipsilateral GP, but typical induction of Fos-LI on the contralateral side (P=0.0317; Fig. 7.3E,F).

7.3.2.3. Substantia Nigra Pars Reticulata. In the 6-OHDAamp group, there was a significant increase in the number of Fos-positive nuclei in the ipsilateral SNR, particularly in the ventromedial region (P=0.0152; Fig. 7.4A,B). The nuclear labeling in these animals was intense and delineated large round nuclei. In 6-OHDAapo animals, there was also a significantly greater number of cells with Fos-LI in the ipsilateral than contralateral SNR (P=0.0215; Fig. 7.4C,D). However, the ipsilateral

SNR of 6-OHDAapo animals had an abundance of small, lightly-stained nuclei, with fewer large, darkly-stained nuclei. When absolute numbers of Fos-positive nuclei were compared between hemispheres, these smaller cells significantly outnumbered the larger nuclei in the contralateral SNR. In contrast, the contralateral SNR of 6-OHDAapo animals expressed abundant Fos-LI that was solely localized to large-diameter, darkly-stained nuclei. This contralateral labeling appeared similar to that observed in the ipsilateral SNR of 6-OHDAamp animals (compare Fig. 7.4A and 7.4D).

In contrast to the significant differences in Fos-LI induced in the SNR between hemispheres of 6-OHDA-lesioned animals, ASF animals had minimal Fos-LI in both ipsilateral and contralateral SNR, with no apparent differences between sides (P=0.2424; Fig. 7.4E,F). The expression of Fos-LI in the SNR of ASF animals was indicative of that induced by d-amphetamine (5 mg/kg) in naive animals (not shown).

7.3.2.4. Entopeduncular Nucleus. The ipsilateral EPN of both 6-OHDAamp and ASF groups exhibited a significantly greater number of Fos-positive nuclei than the contralateral side (P=0.0079; P=0.0023, respectively; Fig. 7.5). Also, the contralateral EPN of 6-OHDAapo animals exhibited significantly more Fos-positive nuclei than the same region in 6-OHDAamp or ASF groups (P=0.00035; P=0.00045, respectively). However, as in the ipsilateral SNR of these animals, the majority of Fos-LI in the ipsilateral EPN was localized to small, lightly-stained nuclei, significantly outnumbering the Fos-positive nuclei of the contralateral side (P=0.0317).

7.3.2.5. Ventromedial Thalamus. The VMT had marked alterations in Fos-LI in all animal groups. Consistent with an increased inhibitory output from the SNR, the ipsilateral VMT had a significant reduction in Fos-LI compared to the contralateral side in 6-OHDAamp animals (P=0.0146; Fig. 7.6A,B). A significant reduction was also observed in the ipsilateral VMT of ASF animals (P=0.0137; Fig. 7.6E,F). In contrast, the 6-OHDAapo group had a significant decrease in Fos-LI expression in the contralateral VMT (P=0.0448; Fig. 7.6C,D).

7.3.2.6. Superior Colliculus. Administration of *d*-amphetamine (5mg/kg) typically induced modest expression of Fos-LI in control SCIG (~80-100 cells; Fig. 7.7B,F). ASF animals had a significant increase in Fos-LI in this region, which produced a band of immunoreactivity in the medio-lateral direction across the SC (P=0.0152; Fig. 7.7E). Animals of the 6-OHDAamp group appeared to show a trend of increased Fos-LI in the ipsilateral SCIG, but this increase did not reach statistical significance (P=0.2249; Fig. 7.7A). In contrast, 6-OHDAapo animals had significantly greater expression of Fos-LI in the contralateral SCIG (P=0.0003; Fig. 7.7D).

Significant alterations in Fos-LI were observed in the SCIW of all animal groups. The Fos-LI induced by *d*-amphetamine was similar in the 6-OHDAamp and ASF animals, with significant reductions in the ipsilateral SCIW in both groups (P=0.0192 and 0.0340, respectively). As in the SCIG, animals of the 6-OHDAapo group had a reciprocal expression pattern, with abundant Fos-LI in the ipsilateral SGIW but significantly reduced expression on the contralateral side (P=0.004; Fig. 7.7).

7.3.2.7. Oral Pontine Reticular Formation. Alterations in the expression of Fos-LI in the RPO were prominent in the 6-OHDAamp group. Most animals in this group had a near total absence of Fos-LI in the ipsilateral RPO, with abundant expression on the contralateral side (P=0.0022; Fig. 7.8A). In contrast, the 6-OHDAapo group appeared to have a larger number of Fos-positive nuclei in the ipsilateral RPO. However, the difference between hemispheres in this group did not reach statistical significance and, in many animals, there were no alterations in this region (P=0.2588; Fig. 7.8B). Animals of the ASF group also had no difference between ipsilateral and contralateral expression of Fos-LI in the RPO (P=0.6472; Fig. 7.8C).

7.4. Discussion

In the present study, comparison of the pharmacological induction of Fos-LI in PD (6-OHDA) and HD (ASF) models revealed similar changes in the striatum, EPN, VMT and SCIW, with corresponding trends in the SNR and the SCIG. In contrast, these treatments produced markedly different alterations in Fos-LI in the GP and RPO. In both models, significant, stimulant-induced locomotor asymmetry was manifested as rotational behavior. In order to assess the extent to which asymmetric activation of these various nuclei contributed to rotational behavior, the pattern of Fos-LI was compared between 6-OHDA animals that were challenged with either d-amphetamine or apomorphine. As these stimulants induced circling in opposite directions in 6-OHDA-lesioned animals, nuclei that did not undergo reciprocal changes in Fos-LI presumably had little contribution to this behavior. The majority of regions analyzed exhibited reciprocal expression of Fos-LI between 6-OHDAamp and 6-OHDAapo groups and, therefore, could not be excluded from contributing to the motor asymmetry in DA-depleted animals. However, the disparity between locomotor bias and alterations of Fos-LI in the GP and RPO of 6-OHDAamp and ASF animals clearly demonstrated the distinct physiological effects produced by alterations of nigral and striatal transmission.

7.4.1. Rotational Behavior. In the present study, the temporal pattern of circling activity elicited by d-amphetamine was similar in 6-OHDAamp and ASF groups. However, compared to ASF animals, those of the 6-OHDAamp group exhibited a longer duration of turning behavior and both a greater peak intensity and total number

of rotations. The heightened response of lesioned animals was paralleled by greater differences in Fos-LI between hemispheres in 6-OHDAamp than in ASF animals, particularly in the striatum, VMT and SNR. Previous studies suggested that the difference in rotational intensity between these groups was produced, in part, by the differential activation of the GP. We have previously demonstrated that increased activity of the GP in ASF animals was correlated with the intensity of circling behavior and that elimination of this pallidal influence increased the total number of rotations three-fold (chapter 5). Thus, the increase and decrease in GP activity of ASF and 6-OHDAamp animals, respectively, could account for the variation in behavioral responses to psychostimulant challenge (Fig. 7.10).

7.4.2. Alterations in c-Fos Expression

7.4.2.1. Striatum. It has been previously reported that 6-OHDA lesions produced a sustained expression of Fos-LI in the ipsilateral striatum that was predominantly confined to neurons projecting to the GP (Jian *et al.*, 1993; Doucet *et al.*, 1996). The diffuse, but relatively abundant, Fos-LI in the ipsilateral striatum of 6-OHDAamp animals prompted us to test our antibody to determine if it recognized Fos antigens in unstimulated, 6-OHDA-lesioned animals. Only sparse Fos-LI (~ 10-15 Fos-positive nuclei/coronal section) was observed in the ipsilateral striatum of unstimulated animals (not shown). The substantially larger number of labeled cells (~ 900 Fos-positive nuclei/coronal section) in the equivalent region of 6-OHDAamp animals indicated that this expression had been stimulant-induced and was not a sustained expression evoked by the lesion. The discrepancy between the previously reported, chronic Fos-LI and

that observed in the present study may be explained by the number of Fos-related antigens (FRAs) that the antibody recognized. For example, Doucet *et al.* (1996) reported that their study used an antibody that recognized all members of the *fos* IEG (at least 5 distinct proteins). In contrast, we have previously shown that the antibody used in our studies recognizes primarily the 65 kDa isoform of c-Fos, and, to a lesser extent, a FRA of ~40 kDa (chapter 4). Therefore, it is likely that the majority of chronically expressed Fos-LI was produced by induction of FRAs and not the authentic c-*fos* gene.

Dopamine that is released into the striatum exerts its effects on striatopallidal (indirect pathway) and striatonigral (direct pathway) neurons predominantly by activation of D1 and D2 receptors, respectively (Robertson and Robertson, 1987; Gerfen *et al.*, 1990; Graybiel, 1990, 1991; LeMoine *et al.*, 1990, 1991). Because D1Rs are positively coupled and D2Rs are negatively coupled, to both adenylate cyclase and inositol phospholipid signaling pathways (Kebabian and Calne, 1979; Stoof and Kebabian, 1981; Mahan *et al.*, 1990), stimulation of these receptors increases transmission through direct, but decreases transmisson through indirect, striatal projections. Therefore, it is possible that the Fos-positive cells in the ipsilateral striatum of 6-OHDAamp animals projected to the SN and had received D1R stimulation by DA that was released from residual nigrostriatal fibers. However, the absence of tyrosine hydroxylase immunoreactivity in the striatum (not shown) and the pattern of Fos expression (i.e., not confined to striosomes) makes this an unlikely explanation. Alternatively, these cells may have projected to the GP and were

stimulated by a reduction in D2R-mediated inhibition, produced by the loss of DAergic innervation. However, the observation that far fewer Fos-positive nuclei were present in unstimulated striata suggested that other influences, i.e., corticostriatal afferents, likely contributed to the stimulation of these neurons in 6-OHDAamp animals. For example, the decrease in D2R-mediated inhibition of striatopallidal neurons in DA-depleted striata may render these cells hypersensitive to glutamatergic stimulation from the cortex. Thus, the reduction in D2R activity and increase in glutamatergic transmission (produced by stimulant administration) could synergistically activate striatopallidal neurons, whereas the reduction in D1R-mediated stimulation of striatonigral neurons would antagonize the cortical influence. This hypothesis is supported by recent studies that demonstrate DA-glutamate interactions in the striatum (Morelli, 1997; Ozer *et al.*, 1997; Lannes and Micheletti, 1997) and also the D2R-antagonist-mediated increase in extracellular glutamate concentrations in the EPN of 6-OHDA-lesioned animals (Biggs *et al.*, 1997).

7.4.2.2. Globus Pallidus. Both 6-OHDAamp and ASF groups had modest, but distinct, expression of Fos-LI in the contralateral GP, typical of that induced by *d*-amphetamine. The mechanism by which *d*-amphetamine induces pallidal Fos is unknown. One possibility is that DA is released onto excitatory D1 receptors from SNC afferents that either directly innervate or extend collaterals into the GP. However, the similar expression of Fos-LI in the ipsilateral GP of 6-OHDAapo animals and the lack of an exaggerated induction by apomorphine (as seen in the striatum, SNR and EPN), suggested that the induction of Fos in this region was mediated by changes

in striatal activity and not directly through dopaminergic stimulation. Alternatively, apomorphine (in DA-depleted striata) and d-amphetamine may reduce striatopallidal transmission through increased D2R activation. This hypothesis is supported by a study by Floran et al. (1997) that showed that methamphetamine or the D2 agonist, quinpirole, inhibited the release of γ-aminobutyric acid (GABA) in the GP of the rat. Also, Black et al. (1997) recently used positron emission tomography (PET) in the baboon to demonstrate that cerebral blood flow to the GP was significantly reduced following intravenous administration of a D2-selective agonist. Finally, in PD patients, Hutchinson et al. (1997) demonstrated that administration of apomorphine increased the firing rate of neurons in the GPe.

Of the regions analyzed, the GP exhibited the greatest difference in Fos-LI between 6-OHDAamp and ASF groups. In 6-OHDAamp animals, this expression was reduced by approximately 60%, but was increased by greater than 10-fold in ASF animals. Because striatopallidal neurons release GABA which suppresses GP activity, it is difficult to attribute the decrease in Fos-LI observed in 6-OHDAamp animals to a reduction in striatal activity. Alternatively, a reduction in striatal DA and subsequent decrease in D2R-mediated inhibition of striatopallidal neurons, would increase the inhibitory tone to the GP. This hypothesis is consistent with previous findings of increased expression of Fos-LI in striatopallidal neurons following 6-OHDA lesioning (Jian et al., 1993; Doucet et al., 1996). As intrastriatal infusion of ASF directly suppressed d-amphetamine-induced Fos-LI, presumably without affecting dopaminergic innervation, this treatment should not have produced a D2-mediated increase in

striatopallidal activity. The marked Fos induction in the ipsilateral GP following intrastriatal ASF infusion indicated that ASF-induced inhibition of striatopallidal activity was sufficient to disinhibit pallidal neurons and increase the Fos-LI in this region.

7.4.2.3. Substantia Nigra Pars Reticulata and Entopeduncular Nucleus. Animals of the 6-OHDAamp group had significant elevation of Fos-LI in both the ipsilateral SNR and EPN, whereas ASF animals had a marked increase in only the EPN. The ipsilateral EPN was altered to a similar extent in the ASF and 6-OHDAamp groups, suggesting that disruption of striato-EPN transmission may be suppressed independently of DA concentrations. As both groups had received equal doses of *d*-amphetamine, the smaller SNR response in ASF animals must be attributed to the influence (direct or indirect) of an intact dopaminergic system. This difference was not due to a lack of asymmetrical activation of motor circuitry in ASF animals, as evident by the widespread alterations in other nuclei, and may account for the greater behavioral effects observed in the 6-OHDAamp group. Additionally, the changes in the striatum and GP of these animals were consistent with the differential Fos-LI observed in the SNR. For example, the striatum of ASF animals appeared to have a reduction in activity of both direct and indirect circuits, whereas previous evidence suggested that 6-OHDA lesioning reduced direct, but increased indirect, neurotransmission (Jian *et al.*, 1993; Doucet *et al.*, 1996). The effects of these changes were observed in the GP and suggested that ASF animals had a decrease in striatonigral inhibition and a reduction in STN-mediated stimulation of the SNR

(produced by increased GP output). In contrast, 6-OHDAamp animals had inhibition of direct, striatonigral transmission and an increase in indirect, striatopallidal activity, thus reducing the inhibitory tone from the direct pathway and increasing STN-mediated stimulation of the SNR (Fig. 7.10). These distinct changes in afferent input to the SNR may have been sufficient to produce the observed differences in Fos-LI between 6-OHDAamp and ASF animals.

Animals of the 6-OHDAapo group exhibited a greater number of Fos-positive nuclei in both the ipsilateral SNR and EPN, relative to the contralateral side. This increase was inconsistent with the changes in other regions of the basal ganglia and brainstem, and with the observed behavioral effects (i.e., contralateral rotation). The Fos-LI on the ipsilateral side was predominantly confined to small, lightly stained nuclei, which may have been the result of a sensitized response to direct dopaminergic stimulation. The appearance of the same type of staining in both SNR and EPN of the 6-OHDA-lesioned hemisphere suggested that DA may play a major role in the regulation of these nuclei. This may have significant clinical implications, as PD therapy with apomorphine or L-DOPA would be expected to produce similar effects.

The pattern of Fos-LI in the ipsilateral SNR and EPN of 6-OHDAapo animals was not observed in 6-OHDAamp animals, excluding the possibility that it was caused by a gliosis-induced increase in endogenous peroxidase and increased diaminobenzidine reaction product. Because the ipsilateral SNR and EPN apparently did not exert a dominant influence on motor activity in 6-OHDAapo animals, the expression of Fos-LI in these regions may have been induced in cells that had only local projections. Also, the typical activation of downstream nuclei (i.e., VMT, SC) indicated that the response

of the ipsilateral SNR and EPN did not influence the activity of these other regions. Notably, however, the contralateral SNR and EPN of 6-OHDAapo animals expressed an increased level of Fos-LI in large, darkly-labeled nuclei. The number of Fos-positive nuclei was similar to that observed in the ipsilateral regions in 6-OHDAamp animals, suggesting that this induction was mediated by afferent projections and not direct stimulation of DA receptors.

7.4.2.4. Ventromedial Thalamus. The changes in Fos-LI in the VMT were consistent with the basal ganglia alterations in all groups and suggested that increased inhibitory tone from the EPN and SNR reduced thalamic stimulation. Because several ASF animals had negligible increases in SNR activity, the EPN was implicated in conveying the dominant input to the VMT. This is consistent with the dense innervation of thalamic regions, including the VMT, by EPN afferents (van der Kooy and Carter, 1981; Jimenez-Castellanos and Reinoso-Suarez, 1985; Moriizumi *et al.*, 1988; Finkelstein *et al.*, 1996).

7.4.2.5. Superior Colliculus. The SC is involved in the initiation of saccadic eye movements, head-eye coordination, postural control and species-specific defensive behaviors (Wurtz and Albano, 1980; Sahibzada *et al.*, 1986; Dean *et al.*, 1988; Dean and Redgrave, 1992). This structure receives projections from various cerebral and peripheral regions, including the cortex, basal ganglia, and retina (Nauta and van Straaten, 1947; Hopkins and Niessen, 1976; Beckstead and Frankfurter, 1983; Harvey and Worthington, 1990; Bickford and Hall, 1992). Two major efferent systems from the SC have been well characterized. 1. A contralateral projection in which the

majority of axons descend medially from the SC and cross the midline at the dorsal tegmental decussation. These fibers join the predorsal bundle (PDB) and innervate the medial pons and medulla, with some fibers projecting directly to the spinal cord. These tecto-reticulo-spinal neurons (TRSNs) represent the main premotor projection from the SC to the brainstem that mediates orientation of the head and eyes. 2. An ipsilateral projection sends fibers that terminate in the dorsolateral pons and cuneiform nucleus (CN), the activation of which produces increased avoidance and defensive behaviors (Waldron and Gwyn, 1969; Dean et al., 1986; Ellard and Goodale, 1986, 1988; Redgrave et al.,1987). Studies of the spatial distribution of ipsilaterally- and contralaterally-projecting cells have shown that they are predominantly localized to the intermediate and deep layers of the SC. Specifically, TRSNs appear to have a higher concentration in lateral regions of the intermediate layers, whereas ipsilaterally-projecting cells are located more medially (Redgrave et al., 1986; Westby et al., 1990).

The significant reduction of Fos-LI in the SCIW, ipsilateral to the hemisphere with increased SNR and EPN activity, was consistent with elevated GABA-mediated inhibition from the basal ganglia. This lateral region corresponds to the termination zones of nigrotectal afferents and contains the majority of TRSNs, the activation of which produces contralateral head and eye movements (Berthoz and Grantyn, 1986; Bickford and Hall, 1992). Thus, unilateral suppression of these cells would be expected to induce ipsiversive posturing, owing to the influence of the contralateral TRSNs. These expectations were met by all three animal groups in the present study.

The mechanism of stimulation and the functional role of SCIG activation is unclear. Previous studies have demonstrated that the expression of Fos-LI in SCIG cells increases with the degree of ipsiversive rotation in the animal (chapter 6). Westby et al. (1990) have used electrophysiological techniques to assign modality preferences to cells of the SC that project to the ipsilateral CN. It was determined that CN-projecting cells throughout the medial to lateral extent of the SCIG respond preferentially to visual stimuli. However, because the superficial layers of the SC are the primary retinorecipient areas of this structure (Linden and Perry, 1983; Dreher et al., 1985), SCIG stimulation may be mediated indirectly by glutamatergic, corticotectal afferents projecting from the frontal eye fields or somatosensory cortex. The paradoxical increase in SCIG activation has not been previously reported in Parkinsonian models, but may help explain the extensive variations in oculomotor abnormalities observed in both PD and HD (Avanzini et al.,1979; Shibasaki et al.,1979; Kennard and Lueck, 1989). In the present study, the changes in Fos-LI in the SC suggest that rotational activity may be caused, in part, by oculomotor and postural deviation that is induced by reciprocal stimulation and inhibition of SC laminae.

7.4.2.6. *Pontine Reticular Formation.* The pontine reticular formation (PRF) can be divided into ventral, lateral and medial components, the last of which contains primary premotor centres for the generation of saccadic eye movements and postural control of the head and neck (reviewed in Buttner-Ennever and Holstege, 1986). The PRF has been implicated in motor control (Peterson, 1979; Siegel, 1979), sensory modulation

(Baldissera *et al.*,1967), grooming and defensive behavior (Berntson, 1973) and learning processes (Kornblith and Olds, 1973; Thompson *et al.*,1984).

The oral division of the PRF (RPO) is a major relay centre in the pons that receives input from higher centres, as well as from the spinal cord. Anatomical tracing of the afferent projections to the RPO revealed dense innervation by the medial prefrontal cortex, zona incerta of the diencephalon, ipsilateral SC, as well as other regions of both the ipsilateral and contralateral reticular formation (Shammah-Lagnado *et al.*,1987). The RPO receives a less significant innervation from the ipsilateral SNR and CN. The RPO and its caudal counterpart, RPC, innervate many common oculomotor-related regions of the brainstem, including the abducens nucleus, SCIG, anterior pretectal nucleus, ventral lateral geniculate nucleus and regions of the central gray directly bordering the oculomotor nucleus (Vertes and Martin, 1988). Efferent fibers from the RPO also innervate numerous ipsilateral and contralateral reticular sites and project fibers throughout the cervico-sacral extent of the spinal cord (Jones and Yang, 1985). The functional differences between the ipsilaterally-projecting, reticulo-spinal neurons (RSNs) and contralaterally-projecting TSRNs have been reviewed by Berthoz and Grantyn (1986). In the cat, ipsiversive orienting behavior was correlated with the activation of RSNs while contraversive orienting behavior was correlated with TRSN activity. It was hypothesized that these two circuits influence head-eye coordination by the convergence of their signals on spinal motoneurons. The final output of RSNs, which receive input from TRSNs, is dependent upon the composite excitatory/inhibitory influences on reticular cells. The authors caution, however, that

the correlation of saccade generation with TRSN activity is relatively low compared to that of other nuclei (i.e., periabducens area) and suggest that the TRSN/RSN influence represents a primitive orienting system that has been superseded by more precise mechanisms.

Our analysis of changes in Fos-LI in the RPO of 6-OHDAamp animals revealed a mean decrease of 66% in the ipsilateral hemisphere. In this group, every animal (n=6) exhibited a marked decrease in ipsilateral Fos-LI, with several animals displaying a near total ipsilateral suppression in this nucleus. In contrast, ASF animals exhibited robust Fos-LI in the RPO of both hemispheres, with no differences between sides. These results support the comments made by Berthoz and Grantyn (1986) that suggested that the orientation bias and rotation in both of these groups were most likely dominated by systems other than the RPO. The influence of the asymmetric RPO activation on motor control in 6-OHDAamp animals remains unclear. If these RPO cells projected to the ipsilateral spinal cord, the unilateral suppression of RPO activity would be expected to produce an orientating response in the contralateral direction. The function of the contralateral spinal projection of RPO neurons remains unclear, but likely acts to reduce motor activity in antagonistic musculature. Therefore, the robust ipsiversive circling exhibited by these animals suggested that: 1. these cells did not project to the ipsilateral spinal cord, or 2. the influence of this system was dominated by alternate descending motor circuits.

Altered Fos-LI in the RPO was only observed in the 6-OHDAamp group. The marked reduction of Fos-LI in the RPO of these animals was likely a combined effect of reduced tecto-reticular stimulation and increased nigro-reticular inhibition. The

negligible increase in SNR stimulation in the ASF group may have prevented the suppression of RPO activity in these animals. Also, while the role of DA in the RPO has not been established, SNC efferents projecting to the RPO have been reported, indicating a source of endogenous DA and the possibility of DA receptors in this region (Shammah-Lagnado *et al.*,1987). Thus, in the 6-OHDAapo group, it is possible that apomorphine acted directly upon DA receptors in the RPO, eliciting responses from both hemispheres.

7.4.3. Clinical Implications of Cerebral Abnormalities. The patterns of Fos-LI that have been observed in the current animal models generally agree with clinical descriptions of cerebral changes in PD and HD. PET studies of ^{18}F-fluorodeoxyglucose (^{18}FDG) uptake have revealed a global reduction in cerebral metabolism in PD brains, with no regional selectivity (Kuhl *et al.*,1984). In contrast, HD brains had a significant decrease in ^{18}FDG uptake in the caudate nucleus and specific cortical areas relative to other brain regions (Kuhl *et al.*,1984,1985). The relatively normal metabolic activity of the caudate-putamen in PD brains may be explained by the shifting of activation from striatal neurons of the direct pathway (striato-nigral, striato-GPi) to those of the indirect pathway (striato-GPe), with no overall decrease in local activity. The pathological processes of HD, however, involve the direct loss of striatal neurons, producing an overall reduction in the functional capacity of the caudate-putamen.

We have shown that depletion of nigrostriatal DA produced a significant reduction in GPe stimulation, whereas direct suppression of striatal efferent

transmission increased the activation of the GPe. Alterations in GPe activity are thought to significantly contribute to the motor symptomatology of PD and HD (reviewed in DeLong, 1990). Hypometabolism of the GPe contributes to the bradykinesia produced in PD by indirectly reducing thalamic and tectal activation. The recent report of reduced glutamate decarboxylase, the rate limiting enzyme for the synthesis of GABA, in the GPe of PD patients further strengthens this hypothesis (Nisbet et al.,1996). In contrast, the hyperkinesia of HD is thought to be produced by the loss of striatopallidal neurons and subsequent increase in GPe activity. Bradykinesia frequently supersedes chorea in late stages of HD and is thought to be caused by the subsequent loss of striato-nigral/striato-GPi (direct pathway) neurons and a resultant increase in basal ganglia output (Albin et al.,1990; Storey and Beal, 1993). Thus, the ASF model of striatal dysfunction represents an end-stage HD paradigm in that both striatopallidal and striatonigral activity is suppressed.

Dramatic changes in the activity of thalamic nuclei have been reported in PD and HD. In PD, the ventral-intermediate (VIM) thalamus appears to contain the neural substrates which mediate tremor, as ablation or high frequency stimulation of this region successfully alleviates these symptoms (Benabid et al.,1991; Krauss and Jankovic, 1996; Boecker et al.,1997). However, bradykinesia and rigidity may be exacerbated by these procedures (Boecker et al.,1997) and have been associated with decreased thalamocortical stimulation and reduced muscle control. This is supported by the significant reduction of VMT activation in 6-OHDAamp animals presented here. In HD, chorea is thought to be produced by an increase in thalamocortical stimulation

and hyperactivity of motor-associated cortical regions (Albin *et al.*,1990; Storey and Beal, 1993). However, the ASF model presented here demonstrated a reduction in Fos-LI in the VMT, similar to that observed in 6-OHDAamp animals. This finding is consistent with the understanding that this model mimics an end-stage HD pathology, which in humans, frequently presents with parkinsonian bradykinesia and rigidity. Individuals with juvenile HD, a more severe form of the disease, usually do not develop chorea, but exhibit marked bradykinesia and rigidity (van Dijk *et al.*, 1986). Although adults with HD typically show a normal or increased thalamic metabolism, Matthews *et al.* (1989) reported a decreased metabolism in the same region of juvenile HD patients. Thus, it is possible that thalamic nuclei undergo biphasic changes during the progression of HD (i.e., initial increase followed by progressive decrease).

Severe oculomotor deficits have been reported in both PD and HD. Decreased saccade velocity, prolonged saccadic reaction time and abnormal smooth pursuit are common symptoms in both diseases (Avanzini *et al.*,1979; Shibasaki *et al.*,1979; Kennard and Lueck, 1989; Nakamura *et al.*,1991). Additionally, impaired vestibulo-ocular reflex and visual neglect have been reported in PD patients (White *et al.*,1983a,b; Ebersbach *et al.*,1996). These abnormalities have been attributed to changes in tectal regulation of reticulospinal neurons that control extraocular muscles. The alterations in Fos-LI demonstrated here support the hypothesis that the SC becomes markedly altered in PD and HD. Additionally, the RPO abnormalities observed in the 6-OHDAamp animals were consistent with a report of a 41% loss of substance P-containing neurons in the same region of PD patients (Gai *et al.*,1991) and

marked atrophy of the brainstem in HD patients, as revealed by computed tomography (Masucci et al, 1990). While the extent to which reduced RPO activity contributed to circling behavior in the present animal models is unclear, the clinical manifestation of such abnormalities would be expected to produce severe oculomotor impairment.

The results of this study suggested that the asymmetry in drug-induced motor behavior produced by unilateral 6-OHDA lesioning or ASF infusion in rats is mediated by similar changes in the striatum, EPN, SNR, SC and VMT. Modulatory influences on the extent of motor deficits are likely regulated by the GP and RPO. The successful application of this technique in rats suggests that it may also provide useful information in higher mammals in which accurate neurological phenotypes of PD and HD may be elicited. Combinations of metabolic mapping with electrophysiological and tracing techniques in primates may ultimately reveal the role of specific cerebral and brainstem nuclei in the production of motor symptomatology in these neurodegenerative diseases.

Figure 7.1 Rotational data from 6-OHDA and ASF animals. Both groups that received intraperitoneal injections of d-amphetamine (6-OHDAamp and ASF groups) exhibited significant ipsiversive circling behavior, whereas the group that received apomorphine (6-OHDAapo) demonstrated a marked contraversive bias. A) Temporal patterns of turning behavior. Line graphs illustrate the intensity of ipsiversive (6-OHDAamp, ASF groups) and contraversive (6-OHDAapo group) circling as assessed in 10-minute intervals. Ipsiversive turns are indicated by positive values, contraversive turns are indicated by negative values. B) Histograms showing the total number of rotations. All groups (denoted by the legend symbols in A) had a significant bias towards either the ipsiversive (6-OHDAamp, ASF) or contraversive (6-OHDAapo) direction (indicated by asterisks).

A

B
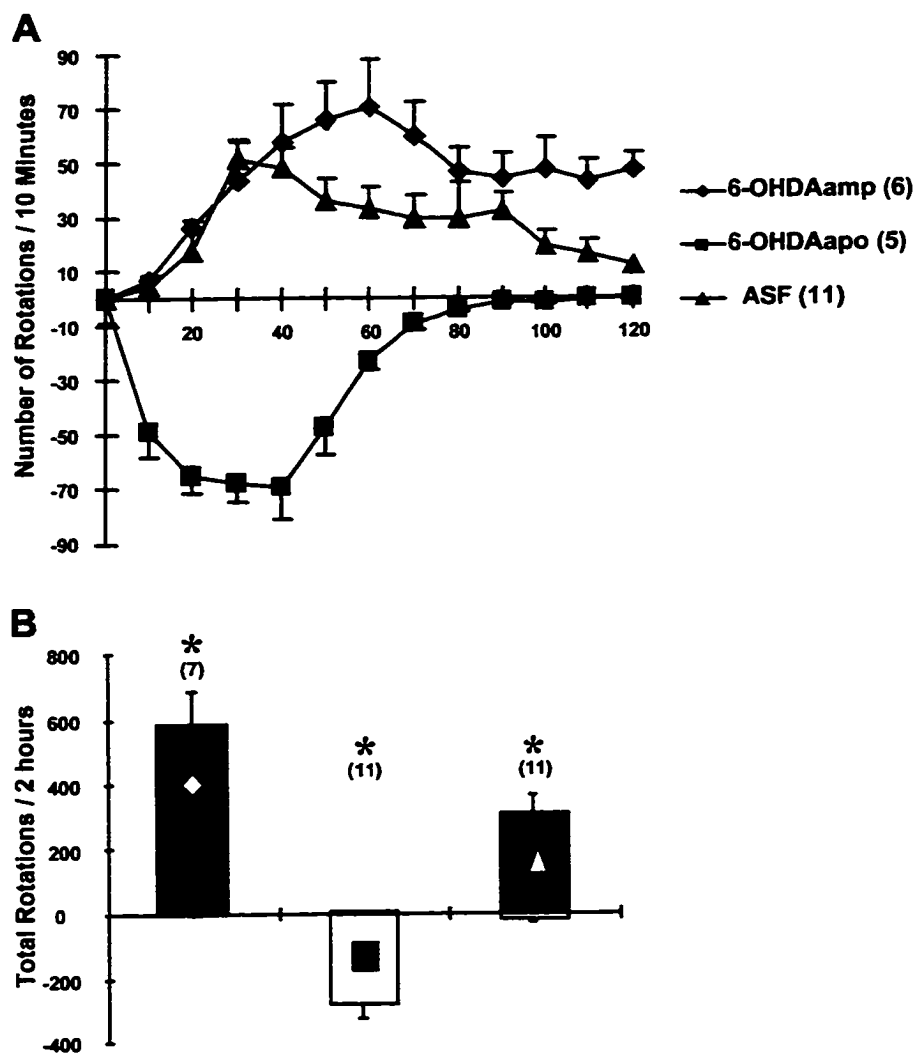
FIGURE 7.1

Figure 7.2 Fos-LI in the ipsilateral (A,C,E) and contralateral (B,D,F) striata of 6-OHDAamp (A,B), 6-OHDAapo (C,D) and ASF (E,F) animals. The ipsilateral striata in 6-OHDAamp and ASF animals had a marked reduction in Fos-LI, with typical striosomal expression on the contralateral side. In contrast, 6-OHDAapo animals had robust induction of Fos-LI in the ipsilateral striata, with negligible expression on the contralateral side. Scale bar = 100 μm.
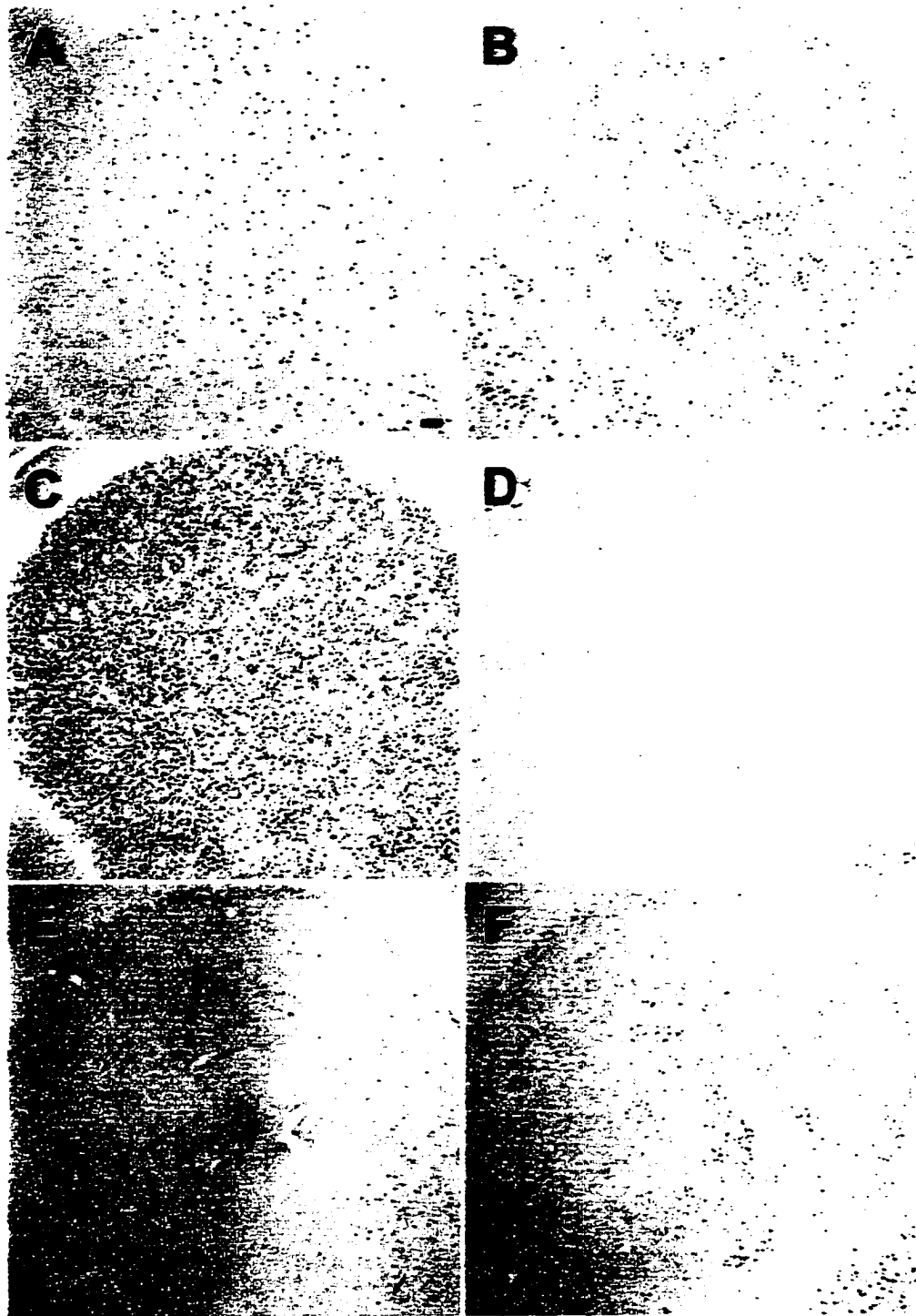
FIGURE 7.2

Figure 7.3 Fos-LI in the GP of 6-OHDAamp (A,B), 6-OHDAapo (C,D) and ASF (E,F) animals. Panels A, C and E represent the ipsilateral GP; panels B, D and F represent the contralateral GP. Note the small but consistent expression in the contralateral GP of 6-OHDAamp (B) and ASF (F) animals, as well as in the ipsilateral GP of 6-OHDAapo (C). This expression was virtually non-existent in the ipsilateral GP of 6-OHDAamp animals (A) and in the contralateral GP of 6-OHDAapo animals (D). In the ASF group, however, there was a significant increase in the Fos-LI of the ipsilateral GP (E). Arrowheads indicate the approximate border between the GP and the overlying striatum. Scale bar = 100 μm.
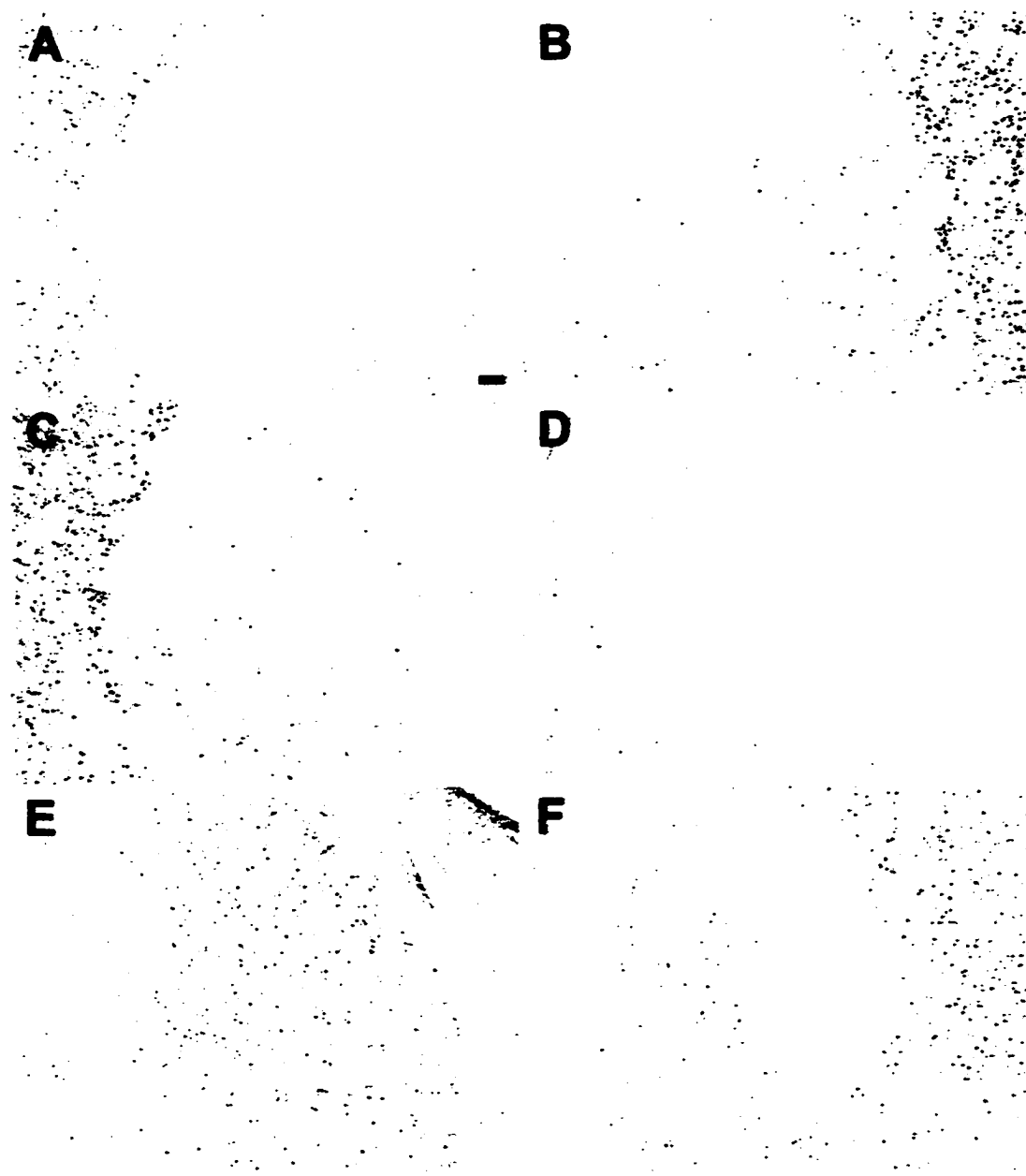
FIGURE 7.3

Figure 7.4 Fos-LI in the EPN of 6-OHDAamp (A,B), 6-OHDAapo (C,D) and ASF

(E,F) animals. Panels A, C and E represent the ipsilateral EPN; panels B, D and F

represent the contralateral EPN. Asymmetrical Fos-LI was observed in all groups.

The ipsilateral EPN of 6-OHDAapo animals exhibited an increase in Fos-LI that

appeared as small, lightly stained nuclei (C). Scale bar = 100 μm.

FIGURE 7.4

Figure 7.5 Fos-LI in the SNR of 6-OHDAamp (A,B), 6-OHDAapo (C,D) and ASF (E,F) animals. Panels A, C and E represent the ipsilateral SNR; panels B, D and F represent the contralateral SNR. Note the marked asymmetry between the SNR in 6-OHDAamp animals compared to those of the ASF group. Also, the staining appearance in the ipsilateral SNR of 6-OHDAapo animals was similar to that in ipsilateral EPN (Fig. 7.4C). Scale bar = 100 μm.
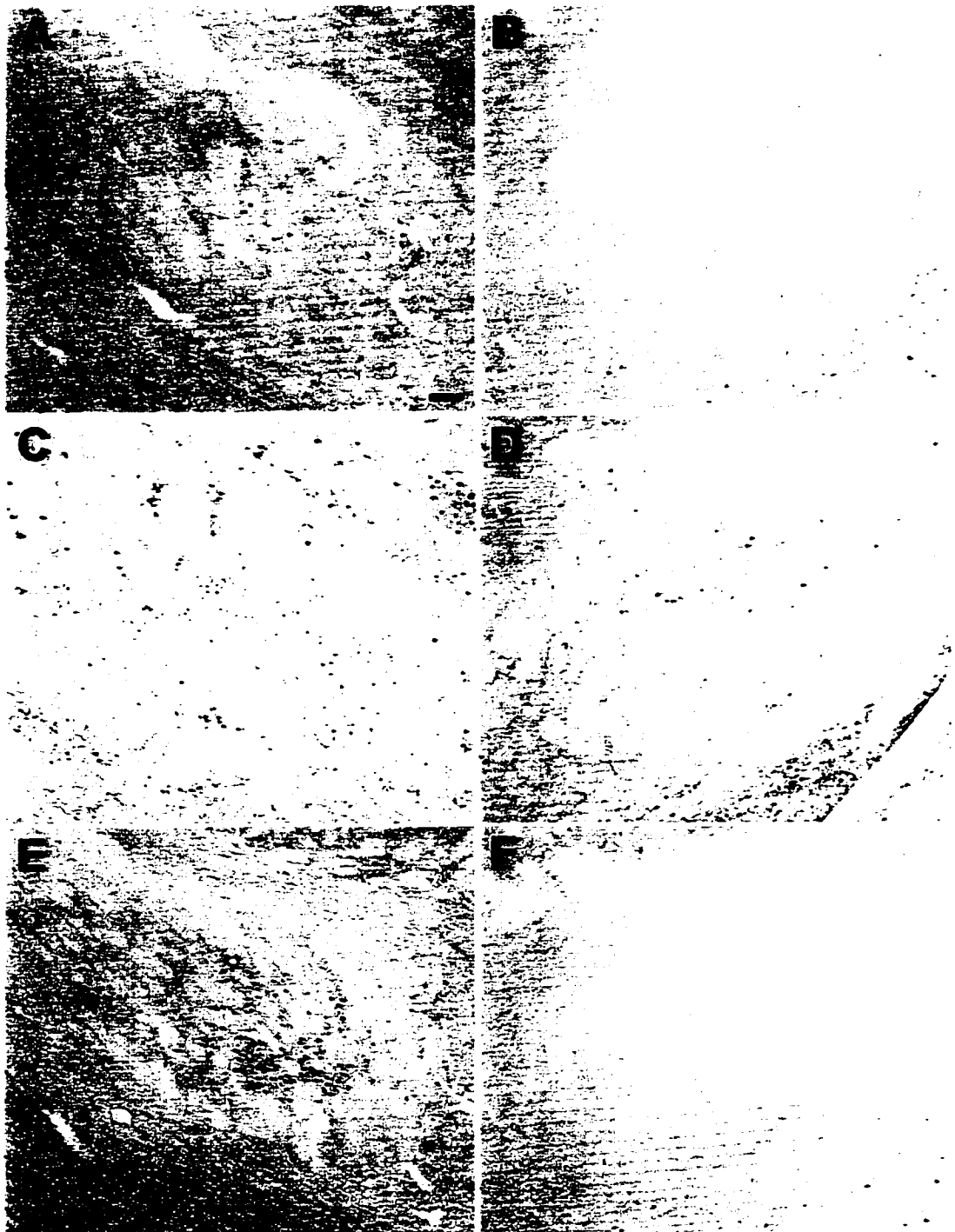
FIGURE 7.5

Figure 7.6 Fos-LI in the VMT of 6-OHDAamp (A,B), 6-OHDAapo (C,D) and ASF (E,F) animals. Panels A, C and E represent the ipsilateral VMT; panels B, D and F represent the contralateral VMT. There was a significant reduction of Fos-LI in the ipsilateral VMT of 6-OHDAamp and ASF groups and in the contralateral VMT of the 6-OHDAapo group. The mammilothalamic tract is indicated for orientation purposes (asterisks). Scale bar = 100 μm.
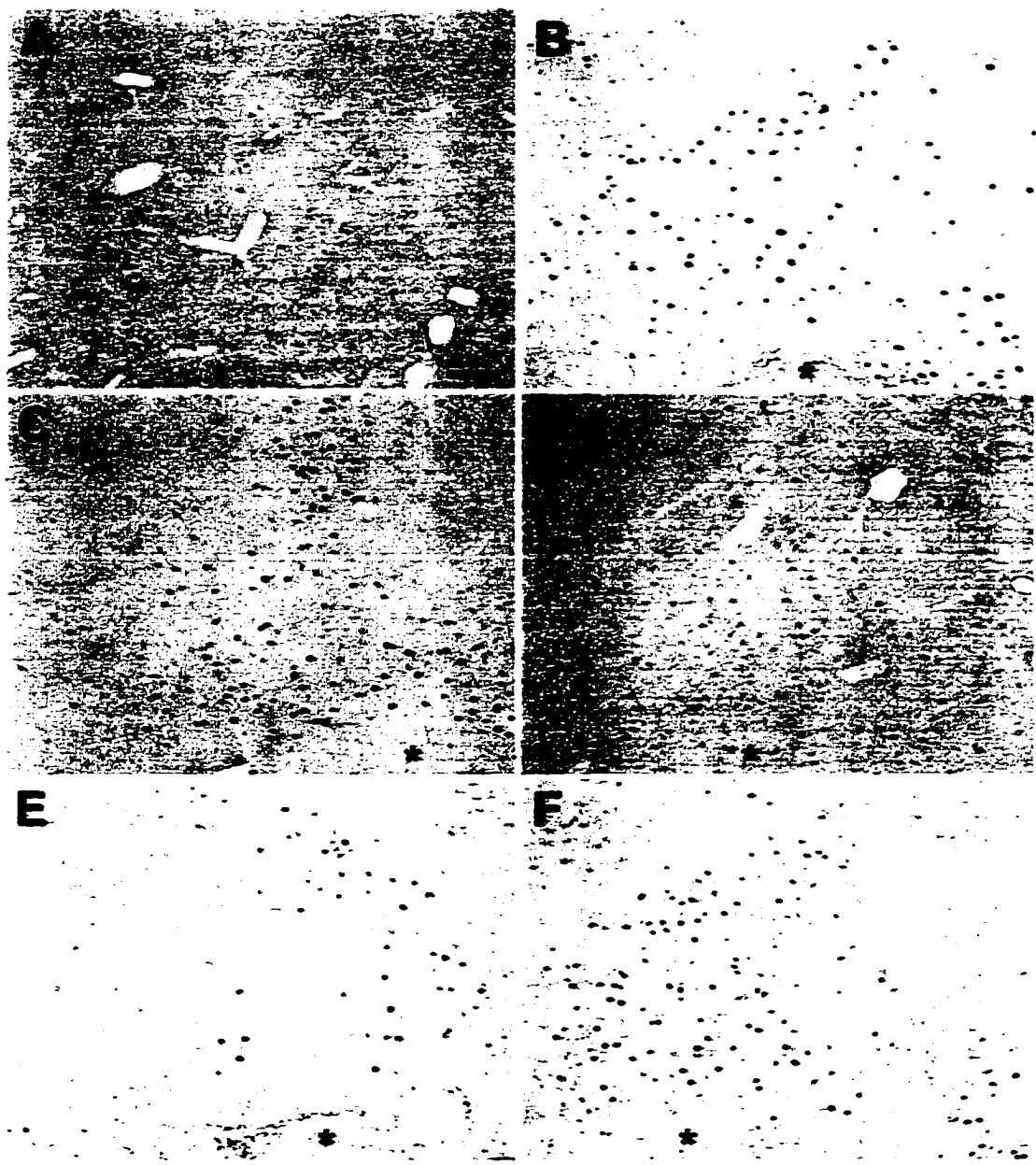
FIGURE 7.6

Figure 7.7 Fos-LI in the SC of 6-OHDAamp (A,B), 6-OHDAapo (C,D) and ASF (E,F) animals. Panels A, C and E represent the ipsilateral SC; panels B, D and F represent the contralateral SC. Animals of the 6-OHDAamp and ASF groups had a significant reduction in Fos-LI in the ipsilateral SCIW, whereas those of the 6-OHDAapo group had reduced expression in the contralateral SCIW. The changes in SCIW Fos-LI were accompanied by a significant increase in expression in the overlying SCIG layer on the ipsilateral (ASF) or contralateral (6-OHDAapo) side. Scale bar = 100 µm.
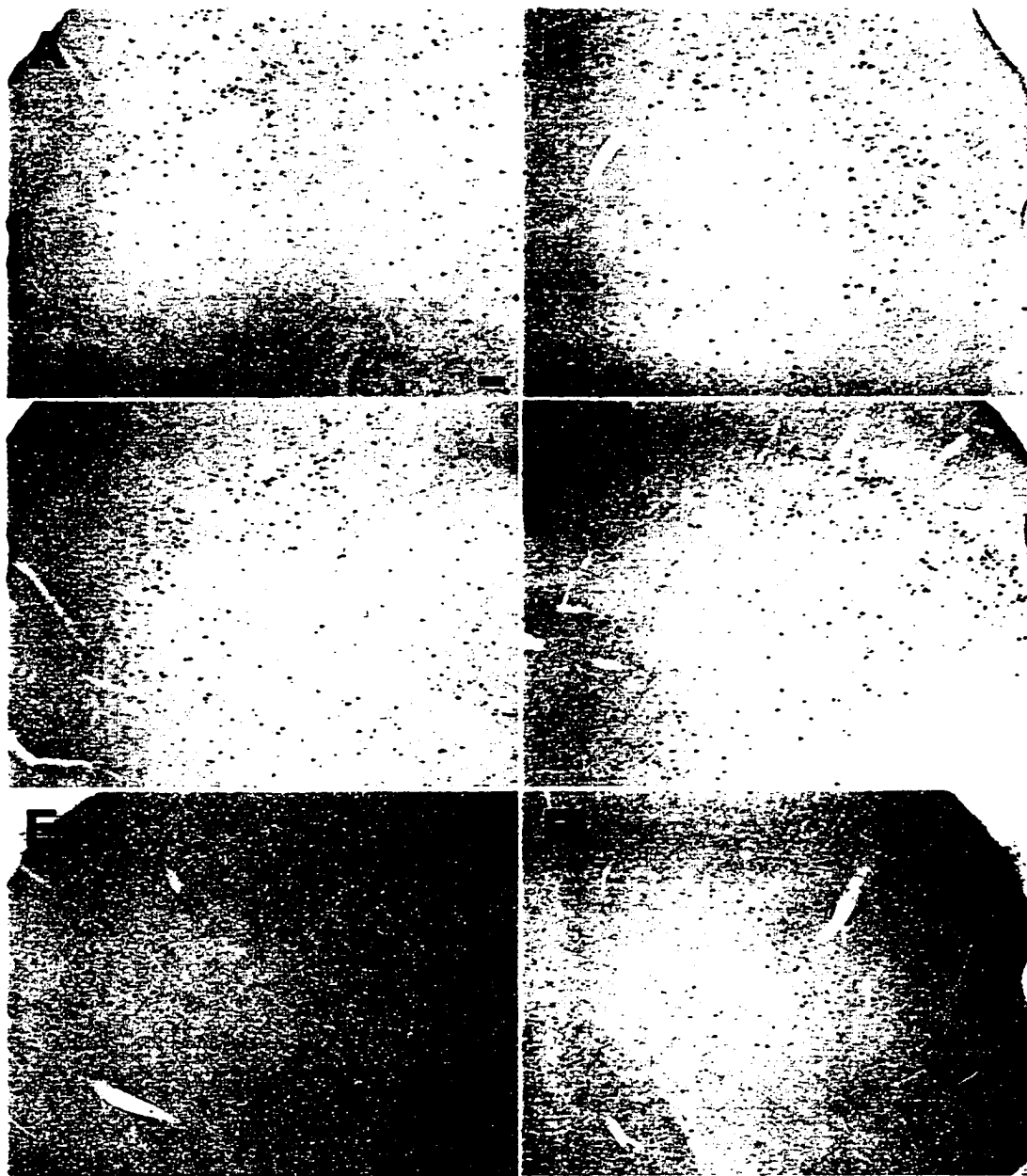
FIGURE 7.7

Figure 7.8 Fos-LI in the RPO of 6-OHDAamp (A), 6-OHDAapo (B) and ASF (C)

animals. The experimental side is on the left in each panel. Note the marked

suppression of Fos-LI in the ipsilateral RPO of 6-OHDAamp animals (A). This

reduction in expression was not observed in either the 6-OHDAapo or ASF groups.

Scale bar = 100 μm.
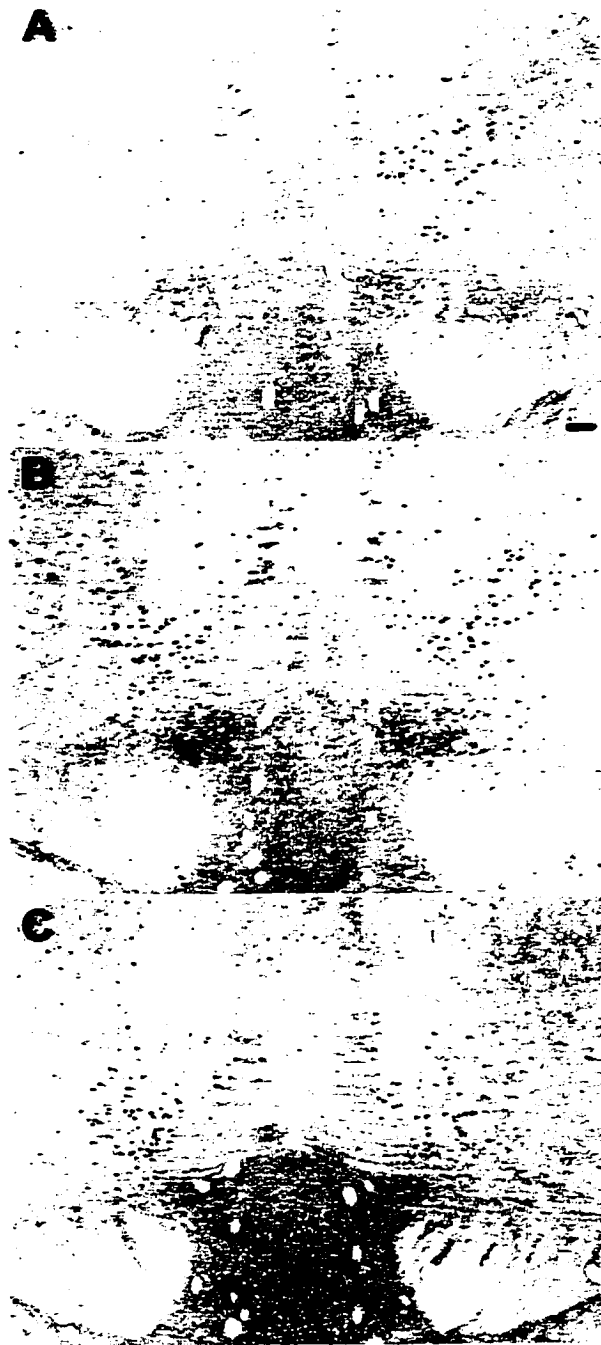
FIGURE 7.8

Figure 7.9 Histograms of Fos-positive cells counts in various subcortical areas. The region analysed is given at the top of each graph. The numbers at the bottom of each histogram denote the animal group, 1: 6-OHDAamp, 2: 6-OHDAapo, 3: ASF. Numbers in parentheses indicate the number of animals used in the analysis of that region. Black bars indicate ipsilateral, white bars indicate contralateral cell counts. Note the differences in the ordinate scale in each histogram. Asterisks indicate significant differences between ipsilateral and contralateral hemispheres ($P < 0.05$). EPN, entopeduncular nucleus; GP, globus pallidus; SCIG, intermediate gray layer of superior colliculus; SCIW, intermediate white layer of superior colliculus; SNR, substantia nigra pars reticulata; STR, striatum; RPO, oral pontine reticular formation; VMT, ventromedial thalamus.
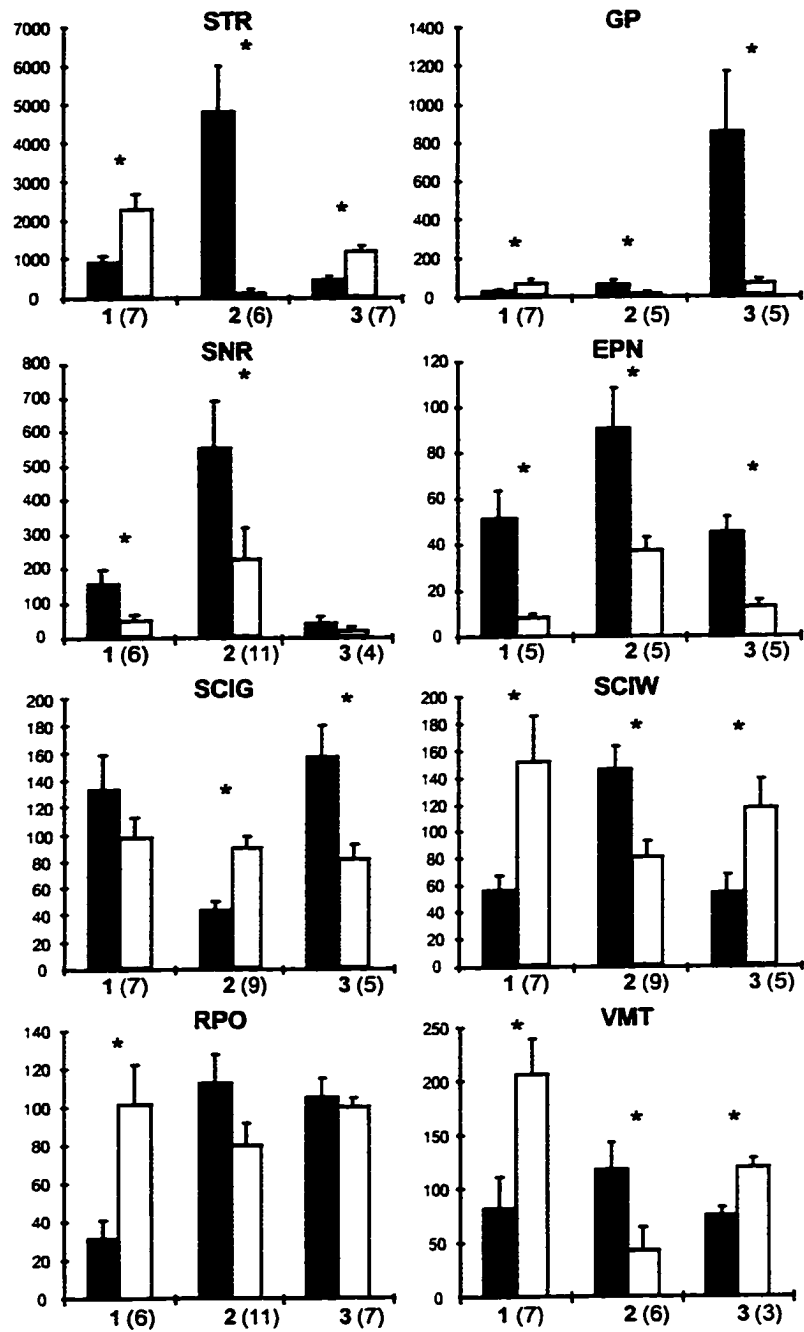
FIGURE 7.9

Figure 7.10 Hypothetical representation of the alterations that occur throughout the extended basal ganglia following a 6-OHDA lesion (A) or intrastriatal infusion of ASF (B). Arrow thickness indicates relative levels of neuronal activity. Filled cicles indicate normal or hyperactive neurons, open circles indicate neurons whose activity has been directly suppressed or abolished by the treatment. A) Following a 6-OHDA ablation of the nigrostriatal DA system, it is hypothesized that striatal neurons that project to the EPN and SNR (direct pathway) become suppressed due to a reduction in D1R-mediated stimulation. In contrast, the striatopallidal neurons (indirect pathway) become hyperactive, presumably due to the reduction in D2R-mediated inhibition of these cells. Reduction of direct activity and an increase in indirect activity would synergistically increase the output of the EPN/SNR via reduced striatal inhibition and increased STN-mediated stimulation, respectively. B) Intrastriatal infusion of ASF effectively reduces activity in neurons of both the direct and indirect circuits. Thus, while there is reduced striatal inhibition of EPN/SNR via the direct pathway, there is also a compensatory increase in GP activation and subsequent reduction in STN-mediated stimulation of these output nuclei. This suggests that the SNR/EPN are stimulated to a greater extent in 6-OHDA animals than ASF animals. This is consistent with the greater locomotor asymmetry and SNR Fos-LI in 6-OHDAamp animals observed here. Also, it is conceivable how an increase in GP activity, without a reduction of striatonigral transmission (as in choreic HD), could produce the opposite effect on the EPN/SNR, reducing the inhibitory drive to the VMT and SC and increasing the motor activity through these nuclei.

A   6-OHDA

B   ASF
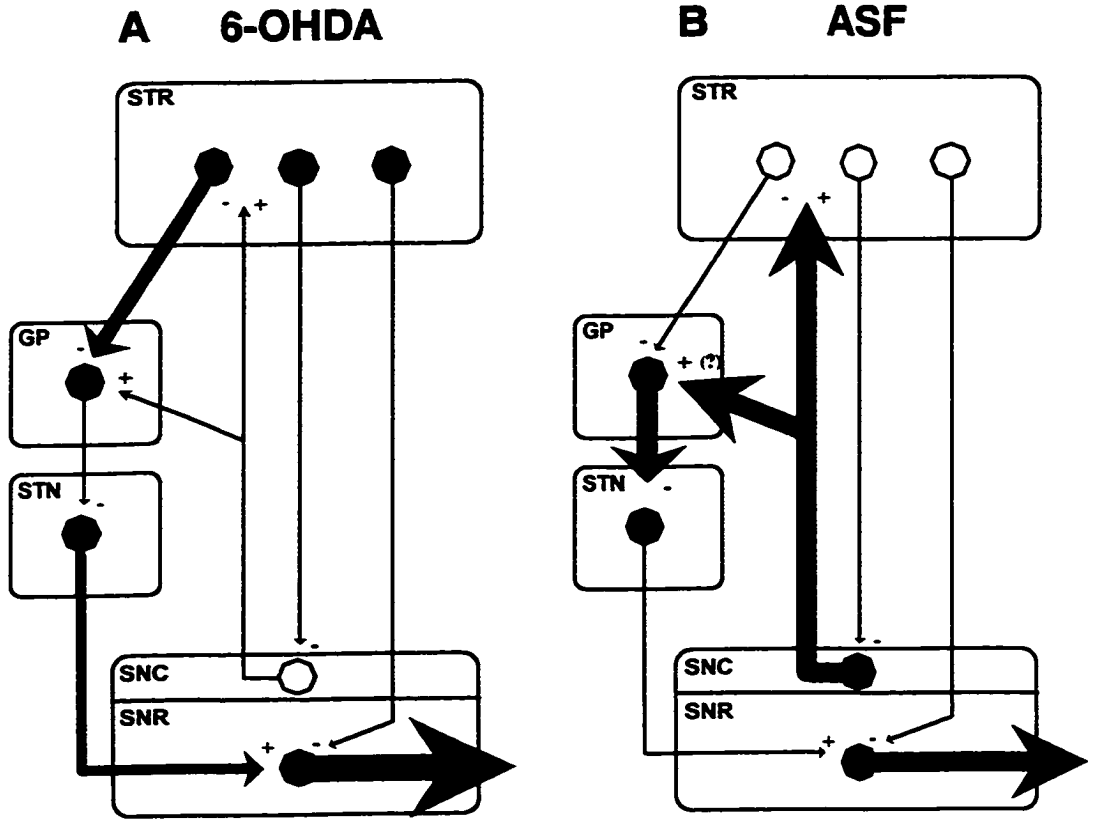
FIGURE 7.10

CHAPTER 8

Identification of a Population of GABAergic Neurons in the Substantia Nigra Pars

Compacta that is Regulated by Dopaminergic Activity[*]

190

8.1. Introduction

The role of dopamine (DA) in the basal ganglia and its contribution to motor and psycho-cognitive functioning has been under investigation for several decades. Loss of mesencephalic DA innervation to the caudate-putamen is the primary cause of motor and cognitive decline in Parkinson's disease (PD), while hyperactivity in limbic DA systems produces psychosis and may contribute to the symptomatology of schizophrenia (Hornykiewicz, 1979; Snyder, 1982). The DAergic neurons of the substantia nigra pars compacta (SNC) project to the striatum and release DA onto striatonigral and striatopallidal neurons to activate D1 and D2 receptors, respectively (Robertson and Robertson, 1987; Gerfen et al., 1990; Graybiel, 1990, 1991; LeMoine et al., 1990, 1991). Because DA D1 receptors (D1R) are positively coupled, whereas D2 receptors (D2R) are negatively coupled, to both adenylate cyclase and inositol phospholipid signaling pathways (Kebabian and Calne, 1979; Stoof and Kebabian, 1981; Mahan et al., 1990), stimulation of these receptors increases transmission through direct, but decreases transmisson through indirect, striatal projections. In addition to modulating efferent transmission from the striatum, DAergic neurons extend dendritic arborizations into the underlying substantia nigra pars reticulata (SNR) where the release of DA regulates SNR activity (Cheramy et al., 1981).

Greater than 85% of neurons in the SNC are DAergic, while the remainder, known as secondary cells, are thought to be cholinergic or γ-aminobutyric acid (GABA)-ergic (Javoy-Agid et al., 1981; Lacey et al., 1989). The function of these secondary cells remains unclear. Electrophysiological studies have revealed similarities

between secondary neurons in the SNC and interneurons of other brain regions (Miles and Wong, 1984; Madison and Nicoll, 1988; Lacey *et al.*, 1989; Yung *et al.*, 1991). However, van der Kooy *et al.* (1981) have shown that a small population of non-DAergic cells in the SNC send projections to the striatum, supporting the notion that secondary cells may also contribute to the regulation of the basal ganglia.

In the present study, we examined the effects of impaired basal ganglia circuitry on the stimulant-induced activation of neurons in the SNC. We used the expression of the immediate early gene (IEG), c-*fos*, to functionally (metabolically) map the activation of cells in the SNC in response to direct (apomorphine) and indirect (*d*-amphetamine) dopamine agonists. We have compared the effects of DA depletion, using 6-hydroxydopamine (6-OHDA) lesioning (Ungerstedt, 1968), and direct suppression of striatal efferent transmission, using intracerebral infusions of antisense oligodeoxynucleotides (ODNs) targeted to c-*fos* mRNA (Chiasson *et al.*,1992,1994; Dragunow *et al.*,1993,1994; Heilig *et al.*,1993; Sommer *et al.*,1993; Hooper *et al.*,1994; chapters 3 and 4), on the stimulation of these cells. Previous studies have shown that, in addition to suppressing IEG expression, intrastriatal infusion of antisense ODNs that are complementary to either c-*fos* or *ngfi*-a mRNA, reduced the release of GABA from striatal projection neurons and increased the stimulation of recipient nuclei (i.e. globus pallidus, substantia nigra) (Sommer *et al.*, 1996; chapter 4). Infusion of control ODNs had no effect on either parameter. Thus, while the mechanism remains unclear, it appears that suppression of striatal IEG expression effectively reduced the efferent transmission from this region. Presently, we have used

antisense ODNs to alter striatal activity without interfering with DA transmission from the SNC. We provide a neuroanatomical and neurochemical description of SNC neurons that are differentially activated following alterations in the striatum and the substantia nigra.

8.2. Materials and Methods

8.2.1. Experimental Design. Refer to section 7.2.1..

8.2.2. Surgical Procedures. Refer to section 7.2.2..

8.2.3. Immunohistochemistry. Following the appropriate recovery periods, animals were given intraperitoneal injections of either d-amphetamine (5 mg/kg; 6-OHDAamp and ASF groups) or apomorphine (0.5 mg/kg; 6-OHDAapo group). Two hours following stimulant administration, animals were deeply anesthetized with sodium pentobarbital (>100 mg/kg) and perfused through the left ventricle, initially with saline, followed by 4% paraformaldehyde in a 0.1 M phosphate buffer solution (pH 7.4). Brains were subsequently removed and post-fixed at 4°C until further analysis. Brains were blocked, cut into 50 μm coronal sections on a Vibratome and subsequently processed for c-Fos, tyrosine hydroxylase (TH) or glutamic acid decarboxylase (GAD, 67 kDa isoform) immunoreactivity.

For immunohistochemistry, the tissue was washed for 10 minutes in 0.1M phosphate-buffered saline containing 0.1% Triton-X (PBS-TX; except for GAD immunoreactivity, see below). This was followed by a 15 minute incubation in 1% hydrogen peroxide to inactivate endogenous peroxidase activity and subsequent 3 X 10 minute washes in PBS-TX at room temperature. Sections were then incubated in a solution containing a polyclonal antibody to c-Fos (1:5000; Genosys, TX), TH (1:4000; Pel-Freez, ARK) or GAD67 (1:5000; Chemicon, CA) for 16-24 hours at 4°C. They were then washed 3 X 10 minutes in PBS-TX and incubated in a 1:500 dilution of an appropriate, biotinylated secondary antibody (Vector Laboratories) for 1-2 hours at

room temperature. Excess antibody was removed by washing 3 X 10 minutes in PBS-TX and the bound secondary was visualized using the avidin-biotin technique (ABC Elite; Vector Laboratories) using diaminobenzidine (DAB; Sigma) as the chromogen. We found that addition of detergents markedly reduced the GAD immunoreactivity in cell soma and, therefore, all immunohistochemical procedures using the GAD67 antibody were performed in solutions that did not contain Triton-X. Processed sections were mounted on gelatin-coated slides, air-dried, dehydrated in graded alcohols, delipidated in xylenes and coverslipped using Entellan adhesive (Merck).

Some tissue sections were double-labeled for Fos-LI and GAD67 using two color DAB immunohistochemistry. Immunolabeling of these two proteins in the same tissue was technically challenging. Because the c-Fos antibody required the presence of Triton-X, whereas the GAD67 antibody required detergent-free PBS, simultaneous incubation in a PBS solution containing both c-Fos and GAD67 antibodies was not feasible. Therefore, we performed complete immunohistochemical reactions with the GAD67 antibody, using conventional (brown) DAB, followed by immunohistochemistry for c-Fos, using nickel-enhanced (blue) DAB, as described above.

Fluorescent double-labeling was performed using c-Fos/TH and c-Fos/GAD67 antibody combinations. All incubations were performed at 4°C. For the c-Fos/TH combination, sections were incubated in a buffer solution of PBS-TX that contained both primary antibodies at the dilutions described above. Following a 24-48 hour incubation, the sections were washed 3 X 10 minutes in PBS-TX and subsequently incubated in CY2-conjugated donkey anti-sheep (c-Fos) and CY3-conjugated donkey

anti-rabbit (TH) antibodies at a dilution of 1:400 (BioCan) for 16-24 hours. Excess antibody was removed by washing 3 X 10 minutes in PBS-TX. The sections were then mounted on gelatin-coated slides and visualized using filter sets to detect CY2 (Zeiss, catalogue no.487710) and CY3 (Zeiss, catalogue no.487715) immunofluorescence.

For the c-Fos/GAD67 antibody combination, the sections were initially incubated in a PBS (without TX) solution containing the GAD67 antibody for 16-24 hours. They were then washed 3 X 10 minutes in PBS and incubated with a CY3-conjugated anti-rabbit antibody, as described above. Sections were subsequently washed and incubated in a PBS-TX solution containing the c-Fos antibody for 16-24 hours. After rinsing, the tissue was incubated with a CY-2-conjugated anti-sheep antibody (in PBS-TX) for 16-24 hours. Following removal of excess antibody, the fluorochromes were viewed as previously described.

Selected sections were also stained for Nissl substance. Briefly, 50 μm sections were mounted on gelatin-coated slides, air-dried, dehydrated in graded alcohols and xylenes, rehydrated and stained with 0.1% cresyl violet.

8.2.4. Oligodeoxynucleotides. Refer to section 7.2.4..

8.2.5. Retrograde Labeling of SNC Neurons. In order to determine whether the Fos-positive cells that were identified in the SNC projected to the striatum, retrograde labeling of nigrostriatal neurons was combined with c-Fos immunofluorescence. Two naïve animals were subjected to stereotaxic surgery, as described above, where a single 25-gauge cannula was inserted into the right striatum (coordinates from bregma: AP 1.0 mm; LAT +3.0 mm; DV -6.0 mm) and 0.5 μl of 4% Fluorogold (Fluorochrome

Inc., Colo.) solution was infused at a rate of 0.1 µl/minute. Following infusion, the cannula was retracted, the skin sutured and the animals were left to recover for 5 days. After this time, the animals received 5 mg/kg d-amphetamine (i.p.) and were placed in their cages for two hours, afterwhich they were anesthetized and perfused as previously described. Sections were cut through the SNC and the tissue was processed for c-Fos immunofluorescence, as described above. Fluorogold fluoresced optimally under a wide band UV filter. However, because both Fluorogold and the CY2 fluorochrome also fluoresced under the Zeiss CY2 filter, we used a CY3-conjugated secondary antibody to visualize the c-Fos immunolabeling. There was no overlap between the emission wavelengths for Fluorogold and the CY3-conjugated antibody.

8.3. Results

8.3.1. Extent of 6-OHDA Lesions and ASF-induced IEG Suppression

8.3.1.1. Tyrosine Hydroxylase Immunoreactivity. Examination of TH-IR following various post-lesion recovery periods revealed a progressive deterioration of dopamine cells in the SN. Three days after infusion of 6-OHDA into the medial forebrain bundle, there was substantial loss of TH-positive dendritic processes and an overall reduction in the number of TH-positive cell bodies in the SNC (Fig. 8.1A,B). After one week, TH-IR revealed extensive pyknosis in the SNC. At this time point, all evidence of dendritic arborization was lost and the SNC appeared as a strip of densely clustered granules (Fig. 8.1C,D). By three weeks after 6-OHDA infusion, there remained only scant traces of TH-IR in the SN, indicating a near total destruction of DAergic cells (Fig. 8.1E,F).

8.3.1.2. Nissl Staining. Nissl staining of lesioned animals with three week recovery periods revealed extensive loss of large diameter soma in the SNC (Fig. 8.1G,H). This confirmed that, at three weeks following 6-OHDA lesioning, the dopamine cells of the SNC were destroyed and did not merely exhibit a suppression of TH expression. All of the 6-OHDA-lesioned animals used in subsequent analyses were examined at this time point.

8.3.2. Fos Immunoreactivity. Suppression of striatal IEG expression in ASF animals was assessed by examination of Fos-LI in the striatum. Infusion of ASF reduced the induction of Fos-LI in the striatum by approximately 65% (not shown). Effective ASF-

mediated suppression of c-*fos* expression in this region has been previously described in several reports (chapters 3, 4 and 5).

Examination of Fos-LI in striata of 6-OHDAamp animals also revealed a significant reduction in expression on the ipsilateral side. In contrast, 6-OHDAapo animals had robust Fos-LI in the ipsilateral striatum, but negligible induction on the contralateral side. The effects of 6-OHDA-lesioning on stimulant-induced c-Fos expression in the striatum were consistent with those previously reported (Cenci *et al.*, 1992; chapter 7).

8.3.3. Differential Expression of c-fos in the SNC. In naïve animals, *d*-amphetamine (5 mg/kg) induced bilateral expression of Fos-LI in the central region of the SNC at the level of the interpeduncular nucleus (Fig. 8.2A). Animals that received *d*-amphetamine following either a 6-OHDA lesion (Fig. 8.2B) or intrastriatal infusion of ASF (Fig. 8.2C) had a near total elimination of Fos-LI in the ipsilateral SNC, but normal expression on the contralateral side. In contrast, animals that received a 6-OHDA lesion followed by apomorphine challenge had elimination of this expression in the contralateral SNC, with apparently normal induction on the ipsilateral side (Fig. 8.2D).

8.3.4. Characterization of Fos-Positive Cells in the SNC

8.3.4.1. Fos and TH Immunohistochemistry. The apomorphine-induced expression of Fos-LI in 6-OHDA-lesioned SNC, which had been shown to contain no TH labeling, indicated that the Fos-positive cells were not DA neurons. However, to confirm this hypothesis, we used double-labeling immunofluorescence for Fos-LI and TH in naïve animals that had been challenged with *d*-amphetamine. The Fos-positive nuclei were

interspersed between large TH-containing neurons, but were never colocalized with TH in the same cells (Fig. 8.3). Also, to confirm that Fos-induction was not altered in the SNC following ablation of the DAergic neurons of this region, similar double-labeling experiments were performed on 6-OHDAapo animals. Although the TH immunolabeling was eliminated, apomorphine still produced robust induction of Fos-LI in the lesioned SNC (Fig. 8.4).

8.3.4.2. Fos and GAD Immunohistochemistry. Previous reports have described the distribution of GAD-positive neurons in the SNC (Oertel *et al.*, 1982; Yung *et al.*, 1991). We were interested in determining whether the Fos-positive cells in the SNC also expressed GAD, indicative of a GABAergic phenotype. We initially performed conventional DAB-immunohistochemistry for Fos or GAD using serial sections through the SNC. Because the Fos antibody worked poorly on 14μm-thick, slide-mounted sections (not shown), it was necessary to use 50 μm-thick, free-floating sections. This method revealed a high concentration of GAD-positive cell bodies in the vicinity of the Fos-positive nuclei (Fig. 8.5).

In order to demonstrate Fos and GAD co-localization, we next performed sequential, two-color DAB immunohistochemistry. This technique revealed several double-labeled neurons in the SNC, confirming our hypothesis that the Fos-expressing cells were GABAergic (Fig. 8.6). Sequential immunofluorescent double-labeling of Fos and GAD also demonstrated co-localization of these proteins (Fig. 8.7). With both DAB and fluorescent methods, there appeared to be Fos-positive nuclei that did not double-label for GAD. This effect was attributed to technical difficulties in

immunolabeling of the cell soma with the GAD antibody. Both methods also revealed GAD-containing neurons that were devoid of Fos-LI.

8.3.4.3. Retrograde Labeling and Fos Immunofluorescence. Five days following tracer injection, the Fluorogold had diffused throughout a substantial portion of the striatum. The fluorescence was confined within the boundaries of this nucleus, except for a small region of diffusion through the cannulae tract into the overlying cortex (Fig. 8.8). Examination of the SNC revealed extensive retrograde labeling of compacta cells, producing a pattern of fluorescence similar to that seen with TH immunofluorescence. Subsequent immunolabeling revealed that the Fos-positive nuclei were not contained within Fluorogold-labeled neurons, but were interspersed between these cells (Fig. 8.8).

8.4. Discussion

Presently, we report the activation of a population of neurons in the SNC by the dopamine agonists, *d*-amphetamine and apomorphine, in intact, 6-OHDA-lesioned and ASF-infused animals. Nuclear expression of Fos-LI in the SNC was not present in TH-positive cells but was co-localized with cytoplasmic GAD, indicating that these neurons were GABAergic. In all groups, elimination of the stimulant-induced Fos-LI corresponded to a reduced expression of c-*fos* in the striatum, suggesting that efferent striatal transmission had mediated the SNC response.

Because DA neurons of the SNC are tonically active, it is thought that the release of DA in the striatum maintains a resting tone which may be modulated by changes in nigral activity (Lacey *et al.*, 1989; Yung *et al.*, 1991). Also, dendritic release of DA into the underlying SNR has been shown to facilitate efferent transmission from this region and attenuate the inhibitory effects of GABA (Ruffieux and Schultz, 1980; Waszczak and Walters, 1983; Martin and Waszczak, 1996). Thus, the effects of DA in the striatum and in the SNR appear to counteract one another, increasing inhibitory tone to the SNR (via activation of direct striatonigral transmission) and facilitating SNR activity, respectively. It may be that the extent to which each of these components affects SNR output is reflected by the level of stimulation of SNC neurons.

While DA regulates the activity of neurons in the striatum and SNR, stimulation of either of these regions markedly suppresses neuronal activity in the SNC (Dray *et al.*, 1976; Gerfen, 1984; Jimenez-Castellanos and Graybiel, 1989; Tepper *et al.*,

1995). For example, Tepper *et al.* (1995) used antidromic stimulation of SNR neurons, while simultaneously recording from the SNC, to show that increases in reticulata firing rates were associated with decreased SNC activity. The physiological role of SNR-SNC interactions remains unclear. One possibility is that this circuit provides a positive feedback mechanism by which increased SNR activity reduces nigrostriatal DAergic transmission and, subsequently, decreases the inhibitory input to the SNR from the striatum. Alternatively, increased suppression of DAergic neurons in the SNC would reduce the dendritic release of DA onto SNR terminals and decrease the facilatory influence of DA on reticulata outflow. This paradoxical influence of reduced SNC tone on SNR activity may be dependent upon the degree of reticulata stimulation. For example, low level SNC inhibition may result only in a decrease of dendritic DA release, increasing inhibitory tone to the SNR. Such localized inhibition may act as a physiological barrier which prevents the transmission of unwanted signals from the SNR to downstream nuclei. Marked increases in SNR activity may overcome this threshold and potentiate SNR output by reducing the release of DA in the striatum and decreasing D1R-mediated striatonigral transmission.

Although the majority of studies that have investigated the SNC have focused on the neurophysiology of DAergic neurons in this region, several electrophysiological and immunocytochemical studies have described at least two types of SNC neurons (Javoy-Agid *et al.*, 1981; van der Kooy *et al.*, 1981; Lacey *et al.*, 1989; Yung *et al.*, 1991). Lacey *et al.* (1989) have described two classes of neurons in the SNC that were distinguished on the basis of their electrophysiological properties. They found that

95% of SNC neurons, which they termed 'principal neurons', had spontaneous, low frequency action potentials of relatively long duration. These neurons were significantly inhibited by dopamine or baclofen (a GABA agonist). In contrast, the remaining 5% of neurons (called 'secondary cells') exhibited rapid, high frequency action potentials that were unaffected by DA, but inhibited by baclofen. In a more recent study, Yung et al. (1991) have also described two populations of SNC neurons that were distinguished by their electrophysiological membrane properties. Consistent with previous reports, the authors classified these cells as either bursting (15% of total cells) or non-bursting (85% of total cells). Double labeling experiments revealed that all of the non-bursting cells were positive for TH-IR and, thus, were assumed to be dopamine neurons. None of the bursting cells were TH-positive and their distribution paralleled that of GAD-positive cells in the SNC. A similar abundance of GAD immunoreactivity in this region has been previously reported by Oertel et al. (1982). Yung and colleagues (1991) suggested that these burster cells were GABAergic neurons and may represent a component of the non-DAergic nigrostriatal pathway implicated in previous anatomical (van der Kooy et al., 1981) and electrophysiological (Guyenet and Aghajanian, 1978) studies. Consistent with the description of secondary cells in the SNC (Lacey et al., 1989), it was found that the burster cells in this region were also DA-insensitive (Yung et al., 1991).

Striatonigral neurons that project to the SNC are predominantly localized to the striosomal compartment of the striatum and are stimulated by D1R activation (Graybiel et al., 1990). The stereotypic effects of d-amphetamine are also mediated primarily

through D1R activation and, consequently, the Fos-LI that is induced in the striatum is mainly confined to striosomes (Graybiel *et al.*, 1990). There is also, however, substantial D1-mediated stimulation of striatal neurons that project to the SNR following *d*-amphetamine challenge. In the present study, administration of *d*-amphetamine consistently induced Fos-LI in TH-negative, GAD-positive neurons of the central region of the SNC. The mechanism by which *d*-amphetamine-induced Fos-LI in the SNC remains unclear. However, the ipsilateral elimination of this expression both in animals that had received an unilateral 6-OHDA lesion or intrastriatal infusion of ASF indicated that striatal activation was necessary for the SNC response. Also, because striatal projection neurons are GABAergic, the stimulation of the SNC must have been produced indirectly through secondary circuits. Results obtained from the 6-OHDAamp and ASF groups suggested two possible mechanisms of SNC stimulation. The first possibility (hypothesis 1) is that, in naive animals, DA acts in the SNC to tonically inhibit activation of the GABAergic neurons, i.e., by D2R stimulation. As *d*-amphetamine increases the inhibitory input to the SNC from the striatum, this influence would effectively reduce the DA-mediated inhibition of GABAergic neurons. Ablation of DAergic neurons by 6-OHDA would chronically remove the inhibition of GABAergic transmission in the SNC, disregulating the activity of these neurons. Because c-Fos is induced in response to changes in metabolic activity, no expression would be observed in these cells that had been rendered tonically active. However, even if the DAergic neurons had remained intact, a similar reduction in striatonigral transmission, by an alternate mechanism, would be expected to suppress the stimulation

of the SNC. This was confirmed in the ASF group, where nigrostriatal DA systems remained intact and only efferent transmission from the striatum was affected.

The second possibility (hypothesis 2) predicts that the GABAergic neurons of the SNC are regulated by GABAergic influences from the SNR. This is supported by previous studies that demonstrated that SNR activity inhibits that of the SNC (Tepper *et al.*, 1995). Thus, in naive animals, administration of *d*-amphetamine increases the inhibition of the SNR, via striatonigral stimulation, which reduces the inhibitory tone of the SNR on the SNC, permitting induction of Fos-LI. In both 6-OHDAamp and ASF groups, the striatonigral influence is drastically reduced (in the ipsilateral hemisphere), increasing both SNR outflow and inhibitory tone to the SNC. This second hypothesis is also supported by the previous observation that animals with reduced striatal activity, particularly 6-OHDAamp animals, have an increase in Fos-LI in the ipsilateral SNR, with a concurrent elimination of the expression in the SNC (chapter 7).

Expression of Fos-LI in the SNC of 6-OHDAapo animals conflicted with the notion of DA-mediated regulation of GABAergic neurons (hypothesis 1) and further supported the possibility that these cells in the SNC were influenced by SNR activity (hypothesis 2). For example, although it is possible that apomorphine acted directly at DA receptors in the SNC to induce Fos-LI, this notion contradicts hypothesis 1 which predicts that DA produces inhibition of these neurons. Furthermore, regions such as the striatum, that are subjected to tonic DA influence, develop supersensitivity to direct DA agonists following depletion of endogenous sources (Ungerstedt, 1971). We have

also observed this phenomenon in both the SNR and the entopeduncular nucleus in 6-OHDA-lesioned animals (chapter 7). Therefore, if the GABAergic neurons in the SNC were directly influenced by DA, it would be expected that a certain degree of sensitization would occur following DA depletion. However, there was no evidence to support this in the current studies. Hypothesis 2, however, was supported by the robust expression of Fos-LI in the ipsilateral, but not contralateral, striatum in 6-OHDAapo animals. This was consistent with the previous observation that induction of Fos-LI in the SNC paralleled that in the striatum. These animals also exhibited an increase in Fos-LI in the contralateral SNR with no expression in the contralateral SNC. Thus, it appeared that, as in the other animal groups, SNC stimulation was mediated by increased striatonigral activity and a reduction in SNR inhibition of the GABAergic neurons in the SNC.

In their discussion of burster neurons in the SNC, Yung et al. (1991) suggested that these cells may comprise a GABAergic nigrostriatal pathway. From the similarities in electrophysiological properties, abundance and location between burster neurons and the 'secondary cells' previously described by Lacey et al. (1989), the authors concluded that they belonged to the same neuronal subpopulation. Our present findings of the location and abundance of the Fos-positive, GABAergic neurons in the SNC are consistent with these earlier reports and suggest that these cells are burster/secondary neurons. Also, the demonstration that the burster cells are insensitive to DA, but markedly inhibited by GABA agonists further supports our hypothesis that these cells are regulated through SNR transmission and not directly by

DAergic colaterals (hypothesis 2). However, the idea that these GABAergic neurons comprise a non-dopaminergic, nigrostriatal circuit was not supported by these studies. Retrograde labeling, using Fluorogold, produced an abundance of filled neurons throughout the entire extent of the SNC. We did not observe any cells in this region that were double-labeled for Fos-LI and Fluorogold. In fact, the distribution of the Fos-positive nuclei amongst the large, Fluorogold-filled neurons was similar to that observed with double immunofluorescence for Fos and TH. Together with the previously reported similarities between secondary neurons and interneurons of other brain regions (Miles and Wong, 1984; Madison and Nicoll, 1988; Lacey et al., 1989; Yung et al., 1991), these results suggest that the Fos-positive, GABAergic neurons reported in this study belong to a class of interneurons. The activation of these cells by DA agonists suggests that they may play a role in inhibitory mechanisms which reduce the DAergic stimulation of striatal neurons. Whether these neurons project to the SNR, or only arborize locally, remains unknown. However, studies that demonstrated a reciprocal relationship between SNR and SNC activity argue against a GABAergic interneuronal connection between these two regions (Grace and Bunney, 1979; Waszczak et al., 1980). Determination of the mechanism of stimulation and the function of these GABAergic neurons will require electrophysiological methods and may provide insight into regulatory processes that exist between the SNC, SNR and the basal ganglia.

Figure 8.1 Progression of SNC deterioration following 6-OHDA infusion. Shown is the TH-IR (A-F) and Nissl staining (G,H) in the SNC, ipsilateral (left panels) and contralateral (right panels) to the infusion of 6-OHDA into the medial forebrain bundle. By 3 days after 6-OHDA infusion, there was marked loss of DAergic dendrites in the SNR as well as cell soma in the SNC (A,B). There was a complete absence of normal TH-positive soma by 7 days after lesioning, with extensive pyknosis evident (C,D). At 21 days post-lesion, >95% of TH-IR was eliminated from the ipsilateral SNC (E, F). Nissl staining confirmed the marked loss of large diameter cell bodies at the 21-day time point (G,H). The tissue sections shown in panels E-H were taken from the same animal. Asterisks in G) and H) indicate corresponding regions of the SNC. Scale bar = 100 μm.
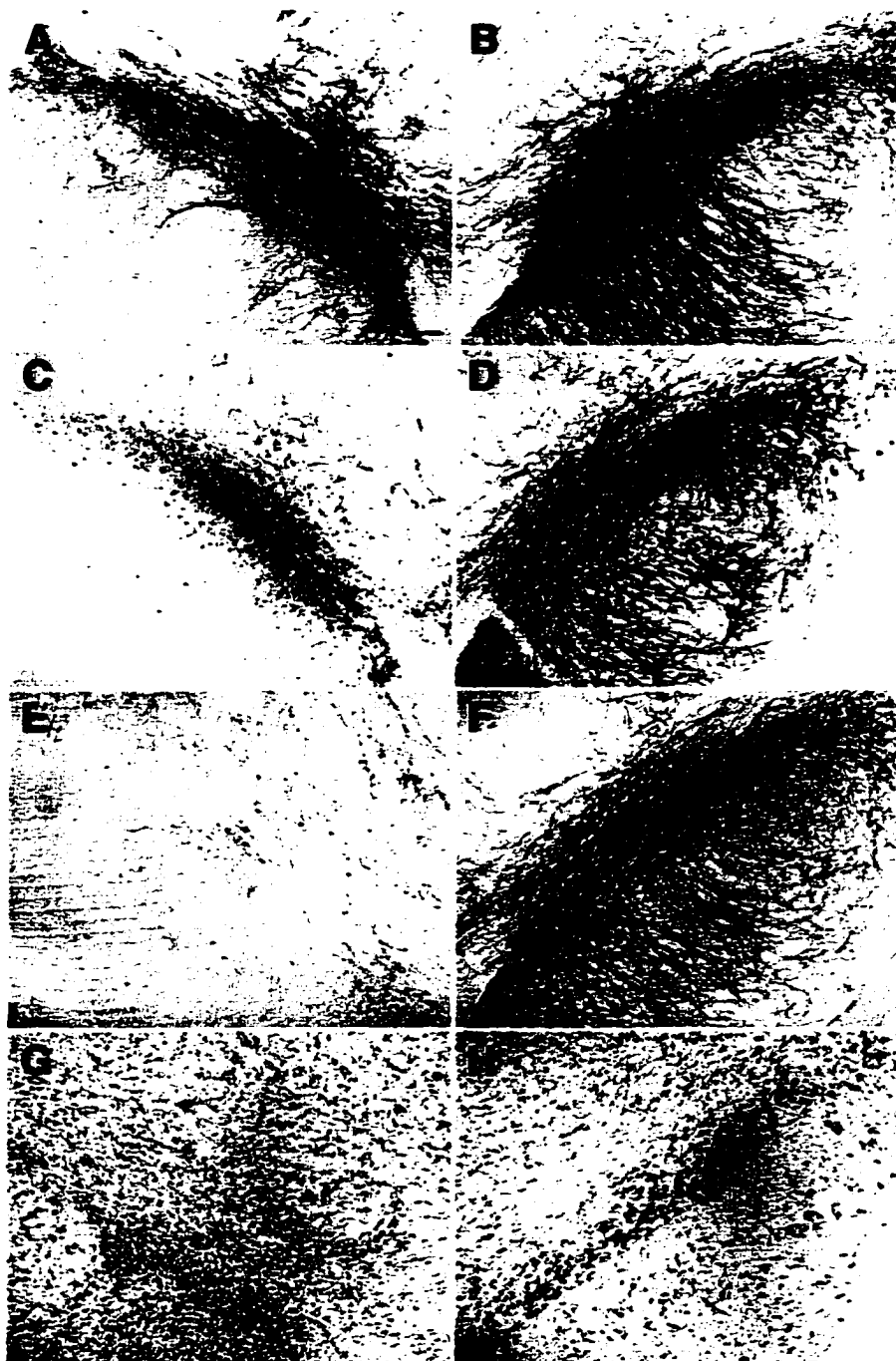
FIGURE 8.1

Figure 8.2 Localization of the differentially-expressed Fos-LI in the SNC following psychostimulant challenge. The left half of the micrographs show the treated SN; the right half show the control SN. A) In naive animals, intraperitoneal administration of *d*-amphetamine induced bilateral expression of Fos-LI in the central region of the SNC. Following an unilateral 6-OHDA lesion (B) or intrastriatal infusion of antisense ODNs (C), the ipsilateral expression was eliminated, while the contralateral Fos-LI remained unaffected. D) In animals that received 6-OHDA lesions followed by apomorphine challenge, the ipsilateral SNC exhibited normal Fos-LI while the expression in the contralateral hemisphere was abolished. Arrows indicate regions of stimulant induced Fos-LI, or the location of its absence. Scale bar = 100 μm.
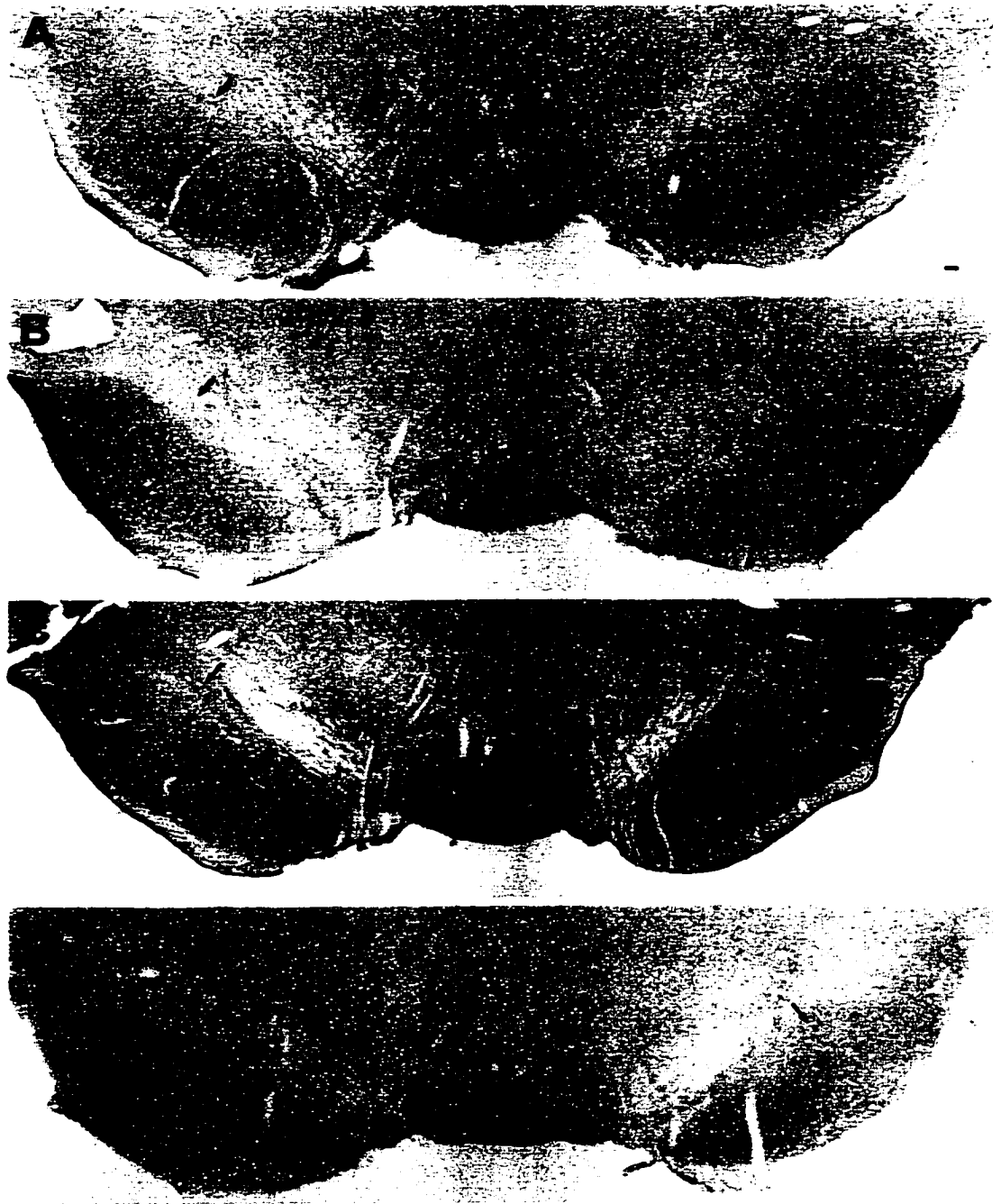
FIGURE 8.2

Figure 8.3 Fluorescent double-labeling of TH and Fos in the SNC of naive animals. Low (A-C) and high (D-F) magnification micrographs showing the *d*-amphetamine-induced expression of Fos-LI (A,D; green) in naive animals. TH-IR is represented in the identical regions in the adjacent panels (B,E; red). Composite exposures showing both antigens clearly demonstrated that the Fos-positive nuclei were not contained within TH-positive cells (C,F). Scale bars represent 100 μm and indicate magnification in each horizontal row of panels.
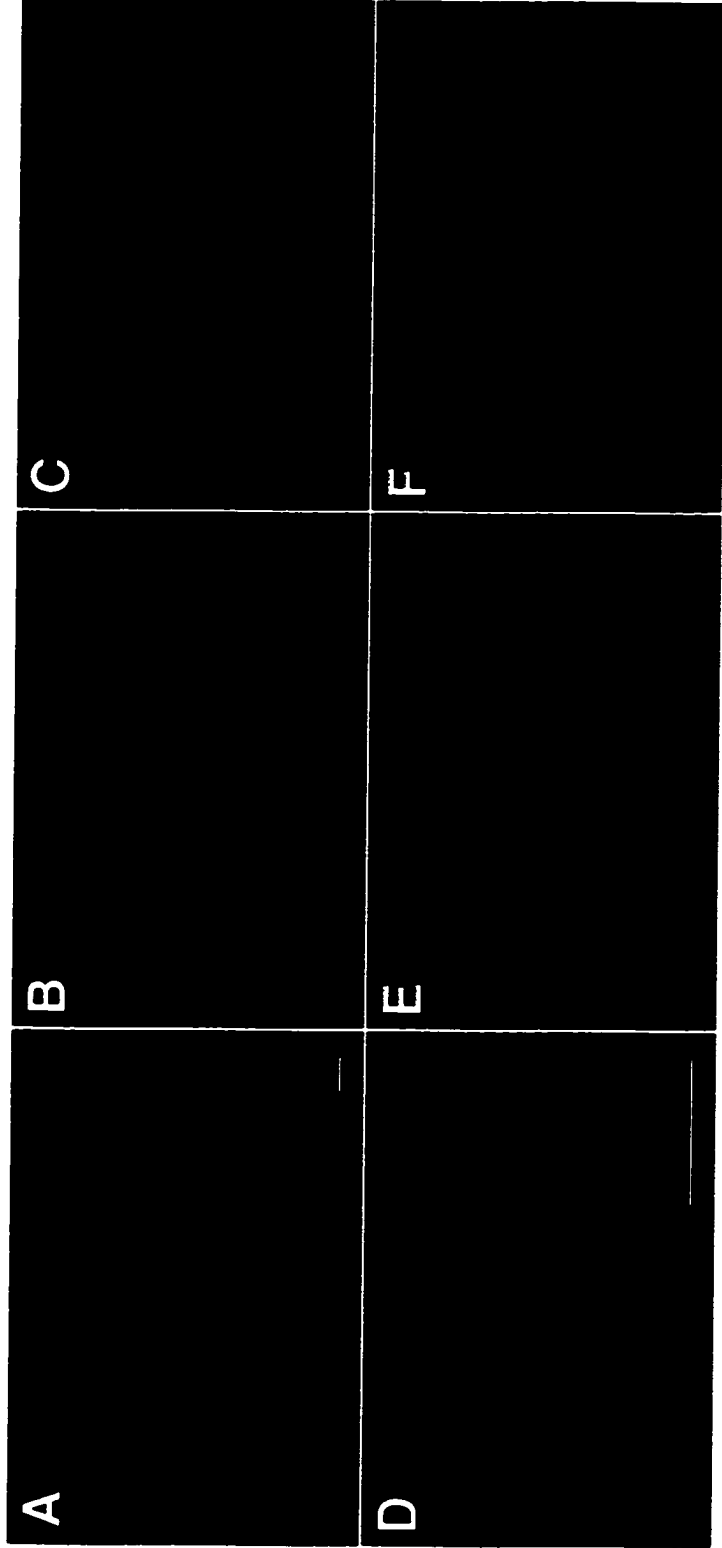
FIGURE 8.3

Figure 8.4 Fluorescent double-labeling of TH and Fos in the SNC of 6-OHDA-lesioned animals. Low (A-C) and high (D-F) magnification micrographs showing the apomorphine-induced expression of Fos-LI (A,D; green) in the SNC in animals that had received a 6-OHDA lesion on the ipsilateral side. The near complete loss of DAergic neurons in the identical region was demonstrated by the lack of TH-IR (B,D; red). Composite exposures of Fos-LI and TH-IR are shown in panels C) and F). It was evident that the stimulant-induced expression of Fos-LI was not affected by a total ablation of the DAergic neurons in this region. Scale bars represent 100 μm and indicate magnification in each horizontal row of panels.
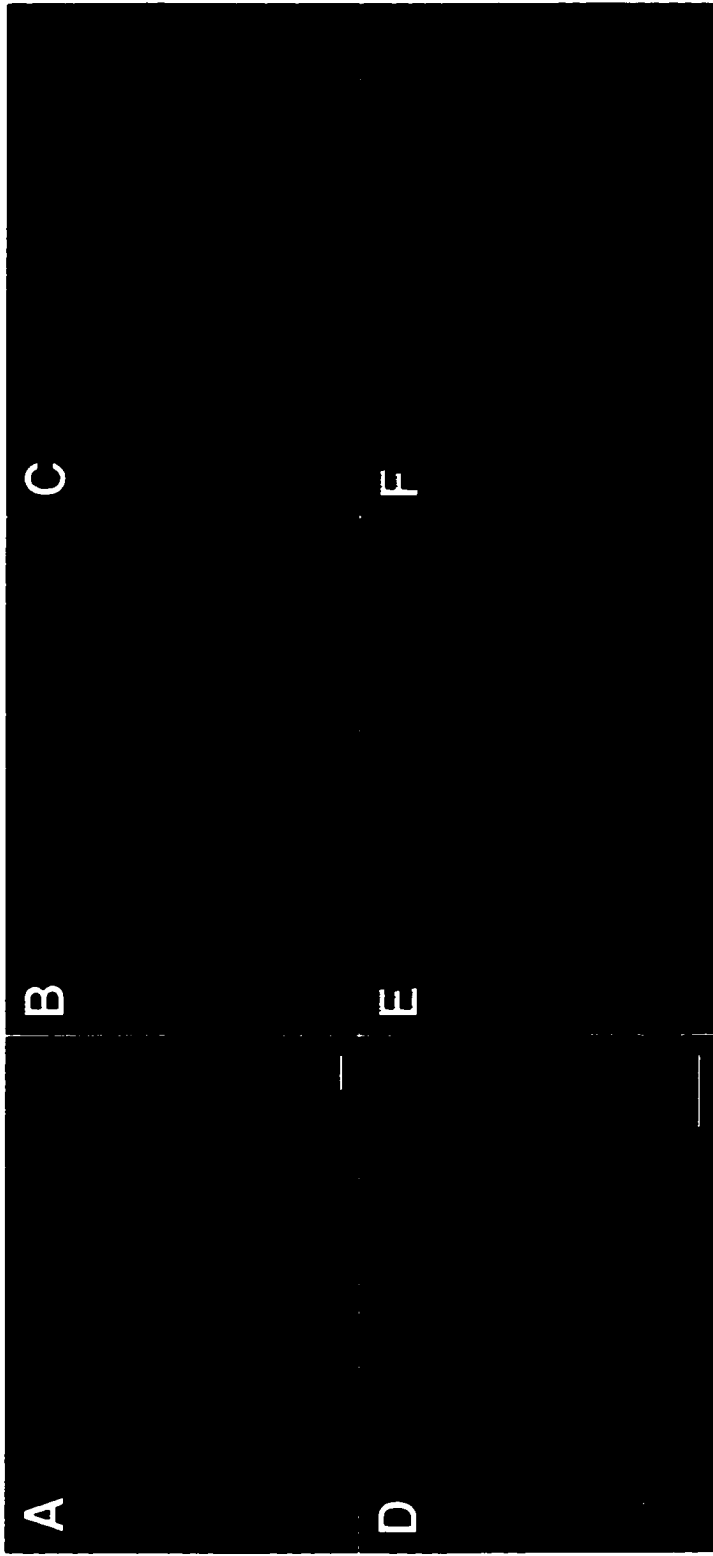
FIGURE 8.4

Figure 8.5 Immunoreactivity of Fos and GAD in serial sections through the SNC. Low (A,B), medium (C,D) and high (E,F) magnification micrographs demonstrating the expression of Fos-LI (left panels) and GAD (right panels) in the SNC of a naive animal following d-amphetamine challenge. The boxed areas in A) and B) indicate the corresponding regions that are shown magnified in panels C - F, respectively. The central region of the SNC (arrows) where Fos-LI was expressed was found to have a high concentration of GAD-positive cells. Scale bars = 100 μm.
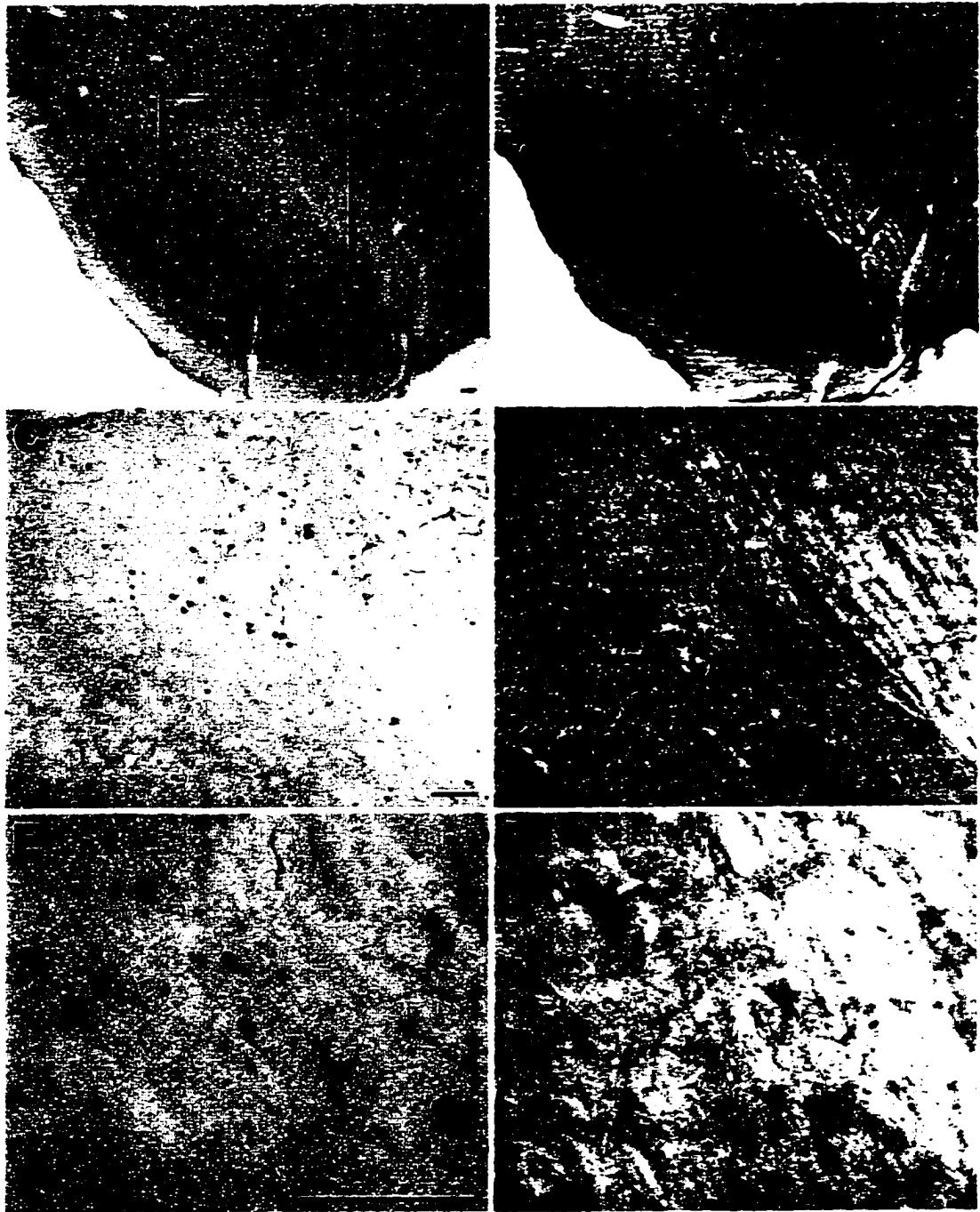
FIGURE 8.5

Figure 8.6 Double-labeling of Fos (dark nuclei) and GAD (light brown cytoplasm) in the SNC using two-color DAB immunohistochemistry. A) Low magnification micrograph showing the location of the double-labeled cells. B), C) Higher magnification of the region shown in A). Many double-labeled cells (arrows) were present, as well as GAD-positive cells that did not express Fos-LI (arrowheads). Also note the abundance of GAD-immunoreactivity in terminal boutons. Scale bars = 100 μm.
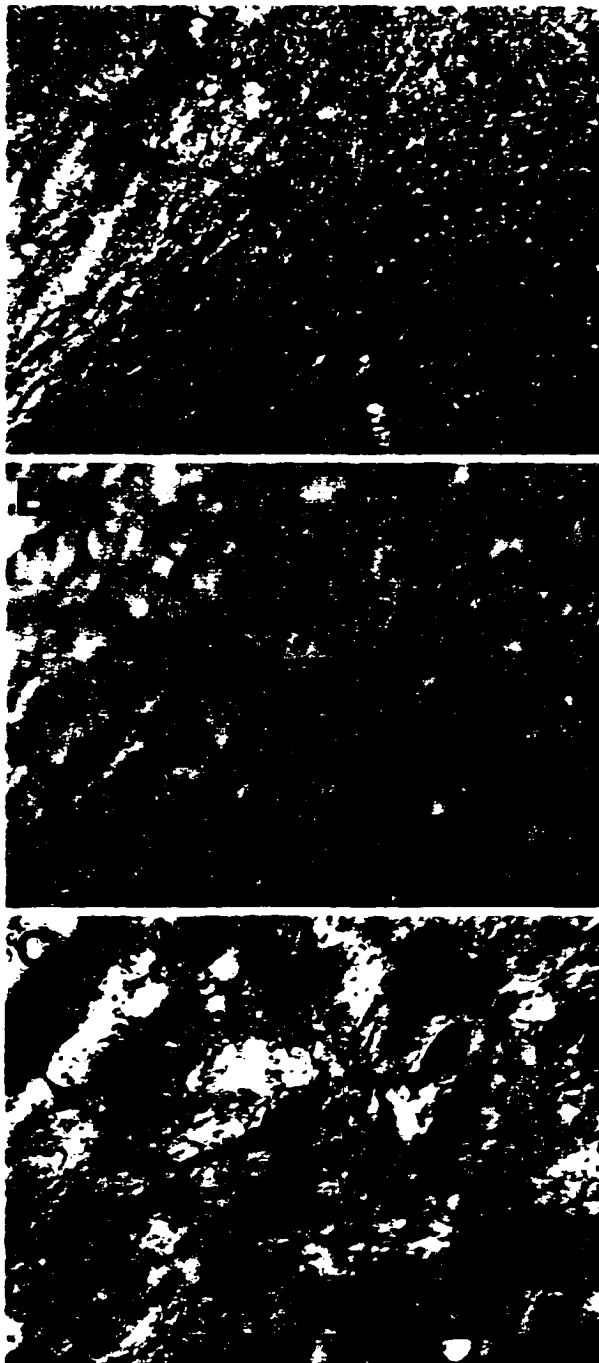
FIGURE 8.6

Figure 8.7 Double immunofluorescent-labeling of Fos (green) and GAD (red), imaged using confocal microscopy. Sections 50 μm-thick were examined in 5 μm increments to reduce obscuring of soma-labeling by GAD-positive fibres. These sections were obtained from naive animals that had been stimulated with d-amphetamine. A) Consistent with the DAB immunohistochemistry, several double-labeled neurons were apparent in the SNC using this method (arrows). Also, there appeared to be GAD-positive, Fos-negative cells in this region (large arrowhead). Fos-positive nuclei that were less intensely labeled were evident in adjacent tissue planes (small arrowheads). B) High magnification of a double-labeled neuron in the SNC. Scale bars = 10 μm.
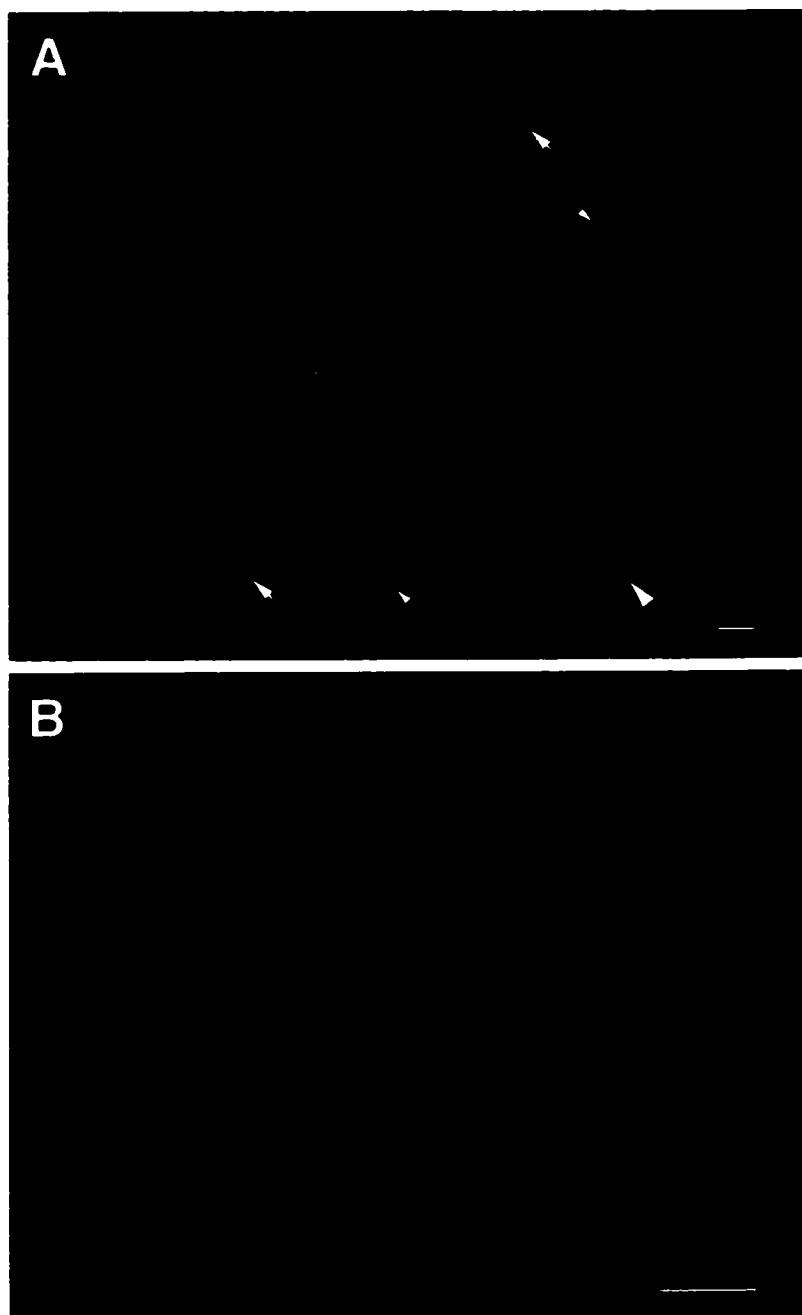
FIGURE 8.7

Figure 8.8 Retrograde labeling of nigrostriatal neurons. A) Fluorogold injection site in the striatum. Diffusion of the tracer was apparent throughout most of the striatum, with no penetration into surrounding brain regions. Dashed line indicates the lateral border of the striatum. cc = corpus callosum. B) Fluorogold-labeled neurons in the SNC five days following tracer injection into the striatum. C) Fluorogold (blue-white) and Fos-LI (red) in the SNC following *d*-amphetamine administration. D) High magnification of the area shwon in C). Scale bars = 100 μm.
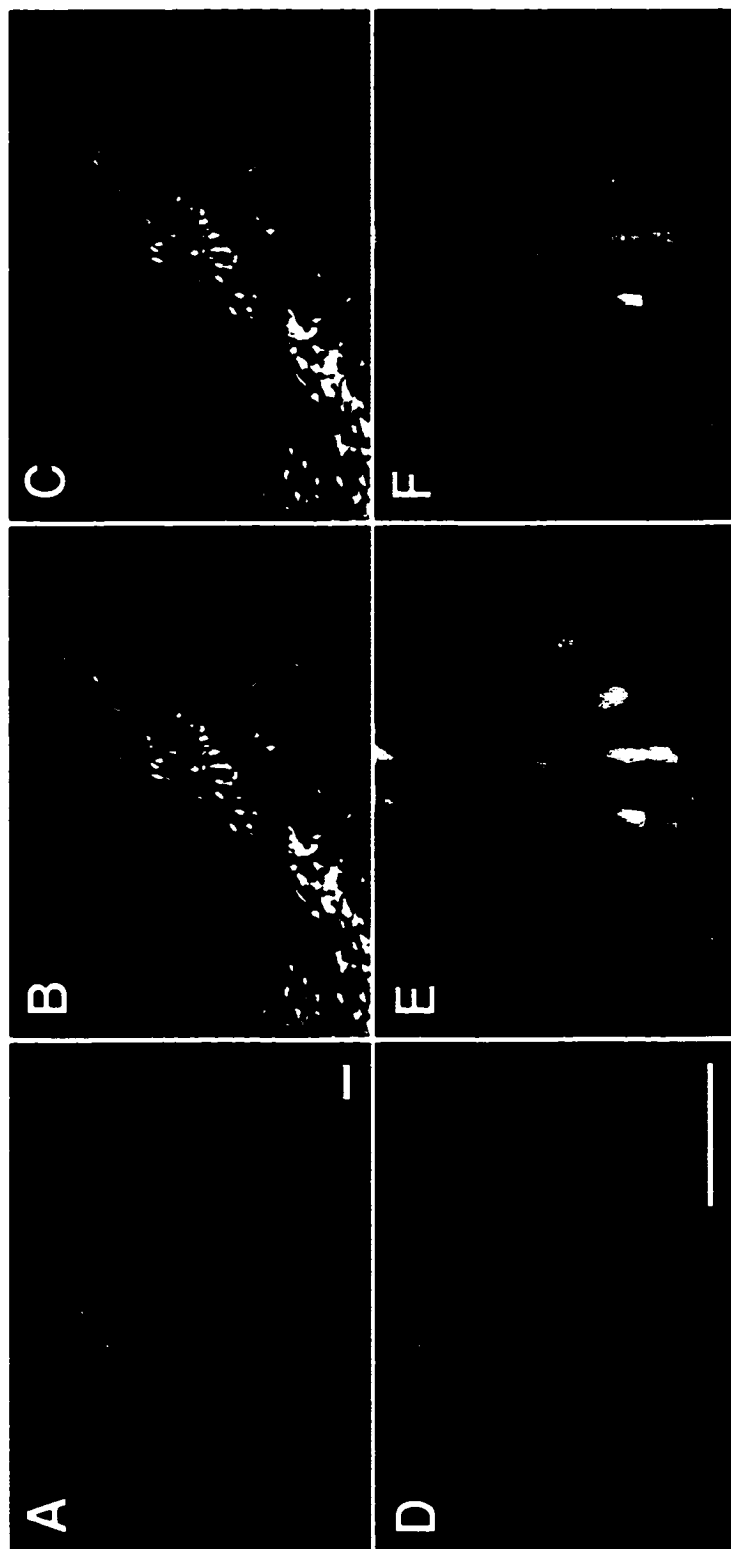
FIGURE 8.8

CHAPTER 9

Uptake and Biodistribution of Intrastriatally-Injected Oligodeoxynucleotides with Various Lengths and Degrees of Phosphorothioate Modification

9.1. Introduction

The *in vivo* application of antisense ODNs has become an increasingly popular method with which to suppress gene expression in the brain. However, systematic assessments of the uptake and biodistribution of intracerebrally-injected ODNs have been scarce. Sommer *et al.*(1998) have described the uptake patterns and transport of both radio-labeled and fluorescein-labeled ODNs in the rat brain and have shown that partially modified, phosphorothioate ODNs are rapidly taken up by neurons in the striatum. The appearance of the internalized ODNs was initially diffuse but changed to a punctate pattern, an effect attributed to encapsulation of the ODNs into intracellular vesicles.

Two important factors which are crucial for effective antisense-mediated gene suppression are the stability of the ODN in the cellular environment and specificity of ODN hybridization. Unmodified, phosphodiester ODNs are rapidly degraded *in vivo* by exo- and endo-nucleases (Eckstein, 1985). A common modification that is used to increase nuclease-resistance is phosphorothioate substitution, in which an oxygen atom of the linkage phosphate group is replaced with a sulfur atom. This modification hinders the activity of the degrading enzyme, possibly by increasing the dissociation time of the enzyme-ODN complex (reviewed in Stein and Cohen, 1989). One disadvantage of phosphorothioate ODNs is decreased cellular uptake, owing to increased protein affinity and non-specific interactions (reviewed in Neckers, 1989).

In this study, we have compared the uptake and distribution of radio-labeled and fluorescein-labeled derivatives of the anti-c-*fos* (ASF) ODNs (15-mers) that had been

used in previous studies (see chapters 3-8). The biodistribution of ASF ODNs with various degrees of sulfur modification were compared following direct infusion of these molecules into the striatum. Also, we were interested in determining whether increasing the length of the ODN would alter its pharmacokinetic properties in the CNS. For this, we infused a relatively large (45-base), end-capped ODN that was complementary to a region of the *huntingtin* mRNA (see chapter 10) into the striatum of adult rats and compared distribution profiles with those of the smaller (15-mer) ODNs. Our results suggest that neither increasing the degree of phosphorothioate modification on smaller ODNs, nor lengthening the ODN by three-fold, significantly alter the cerebral uptake and distribution patterns of these molecules.

9.2. Materials and Methods

9.2.1. Experimental Design

Male Sprague-Dawley rats, weighing between 250-350 grams, were anesthetized with halothane and subsequently mounted on a Kopf stereotaxic apparatus in a flat skull position. Animals were supplemented with halothane (Fluothane) during the course of the surgery. Once mounted in the apparatus, the scalp was retracted and the skull exposed. A burr hole was drilled in the skull and a 25-gauge cannula was guided into the right striatum (from bregma: AP, 1.0 mm; DV, 6.0 mm; LAT, 3.0 mm). Solutions of oligodeoxynucleotides were then infused at a rate of 0.25 μl/min using a CMA 100 (Carnegie-Medicin) microinjection pump until a total volume of 2.0 μl (2.0 nmol) was reached. Following infusion, the cannula was left in place for an additional two minutes to allow for diffusion away from the injection site. Following removal of the cannulae, the animals were sutured and placed in their home cage for the appropriate recovery periods.

In a preliminary study, animals received an intrastriatal infusion of a 45-base antisense ODN targeting the *huntingtin* gene (HDO). Following infusion, animals were given a recovery period of 30 minutes, 1 hour, 3 hours or 5 hours (n=1 each), afterwhich they were deeply anesthetized with pentobarbital (>100 mg/kg) and sacrificed. These animals were transcardially perfused, initially with saline, followed by 4% paraformaldehyde in a 0.1 M phosphate buffer solution (pH 7.4). Brains were subsequently removed and post-fixed at 4°C until further analysis. Brains were blocked and cut on a vibratome in 50 μm coronal sections. Sections were mounted on gelatin-coated glass slides and visualized under fluorescent illumination.

In a second study group, animals were infused with ODNs that had been labeled at the 3'-terminal with fluorescein and at the 5'-terminal with $[^{33}P]\alpha$-dATP (see below). These animals were allowed recovery periods of 1, 4 or 24 hours (n=1 each), following which they were sacrificed. These animals were swiftly decapitated and had their brains removed and frozen on dry ice until further analysis. Brains were cut on a cryostat into 14 μm sections. After air-drying, some sections through the striatum, GP and SN were analyzed microscopically, under fluorescent illumination to visualize the fluorochrome, while adjacent sections were exposed on Biomax MR autoradiographic film (Kodak) for 2 (striatum, GP) or 5 (SN) days to identify the radiolabeled ODN. Selected sections were coated with autoradiographic emulsion (Kodak NTB2) and exposed for 4 weeks at 4°C, prior to developing with Kodak D19 developer and fixer. After developing, the slides were counterstained for Nissl substance by being air-dried, dehydrated in graded alcohols and xylene, rehydrated and stained with 0.1% cresyl violet.

9.2.2. Oligodeoxynucleotides

9.2.2.1. General   The two ODN sequences used in these studies have both been described in alternate chapters. The 15-base ASF sequence is described in section 3.2.3.. Presently, this sequence was used in two different chimeric phosphodiester / phosphorothioate ODN derivatives: ASF1 was the single end-capped ODN that had been used in the previously described experimental work in chapters 3-8. This ODN had a single phosphorothioate substitution at the terminal phosphate groups. A second ODN, ASF2, contained significantly greater sulfur modification in that every second

phosphate linkage group had a phosphorothioate substitution. A third ODN, HDO, was a 45-mer, with the sequence 5'-CTT-GTT-CTA-CAA-TCC-CTC-TGA-TCA-TGC-TCA-ACT-TTC-TTC-CAA-ATC-3'. The sequence of this ODN was complementary to bases 7570-7614 of the huntingtin RNA (GenBank accession no. U18650) and had been used in both *in situ* and Northern blot analyses of the huntingtin transcript (see chapter 10). Both ASF1 and HDO were obtained from Genosys while ASF2 was obtained from BIOTEZ (Berlin).

9.2.2.2. ODN-Labeling and Gel Purification

All ODNs had three molecules of fluorescein linked to the 3'-amino terminal (as performed by the manufacturer). The ODNs used in the second study group were also radiolabeled at the 5'-terminal. For this, 0.5 nmole of the fluorescein-tagged ODNs were labeled at the 5'-carboxy terminal with [^{33}P]α-dATP using T4 polynucleotide kinase (Pharmacia), according to the suppliers protocol. When labeling was complete, the entire reaction mixture (~ 30 μl) was loaded on a 12% polyacrylamide minigel and electrophoresed until the ODNs had migrated approximately 3 cm into the gel. The position of the migration front was monitored by the addition of 1 μl bromophenol blue to the reaction mixture. (Bromophenol blue co-migrates with ODNs of approximately 15-bases in a 12% polyacrylamide gel.) The gel was then wrapped in 'Saran Wrap' and exposed to Biomax MR autoradiographic film (Kodak) for 4-6 hours, afterwhich the film was developed. The band of appropriate size was cut out of the gel using a razorblade and the ODNs were eluted in 400 μl sterile water at 60°C overnight. The next day, the ODN solution was transferred to a fresh tube. Aliquots of 2 μl were used to measure

the amount of radioactivity and 3 µl was loaded onto a 12% polyacrylamide gel to verify ODN size and purity. The purified ODNs were stored at -20°C until used.

9.2.2.3. Intracerebral ODN Infusions Following quantification of radioactivity in the gel-purified, labeled ODNs, 500 000 cpm of each ODN was transferred to a fresh eppendorf tube and lyophilized under vacuum centrifugation. The dried ODNs were reconstituted in a 1 mM solution of the respective, non-radioactive (but fluorescein-tagged) ODN. This was the concentration of ASF that had been utilized in the previous functional studies (see chapters 3-8). The ODNs were infused into the striatum as described above.

9.3. Results

9.3.1. Purification of Labeled ODNs

Initial PAGE of ODN samples revealed broad bands of radioactive signal when exposed to film (Fig.9.1A). This was attributed to a certain degree of ODN degradation during storage and handling, resulting in ODNs of various lengths being labeled with $[^{33}P]\alpha$-dATP. Removal of the appropriate sized bands from this gel successfully isolated the desired ODNs and eliminated the majority of degradation products and unincorporated radioactivity (Fig.9.1B).

9.3.2. Distribution and Uptake of ODNs in the Striatum

Because the majority of functional studies that used ASF1 had been performed with the animals receiving a recovery period of 1 hour, we were interested in determining the extent of ODN diffusion and transport in the brain at this time point. In these animals, the radioactive signal was diffuse throughout the infused striatum, but appeared to be restricted from adjacent brain regions by the corpus callosum and ventral striatal borders (Fig.9.2A,B). We found that the radioactive signal rapidly appeared in the GP, but not the SN, and was evident at 1 hour post-infusion (Fig.9.2C-F).

The distribution of radioactivity and fluorescence was similar for all ODNs at each time point observed. Also, the microscopic and autoradiographic results were consistent between animals. Figure 9.3 shows representative micrographs of the fluorescent signal observed in the striatum and GP at 1 hour after the delivery of the ODNs. Note the extensive cellular uptake in the striatum and the GP. However, both the fluorescent and radioactive signals were very low or completely absent in the

extreme caudal striatum, immediately overlying the GP. Thus, the robust signal in the GP could not be attributed to a general diffusion of the ODNs into this area and must have occurred through cellular transport from the striatum. Examination of the distribution of the fluorescence in the GP revealed both prominent cell soma incorporation as well as dense fibre labeling, indicative of both anterograde and retrograde transport from the striatum to the GP (Fig.9.3B). Paraformaldehyde-fixed brains that had been infused with the fluorescein-tagged HDO provided greater morphological detail of cellular distribution of the ODN than did the unfixed, frozen sections. Figure 9.4A shows substantial ODN incorporation into striatal neurons at 30 minutes post-infusion. While there were many neurons labeled at this time point, there appeared to be greater uptake with longer latencies (not shown). In addition to neuronal uptake of HDO in the striatum at 30 minutes post-infusion, we observed dramatic labeling of GP neurons and fibres (Fig.9.4B-D). The fluorescence was completely localized to the GP at this antero-posterior level, producing a spotlight appearance of this nucleus (Fig.9.4B). Numerous cell bodies were fluorescently labeled, with the signal apparent in both the cytoplasm and nucleus. Consistent with the dense fibre labeling observed in the frozen sections, there was strong fluorescence in boutons in the GP (Fig.9.4D). Thus, it appeared that the GP received both anterograde and retrograde transport of ODNs following striatal infusion.

Fluorescent labeling was not detected in the SN at any time point, likely due to imperceptible amounts of the transported fluorochrome. There was also no radioactive signal detected at 1 hour post-infusion (Fig.9.2F). However, at the 4 and 24 hour time

points, all animals exhibited significant ODN transport to the SN, independent of the sequence and length of the ODN (Fig.9.2G).

Emulsion autoradiography in the GP and the SN revealed a very dense clustering of silver grains that was diffusely distributed throughout the region (not shown). Thus, using this technique, it was difficult to determine whether the signal was emanating from both intracellular and extracellular sources or, perhaps, exclusively from neurons, including those out of the plane of Nissl staining. However, this diffuse distribution of silver grains was consistent with the previous observation that ODNs undergo anterograde transport along striatopallidal fibres and retrograde transport to somata in the GP via pallidostriatal fibres. Thus, it is likely that the ODN signal in the SN resulted from similar mechanisms.

9.4. Discussion

Phosphorothioate ODNs, like their phosphodiester congeners, are large anionic molecules that do not readily pass through hydrophobic cellular membranes. Internalization of phosphorothioate ODNs is believed to occur through active pinocytotic mechanisms, although there have also been reports of receptor-mediated ODN transport into cells (Loke *et al.*,1989; Yakubov *et al.*,1989). Although the molecular charge of phosphodiester ODNs is conserved by phosphorothioate modification, the sulfur substitution confers significant resistance to ODN degradation by endo- and exo-nucleases (Eckstein, 1985). The sulfur atom is, however, much larger and more polarizable than the oxygen atom, increasing the ionic affinity of sulfur-modified ODNs for other charged cellular constituents. Thus, a major drawback of this derivatization is the increased affinity to cellular proteins that is produced by the sulfur substitution (reviewed in Stein and Cohen, 1989). In the brain, extensive interactions have been demonstrated to occur between phosphorothioate ODNs and several heparin-binding proteins, including basic fibroblast growth factor (bFGF) (Guvakova *et al.*,1995). Also, phosphorothioate have been shown to bind to several cell surface proteins, further contributing to their non-specific effects and impeding their internalization (reviewed in Neckers, 1989).

The antisense studies described in the previous chapters have utilized single end-capped ODNs. These chimeric molecules possess a phosphorothioate substitution at the terminal phosphate groups, endowing them with a portion of the nuclease resistance of fully modified molecules (Stein *et al.*,1988). Also, it has been reported

that end-capped ODNs are internalized into cells at a rate similar to phosphodiester ODNs (reviewed in Neckers, 1989). To date, however, there have been no descriptions of the uptake and distribution of single-end-capped ODNs in the brain. Thus, the purpose of this study was to demonstrate the extent of striatal diffusion and cellular uptake of the c-*fos* antisense ODN (ASF1) that had been used in previous functional studies (see chapters 3-8). Also, we were interested in determining whether an increased degree of phosphorothioate modification on the ASF sequence would alter the pharmacokinetic properties of this ODN, relative to the end-capped derivative. Finally, we examined whether a relatively large, 45-base ODN (HDO) would be incorporated into striatal neurons or if the size of this ODN would hinder its uptake. We found that all three ODNs were extensively taken up by striatal neurons at 1 hour following infusion. The widespread distribution of ODN throughout the infused striatum, but not the contralateral side or cortex is consistent with the extent of c-*fos* suppression previously reported (see chapters 3-5, 7). In agreement with a recent report by Sommer *et al.* (1998), the intracellular distribution at this time point appeared diffuse throughout the cytoplasm of the cells. In addition to striatal uptake, it appeared that all ODNs were transported to the GP and SN, apparently by both anterograde and retrograde mechanisms.

The transport of ODNs from the striatum to the GP occurred very rapidly, appearing in pallidal fibres and cell bodies at 30 minutes post-infusion. The greater physical distance from the striatum likely accounted for the delayed (4 hrs) appearance of ODN signal in the SN. While the functional consequences of ODN transport to

these projection nuclei remain speculative, our previous experience with ASF suggests that, if intact ODNs are indeed transported to the GP and SN, they do not exert an antisense effect in these regions. For example, we have found that marked suppression of *d*-amphetamine-induced c-*fos* expression is produced by intrastriatal infusion of ASF. This striatal suppression has been associated with a dramatic increase in pallidal expression (see chapters 3 and 4), discounting the possibility that transported ODNs had an antisense (suppression) effect. These findings also raise the possibility that the previously reported increase in pallidal Fos-LI (see chapters 3 and 4) may not have resulted from a suppression of inhibitory striatopallidal transmission, but rather as a cellular response to the influx of transported ODNs. Several previous findings discount this possibility, however. The demonstration of the functional motor effect of pallidal activation in animals that received striatal ASF suggested that these changes were mediated through alterations in motor circuitry, in attempt to maintain intercerbral symmetry, and did not result from unrelated changes in intracellular constituents (see chapter 5). This is further supported by the alterations in GP Fos-LI produced by *d*-amphetamine and apomorphine in animals that had received 6-OHDA lesions and were not administered antisense ODNs (see chapter 7).

It is difficult to explain the apparent efficiency of ODN transport and the lack of functional antisense effect of these molecules in the striatal projection nuclei. It is possible that the ODNs were contained within intracellular vesicles that restricted their access to cytoplasmic RNA. Alternatively, terminal degradation by nuclease activity may have played a role. Many endo-nucleases function in the 3'-5' direction, but there

are also those that degrade fragmented DNA from 5'-3'. Thus, the removal of the 3'-fluorochrome or the 5'-radiolabel from the parent ODN would effectively produce an abundance of small molecular weight tracer molecules that could easily and rapidly be transported or diffuse throughout intracellular systems. We have attempted to avoid misinterpretation of distributed ODN signals by labeling both ends of the molecule, and comparing the biodistribution of both fluorescence and radioactivity in the tissue. Also, the initial gel purification of the ODNs significantly minimized the amount of free radiolabel or fluorescein in the ODN solutions. Finally, the terminal phosphorothioate modifications on all of the ODNs should have afforded a certain degree of nuclease resistance to the ODNs. However, in order to conclusively determine whether the signals that are observed in the projection nuclei are intact ODNs or free labels, one must carefully dissect out these regions and recover the transported ODNs. One major difficulty with this approach (that we have experienced first hand) is that there may only be minute amounts of labeled ODN present in these distant projection regions. An alternate, but less conclusive, method would be to label the ODNs at the internal phosphate groups, affording them more substantial protection from enzymatic dissociation.

The results of this study demonstrate that 15-base, end-capped ODNs are effectively internalized in striatal neurons and that this process does not appear to be significantly affected by additional phosphorothioate modifications or lengthening the ODN to 45-bases. Additionally, it suggests that there is rapid transport of ODNs from the striatum to proximal (GP) and distal (SN) projection nuclei. These findings provide rationale for future investigations into the functional consequences of such transport.

Figure 9.1   Autoradiographs showing PAGE of total (A) and purified (B) 5'-[^{33}P]α-dATP-labeled ODNs. A) Samples of each ODN were loaded into 2 lanes, as indicated at the top of the autoradiograph. The boxes indicate the bands which were removed and eluted. B) Purified ODNs eluted from the gel shown in A). ODNs migrated as would be expected from their lengths (HDO, 45-mer; ASF1 and ASF2, 15-mer). Purified ODNs were used for intracerebral injections.

A HDO ASF1 ASF2

B HDO ASF1 ASF2
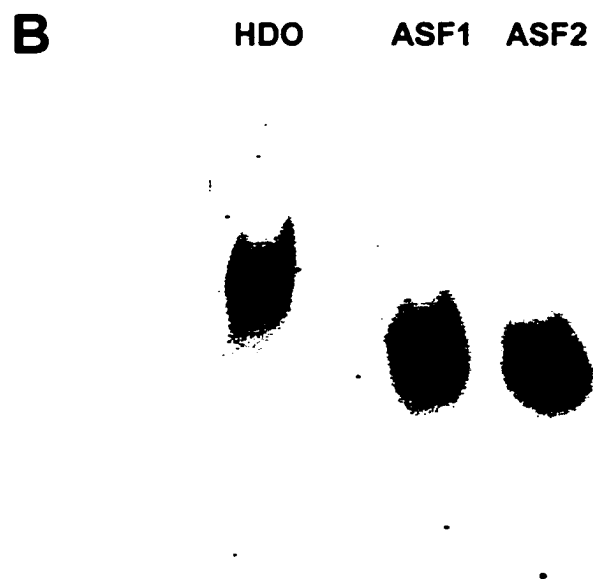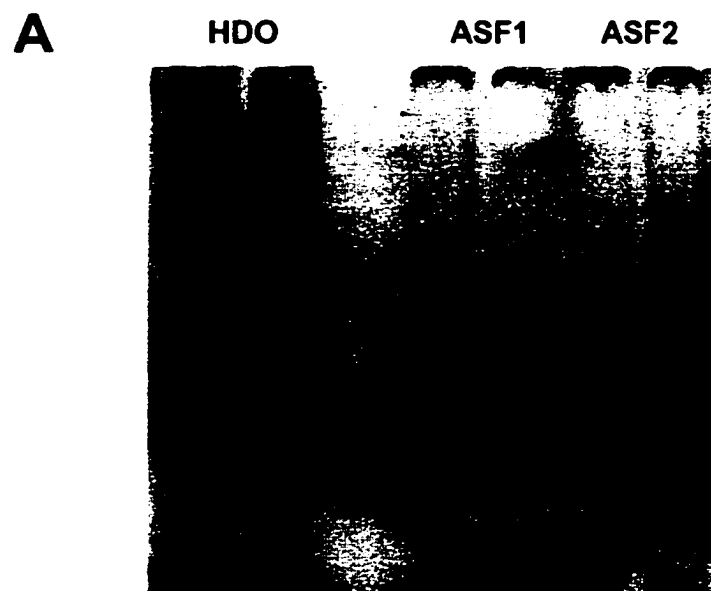
FIGURE 9.1

Figure 9.2 Distribution of radioactivity following intrastriatal infusion of ASF1 with a 1-hour recovery period. Panels A,C and E show schematically the region of interest in corresponding panels B,D and F. The areas shaded in gray correspond to the regions show in the panel to the right of the diagram. At this time point, there was extensive striatal diffusion (B) as well as robust signal emanating from the GP (D). No radioactivity was detected in the SN at 1 hour post-infusion (F). The sections in panel F and G have been overexposed to reveal the tissue morphology. At 4 and 24 hours after ODN infusion, however, there was a strong radioactive signal in the SN (G). The pattern of distribution shown in this figure is representative of that seen with all ODNs. Diagrams have been modified from Paxinos and Watson (1997).

A **B** **C** **D** **E** **F** **G**
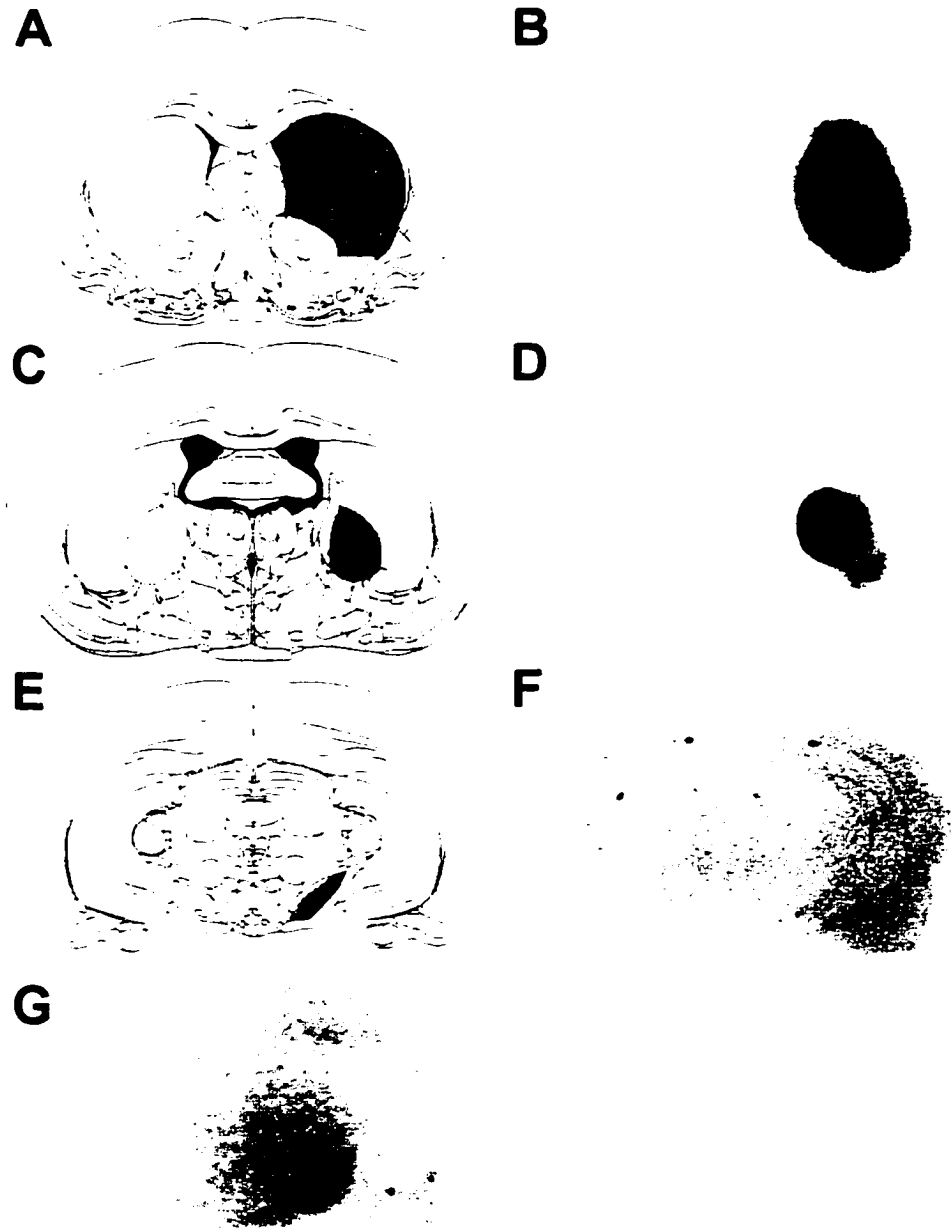
FIGURE 9.2

Figure 9.3 Distribution and uptake of fluorescein-labeled ASF1 in the striatum (A) and GP (B) in unfixed, frozen sections. Consistent with the autoradiographic results, there was extensive cellular labeling surrounding the striatal infusion site (A). The GP also had marked cellular labeling as well as dense fibre labeling (B). The arrowheads in B) indicate the striatum-GP border. Note the lack of labeling in the caudal striatum, indicating the fluorescence in the GP was not produced by general diffusion from the infusion site, but rather intracellular transport. These micrographs are representative of the results obtained from all ODNs. Scale bar represents 100 μm.
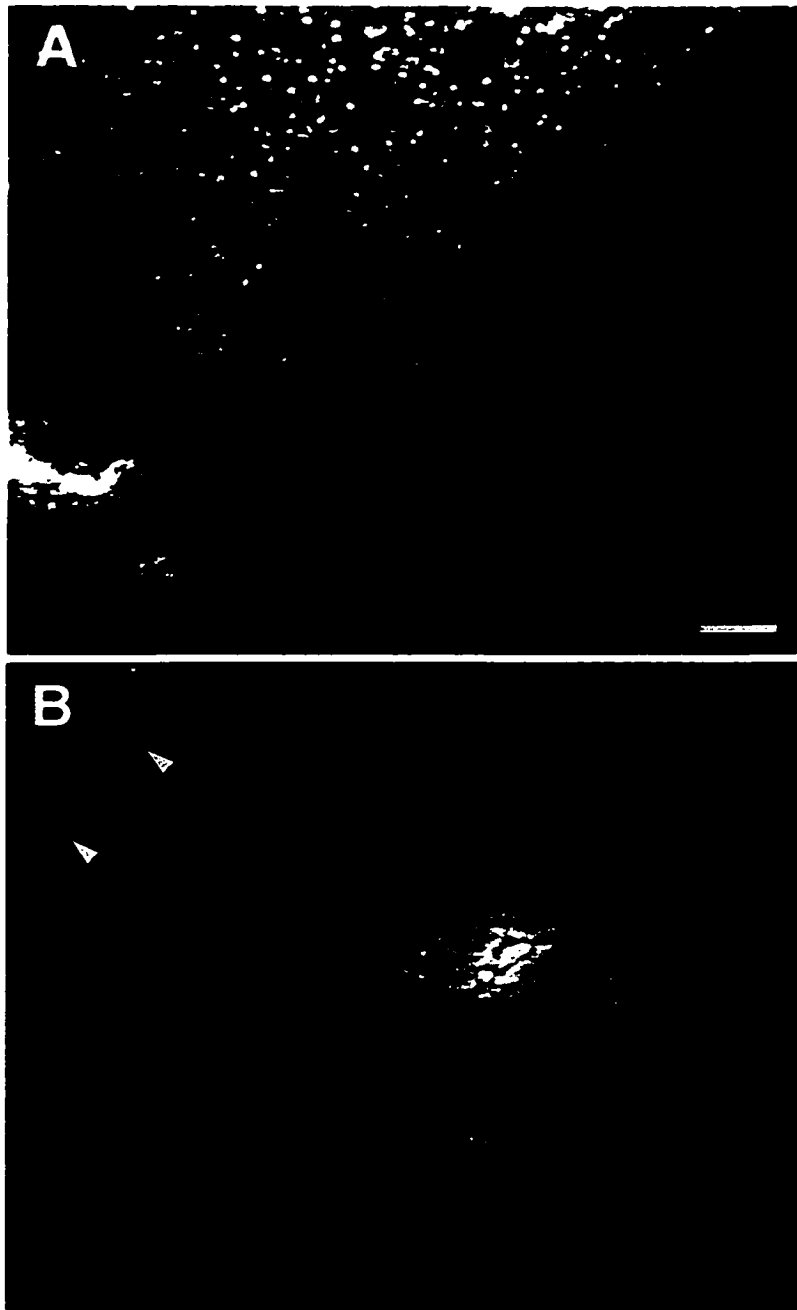
FIGURE 9.3

Figure 9.4   Cellular uptake of HDO in the striatum and GP at 30 minutes post-infusion in paraformaldehyde-fixed tissue. A) Numerous filled neurons were present in the striatum in the region surrounding the infusion site. B) The GP of these animals displayed robust fluorescence, taking on a spotlight appearance in the midst of the overlying, unlabeled striatum. Medium (C) and high (D) magnification micrographs of the GP show cellular morphology of the filled neurons. Also note the labeled boutons in this region (D), indicative of anterograde transport via striatopallidal fibres. Scale bar in A) indicates magnification of A) and D). All scale bars represent 100 μm.
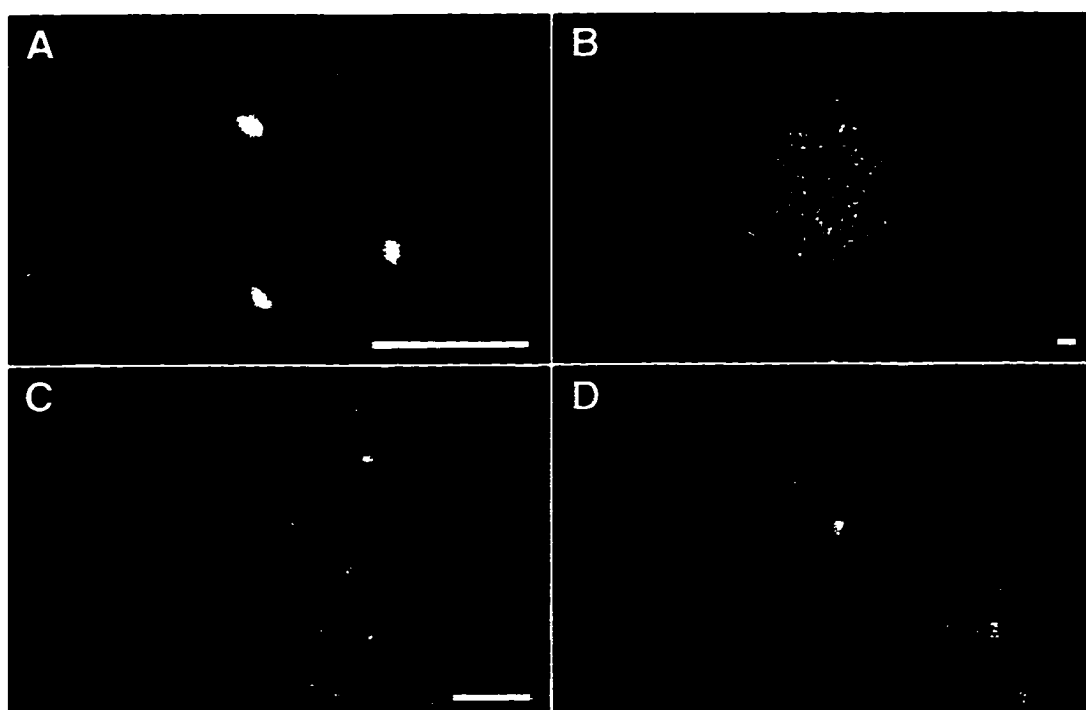
FIGURE 9.4

CHAPTER 10

Expression of the Huntington's Disease Gene in the Hypothalamus: Evidence of Involvement in Neuroendocrine Plasticity[*]

[*] Results presented in this chapter have been submitted for publication.

10.1. Introduction

Huntington's Disease (HD) is a genetic neuropathological disorder which presents with progressive motor and cognitive impairment, marked atrophy of specific brain regions, and neuronal loss (Folstein, 1989). The genetic mutation which leads to HD is an expansion of a trinucleotide (CAG) repeat in exon 1 of the IT15 gene located at chromosome 4p16.3 that encodes the protein, huntingtin (The Huntington's Disease Collaborative Research Group, 1993; Trottier *et al.*, 1995b). Currently, neither the function of the normal form of huntingtin nor any aberrant interactions that are induced by the mutation of this protein are known. Also, while alterations in the expression of this gene have been reported to be induced by excitotoxins (Carlock *et al.*,1995; Tatter *et al.*,1995), its regulation during naturally occurring physiological changes has not been demonstrated.

The hypothalamus, particularly the arcuate nucleus (AN), undergoes marked alterations in metabolic activity during the late stages of pregnancy, parturition and post-parturition. Changes in physiology and cellular morphology in this region have been shown to be regulated by gonadal hormones, the levels of which change markedly following parturition (Pfaff and Keiner, 1973; Garcia-Segura *et al.*, 1986; Olmos *et al.*, 1989; Keefe *et al.*, 1991). For example, the activity of the tuberinfundibular dopamine (TIDA) neurons of the AN is suppressed in lactating animals, an effect which is enhanced and maintained by the suckling stimulus (Moore, 1987; Hoffman *et al.*, 1994). However, the mechanisms by which these alterations occur remain unknown. In this report, we describe the induction of the Huntington's Disease gene in the

subependymal zone (SEZ) of the third ventricle and the AN of the hypothalamus in postpartum, lactating animals.

10.2. Materials and Methods

10.2.1. Animal Treatment Adult Sprague-Dawley rats were used in this study. Postpartum female rats were purchased with 2-day old litters and housed with their litters under a 12-hour light-dark cycle with free access to food and water. The mothers were removed at postnatal day 7 and anesthetized using > 100 mg/kg sodium pentobarbital. Rats were perfused through the left ventricle with 60 ml saline followed by 120 ml 4% (w/v) paraformaldehyde in a 0.1M phosphate ($NaH_2PO_4 \bullet H_2O$) buffer solution (pH 7.4). Following perfusion, the brains were removed and post-fixed for 10-16 hours in equivalent paraformaldehyde solution. For RNA isolation, animals were decapitated and the hypothalami were excised and stored in liquid nitrogen. All animal groups were analyzed by immunohistochemistry (postpartum n=11; naïve female n=4; male n=7) and *in situ* hybridization (postpartum n=4; naïve female n=4; male n=4) techniques. Northern blot analysis was performed on individual RNA extractions from 3 male animals.

10.2.2. Immunohistochemistry Brains were blocked and 50 μm coronal sections were cut on a vibratome. Sections were collected through the rostrocaudal axis of the third ventricle and the hypothalamus and processed for huntingtin immunohistochemistry and *in situ* hybridization analysis. For immunohistochemistry, the tissue was washed for 10 minutes in 0.1M phosphate-buffered saline containing 0.1% Triton-X (PBS-TX). This was followed by a 15 minute incubation in 1% hydrogen peroxide to inactivate endogenous peroxidase activity and subsequent 3 X 10 minute washes in PBS-TX at room temperature. The sections were then incubated in a

1:500 dilution of a monoclonal antibody to the huntingtin protein (Chemicon; MAB2166) for 16-24 hours at 4°C. (This antibody has been previously characterized by Trottier *et al.*, 1995a,b.) Following incubation with the primary antibody, the sections were washed 3 X 10 minutes in PBS-TX and incubated in a 1:500 dilution of horse anti-mouse secondary antibody (Vector Laboratories) for 1-2 hours at room temperature. Excess antibody was removed by washing 3 X 10 minutes in PBS-TX and the bound secondary was visualized using the avidin-biotin technique (ABC Elite; Vector Laboratories) using diaminobenzidine (DAB; Sigma) as the chromogen. The sections were mounted on gelatin-coated slides, air-dried, dehydrated in graded alcohols, delipidated in xylene and coverslipped using Entellan adhesive (Merck).

Sections were also double-labeled for huntingtin and glial fibrillary acidic protein (GFAP). The primary incubation media contained both the monoclonal antibody to huntingtin (1:500) and a rabbit polyclonal antibody to GFAP (1:2000; DAKO) in PBS-TX. Following incubation (16-24 hours) with the primary antibodies, the sections were washed 3 X 10 minutes in PBS-TX and subsequently incubated in CY2-conjugated donkey anti-mouse and CY3-conjugated donkey anti-rabbit (1:400; BioCan) for 16-24 hours at 4°C. The sections were then washed 3 X 10 minutes in PBS-TX, mounted on gelatin-coated slides and coverslipped using Citifluor (Marivac). Fluorochromes were visualized using filter sets to detect CY2 (Zeiss, catalogue no.487710) and CY3 (Zeiss, catalogue no.487715) immunofluorescence.

10.2.3. Determination of Transcript Size

10.2.3.1. Northern blot analysis   Hypothalami were removed from adult rats and stored individually in liquid nitrogen. Total cellular RNA was isolated from individual samples using TRIzol reagent (GibcoBRL) according to the manufacturer's protocol. A northern blot was prepared by fractionating 10 µg aliquots of RNA on a 1% denaturing agarose gel followed by transfer of the RNA to Zetaprobe (BioRad) membrane using standard methodology (Sambrook *et al.*,1989).

10.2.3.2. Hybridization Probe   A 45-base oligonucleotide probe (5'-CTT-GTT-CTA-CAA-TCC-CTC-TGA-TCA-TGC-TCA-ACT-TTC-TTC-CAA-ATC-3')   was designed which was complimentary to bases 7570-7614 of the huntingtin RNA (GenBank accession no. U18650). The oligonucleotide (5 pmoles) was radiolabeled with [^{32}P]α-dATP using terminal transferase (3'-end labeling kit; Amersham). Unincorporated radionucleotides were removed from the labeled probe by centrifugation through a Microspin-G25 column (Pharmacia Biotech).

10.2.3.3. Hybridization Conditions   The northern blot was prehybridized in buffer containing 5X standard saline citrate (SSC), 5X Denhardt's solution, 50mM sodium phosphate, 1% sodium dodecyl sulfate (SDS), 5mM EDTA, 10 µg/ml tRNA, 50 µg/ml denatured salmon sperm DNA, 50 µg/ml denatured yeast RNA and 50% formamide at 42°C for 4-6 hours. Following prehybridization, the blot was transferred to a hybridization buffer (5X SSC, 1X Denhardt's solution, 20mM sodium phosphate, 2% sodium dodecyl sulfate (SDS), 5mM EDTA, 10 µg/ml tRNA, 100 µg/ml denatured salmon sperm DNA, 100 µg/ml denatured yeast RNA, 50% formamide and 100 mg/ml dextran sulfate) containing 2 X 10^6 counts/ml of radiolabeled oligonucleotide. The blot

was hybridized for a minimum of 18 hours at 42°C, afterwhich it was washed for 15 minutes in 2X SSC / 0.1% SDS (42°C), 2X SSC / 0.1% SDS (50°C), then twice in 1X SSC / 0.1% SDS (50°C). The blot was subsequently washed in 0.5X SSC / 0.1% SDS at 50°C and exposed to Biomax MR autoradiographic film (Kodak) with an intensifying screen for 4 days at -70°C.

10.2.4. Localization of huntingtin mRNA transcripts

10.2.4.1. In situ hybridization and emulsion autoradiography   Coronal sections (50 μm) were mounted on Superfrost Plus slides and air-dried overnight. The sections were dehydrated and cleared in graded alcohols and xylene, respectively. Following rehydration, sections were washed 3 X 5 minutes in 1X PBS followed by 3 X 5 minutes in 2X SSC and air-dried.

10.2.4.2. Hybridization Probe   The 45-base huntingtin oligonucleotide probe which was used in the northern blot analysis was also used for *in situ* hybridization. The oligonucleotide (5 pmoles) was radiolabeled at the 3'-end with [^{33}P]α-dATP as described above.

10.2.4.3. Hybridization Conditions   The sections were covered with hybridization buffer (5X SSC, 1X Denhardt's solution, 20mM sodium phosphate, 2% sodium dodecyl sulfate (SDS), 5mM EDTA, 10 μg/ml tRNA, 100 μg/ml denatured salmon sperm DNA, 100 μg/ml denatured yeast RNA, 50% formamide and 100 mg/ml dextran sulfate) containing 5 x 10^6 counts/ml of labeled huntingtin probe and incubated at 38°C in a humidified chamber for a minimum of 18 hours. Following hybridization, the slides were washed for 4 x 15 minutes each in 1X, 0.5X, 0.25X SSC at 50°C,

rinsed in H$_2$O and air-dried overnight. The slides were exposed to Biomax MR (Kodak) autoradiographic film for 7 days, afterwhich they were coated in autoradiographic emulsion (Kodak NTB2) and exposed for 4 weeks at 4°C, prior to developing with Kodak D19 developer and fixer.

Following the processing of slides for autoradiographic emulsion, the sections were counterstained for Nissl substance. Briefly, the sections were dehydrated and rehydrated in a series of graded alcohols (50%, 70%, 90%, 100%), then washed in cold water. Slides were immersed in 1% (w/v in H$_2$O) Cresyl Violet (ICN Biochemicals) for approximately 1 minute. Excess stain was removed by washing in dilute acetic acid, then the slides were dehydrated, delipidated in xylenes and coverslipped.

10.2.5. Statistical Analysis Densitometric analysis of *in situ* autoradiographs was performed using Molecular Analyst software (BioRad) to determine the optical density (OD) of the radiolabel in hypothalamic regions. Autoradiographic films were scanned into the computer using a BioRad GS-690 Imaging Densitometer. The sections were numbered in a random fashion, with the observer blind to the animal group from which they were obtained. There were four animals per group included in this analysis. Optical density units were calculated by blocking individual arcuate regions for each animal and calculating these values for 3-4 sections of the hypothalamus per animal to obtain a total of 6-8 OD values per animal. To account for non-specific radioactivity in the sections, the OD value for the ventromedial nucleus of the thalamus was taken as the background signal and this value was subtracted from all values obtained from the

arcuate nucleus in each section. The mean value of this difference was calculated for each animal and used as a representation of the intensity of hybridization signal in the arcuate nucleus.

Once all densitometric values had been calculated, the number code for the animals was revealed and the mean OD values were grouped as postpartum female, naïve female or male. These values were then subject to a one-way analysis of variance (ANOVA) followed by a post-hoc Newman-Keuls test. Significance was assumed at $P < 0.05$. Data was converted to relative OD values by expressing the raw data as a percentage of the highest OD value obtained in the postpartum group.

10.3. Results

10.3.1. Expression of the huntingtin Protein in the Subependymal Zone Huntingtin-immunoreactivity (huntingtin-IR) was observed in several brain regions, including cortex, thalamus, hippocampus and hypothalamus. In naïve female and male animals, huntingtin-IR was evident in the SEZ and defined a continuous cellular monolayer immediately adjacent to the ependymal lining of the ventricle (Fig. 10.1A,C,E). The distribution of huntingtin-IR in the cytoplasm of these cells revealed an ovoid cellular morphology with a large, central nucleus and no evidence of extending processes (Fig. 10.1E). This pattern of immunolabeling was specific to the huntingtin antibody as sections processed without primary antibody had no definition of these cells (data not shown).

In postpartum, lactating animals, the intensity of huntingtin-IR was markedly amplified in the SEZ compared to naïve animals. The cellular monolayer immediately adjacent to the ventricular ependyma immunolabeled intensely for huntingtin throughout the majority of the ventricular surface, with the exception of the most dorsal regions (Fig. 10.1B). Unlike the continuous chain of huntingtin-positive cells seen in naïve animals, the SEZ of postpartum animals appeared disrupted in several areas, with intensely labeled cells in and adjacent to the SEZ (Fig. 10.1D). It was evident that the huntingtin-IR was confined to the cytoplasm as the nuclei were clearly defined. Where the integrity of this region was disrupted, huntingtin-IR positive cells were often seen in the neuropil immediately adjacent to the SEZ. As evident in Fig. 10.1F, the huntingtin-IR defined several small processes that resembled sprouting

neurites which extended from the perikarya. Disruption of the SEZ and the identification of neurites with huntingtin-IR was not seen in any of the naïve female or male animals.

10.3.2. Expression of huntingtin Protein in the Arcuate Nucleus Neuronal expression of huntingtin was evident in the AN and the surrounding neuropil (Fig. 10.2). In addition to ubiquitous neuronal labeling, the AN of naïve female and male rats expressed low levels of huntingtin in cells that were morphologically characteristic of glia (Fig. 10.2D,F). In postpartum animals, however, the expression of huntingtin was markedly increased in these cells (Fig. 10.2A,B). This observation was consistent in all postpartum animals examined. Omission of the primary antibody eliminated immunolabeling in all animal groups (Fig. 1G,H). These control experiments excluded the possibility that the diaminobenzidine (DAB) product observed in the AN was a result of endogenous peroxidase activity. This enzyme has been previously shown to be affected by changes in estradiol concentrations in various estrogen target tissues (Anderson *et al.*,1975; Lyttle and DeSombre, 1977; Schipper *et al.*,1990).

10.3.3. Specificity of the huntingtin Oligonucleotide We designed a 45-base oligonucleotide probe that was complementary to bases 7570-7614 of the huntingtin mRNA for use in *in situ* hybridization analysis. To ensure that this short, synthetic oligonucleotide would hybridize exclusively to huntingtin transcripts, we used this probe in northern blot analysis against electrophoretically-fractionated total RNA isolated from the hypothalamus. Figure 10.3 shows a representative hybridization result from these studies. In each of three individual RNA samples that were subjected

to northern blot analysis, the radiolabeled oligonucleotide annealed exclusively with discrete bands of approximately 11 kb and 13 kb. The size of these hybridizing bands correspond to those previously reported for the huntingtin transcripts (Li *et al.*,1993; Lin *et al.*,1993, 1994). These results confirmed that the oligonucleotide probe used for northern blot and subsequently *in situ* hybridization analyses was specific for transcripts whose sizes correspond precisely to those of the huntingtin mRNA.

10.3.4. Localization of huntingtin mRNA in the Hypothalamus In situ hybridization was performed on coronal brain sections through the hypothalamus from male, naïve female and postpartum female rats using the 45-base antisense oligonucleotide to the huntingtin transcript. Examination of autoradiographs from naïve female and male animals revealed pronounced huntingtin-radiolabeling in the piriform cortex, hippocampus and the hypothalamus (Fig. 10.4A). Thus, the pattern of huntingtin mRNA and protein expression were consistent in these regions. While naïve female and male animals expressed huntingtin mRNA in the arcuate nucleus, the level of expression was low and was only particularly evident when viewed following emulsion autoradiography (discussed below). In contrast, postpartum, lactating animals showed intense radiolabeling in the arcuate region of the hypothalamus (Fig. 10.4A). This signal was evident throughout the rostrocaudal axis of the arcuate nucleus, consistent with the huntingtin immunolabeling previously observed. Densitometric analysis of huntingtin hybridization signal in the arcuate region revealed a significant increase of approximately seven-fold in the postpartum animals compared to naïve female and male animals (P= 0.029; Fig. 10.4B). Post-hoc analysis revealed significant differences in

huntingtin hybridization signal between postpartum females and naïve females (P=0.022) and male animals (P=0.043). In contrast, there was no difference in the expression between naïve female and male animals (P=0.902).

Examination of the arcuate nucleus following emulsion autoradiography of coronal sections that were radiolabeled with the huntingtin probe revealed a clustered distribution of silver grains in a pattern analogous to that observed with huntingtin-IR (Fig. 10.5). This pattern was observed in postpartum and, to a lesser extent, naïve animals. The sections processed for emulsion autoradiography were counterstained for Nissl substance in order to reveal the location of huntingtin-expressing glial cells relative to neurons of this region. The clusters of silver grains were consistently found in close apposition to neuronal soma. Under brightfield illumination, it was evident that the clusters were not directly overlying the neuronal soma but appeared juxtaposed to these cells, suggesting physical interactions between these cell types (Fig. 10.6A). High magnification comparison of huntingtin mRNA and protein expression in the AN revealed similar patterns of distribution (compare Fig. 10.6A with Fig. 10.6B).

10.3.5. Characterization of huntingtin-Expressing Cells in the AN

10.3.5.1. Morphology of huntingtin-expressing cells in the AN   The cellular distribution of huntingtin mRNA in the AN (Fig. 10.7A), as detected by *in situ* emulsion autoradiography, and the huntingtin protein (Fig. 10.7B), as observed by immunohistochemistry, revealed expression of this gene in cell soma as well as in several cellular processes. The distribution pattern of the mRNA and protein both defined a stellate conformation characteristic of astrocytes, but not neurons.

10.3.5.2. Co-localization of huntingtin and GFAP To characterize the cells that

had elevated huntingtin expression in postpartum animals, we performed

immunohistochemistry for the astrocytic marker, glial fibrillary acidic protein (GFAP)

and huntingtin in fluorescent double-labeling experiments. The expression of GFAP

was ubiquitous and immunofluorescence was intense in several regions of the brain.

To ensure that the immunofluorescence of the huntingtin signal (CY2) was only

observed under the appropriate filter and not seen with the filter used to view the

GFAP signal (CY3), we examined various regions of the brain for penetrance of

immunofluorescence. When tissue sections through the hippocampus (dentate gyrus)

were immunolabeled for both huntingtin (Fig. 10.8A) and GFAP (Fig. 10.8B), it was

evident that fluorescent signal from the labeled antigens were not observed when the

tissue was viewed with a filter that was specific for the emission wavelength of the

other fluorochrome (Fig. 10.8C).

Huntingtin immunofluorescence was pronounced in the AN of postpartum

animals (Fig. 10.8D). In the AN, the cells that were expressing huntingtin were also

positive for GFAP immunofluorescence (Fig. 10.8E, F). Several huntingtin-positive,

GFAP-negative cells were observed in the peripheral regions of the AN. Close

examination of this region revealed that many cells that had abundant huntingtin

expression only labeled positively for GFAP in portions of the cell soma, but not in

cellular processes (Fig. 10.8G-I).

While these results demonstrate that the fluorescent signals were specific to

huntingtin and GFAP and, hence, that huntingtin and GFAP are co-localized in these

cells, it is important to recognize the possibility of autofluorescence. It has been previously reported that glial cells in the AN autofluoresce under UV light, an effect which is thought to be caused by the presence of porphyrins in these cells (Goldgefter et al.,1980). We examined sections that were processed for immunofluorescence without incubating the tissue in primary antibody and found that cells in the AN autofluoresced under a wide-band ultraviolet filter. This autofluorescence in the AN was markedly reduced under the CY2 filter and completely eliminated under the CY3 filter (data not shown). Also, the pattern of autofluorescence was unlike that observed with huntingtin-IR or GFAP-IR and cellular resolution of the autofluorescing cells was not possible. Unlike the huntingtin-IR, there was no difference in intensity of this non-specific signal between the animal groups. These results demonstrate that these huntingtin-immunoreactive cells are GFAP-positive and support their morphology-based classification as astrocytes. We were not, however, able to confirm the co-localization of huntingtin and GFAP in the cells of the SEZ.

10.4. Discussion

We have demonstrated the induction of the Huntington's Disease (HD) gene in a population of subependymal cells in the third ventricle of postpartum animals. In naïve female and male animals, these cells possess an ovoid morphology, devoid of huntingtin-expressing cellular processes. In postpartum females, a substantial portion of these cells in the SEZ appears to migrate from the ventricular lining, producing obvious changes in the cytoarchitecture of this region. These cells are elongated and have several identifiable neuritic processes. As this subependymal zone (SEZ) has been shown to contain pleuripotent progenitor cells that may be induced to differentiate and express neuronal or glial phenotypes, it is possible that the cells described here are stem cells or are associated with stem cells (Weiss at al., 1996). The induction of huntingtin in the cells of the SEZ and their apparent differentiation and migration strongly implicate this protein's involvement in mediating trophic responses.

Our results also show that astrocytic expression of the huntingtin protein is increased in the arcuate nucleus (AN) of the hypothalamus in postpartum, lactating animals. The AN regulates the release of the lactogenic hormone, prolactin, from the anterior pituitary gland in postpartum animals. The tuberoinfundibular dopamine (TIDA) neurons of this region produce a tonic inhibition of prolactin release, thus preventing milk production in naïve animals (Moore, 1987; Neill and Nagy, 1994). The hormonal changes that occur following parturition produce cellular alterations that are believed to inhibit the activity of the DA system and permit secretion of prolactin. It has been demonstrated that suckling produces a marked increase in prolactin secretion and a concomitant reduction in dopamine release (Moore, 1987; Neill and

Nagy, 1994). Although the mechanisms by which these changes occur remain unclear, there is mounting evidence to suggest the involvement of glia in hypothalamic regulation (Brawer *et al.*, 1978; Tranque *et al.*, 1987; Garcia-Segura *et al.*, 1989; Ojeda *et al.*, 1990; Torres-Aleman *et al.*, 1992; Ma *et al.*, 1994, 1997).

Estradiol treatment has been shown to modify the shape of astrocytes in the AN and produce alterations in the distribution of glial fibrillary acidic protein (GFAP) in these cells (Tranque *et al.*, 1987; Garcia-Segura *et al.*, 1989; Torres-Aleman *et al.*, 1992). As these effects were dependent on the presence of neurons, it was postulated that stimulation of neuronal estrogen receptors (ER) induced the release of stimulatory factor(s) which produced the astrocytic changes (Torres-Aleman *et al.*, 1992). Astrocytes in the hypothalamus express transforming growth factor-alpha (TGF-α) and the epidermal growth factor receptor (EGFR) (Ferrer *et al.*, 1996). Estradiol has been shown to increase the expression of TGF-α in hypothalamic astrocytes, but not in astrocytes of the cerebellum, indicating that hormonal responsiveness in these cells is greater in specific regions of the brain (Ma *et al.*, 1994). The increased expression of TGF-α by estradiol is blocked by inhibition of EGFR. As ERs are expressed in as few as 10% of hypothalamic glial cells, it is thought that the stimulation of TGF-α expression and release produces a paracrine/autocrine enhancement of this factor in adjacent cells which do not express ERs (Ojeda *et al.*, 1992; Ma *et al.*, 1994). These results demonstrate that changes in circulating estrogen can have profound effects on trophic expression in the AN.

It has been reported that stimulation of hypothalamic astrocytes with TGF-α produces an increase in the release of luteinizing hormone-releasing hormone (LHRH) from neurons in this region (Ojeda *et al.*, 1990; Ma *et al.*, 1997). The exposure of hypothalamic astrocytes to TGF-α produced an increase in prostaglandin E2 (PGE$_2$) release, the blockade of which prevented the astrocytic medium from inducing LHRH release from neurons. Thus, it appears that the release of LHRH from the hypothalamus is regulated by hormonal changes that stimulate local astrocytes to secrete soluble factor(s), including PGE$_2$, which induce neuronal LHRH release. It is possible that the release of prolactin-inhibiting (DA) and prolactin-stimulating hormones are under similar regulatory control. In addition, glia to neuron apposition in the hypothalamus is substantial and has been shown to be altered by gonadal steroids, suggesting that the astrocytic regulation of neuronal function may be mediated by physical alterations in synaptic connectivity (Witkin and Silverman, 1985; Witkin *et al.*, 1991; King and Letourneau, 1994). These results are consistent with the current finding that, in postpartum animals, upregulation of huntingtin expression occurs in hypothalamic astrocytes that are juxtaposed to neuronal soma.

Currently, the mechanisms that mediate physiological changes in the AN during the reproductive cycle remain unknown. While estrogen has no documented influence on stem cells of the SEZ, it has been shown to inhibit various hemopoietic cell lines and induce granulocytic differentiation in myeloblasts, as well as inhibit osteoblast proliferation (Egrise et al., 1992; Modrowski et al., 1993; Dietsch et al. 1996; Shevde and Pike, 1996). Also, it may be relevant that estrogen increases the release of TGF-α

from hypothalamic astrocytes (Ma *et al.*, 1994). Epidermal growth factor (EGF) and TGF-α have been repeatedly shown to induce multipotent stem cells from ventricular SEZ to migrate and differentiate to express neuronal and astrocytic phenotypes (Reynolds *et al.*, 1992; Reynolds and Weiss, 1992). More recently, these stem cells have been shown to express EGFR and have been isolated from spinal cord and all regions of the ventricular neuroaxis, including the third ventricle (Okano *et al.*, 1996; Weiss *et al.*, 1996). Our results raise the possibility that neuroendocrine modifications in the AN are mediated through the recruitment of multipotent stem cells of the SEZ which migrate to the AN and differentiate into astrocytes. As it is unlikely that every naïve female examined in this study was at the identical stage of estrous when sacrificed, the minimal expression of huntingtin consistently observed in the SEZ and AN in this group and in male animals suggests that the process observed in postpartum animals does not occur during the course of normal cycling.

A recent study by Liu *et al.* (1997) investigated the possible association of huntingtin with various signaling molecules involved in EGFR signaling cascade. The presence of multiple proline-rich motifs in the huntingtin sequence led this group to investigate the possibility that huntingtin would associate with signaling modules through binding of *src* homology 3 (SH3) domains. Experiments demonstrated that huntingtin associates with the EGFR signaling complex through binding of SH3 domains on growth factor receptor-binding protein (Grb2) and Ras-GTPase-activating protein (RasGAP). These associations were highly dependent upon EGFR activation and autophosphorylation (Liu *et al.*, 1997). Interestingly, huntingtin

immunoprecipitates were found to contain Grb2, but not the Ras guanine nucleotide releasing factor, Sos. In contrast, Grb2 immunoprecipitates were found to contain Sos. As Sos is the normal associative molecule which complexes with the SH3 domains on Grb2, the authors suggested that huntingtin may be a competitive inhibitor of Sos-Grb2 binding and transduction of Ras-dependent signaling. The nature of the huntingtin-RasGAP association remains unclear.

The present study implicates the huntingtin protein as an important component of the cellular mechanism that mediates hormone-induced transcriptional and morphological changes in the neuroendocrine brain. The role of huntingtin as a regulator of receptor tyrosine kinase signaling and modulator of cellular plasticity would account for the widespread expression of this protein. This would also offer an explanation for the embryonic mortality observed in mutant mice that are nullzygous for the huntingtin gene (Nasir et al., 1995; Zeitlin et al., 1995). As the expression of this protein is constitutive in neurons throughout most brain regions, it is conceivable that huntingtin may not only be involved in EGFR signaling, but may be a component of other receptor kinase signaling cascades as well.

The function of the huntingtin protein remains unknown. Because mutation of the IT15 gene produces an altered protein that induces the irreversible neuropathology of HD, major therapeutic potential is thought to lie in the development of agents that will inhibit its expression. However, if huntingtin is an essential component of stem cell development, as our results suggest, suppression of this gene may accelerate or

have further detrimental consequences for the normally prolonged course of

Huntington's disease.

Figure 10.1 Induction of *huntingtin* expression in the subependymal zone. Huntingtin-IR surrounding the third ventricle and in the adjacent neuropil of naïve female and male animals (A,C,E) and in postpartum animals (B,D,F) demonstrated the pronounced expression of this protein in the ventricular lining of lactating females. (C) Low levels of huntingtin-IR were evident in a monolayer of subependymal cells immediately adjacent to the ventricular ependyma in naïve animals. (D) In postpartum animals, this region had undergone marked alterations in cytoarchitecture as many cells with intense huntingtin-IR appeared to have migrated from the SEZ into deeper layers of the adjacent neuropil. Note the absence of the definable chain of SEZ cells seen in C). The arrows in C) and D) indicate regions which are shown at high magnification in E) and F), respectively. E) The huntingtin-expressing cells of the SEZ in naïve animals appeared ovoid in morphology, with no evidence of cellular processes. F) In postpartum animals, cells were elongate and had several cellular processes that were huntingtin-positive (arrowheads). Scale bar represents 200 μm for A) and B), 20 μm for C) and D) and 5 μm for E) and F).
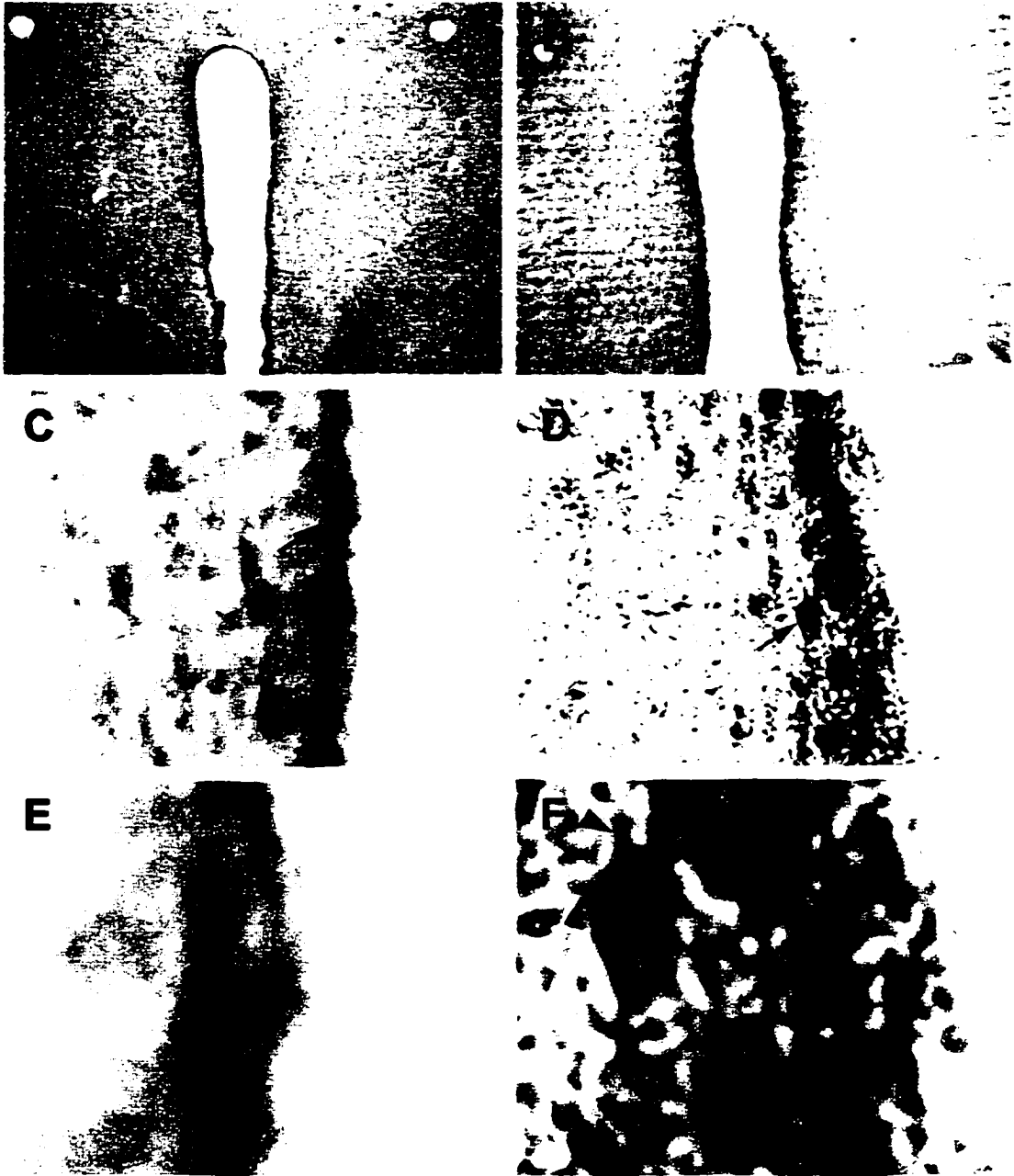
FIGURE 10.1

Figure 10.2 Expression of the huntingtin protein in the arcuate nucleus. The images in the left column have been magnified in the corresponding panel on the right. Postpartum animals had robust expression of huntingtin in cells with glia-like morphology (A,B). This expression was evident in low abundance in naïve female (C,D) and male (E,F) animals (arrows). Omission of the primary antibody during immunohistochemical processing eliminated labeling in both neuronal and glial cells (G,H). Scale bar represents 80 μm.
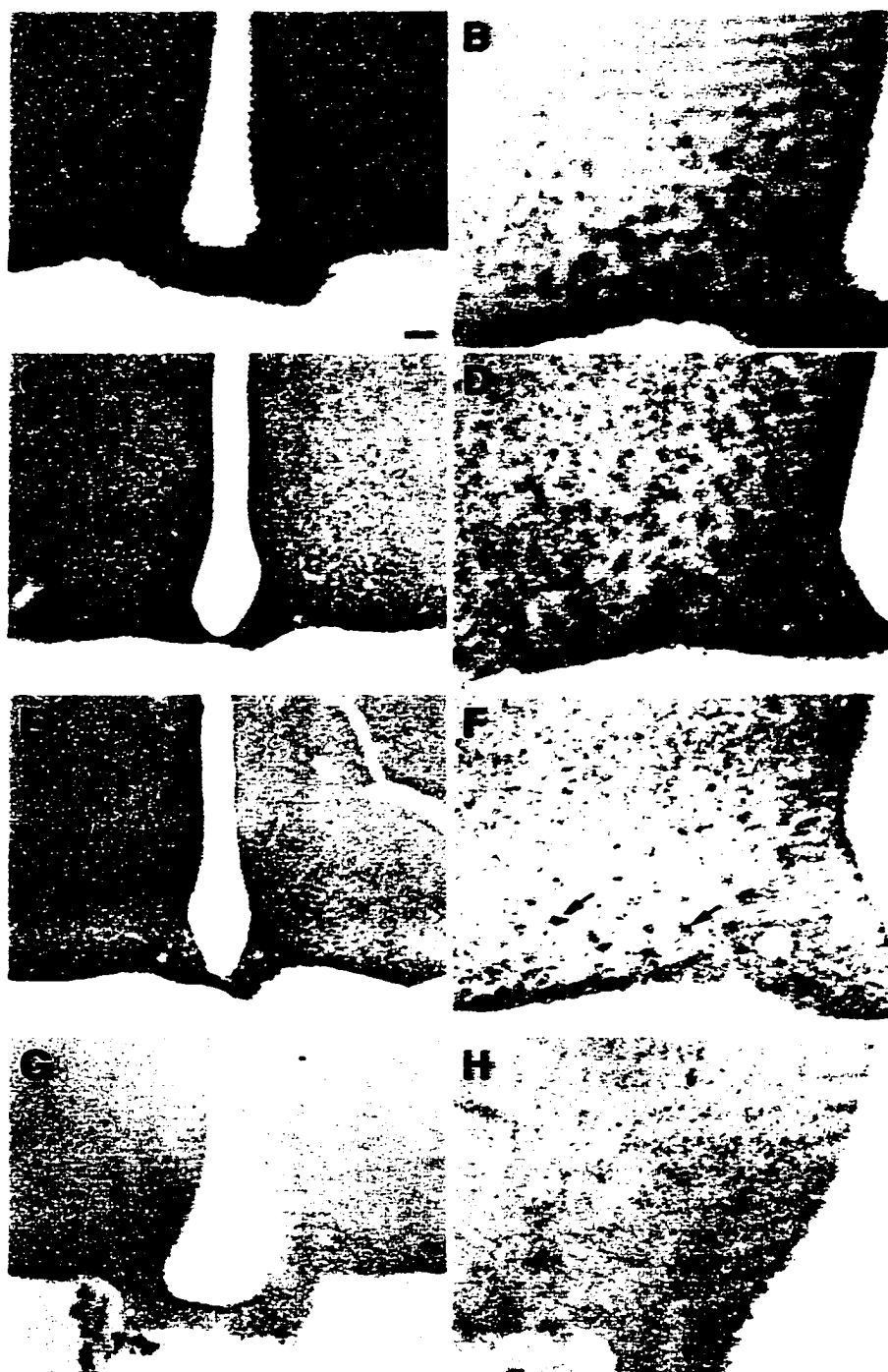
FIGURE 10.2

Figure 10.3 Northern blot analysis confirmed the specificity of the 45-base oligonucleotide probe targeted to the huntingtin mRNA. This probe identified bands of approximately 11 and 13 kb, corresponding to previously confirmed sizes of the two *huntingtin* transcripts.

9.5
7.5

4.4

2.4

1.4

0.24
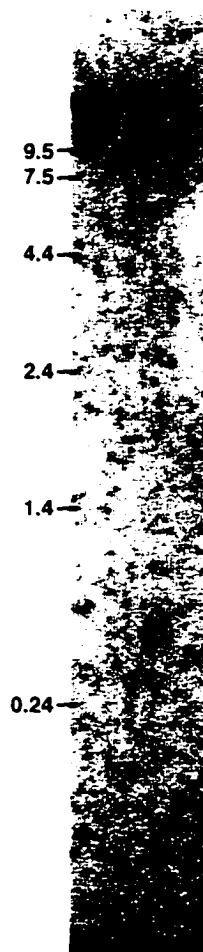
FIGURE 10.3

Figure 10.4 Distribution of *huntingtin* mRNA in the arcuate nucleus. A) *In situ* autoradiography indicating rostral (I,III,V) and caudal (II,IV,VI) expression of the *huntingtin* mRNA in the arcuate nucleus in postpartum (I,II), naïve female (III,IV) and male (V,VI) animals. Consistent with immunohistochemical analysis, this region had significantly greater expression of the huntingtin mRNA in postpartum animals relative to naïve female or male animals. Each section in the animal groups shown was taken from a different animal. Note the intense hybridization signal in the piriform cortex and the hippocampus which is also consistent with the distribution of the huntingtin protein. B) Quantification of huntingtin hybridization signal in the arcuate nucleus revealed a significant increase in mRNA expression in postpartum animals. M=male; NF=naïve female; PPF= postpartum female. Asterisks indicate significant difference from postpartum group (P<0.05).

A

B
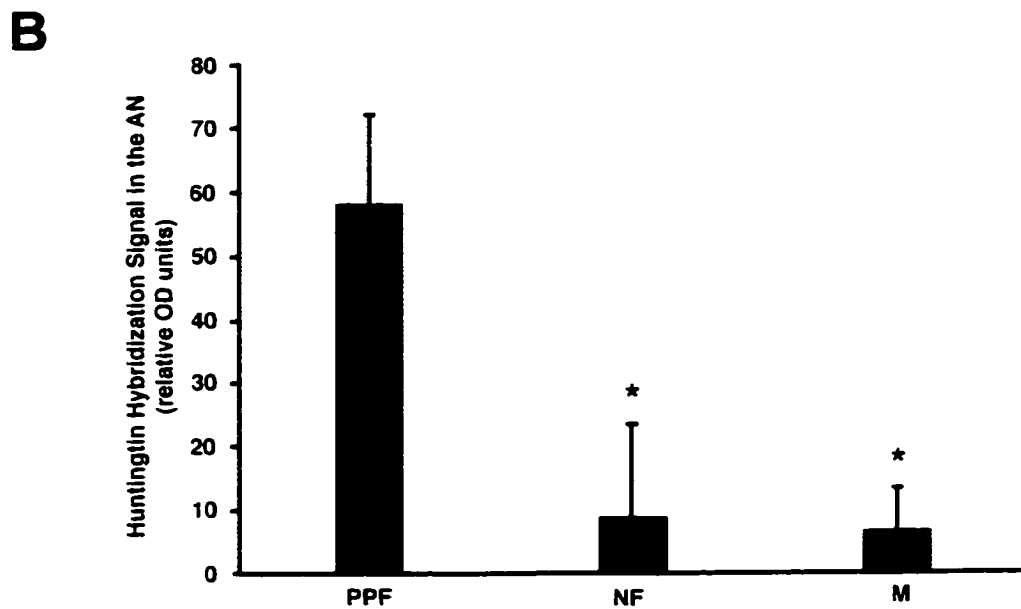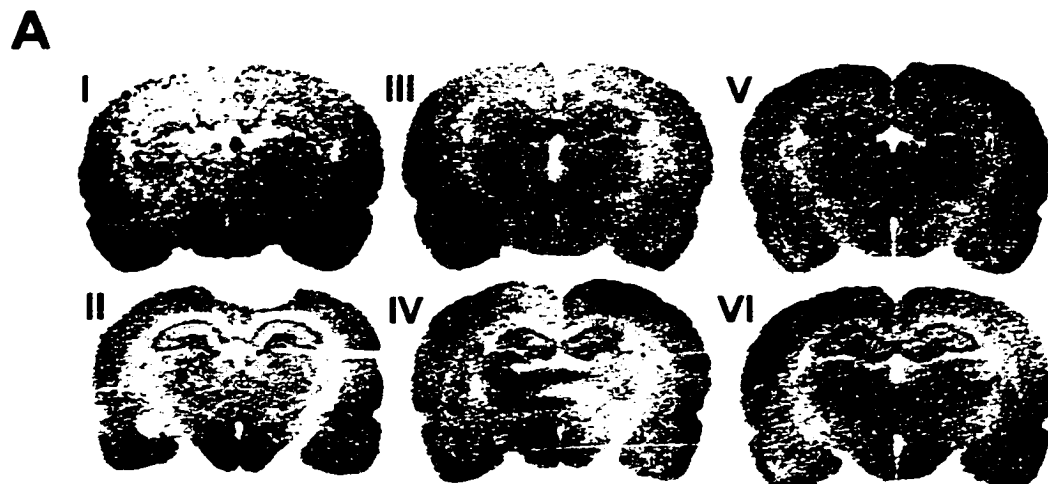
FIGURE 10.4

Figure 10.5 Emulsion autoradiography of huntingtin hybridization signal in the arcuate nucleus. Low (A) and high (B) magnification autoradiographs viewed under darkfield illumination revealed a pattern of mRNA expression that was consistent with the distribution of the huntingtin protein. This robust signal was confined to the arcuate nucleus and was evident throughout the rostrocaudal axis of this region. Arrows point to the same cluster in both A) and B). Scale bars represent 100 μm. V; third ventricle.
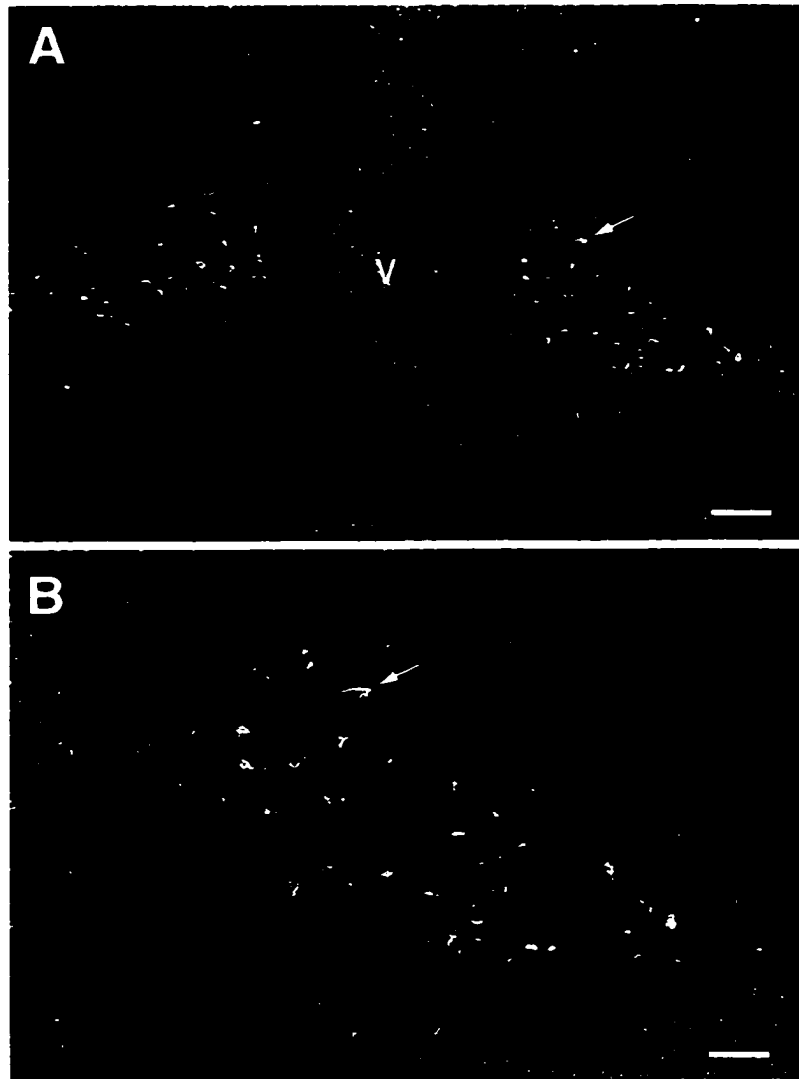
FIGURE 10.5

Figure 10.6 Neuronal and glial expression of huntingtin mRNA and protein in the arcuate nucleus of postpartum animals. A) Emulsion autoradiograph counterstained for Nissl substance. The hybridization signal was not found directly overlying Nissl-stained cells, but consistently appeared in close apposition to neuronal soma. Arrowheads indicate two of several prominent complexes of huntingtin hybridization signal with neuronal soma. B) High magnification photomicrograph of huntingtin immunolabeling in the arcuate nucleus. Note the intense expression of the protein in glia-like cells (large arrows) relative to the neuronal (small arrows) labeling. Scale bars represent 100 μm.
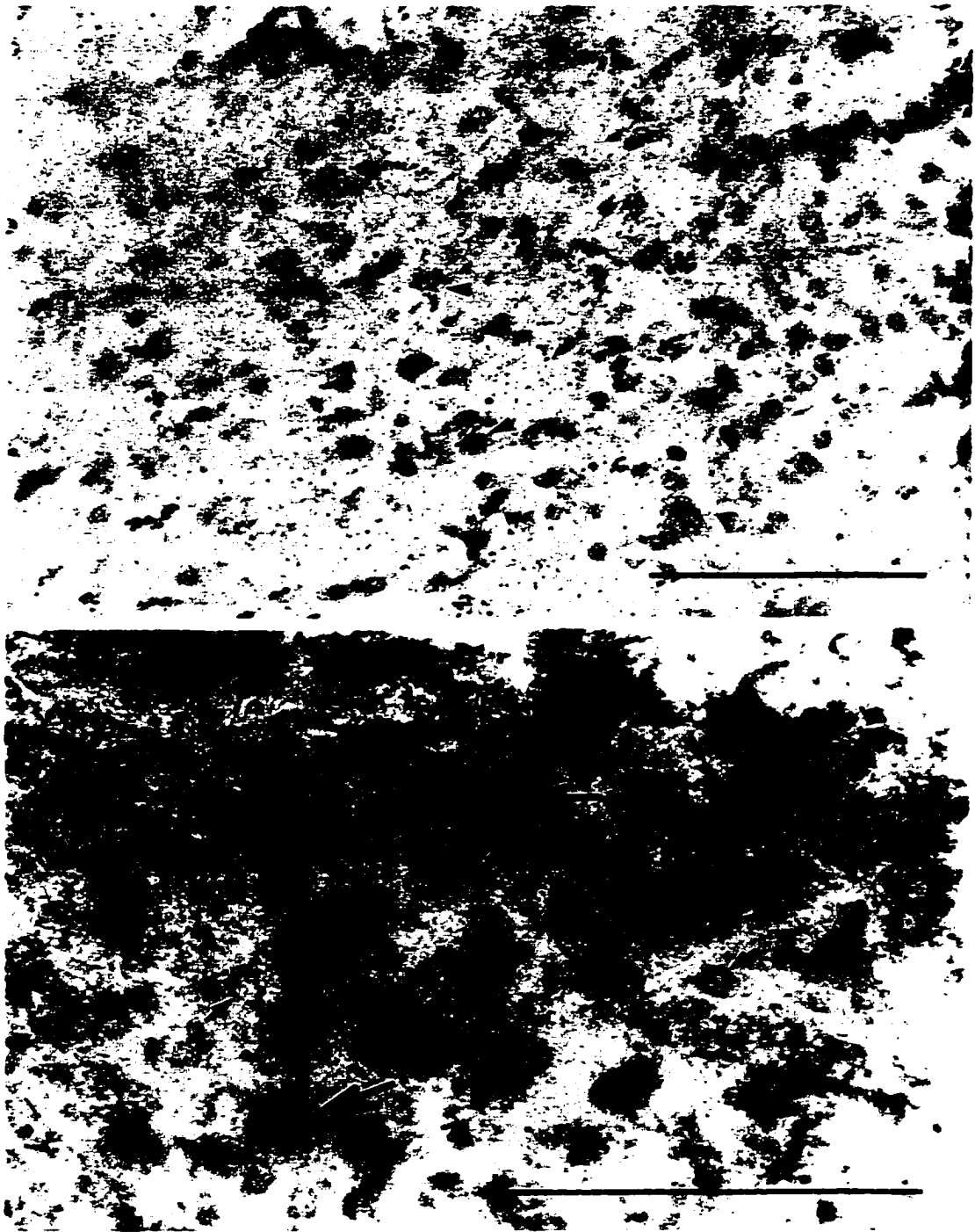
FIGURE 10.6

Figure 10.7 Morphology of huntingtin-expressing cells in the arcuate nucleus. A) The hybridization signal obtained from emulsion autoradiographs revealed that *huntingtin* mRNA was distributed throughout the cell soma as well as the processes. The pattern of distribution revealed a stellate morphology that was indicative of astrocytes. B) High magnification of huntingtin immunohistochemistry revealed a cellular distribution of protein expression which was consistent with the mRNA distribution that was observed with emulsion autoradiography. Arrowhead indicates one of several processes that are immunopositive for the huntingtin protein. Scale bar represents 10 μm.
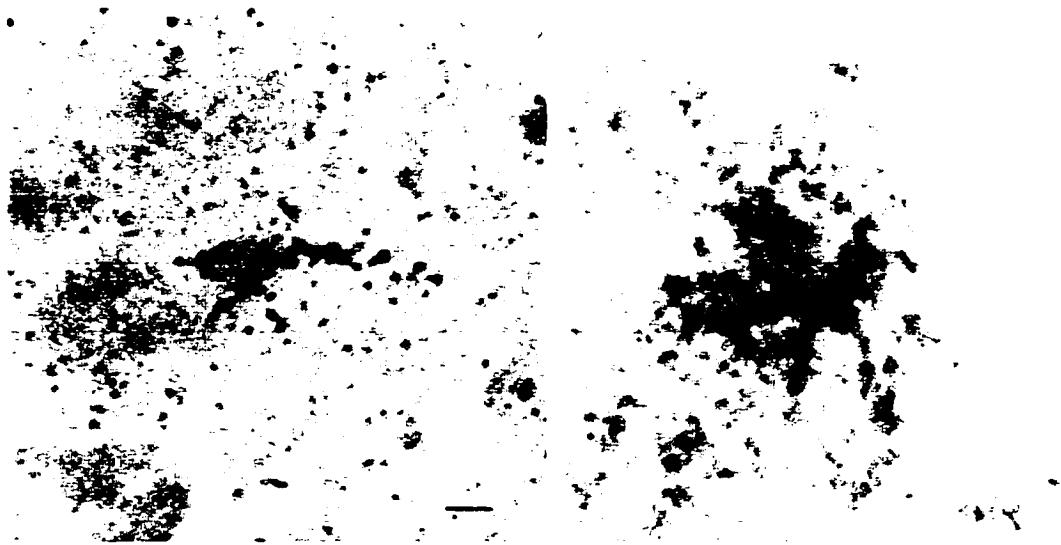
FIGURE 10.7

Figure 10.8 Co-localization of huntingtin and GFAP proteins. A) Huntingtin immunohistochemistry in the dentate gyrus of the hippocampus revealed predominantly process and terminal labeling. B) Double immunolabeling in the same section as in A) revealed a distinct expression of GFAP with a distribution that was dissimilar to that of huntingtin. C) Composite overlay of the exposures in A) and B) confirmed the specificity of the fluorochrome signals to the appropriate fluorescent filter. D) Huntingtin immunofluorescence in the arcuate nucleus of postpartum rats revealed a protein distribution which was consistent with that seen using DAB immunohistochemistry. E) When the section in D) was double labeled for GFAP it was evident that these huntingtin-expressing cells were also GFAP-positive. F) Composite imaging of the distribution of the two proteins confirmed the co-localization of huntingtin and GFAP (as indicated by the yellow cells). Arrows in D)-F) indicate cells that immunolabeled for both huntingtin and GFAP. Panels G)-H) show a magnified view of the boxed region in D). These peripheral cells had strong huntingtin immunofluorescence (G), but only weak labeling of GFAP (H). Panel I) shows a composite exposure of panel G) and H). Scale bars represents 100 μm.
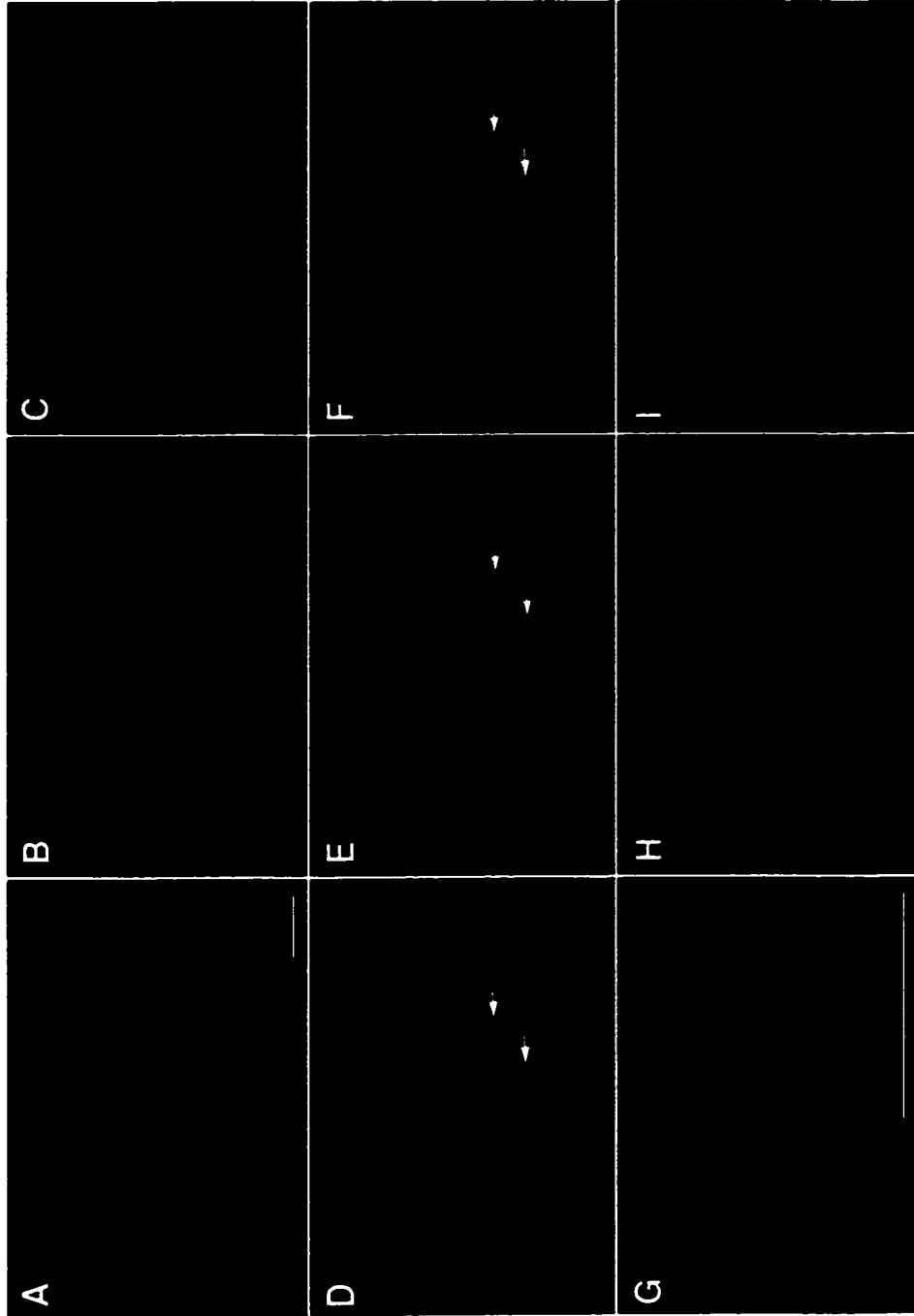
FIGURE 10.8

CHAPTER 11

General Summary and Conclusions

The basal ganglia represent a model system with which to study cellular and molecular interactions between cerebral nuclei. While much knowledge has amassed in the last three decades about the structure and function of these systems, there remains a great deal to be learned about the organization of information processing into and out of the basal ganglia. The striatum, GP and SNR are intricately connected via reciprocal GABAergic projections and the primary output nuclei of the basal ganglia, the SNR and EPN, provide tonic inhibitory tone to recipient regions such as the thalamus and SC. Thus, changes in the activity of basal ganglia nuclei exert their effects by increasing or decreasing this tonic inhibition (reviewed in Mink, 1996).

Learning and planning of motor activities involves the premotor and supplementary motor areas (PMA, SMA) of the cortex, which (among other cortical regions) send extensive projections to the striatum. This cortico-striatal interaction is thought to modulate the inhibitory tone of the basal ganglia onto thalamic regions and, thus, regulate thalamo-cortical input to the motor cortex (Mink, 1996). In this regard, the activity of the basal ganglia is thought to involve selective inhibitory programs, which focus information that is transmitted from several cortical regions onto neural substrates that allow execution of precise motor movements. While there exists vast information on the cytoarchitecture and neurochemistry of the basal ganglia, there is far less known about the mechanisms by which neuronal information is organized to mediate controlled locomotor activity.

Studies of the basal ganglia that compare alterations in neurochemistry and stimulus-response profiles with changes in motor behavior permit correlative analysis between the activity of specific brain regions and the functional abilities of an animal.

This concept underlies the rationale of using rotational behavior in 6-OHDA-lesioned animals to investigate the efficacy of various treatments on restoration of DAergic function (Pycock, 1980; Pycock and Kilpatrick, 1989; Miller and Beninger, 1991). Presently, we have investigated the alterations in, and function of, several subcortical motor regions in animal models of HD and PD. The majority of these studies have involved the application of antisense ODNs to suppress stimulant-induced IEG expression in the striatum. We contend that this technique provides a model which mimicks the striatal dysfunction that occurs in HD and offers a viable alternative to more severe lesioning (i.e. using quinolinic acid) methods. There are two primary advantages of this ODN model of HD that are not provided by striatal lesioning models. The first advantage is the relative selectivity of neuronal suppression that is obtained. While intrastriatal infusions of antisense ODNs to c-*fos* mRNA (called ASF) have been shown to decrease the basal expression of this gene, no locomotor or postural bias was observed in the absence of psychostimulant challenge (Hebb and Robertson, unpublished observations; W. Sommer, personal communication; Sommer *et al.*, 1996). Administration of *d*-amphetamine produces robust neuronal stimulation and induction of c-*fos* in the striatum (Graybiel *et al.*, 1990). Pre-treatment with ASF prevents either the transcription or translation (the mechanism remains unclear) of the c-*fos* gene or mRNA, respectively, leading to suppression of functional protein. Thus, unilateral infusion of ASF prevents neuronal stimulation and has negligible effects on other cells, leaving the cytoarchitecture intact. This is in stark contrast to QA models

where both neurons and glia are ablated, with subsequent and extensive gliosis (Bjorklund *et al.*, 1986; Popoli *et al.*, 1994).

A second advantage to using the ODN HD model is the reversibility of the treatment. We have shown that, with end-capped ODNs, the antisense effect has dissipated after 4 hours (chapter 3). Thus, in studies investigating the effects of striatal dysfunction on, for example, cognitive function and learning, the animal could be trained in a task then treated with ODNs and re-evaluated for changes in its abilities. After a sufficient recovery period, the animal could be tested again to determine if the ability to perform the task had returned to normal levels. Such reversibility of effect would not be possible with conventional lesioning techniques.

The results of the current studies have provided novel information regarding the functional changes in the basal ganglia, particularly in respect to the etiology of the locomotor bias observed (rotational behavior). For example, evidence that suppression of striatal IEG expression produced a robust increase in expression in the GP demonstrated the marked influence of the striatopallidal pathway on GP activity (chapter 4). Furthermore, elimination of the pallidal stimulation produced a dramatic (3-fold) increase in the locomotor bias observed in these animals, demonstrating the significant functional influence of the GP on motor control (chapter 5). This provided support for the theory that the choreiform movements in HD are produced by a disinhibition of the GP (Storey and Beal, 1993). Further examination of the neurophysiological changes that occurred in animals with striatal and/or GP dysfunction showed that the SC undergoes marked alterations in its stimulus-reponse

abilities, an effect which becomes progressively more pronounced as the motor bias of the animal increases (chapter 6). This suggested that the motor (including oculomotor) symptomatology of HD may be mediated by changes that occur in both the thalamus and the SC. In chapter 7, we provided an extensive comparison of changes that occurred in subcortical, motor-related nuclei between animals that had received a 6-OHDA lesion of the nigrostriatal DA system (PD model) or intrastriatal infusion of ASF (HD model). Our results suggested that several regions in the brain undergo similar changes as a result of these conditions. However, consistent with other experimental and clinical data, we found marked distinctions in the stimulus-response abilities of the GP between these models. Another site of distinct alterations was the RPO, a region that was markedly suppressed following DA depletion, but remained unaffected by striatal dysfunction alone.

The results presented in chapter 8 are somewhat of an extension of those in chapter 7. However, the characterization of such a population of GABAergic neurons in the SNC warranted a thorough discussion. These findings strongly support the idea of a second modulatory system (other than DA) in the SNC that contributes to the regulation of activity in input (striatum) and output (SNR) nuclei. It would be of interest to determine, using electrophysiological methods, if the Fos-positive cells in the SNC were the same as those previously described as 'secondary' or 'burster' neurons (Lacey *et al.*, 1989; Yung *et al.*, 1991). These future experiments may provide clues to the functional role of these neurons in basal ganglia regulation.

Perhaps the most unique study performed in this collection of research was the investigation of *huntingtin* expression described in chapter 10. Our findings provide novel insight into the possible role of the *huntingtin* gene in the adult brain and also suggest that similar mechanisms in embryonic systems may be responsible for the apparent necessity of this gene during development (Duyao *et al.*, 1995; Nasir *et al.*, 1995; Zeitlin *et al.*, 1995). The results presented here provide the basis and rationale for future investigations into the function and significance of htt with respect to: 1. primordial stem cell differentiation, 2. neuroendocrine regulation, 3. possible trophic or chemotactic induction of htt and 4. mechanisms of plasticity induced in other brain regions under natural or experimental conditions.

As discussed in the General Introduction, one of the initial goals of this research was to effectively suppress the expression of the *huntingtin* gene in the adult CNS using antisense ODNs. However, successful antisense-mediated gene suppression relies heavily on the ability of the cells to take up the ODN and, once inside the cell, the selective hybridization of the ODN to the targeted mRNA. The 45-base ODN that was designed to hybridize specifically to the *huntingtin* transcript was investigated for its ability to be incorporated into the cytoplasm of cells (chapter 9). When compared to the uptake and biodistribution profiles of 15-base ODNs that had been successfully used in antisense experiments, the 45-base ODN (called HDO) demonstrated similar pharmacokinetics. It was further shown, using *in situ* hybridization and Northern blot analysis, that HDO effectively and specifically hybridized to mRNA transcripts that corresponded precisely to the size and location of huntingtin transcripts (chapter 10).

Taken together, the results of chapters 9 and 10 suggest that HDO is a prime candidate for use in antisense experiments designed to suppress the expression of the *huntingtin* gene in the adult brain. While the demonstrated sequence specificity of HDO provides researchers with a convenient tool with which to investigate changes in *huntingtin* expression, future demonstration of its ability to suppress gene expression *in vivo* would enormously expand the experimental applications of HDO and antisense technology in HD research.

BIBLIOGRAPHY

Agid, Y. (1991) Parkinson's disease: pathophysiology. Lancet *337*: 1321-1324.

Albin, R.L., Reiner, A., Anderson, K.D., Penney, J.B. and Young, A.B. (1990) Striatal and nigral neuron subpopulations in rigid Huntington's disease: implications for the functional anatomy of chorea and rigidity-akinesia. Ann. Neurol. *27*: 357-365.

Altschul, S.F., Gish, W., Miller, W., Myers, E.W. and Lipman, D.J. (1990) Basic local alignment search tool. J. Mol. Biol. *215*: 403-410.

Anderson W.A., Kang Y., DeSombre E.R. (1975) Endogenous peroxidase: specific marker enzyme for tissues displaying growth dependency on estrogen. J. Cell. Biol. *64*: 668-681.

Anderson, M. and Yoshida, M (1977) Electrophysiological evidence for branching nigral connections to the thalamus and superior colliculus. Brain Res. *137*: 361-364.

Aquilonius, S.M. and Eckernas, S.A. (1977) Choline therapy in Huntington's chorea. Neurol. *27*: 887-889.

Aronin, N., Chase, K., Sagar, S.M., Sharp, F.R. and DiFiglia, M. (1991) N-methyl-D-aspartate receptor activation in the neostriatum increases c-Fos and Fos-related antigens selectively in medium-sized neurons. Neurosci. *44*: 409-420.

Avanzini, G., Girotti, F., Caraceni, T. and Spreafico, R. (1979) Oculomotor disorders in Huntington's chorea. J. Neurol. Neurosurg. Psychiatry *42*: 581-589.

Aylward, E.H., Li, Q., Stine, O.C., Ranen, N., Sherr, M., Barta, P.E., Bylsma, F.W., Pearlson, G.D. and Ross, C.A. (1997) Longitudinal change in basal ganglia volume in patients with Huntington's disease Neurol. *48*: 394-399.

Baldissera, F., Broggi, G. and Mancia, M. (1967) Depolarization of trigeminal afferents induced by stimulation of brainstem and peripheral nerves. Exp. Brain Res. *4*: 1-17.

Bao, J., Sharp, A.H., Wagster, M.V., Becher, M., Schilling, G., Ross, C.A., Dawson, V.L. and Dawson, T.M. (1996) Expansion of polyglutamine repeat in huntingtin leads to abnormal protein interactions involving calmodulin. Proc. Natl. Acad. Sci. (USA) *93*: 5037-5042.

Barr, A.N., Fischer, J.H., Koller, W.C., Spunt, A.L. and Singhal, A. (1988) Serum haloperidol concentration and choreiform movements in Huntington's disease. Neurol. *38*: 84-88.

Barr, A.N., Heinze, W., Mendoza, J.E. and Perlik, S. (1978) Longterm treatment of Huntington's disease with L-glutamate and pyridoxine. Neurol. *28*: 1280-1282.

Bartel, D., Sheng, M., Lau, L. and Greenberg, M. (1989) Growth factors and membrane depolarization activate distinct programs of early response gene expression: dissociation of *fos* and *jun* induction. Genes and Dev. *3*, 304-313.

Beckstead, R.M. and Frankfurter, A. (1983) A direct projection from the retina to the intermediate gray layer of the superior colliculus demonstrated by anterograde transport of horseradish peroxidase in monkey, cat and rat. Exp. Brain Res. *52*: 261-268.

Benabid, A.L., Pollak, P., Gervason, C., Hoffman, D., Gao, D.M., Hommel, M., Perret, J.E. and deRougemont, J. (1991) Long-term suppression of tremor by chronic stimulation of the ventral intermediate thalamic nucleus. Lancet *337*: 403-406.

Bentivoglio, M., VanDerKooy, D. and Kuypers, H. (1979) The organization of efferent projections of the substantia nigra of the rat: a retrograde fluorescent double-labeling study. Brain Res. *174*, 1-17.

Berkowitz, L.S., Riabowol, K.T. and Gilman, M.Z. (1989) Multiple sequence elements of a single functional class are required for cyclic AMP responsiveness of the mouse c-*fos* promoter. Mol. Cell. Biol. *9*: 4272-4281.

Berntson, G.G. (1973) Attack, grooming and threat elicited by stimulation of the pontine tegmentum in cats. Physiol. Behav. *11*: 81-87.

Berretta, S., Robertson, H. and Graybiel, A. (1992) Dopamine and glutamate agonists stimulate neuron-specific expression of Fos-like protein in the striatum. J. Neurophysiol. *68*: 767-777.

Berridge, M. (1986) Second messenger dualism in neuromodulation and memory. Nature *323*: 294-295.

Berthoz, A. and Grantyn, A. (1986) Neural mechanisms underlying eye-head coordination. Progress Brain Res. *64*: 325-343.

Bhide, P.G., Day, M., Sapp, E., Schwarz, C., Sheth, A., Kim, J., Young, A.B., Penney, J., Golden, J., Aronin, N. and DiFiglia, M. (1996) Expression of

normal and mutant huntingtin in the developing brain. J. Neurosci. *16*: 5523-5535.

Bianchi, G., Landi, M. and Garattini, S. (1986) Disposition of apomorphine in rat brain areas: relationship to stereotypy. Eur. J. Pharmacol. *131*: 229-236.

Bickford, M.E. and Hall, W.C. (1992) The nigral projection to predorsal bundle cells in the superior colliculus of the rat. J. Comp. Neurol. *319*: 11-33.

Biggs, C.S., Fowler, L.J., Whitton, P.S. and Starr, M.S. (1997) Extracellular levels of glutamate and aspartate in the entopeduncular nucleus of the rat determined by microdialysis: regulation by striatal dopamine D2 receptors via the indirect striatal output pathway? Brain Res. *753*: 163-175.

Bjorklund, H., Olson, L., Dahl, D. and Schwarcz, R. (1986) Short- and long-term consequences of intracranial injections of the excitotoxin, quinolinic acid, as evidenced by GFA immunohistochemistry of astrocytes. Brain Res. *371*: 267-277.

Black, K.J., Gado, M.H. and Perlmutter, J.S. (1997) PET measurement of dopamine D2 receptor-mediated changes in striatopallidal function. J. Neurosci. *17*: 3168-3177.

Boecker, H., Wills, A.J., Ceballos-Baumann, A., Samuel, M., Thomas, D.G., Marsden, C.D. and Brooks, D.J. (1997) Stereotactic thalamotomy in tremor-dominant Parkinson's disease: an H2(15)O PET motor activation study. Ann. Neurol. *41*: 108-111.

Bollen, E., Reulen, J.P., DenHeyer, J.C. VanderKamp, W., Roos, R.A. and Buruma, O.J. (1986) Horizontal and vertical saccadic eye movement abnormalities in Huntington's chorea. J. Neurol. Sci. *74*: 11-22.

Bolt, J.M. (1970) Huntington's chorea in the west of Scotland. Brit. J. Psychiatry *116*: 259-270.

Bourson, A., Borroni, E., Austin, R.H., Monsma, F.J. and Sleight, A.J. (1995) Determination of the role of the 5-ht$_6$ receptor in the rat brain: a study using antisense oligonucleotides. J. Pharmacol. Exp. Ther. *274*: 173-180.

Brawer J.R., Naftolin F., Martin J., Sonnenschein C. (1978) Effects of a single injection of estradiol valerate on the hypothalamic arcuate nucleus and on reproductive function in the female rat. Endocrinol. *103*: 501-512.

Bruyn, G.W. (1968) Handbook of Clinical Neurology *6*: 298-378.

Burke, J.R., Enghild, J.J., Martin, M.E., Jou, Y.S., Myers, R.M., Roses, A.D., Vance, J.M. and Strittmatter, W.J. (1996) Huntingtin and DRPLA proteins selectively interact with the enzyme GAPDH. Nature .Med. 2: 347-350.

Buttner-Ennever, J. and Holstege, G. (1986) Anatomy of premotor centers in the reticular formation controlling oculomotor, skeletomotor and autonomic motor systems. Progress Brain Res. 64: 89-98.

Campbell, J.M., Bacon, T.A. and Wickstrom, E. (1990) Oligodeoxynucleoside phosphorothioate stability in subcellular extracts, culture media, sera and cerebrospinal fluid. J. Biochem. Biophys. Meth. 20: 259-267.

Campbell, K., Takada, M. and Hattori, T. (1991) Co-localization of tyrosine hydroxylase and glutamate decarboxylase in a subpopulation of single nigrotectal projection neurons. Brain Res. 558: 239-244.

Carlock L., Walker P.D., Shan Y., Gutridge K. (1995) Transcription of the Huntington disease gene during the quinolinic acid excitotoxic cascade. Neuroreport 6: 1121-1124.

Cheramy, A., Leviel, V. and Glowinski, J. (1981) Dendritic release of dopamine in the substantia nigra. Nature 289: 537-542.

Chiasson, B., Armstrong, J., Hooper, M., Murphy, P. and Robertson, H. (1994) The application of antisense oligonucleotide technology to the brain: some pitfalls. Cell. Mol. Neurobiol. 14: 507-521.

Chiasson, B., Dennison, Z. and Robertson, H. (1995) Amygdala kinding and immediate early genes. Mol. Brain Res. 29: 191-199.

Chiasson, B., Hong, M., Hooper, M.L., Armstrong, J.N., Murphy, P. and Robertson, H.A. (1996) Antisense Therapeutics in the Central Nervous System. In Methods in Molecular Medicine: Antisense Therapeutics pp. 225-245. S. Agrawal Humana Press Inc., Totowa, N.J..

Chiasson, B., Hong, M. and Robertson, H. (1997) Putative roles for the inducible transcription factor c-fos in the central nervous system: studies with antisense oligonucleotides. Neurochem. Int. 31: 459-475.

Chiasson, B., Hooper, M., Murphy, P. and Robertson, H. (1992) Antisense oligonucleotide eliminates in vivo expression of c-fos in mammalian brain. Eur. J. Pharmacol. 227: 451-453.

Chiu, R., Angel, P. and Karin, M. (1989) Jun-B differs in its biological properties from, and is a negative regulator of, c-Jun. Cell 59: 979-986.

Chiu, R., Boyle, W.J., Meek, J., Smeal, T., Hunter, T. and Karin, M. (1988) The c-Fos protein interacts with c-JUN/AP-1 to stimulate transcription of AP-1 responsive genes. Cell 54: 541-552.

Christy, B.A., Lau, L.F. and Nathans, D. (1988) A gene activated in mouse 3T3 cells by serum growth factors encodes a protein with "zinc finger" sequences. Proc. Natl. Acad. Sci. (USA) 85: 7857-7861.

Cirelli, C., M. Pompeiano, P. Arrighi, and G. Tononi (1995) Sleep-waking changes after c-fos antisense injections in the medial preoptic area. Neuroreport 6: 801-805.

Cohen, D. and Curran, T. (1988) fra-1 inducible cellular immediate-early gene that encodes a Fos-related antigen. Mol. Cell. Biol. 8: 2063-2069.

Cole, A., Bhat, R., Patt, C., Worley, P. and Baraban, J.M. (1992) D1 dopamine receptor activation of multiple transcription factor genes in rat striatum. J. Neurochem. 58: 1420-1426.

Conneally, P.M. (1993) Suicide risk in Huntington's disease. J. Med. Genet. 30: 293-295.

Crossman, A.R., Mitchell, I.J., Sambrook, M.A. and Jackson, A. (1988) Chorea and myoclonus in the monkey induced by gamma-aminobutyric acid antagonism in the lentiform complex. The site of drug action and a hypothesis for the neural mechanisms of chorea. Brain 111: 1211-1233.

Curran, D. (1930) Huntington's chorea without choreiform movements. J. Neurol. Psychopathol. 10: 305-310.

Curran, E.J., Akil, H.and Watson, S.J. (1996) Psychomotor stimulant- and opiate-induced c-fos mRNA expression patterns in the rat forebrain: comparisons between acute drug treatment and a drug challenge in sensitized animals. Neurochem. Res. 21: 1425-1435.

Curran, T. (1988) The fos oncogene, in The Oncogene Handbook. (Reddy, E., Skalka, A. and Curran, T. ,eds.) Elsevier Science, Amsterdam. pp. 307-325.

Curran, T. and Franza, B. (1988) Fos and Jun: the AP-1 connection. Cell 55: 395-397.

Curran, T. and Morgan, J. (1987) Memories of fos. BioEssays 6: 255-258.

Curran, T. and Morgan, J. (1995) Fos: an immediate early transcription factor in neurons. J. Neurobiol. *26*: 403-412.

Davies, S.W., Turmaine, M., Cozens, B.A., DiFiglia, M., Sharp, A.H., Ross, C.A., Scherzinger, E., Wanker, E.E., Mangiarini, L. and Bates, G.P. (1997) Formation of neuronal intranuclear inclusions underlies the neurological dysfunction in mice transgenic for the HD mutation. Cell *90*: 537-548.

Dean, P. and Redgrave, P. (1992) Behavioral consequences of manipulating GABA neurotransmission in the superior colliculus. Prog. Brain Res. *90*: 263-281.

Dean, P., Mitchell, I.J. and Redgrave, P. (1988) Responses resembling defensive behavior produced by microinjection of glutamate into superior colliculus of rats. Neurosci. *24*: 501-510.

Dean, P., Redgrave, P., Sahibzada, N. and Tsuji, K. (1986) Head and body movements produced by stimulation of the superior colliculus in rats: effects of interuption of the crossed tectoreticulospinal pathway. Neurosci. *19*: 367-380.

DeLong, M.R. (1990) Primate models of movement disorders of the basal ganglia. Trends Neurosci. *13*: 281-285.

Deniau, J., Hammond, C., Riszk, A. and Feger, J. (1978) Electrophysiological properties of identified output neurons of the rat substantia nigra (pars compacta and pars reticulata): evidence for the existence of branched neurons. Exp. Brain Res. *32*: 402-422.

DeRooij, K., DeKoningGans, P., Roos, R.A., VanOmmen, G.B. and DenDunnen, J.T. (1995) Somatic expansion of the $(CAG)_n$ repeat in Huntington disease brains. Hum. Genet. *95*: 270-274.

Dewhurst, K. (1970) Personality disorder in Huntington's disease. Psychiatrica Clinica *3*: 221-229.

Di Maio, L., Squitieri, F., Napolitano, G., Campanella, G., Trofatter, J.A. and Conneally, P.M. (1993) Suicide risk in Huntington's disease. J. Med. Genet. *30*: 293-295.

DiChiara, G., Porceddu, M., Imperato, A. and Morelli, M. (1981) Role of GABA neurons in the expression of striatal motor functions. Adv. Biochem. Psychopharmacol. *30*: 129-163.

Dietsch V., Kalf G.F., Hazel B.A. (1996) Induction of granulocytic differentiation in myeloblasts by 17-beta-estradiol involves the leukotriene D4 receptor. Recept Signal Transduct. 6: 63-75.

Dragunow, M. and Faull,R. (1989) The use of c-*fos* as a metabolic marker in neuronal pathway tracing. J. Neurosci. Methods 29: 261-265.

Dragunow, M. and Robertson, H. (1987) Kindling stimulation produces c-*fos* protein in granule cells of the rat dentate gyrus. Nature 329: 441-442.

Dragunow, M., Lawlor, P., Chiasson, B. and Robertson, H. (1993) c-*fos* antisense generates apomorphine and amphetamine-induced rotation. Neuroreport 5: 305-306.

Dragunow, M., Tse, C., Glass, M. and Lawlor, P. (1994) c-*fos* antisense reduces expression of Krox 24 in rat caudate and neocortex. Cell. Mol. Neurobiol. 14: 395-405.

Dragunow, M., Yamada, N., Bilkey, D. and Lawlor, P. (1992) Induction of immediate early gene proteins in dentate granule cells and somatostatin interneurons after hippocampal seizures. Mol. Brain Res. 13: 119-126.

Draisci, G. and Iadarola, M. (1989) Temporal analysis of increases in c-*fos*, preprodynorphin and preproenkephalin mRNAs in rat spinal cord. Mol. Brain. Res. 6: 31-37.

Dray, A., Gonye, T.J. and Oakley, N.R. (1976) Caudate stimulation and substantia nigra activity in the rat. J. Physiol. 259: 825-849.

Dreher, B., Barker, D., Bath, M. and Keay, K. (1996) Spatiotemporal pattern of ontogenetic expression of calbindin-28/kD in the retinorecipient layers of rat superior colliculus. J. Comp. Neurol. 376: 223-240.

Dreher, B., Sefton, A.J., Ni, S.K. and Nisbett, G. (1985) The morphology, number, distribution and central projections of class I retinal ganglion cells in albino and hooded rats. Brain Behav.Evol. 26: 10-48.

Duncan, R.L., Kizer, N., Barry, E.L.R., Friedman, P.A. and Hruska, K.A. (1996) Antisense oligonucleotide inhibition of a swelling-activated cation channel in osteoblast-like sarcoma cells. Proc. Natl. Acad. Sci. (USA) 93: 1864-1869.

Duyao, M.P., Auerbach, A.B., Ryan, A., Persichetti, F., Barnes, G., McNeil, S.M., Ge, P., Vonsattel, J., Gusella, J., Joyner, A. and MacDonald, M. (1995)

Inactivation of the mouse Huntington's disease gene homolog *Hdh*. Science *269*: 407-410.

Ebersbach, G., Trottenberg, T., Hattig, H., Schelosky, L., Schrag, A. and Poewe, W. (1996) Directional bias of initial visual exploration. A symptom of neglect in Parkinson's disease. Brain *119*: 79-87.

Eckstein, F. (1985) Investigations of enzyme mechanisms with nucleoside phosphorothioates. Ann. Rev. Biochem. *54*: 367-402.

Egrise D., Vienne A., Martin D., Schoutens A. (1992) Trabecular bone cell proliferation *ex vivo* increases with donor age in the rat: it is correlated with the extent of bone loss and not with histomorphometric indices of bone formation. Calcif. Tissue Int. *59*: 45-50.

Ellard, C.G. and Goodale, M.A (1988) A functional analysis of the collicular output pathways: a dissociation of deficits following lesions of the dorsal tegmental decussation and the ipsilateral collicular efferent bundle in the Mongolian gerbil. Exp. Brain Res. *71*: 307-319.

Ellard, C.G. and Goodale, M.A. (1986) The role of the predorsal bundle in head and body movements elicited by electrical stimulation of the superior colliculus in the Mongolian gerbil. Exp.Brain Res. *64*: 421-433.

Farrer, L.A. (1986) Suicide and attempted suicide in Huntington's disease: implications for preclinical testing of persons at risk. Am. J. Med. Genet. *24*: 305-311.

Ferrante, R.J., Kowall, N.W., Beal, M.F., Martin, J.B., Bird, E.D. and Richardson, E.P. (1987) Morphologic and histochemical characteristics of a spared subset of striatal neurons in Huntington's disease. J. Neuropathol. Exp. Neurol. *46*: 12-27.

Ferrante, R.J., Kowall, N.W., Beal, M.F., Richardson, E.P., Bird, E.D. and Martin, J.B. (1985) Selective sparing of a class of striatal neurons in Huntington's disease. Science *230*: 561-563.

Ferrer I., Alcantara S., Ballabriga J., Olive M., Blanco R., Rivera R., Carmona M., Berruezo M., Pitarch S., Planas A. (1996) Transforming growth factor-α (TGF-α) and epidermal growth factor-receptor (EGF-R) immunoreactivity in normal and pathologic brain. Prog. Neurobiol. *49*: 99-123.

Finkelstein, D.I., Reeves, A.K. and Horne, M.K. (1996) An electron microscopic tracer study of the projections from entopeduncular nucleus to the ventrolateral nucleus of the rat. Neurosci. Lett. *211*: 33-36.

Fisher, R., Norris, J.W. and Gilka, L. (1974) GABA in Huntington's chorea. Lancet *I*: 506.

Floran, B., Floran, L., Sierra, A. and Aceves, J. (1997) D2 receptor-mediated inhibition of GABA release by endogenous dopamine in the rat globus pallidus. Neurosci. Lett. *237*: 1-4.

Folstein, S.E. (1989) Huntington's Disease: A Disorder of Families. Baltimore, The Johns Hopkins University Press.

Folstein, S.E., Chase, G.A., Wahl, W.E., McDonnell, A.M. and Folstein, M.F. (1987) Huntington's disease in Maryland: clinical aspects of racial variation. Amer. J. Hum. Genet. *41*: 168-179.

Gai, W.P., Halliday, G.M., Blumbergs, P.C., Geffen, L.B. and Blessing, W.W. (1991) Substance P-containing neurons in the mesopontine tegmentum are severely affected in Parkinson's disease. Brain *114*: 2253-2267.

Gale, K. and Iadorola, M. (1980) GABAergic denervation of rat substantia nigra: functional and pharmacological properties. Brain Res. *183*: 217-223.

Garcia-Segura L.M., Baetens D., Naftolin F. (1986) Synaptic remodeling in arcuate nucleus after injection of estradiol valerate in adult female rats. Brain Res. *366*: 131-136.

Garcia-Segura L.M., Torres-Aleman I., Naftolin F. (1989) Astrocytic shape and glial fibrillary acidic protein immunoreactivity are modified by estradiol in primary rat hypothalamic cultures. Dev. Brain Res. *47*: 298-302.

Garrett, B.E. and Holtzman, S.G. (1996) Comparison of the effects of prototypical behavioral stimulants on locomotor activity and rotational behavior in rats. Pharmacol. Biochem. Behav. *54*: 469-477.

Gerfen, C.R. (1984) The neostriatal mosaic: compartmentalization of corticostriatal input and striatonigral output systems. Nature *311*: 461-464.

Gerfen, C.R., Engber, T.M., Mahan, L.C., Susel, Z., Chase, T.N., Monsma, F.J. and Sibley, D.R. (1990) D1 and D2 dopamine receptor regulated gene expression of striatonigral and striatopallidal neurons. Science *250*: 1429-1432.

Gillardon, F., Beck, H., Uhlmann, E., Herdegen, T., Sandkuhler, J., Peyman, A. and Zimmermann, M. (1994) Inhibition of c-Fos protein expression in rat spinal

cord by antisense oligodeoxynucleotide superfusion. Eur. J. Neurosci. *6*: 880-884.

Gillardon, F., Vogel, J., Hein, S., Zimmermann, M. and Uhlmann, E. (1997) Inhibition of carrageenan-induced spinal c-Fos activation by systemically administered c-*fos* antisense oligodeoxynucleotides may be facilitated by local opening of the blood-spinal cord barrier. J. Neurosci. Res. *47*: 582-589.

Goddard, G., McIntyre, D. and Leech, C. (1969) A permanent change in brain function resulting from daily electrical stimulation. Exp. Neurol. *25*,:295-330.

Goelet, P., Castellucci, V.F., Schacher, S. and Kandel, E. (1986) The long and short of long-term memory- a molecular framework. Nature *322*: 419-422.

Goldgefter L, Schejter AS, Gill D (1980) Structural and microspectrofluorometric studies on glial cells from the periventricular and arcuate nuclei of the rat hypothalamus. Cell Tissue Res. *211*: 503-510.

Gonzalez, G. and Montminy, M. (1989) Cyclic AMP stimulates somatostatin gene transcription by phosphorylation of CREB at serine 133. Cell *59*: 675-680.

Grace, A.A. and Bunney, B.S. (1979) Paradoxical GABA excitation of nigral dopaminergic cells: indirect mediation through reticulata inhibitory neurons. Eur. J. Pharmacol. *59*: 211-218.

Gray, J.M., Young, A.W., Barker, W.A., Curtis, A. and Gibson, D. (1997) Impaired recognition of disgust in Huntington's disease gene carriers. Brain *120*: 2029-2038.

Graybiel, A. (1990) Neurotransmitters and neuromodulators in the basal ganglia. Trends Neurosci. *13*:244-254.

Graybiel, A., Moratalla, R. and Robertson, H. (1990) Amphetamine and cocaine induce drug-specific activation of the c-*fos* gene in striosome-matrix compartments and limbic subdivisions of the striatum. Proc. Natl. Acad. Sci. (USA) *87*: 6912-6916.

Graybiel, A.M. (1991) Basal ganglia - input, neural activity and relation to the cortex. Curr. Opin. Neurobiol. *1*: 644-651.

Graybiel, A.M. (1995) The basal ganglia. Trends Neurosci. *18*: 60-62.

Guo, H., Tian, J., Wang, X., Fang, Y., Hou, Y. and Han, J. (1996) Brain substrates activated by electroacupuncture (EA) of different frequencies (II): role of

Fos/Jun proteins in EA-induced transcription of preproenkephalin and preprodynorphin genes. Mol. Brain Res. *43*: 167-173.

Gutekunst, C.A., Levey, A.I., Heilman, C.J., Whaley, W.L., Yi, H., Nash, N.R., Rees, H.D., Madden, J.J. and Hersch, S.M. (1995) Identification and localization of huntingtin in brain and human lymphoblastoid cell lines with anti-fusion protein antibodies. Proc. Natl. Acad. Sci. (USA) *92*: 8710-8714.

Guvakova, M.A., L.A. Yakubov, I. Vlodavsky, J.L. Tonkinson, and C.A. Stein (1995) Phosphorothioate oligodeoxynucleotides bind to basic fibroblast growth factor, inhibit its binding to cell surface receptors, and remove it from low affinity binding sites on extracellular matrix. J. Biol. Chem. *270*: 2620-2627.

Guyenet, P.G. and Aghajanian, G.K. (1978) Antidromic identification of dopaminergic and other output neurons of the rat substantia nigra. Brain Res. *150*: 69-84.

Halligan, P.W. (1998) Inability to recognise disgust in Huntington's disease. Lancet *351*: 464.

Haque, N. and Isacson, O. (1996) Antisense gene therapy for neurodegenerative disease? Exp. Neurol. *144*: 139-146.

Harper, P.S. and Morris, M. (1996) Huntington's disease. (P.S. Harper, ed.) London, W.B. Saunders Company Ltd.

Harrison, M., Wiley, R.G. and Wooten, G.F. (1990) Selective localization of striatal D1 receptors to striatonigral neurons. Brain Res. *528*: 317-322.

Harvey, A.R. and Worthington, D.R. (1990) The projection from different cortical areas to the rat superior colliculus. J. Comp. Neurol. *298*: 281-292.

Hayden, M.R. (1981) Huntington's Chorea. Berlin: Springer-Verlag

Heathfield, K.W. (1967) Huntington's chorea. Investigation into the prevalence of this disease in the area covered by the North East Metropolitan Rgional Hospital Board. Brain *90*: 203-232.

Hebb, D.O. (1949) The organization of behavior. Wiley Press, New York.

Heilig, M., Engel, J. and Soderpalm, B. (1993) C-*fos* antisense in the nucleus accumbens blocks the locomotor stimulant action of cocaine. Eur. J. Pharmacol. *236*: 339-340.

Hess, W.R., Burgi, S. and Bucher, V. (1946) Motor function of tectal and tegmental area. Mschr. Psychiat. Neurol. *112*: 1-52.

Hikosaka, O. and Wurtz, R. (1983) Visual and oculomotor functions of monkey substantia nigra pars reticulata. IV. Relation of substantia nigra to superior colliculus. J. Neurophysiol. *49*: 1285-1301.

Hikosaka, O. and Wurtz, R. (1989) The basal ganglia. In: The Neurobiology of Saccadic Eye Movements (Wurtz, Goldberg, eds.) pp.257-281. Amsterdam: Elsevier.

Hoffman G.E., Le W., Abbud R., Lee W., Smith M.S. (1994) Use of Fos-related antigens (FRAs) as markers of neuronal activity: FRA changes in dopamine neurons during proestrus, pregnancy and lactation. Brain Res. *654*: 207-215.

Honkaniemi, J. (1992) Colocalization of peptide- and tyrosine hydroxylase-like immunoreactivities with Fos-immunoreactive neurons in rat central amygdaloid nucleus after immobilization stress. Brain Res. *598*: 107-113.

Honkaniemi, J., Kainu, T., Ceccatelli, S., Rechardt, L., Hokfelt, T. and Pelto-Huikko, M. (1992) Fos and *jun* in rat central amygdaloid nucleus and paraventricular nucleus after stress. Neuroreport *3*: 849-852.

Honkaniemi, J., Kononen, J., Kainu, T., Pyykonen, I.and Pelto-Huikko, M. (1994) Induction of multiple immediate early genes in rat hypothalamic paraventricular nucleus after stress. Mol. Brain Res. *25*: 234-241.

Honkaniemi, J., Sagar, S.M., Pyykonen, I., Hicks, K.J. and Sharp, F.R. (1995) Focal brain injury induces multiple immediate early genes encoding zinc finger transcription factors. Mol. Brain Res. *28*: 157-163.

Hooper, M., Chiasson, B. and Robertson, H. (1994) Infusion into the brain of an antisense oligonucleotide to the immediate-early gene c-*fos* suppresses production of Fos and produces a behavioral effect. Neurosci. *63*: 917-924.

Hopkins, D.A. and Niessen, L.W. (1976) Substantia nigra projections to the reticular formation, superior colliculus and central gray in the rat, cat and monkey. Neurosci.Lett. *2*: 253-259.

Hornykiewicz, O. (1979) Dopamine in Parkinson's disease and other neurological disturbances. In: The neurobiology of dopamine (Horn, A.S., Korf, J., Westerink, B.H., eds.), London: Academic pp. 633-654.

Hou, W., Shyu, B., Chen, T., Lee, J., Shieh, J., Sun, W. (1997) Intrathecally administered c-*fos* antisense oligodeoxynucleotide decreases formalin-induced nociceptive behavior in adult rats. Eur. J. Pharmacol. *329*: 17-26.

Housman, D. (1995) Gain of glutamines, gain of function? Nature Genet. *10*: 3-4.

Hughes, P. and Dragunow, M. (1995) Induction of immediate early genes and the control of neurotransmitter-regulated gene expression within the nervous system. Pharmacol. Rev. *47*: 133-179.

Hughes, P., Singleton, K. and Dragunow, M. (1994) MK-801 does not attenuate immediate early gene expression following an amygdala afterdischarge. Exp. Neurol. *128*: 276-283.

Hunt, S., Pini, A. and Evan, G. (1987) Induction of c-*fos*-like protein in spinal cord neurons following sensory stimulation. Nature *328*: 632-634.

Hunter, J., Woodburn, V., Durieux, C., Pettersson, E., Poat, J. and Hughes, J. (1995) c-*fos* antisense oligodeoxynucleotide increases formalin-induced nociception and regulates preprodynorphin expression. Neurosci. *65*: 485-492.

Huntington, G. (1872) On Chorea. Med. Surg. Reporter *26*: 320-321.

Hutchinson, W.D., Levy, R., Dostrovsky, J.O., Lozano, A.M. and Lang, A.E. (1997) Effects of apomorphine on globus pallidus neurons in parkinsonian patients. Ann. Neurol. *42*: 767-775.

Igarashi, S., Koide, R., Shimohata, T., Yamada, M., Hayashi, Y., Takano, H., Date, H., Oyake, M., Sato, T., Sato, A., Egawa, S., Ikeuchi, T., Tanaka, H., Nakano, R., Tanaka, K., Hozumi, I., Inuzuka, T., Takahashi, H. and Tsuji, S. (1998) Suppression of aggregate formation and apoptosis by transglutaminase inhibitors in cells expressing truncated DRPLA protein with an expanded polyglutamine stretch. Nature Genet. *18*: 111-117.

Javoy-Agid, F., Ploska, A. and Agid, Y. (1981) Microtopography of TH, GAD and CAT in the substantia nigra and ventral tegmental area of control and Parkinsonian brains. J. Neurochem. *36*: 1218-1227.

Jian, M., Staines, W.A., Iadarola, M.J. and Robertson, G.S. (1993) Destruction of the nigrostriatal pathway increases Fos-like immunoreactivity predominantly in striatopallidal neurons. Mol. Brain Res. *19*: 156-160.

Jimenez-Castellanos, J. and Graybiel, A.M. (1989) Compartmental origins of striatal efferent projections in the cat. Neurosci. *32*: 297-321.

Jimenez-Castellanos, J. and Reinoso-Suarez, F. (1985) Topographical organization of the afferent connections of the principal ventromedial thalamic nucleus in the cat. J. Comp. Neurol. *236*: 297-314.

Johansson, B., Lindstrom, K. and Fredholm, B (1994) Differences in the regional and cellular localization of c-*fos* messenger RNA induced by amphetamine, cocaine and caffeine in the rat. Neurosci. *59*: 837-849.

Jones, B.E. and Yang, T. (1985) The efferent projections from the reticular formation and the locus coeruleus studied by anterograde and retrograde axonal transport in the rat. J. Comp. Neurol. *242*: 56-92.

Jou, Y. and Myers, R. (1995) Evidence from antibody studies that the CAG repeat in the Huntington disease gene is expressed in the protein. Hum. Mol. Genet. *4*: 465-469.

Kaczmarek, L. (1993a) Glutamate receptor driven gene expression in learning. Acta Neurobiol. Exp. *53*: 187-196.

Kaczmarek, L. (1993b) Molecular biology of vertebrate learning: is c-*fos* a new beginning? J. Neurosci. Res. *34*: 377-381.

Kalchman, M.A., Graham, R.K., Xia, G., Koide, H.B., Hodgson, J.G., Graham, K.C., Goldberg, Y.P., Gietz, R.D., Pickart, C.M. and Hayden, M.R. (1996) Huntingtin is ubiquitinated and interacts with a specific ubiquitin-conjugating enzyme. J. Biol. Chem. *271*: 19385-19394.

Kato, M., Miyashita, N., Hikosaka, O., Matsumura, M., Usui, S. and Kori, A. (1995) Eye movements in monkeys with local dopamine depletion in the caudate nucleus. I. deficits in spontaneous saccades. J. Neurosci. *15*: 912-927.

Kebabian, J.W. and Calne, D.B. (1979) Multiple receptors for dopamine. Nature *277*: 93-96.

Keefe D.L., Michelson D.S., Lee S.H., Naftolin F. (1991) Astrocytes within the hypothalamic arcuate nucleus contain estrogen-sensitive peroxidase, bind fluorescein-conjugated estradiol, and may mediate synaptic plasticity in the rat. Am. J. Obstet. Gynecol. *164*: 959-966.

Kennard, C. and Lueck, C.J. (1989) Oculomotor abnormalities in diseases of the basal ganglia. Rev. Neurol. Paris *145*: 587-595.

Kieburtz, K., Feigin, A., McDermott, M., Como, P., Abwender, D., Zimmerman, C., Hickey, C., Orme, C., Claude, K., Sotack, J., Greenamyre, J., Dunn, C. and

Shoulson, I. (1996) A controlled trial of remacemide hydrochloride in Huntington's disease. Mov. .Disorders *11*: 273-277.

Kilpatrick, I., Starr, M., Fletcher, A., James, T. and MacLeod, N. (1980) Evidence for a GABAergic nigrothalamic pathway in the rat. Exp. Brain Res. *40*: 45-54.

King J.C. and Letourneau, R.L. (1994) Luteinizing hormone-releasing hormone terminals in the median eminence of rats undergo dramatic changes after gonadectomy, as revealed by electron microscopic image analysis. Endocrinol. *134*: 1340-1351.

Koeppen, A.H. (1989) The nucleus pontis centralis caudalis in Huntington's disease. J. Neurol. Sci. *91*: 129-141.

Koh, J.Y. and Choi, D.W. (1988a) Cultured striatal neurons containing NADPH-diaphorase or acetylcholinesterase are selectively resistant to injury by NMDA receptor agonists. Brain Res. *446*: 374-378.

Koh, J.Y. and Choi, D.W. (1988b) Vulnerability of cultured cortical neurons to damage by excitotoxins: differential susceptibility of neurons containing NADPH-diaphorase. J. Neurosci. *8*: 2153-2163.

Koide, R., Ikeuchi, T., Onodera, O., Tanaka, H., Igarashi, S., Endo, K., Takahashi, H., Kondo, R., Ishikawa, A., Hayashi, T., et al (1994) Unstable expansion of CAG repeat in hereditary dentatorubral-pallidoluysian atrophy (DRPLA). Nature Genet. *6*: 9-13.

Koller, W.C. and Trimble, J. (1985) The gait abnormality of Huntington's disease. Neurol. *35*: 1450-1454.

Konradi, C., Cole, R.L., Heckers, S. and Hyman, S.E. (1994) Amphetamine regulates gene expression in rat striatum via transcription factor CREB. J. Neurosci. *14*: 5623-5634.

Koob, G.F. and Bloom, F.E. (1988) Cellular and molecular mechanisms of drug dependence. Science *242*: 715-723.

Kornblith, C. and Olds, J. (1973) Unit activity in brainstem reticular formation of the rat during learning. J. Neurophysiol. *36*: 489-501.

Kouzarides, T. and Ziff, E. (1988) The role of the leucine zipper in the *fos-jun* interaction. Nature *336*: 646-651.

Kouzarides, T. and Ziff, E. (1989) Leucine zippers of Fos, Jun and GCN4 dictate dimerization and thereby control DNA binding. Nature *340*: 568-571.

Krauss, J.K. and Jankovic, J. (1996) Surgical treatment of Parkinson's disease. Am. Fam. Physician *54*: 1621-1629.

Kuhl, D.E., Markham, C.H., Metter, E.J., Riege, W.H., Phelps, M.E. and Mazziotta, J.C. (1985) Local cerebral glucose utilization in symptomatic and presymptomatic Huntington's disease. Res.Publ.Assoc.Res. Nerv. Ment. Dis. *63*: 199-209.

Kuhl, D.E., Metter, E.J. and Riege, W.H. (1984) Patterns of local cerebral glucose utilization determined in Parkinson's disease by the [18F]fluorodeoxyglucose method. Ann. Neurol. *15*: 419-424.

Kuhl, D.E., Metter, E.J., Riege, W.H. and Markham, C.H. (1984) Patterns of cerebral glucose utilization in Parkinson's and Huntington's disease. Ann. Neurol. *15 Suppl*: S119-125.

Lacey, M.G., Mercuri, N.B. and North, R.A. (1989) Two cell types in rat substantia nigra zona compacta distinguished by membrane properties and the actions of dopamine and opioids. J. Neurosci. *9*: 1233-1241.

Lannes, B. and Micheletti, G. (1997) Sensitization of the striatal dopaminergic system induced by chronic administration of a glutamate antagonist in the rat. Neurosci. Biobehav. Rev. *21*: 417-424.

Lasker, A.G., Zee, D.S., Hain, T.C., Folstein, S.E. and Singer, H.S. (1987) Saccades in Huntington's disease: initiation defects and distractability. Neurol. *37*: 364-370.

Lee, R.G. (1987) Physiology of the basal ganglia and pathophysiology of Parkinson's disease. Can. J. Neurol. Sci. *14*: 373-380.

Leigh, P., Reavill, C., Jenner, P. and Marsden, C. (1983) Basal ganglia outflow pathways and circling behavior in the rat. J. Neural Trans. *58*: 1-41.

Leigh, R.J., Newman, S.A., Folstein, S.E., Lasker, A.G. and Jensen, B.A. (1983) Abnormal ocular motor control in Huntington's disease. Neurol. *33*: 1268-1275.

Lemaire, P., Revelant, O., Bravo, R. and Charnay, P. (1988) Two mouse genes encoding potential transcription factors with identical DNA-binding domains are

activated by growth in cultured cells. Proc. Natl. Acad. Sci.(USA) *85*:4691-4695.

LeMoine, C., Normad, E. and Bloch, B. (1991) Phenotypical characterization of rat striatal neurons expressing the D1 dopamine receptor gene. Proc. Natl. Acad. Sci. (USA) *88*: 4205-4209.

LeMoine, C., Normad, E., Guitteny, A.F., Fouque, B., Teoule, R. and Bloch, B. (1990) Dopamine receptor gene expression by enkephalin neurons in rat forebrain. Proc. Natl. Acad. Sci. (USA) *87*: 230-234.

Li, S.H., Schilling, G., Young, W.S., Li, X.J., Margolis, R.L., Stine, O.C., Wagster, M.V., Abbott, M.H., Franz, M.L., Ranen, N.G., Folstein, S.E., Hedreen, J.C. and Ross, C.A. (1993) Huntington's Disease gene (IT15) is widely expressed in human and rat tissues. Neuron *11*: 985-993.

Li., X., Li, S., Sharp, A., Nuclfora, F., Schilling, G., Lanahan, A., Worley, P., Snyder, S. and Ross, C. (1995) A huntingtin-associated protein enriched in brain with implications for pathology. Nature *378*: 398-402.

Li., X., Sharp, A., Li, S., Dawson, T., Snyder, S. and Ross, C. (1996) Huntingtin-associated protein (HAP1): discrete neuronal localizations in the brain resemble those of neuronal nitric oxide synthase. Proc. Natl. Acad. Sci. (USA) *93*: 4839-4844.

Lin, B., Nasir, J., MacDonald, H., Hutchinson, G., Graham, R., Rommens, J. and Hayden, M. (1994) Sequence of the murine Huntington disease gene: evidence for conservation and polymorphism in a triplet (CCG) repeat alternate splicing. Hum. Mol. Genet. *3*: 85-92.

Lin, B.Y., Rommens, J.M., Graham, R.K., Kalchman, M., MacDonald, H., Nasir, J., Delaney, A., Goldberg, Y.P. and Hayden, M.R. (1993) Differential 3' polyadenylation of the Huntington disease gene results in two mRNA species with variable tissue expression. Hum. Mol. Genet. *2*: 1541-1545.

Lin, J.S., Hou, Y. and Jouvet, M. (1996) Potential brain neuronal targets for amphetamine-, methylphenidate-, and modafinil-induced wakefulness, evidenced by c-*fos* immunocytochemistry in the cat. Proc. Natl. Acad. Sci. (USA) *93*: 14128-14133.

Linden, R. and Perry, V.H. (1983) Massive retinotectal projections in rats. Brain Res. *272*: 145-149.

Liu, Y.F., Deth, R.C. and Devys, D. (1997) SH3 domain-dependent association of huntingtin with epidermal growth factor receptor signaling complexes. J Biol Chem 272: 8121-8124.

Loke, S.L., Stein, C.A., Zhang, X.H., Mori, K., Nakanishi, M., Subasinghe, C. and Cohen, J. (1989) Characterization of oligonucleotide transport into living cells. Proc.Natl.Acad.Sci. (USA) 86: 3474-3478.

Lucas, J., Mellstrom, B., Colado, M. and Naranjo, J. (1993) Molecular mechanisms of pain: serotonin 1A receptor agonists trigger transactivation by c-fos of the prodynorphin gene in spinal neurons. Neuron 10: 599-611.

Lyttle, C.R. and DeSombre, E.R. (1977) Generality of oestrogen stimulation of peroxidase activity in growth-responsive tissues. Nature 268: 337-339.

Ma, Y.J., Berg-von der Emde, K., Moholt-Siebert, M., Hill, D.F. and Ojeda, S.R. (1994) Region-specific regulation of transforming growth factor α (TGFα) gene expression in astrocytes of the neuroendocrine brain. J. Neurosci. 14: 5644-5651.

Ma, Y.J., Berg-von der Emde, K., Rage, F., Wetsel, W.C. and Ojeda, S.R. (1997) Hypothalamic astrocytes respond to transforming growth factor-α with the secretion of neuroactive substances that stimulate the release of luteinizing hormone-releasing hormone. Endocrinol. 138: 19-25.

Madison, D.V. and Nicoll, R.A. (1988) Enkephalin hyperpolarizes interneurons in the rat hippocampus. J. Physiol. 398: 123-130.

Mahan, L.C., Burch, R.M., Monsma, F.J. and Sibley, D.R. (1990) Expression of striatal D1 dopamine receptors coupled to inositol phosphate production and Ca²⁺ mobilization in Xenopus oocytes. Proc. Natl. Acad. Sci. (USA) 87: 2186-2200.

Maki, Y., Bos, T., Davis, C., Starbuck, M. and Vogt, P. (1987) Avian sarcoma virus 17 carries a new oncogene jun. Proc. Natl. Acad. Sci. (USA) 84: 2848-2852.

Mangiarini, L., Sathasivam, K., Seller, M., Cozens, B., Harper, A., Hetherington, C., Lawton, M., Trottier, Y., Lehrach, H., Davies, S. and Bates, G. (1996) Exon 1 of the HD gene with an expanded CAG repeat is sufficient to cause a progressive neurological phenotype in transgenic mice. Cell 87: 493-506.

Marsden, C.D. and Jenner, R. (1980) Pathophysiology of extrapyramidal side effects of neuroleptic drugs. Psychol. Med. 10: 55-72.

Martin, L.P. and Waszczak, B.L. (1996) Dopamine D2 receptor-mediated modulation of the GABAergic inhibition of substantia nigra pars reticulata neurons. Brain Res. *729*: 156-169.

Massieu, L., Rocamora, N., Palacios, J.M. and Boddeke, H. (1992) Administration of quinolinic acid in the rat hippocampus induces expression of c-*fos* and *ngfi*-a. Mol. Brain Res. *16*: 88-96.

Masucci, E.F., Borts, F.T. and Kurtzke, J.F. (1990) CT brainstem abnormalities in the differential diagnosis of Huntington's disease. Comput. Med. Imaging Graph. *14*: 205-212.

Matthews, P.M., Evans, A.C., Andermann, F. and Hakim, A.M. (1989) Regional cerebral glucose metabolism in adult and rigid forms of Huntington disease. Pediatr. Neurol. *5*: 353-356.

McLean, D.R. (1982) Failure of isoniazid therapy in Huntington's disease. Neurol. *32*: 1189-1191.

Merchant, K.M. (1994) c-*fos* antisense oligonucleotide specifically attenuates haloperidol-induced increases in neurotensin/neuromedin N mRNA expression in rat dorsal striatum. Mol. Cell. Neurosci. *5*: 336-344.

Milbrandt, J. (1987) A nerve growth factor induced gene encodes a possible transcriptional regulatory factor. Science *238*: 797-799.

Miles, R. and Wong, R.K. (1984) Unitary inhibitory synaptic potentials in the guinea-pig hippocampus *in vitro*. J. Physiol. *356*: 97-113.

Mileusnic, R., K. Anokhin, and S.P. Rose (1996) Antisense oligodeoxynucleotides to c-*fos* are amnestic for passive avoidance in the chick. Neuroreport *7*: 1269-1272.

Miller, R. and Beninger, R.J. (1991) On the interpretation of asymmetries of posture and locomotion produced with dopamine agonists in animals with unilateral depletion of striatal dopamine. Progress Neurobiol. *36*: 229-256.

Mink, J. (1996) The basal ganglia: focused selection and inhibition of competing motor programs. Prog. Neurobiol. *50*: 381-425.

Mize, R. (1988) Immunocytochemical Localization of gamma-aminobutyric acid (GABA) in the cat superior colliculus. J. Comp. Neurol. *276*: 38-41.

Mize, R., Spencer, R. and Sterling, P. (1981) Neurons and glia in the cat superior colliculus accumulate [3H]-gamma-aminobutyric acid (GABA). J. Comp. Neurol. 202: 385-396.

Mize, R., Spencer, R. and Sterling, P. (1982) Two-types of GABA-accumulating neurons in the superficial layer of the cat superior colliculus. J. Comp. Neurol. 206: 180-192.

Modrowski, D., Miravet, L., Feuga, M. and Marie, P.J. (1993) Increased proliferation of osteoblast precursor cells in estrogen-deficient rats. Am. J. Physiol. 264: E190-196.

Moller, C., Bing, O. and Heilig, M. (1994) c-fos expression in the amygdala: in vivo antisense modulation and role in anxiety. Cell. Mol. Neurobiol. 14: 415-423.

Monckton, D. and Caskey, C. (1995) Unstable triplet repeat diseases. Circulation 91: 513-520.

Moore, K.E. (1987) Interactions between prolactin and dopaminergic neurons. Biol. Reprod. 36: 47-58.

Moratalla, R., Robertson, H.A. and Graybiel, A. (1992) Dynamic regulation of ngfi-a (zif268, egr1) gene expression in the striatum. J. Neurosci. 12: 2609-2622.

Moratalla, R., Vickers, E., Robertson, H., Cochran, B. and Graybiel, A. (1993) Coordinate expression of c-fos and junB is induced in the striatum by cocaine. J. Neurosci. 13: 423-433.

Morelli, M. (1997) Dopamine/glutamate interaction as studied by combining turning behaviour and c-Fos expression. Neurosci. Biobehav. Rev. 21: 505-509.

Morgan, J.I. and Curran, T. (1989) Stimulus-transcription coupling in neurons: role of cellular immediate-early genes. Trends Neurosci. 12: 459-462.

Morgan, J. I. and Curran, T (1991) Stimulus-transcription coupling in the nervous system: involvement of the inducible proto-oncogenes fos and jun. Ann. Rev. Neurosci. 14: 421-451.

Moriizumi, T., Nakamura, Y., Tokuno, H., Kudo, M. and Kitao, Y. (1988) Convergence of afferent fibers from the entopeduncular nucleus and the substantia nigra pars reticulata onto single neurons in the ventromedial thalamic nucleus: an electron microscope study in the cat. Neurosci. Lett. 95: 125-129.

Nakamura, T., Kanayama, R., Sano, R., Ohki, M., Kimura, Y., Aoyagi, M. and Koike, Y. (1991) Quantitative analysis of ocular movements in Parkinson's disease. Acta Otolaryngol. Suppl. Stockh. *481*: 559-562.

Naranjo, J., Mellstrom, B., Achaval, M., Lucas, J., DelRio, J. and Sassone-Corsi, P. (1991) Co-induction of junB and c-*fos* in a subset of neurons in the spinal cord. Oncogene *6*: 223-227.

Nasir J, Floresco S, O'Kusky J, Diewert V, Richman JM, Zeisler J, Borowski A, Marth JD, Phillips AG, Hayden MR (1995) Targeted disruption of the Huntington's Disease gene results in embryonic lethality and behavioral and morphological changes in heterozygotes. Cell *81*: 811-823.

Nauta, V.J.H. and van Straaten, J.J. (1947) The primary optic centres of the rat: an experimental study by the "bouton" method. J. Anat. (London) *81*: 127-135.

Neal, J.W., Pearson, R.C., Cole, G. and Powell, T.P. (1991) Neuronal hypertrophy in the pars reticulata of the substantia nigra in Parkinson's disease. Neuropathol. Appl. Neurobiol. *17*: 203-206.

Neckers, L.M. (1989) Antisense Oligodeoxynucleotides as a tool for studying cell regulation: mechanism of uptake and application to the study of oncogene function In: Oligodeoxynucleotides: Antisense Inhibitors of Gene Expression (J.Cohen, ed.) pp 211-231.

Neill J, Nagy G (1994) Prolactin secretion and its control. In: The Physiology of Reproduction (Knobil E, Neill J, eds.),pp 1833-1860. New York: Raven Press Ltd.

Nestler, E.J., Hope, B.T. and Widnell, K.L. (1993) Drug addiction: a model for the molecular basis of neural plasticity. Neuron *11*: 995-1006.

Nisbet, A.P., Eve, D.J., Kingsbury, A.E., Daniel, S.E., Marsden, C.D., Lees, A.J. and Foster, O.J. (1996) Glutamate decarboxylase-67 messenger RNA expression in normal human basal ganglia and in Parkinson's disease. Neurosci. *75*: 389-406.

Nishina, H., Sato, H., Suzuki, T., Sato, N. and Iba, H. (1990) Isolation and characterisation of Fra-2, an additional member of the *fos* gene family. Proc. Natl. Acad. Sci. (USA) *87*: 3619-3623.

Noguchi, K., Kowalski, K., Traub, R., Solodkin, A., Iadarola, M. and Ruda, M. (1991) Dynorphin expression and Fos-like immunoreactivity following

inflammation induced hyperalgesia are colocalized in spinal cord neurons. Mol. Brain Res. *10*: 227-233.

Nutt, J.G., Rosin, A. and Chase, T.N. (1978) Treatment of Huntington's disease with a cholinergic agonist. Neurol. *28*: 1061-1064.

Oertel, W.H., Tappaz, M.L., Berod, A. and Mugnaini. E. (1982) Two color immunohistochemistry for dopamine and GABA neurons in rat substantia nigra and zona incerta. Brain Res. Bull. *9*: 463-474.

Ojeda, S.R., Dissen, G.A. and Junier, M.P. (1992) Neurotrophic factors and female sexual development. Front. Neuroendocrinol. *13*: 120-162.

Ojeda S.R., Urbanski H, Costa M, Hill D, Moholt-Siebert M (1990) Involvement of transforming growth factor α in the release of luteinizing hormone-releasing hormone from the developing female hypothalamus. Proc. Natl. Acad. Sci. (USA) *87*: 9698-9702.

Okano, H., Pfaff, D. and Gibbs, R. (1996) Expression of EGFR-, p75NGFR- and PSTAIR (cdc2)-like immunoreactivity by proliferating cells in the adult rat hippocampal formation and forebrain. Dev. Neurosci. *15*: 199-209.

Oliver, J.E. (1970) Huntington's chorea in Northamptonshire. Brit. J. Psychiatry *116*: 241-253.

Olmos, G., Naftolin, F., Perez, J., Tranque, P. and Gracia-Segura, L.M. (1989) Synaptic remodeling in the arcuate nucleus during the estrous cycle. Neurosci. *32*: 663-667.

Ordway, J.M., Tallaksen-Greene, S., Gutekunst, C.A., Bernstein, E.M., Cearley, J.A., Wiener, H.W., Dure, L.S., Lindsey, R., Hersch, S.M., Jope, R.S., Albin, R.L. and Detloff, P.J. (1997) Ectopically expressed CAG repeats cause intranuclear inclusions and a progressive lateonset neurological phenotype in the mouse. Cell *91*: 753-763.

Ozer, H., Ekinci, A.C. and Starr, M.S. (1997) Dopamine D1- and D2-dependent catalepsy in the rat requires functional NMDA receptors in the corpus striatum, nucleus accumbens and substantia nigra pars reticulata. Brain Res. *777*: 51-59.

Parent, A. (1990) Extrinsic connections of the basal ganglia. Trends Neurosci. *13*: 254-258.

Paul, M., Graybiel, A., David, J. and Robertson, H. (1992) D1-like and D2-like dopamine receptors synergistically activate rotation and c-*fos* expression in the

dopamine-depleted striatum in a rat model of Parkinson's disease. J. Neurosci. *12*: 3729-3742.

Paxinos, G. and Watson, C. (1997) The rat brain in stereotaxic coordinates. Academic Press.

Peiris, J.B., Boralessa, H. and Lionel, N.D. (1976) Clonazepam in the treatment of choreiform activity. Med. J. Austral. *1*: 225-227.

Peterson, B.W. (1979) Reticulospinal projections to spinal motor nuclei. Ann. Rev. Physiol. *41*: 127-140.

Pfaff, D. and Keiner, M. (1973) Atlas of estradiol-concentrating cells in the central nervous system of the female rat. J. Comp. Neurol. *151*: 121-158.

Pflanz, S., Besson, J.A., Ebmeier, K.P. and Simpson, S. (1991) The clinical manifestation of mental disorder in Huntington's disease: a retrospective case record study of disease progression. Acta Psychiatrica Scand. *83*: 53-60.

Phillips, J.G., Bradshaw, J.L., Chiu, E., Teasdale, N., Iansek, R., Bradshaw, J.A. *et al.* (1996) Bradykinesia and movement precision in Huntington's disease. Neuropsychologia *34*: 1241-1245.

Phillips, M.L., Young, A.W., Senior, C., Brammer, M., Andrew, C., Calder, A.J., Bullmore, E.T., Perrett, D.I., Rowland, D., Williams, S.C., Gray, J.A. and David, A.S. (1997) A specific neural substrate for perceiving facial expressions of disgust. Nature *389*: 495-498.

Popoli, P., Pezzola, A., Domenici, M.R., Sagratella, S., Diana, G., Caporali, M.G., Bronzetti, E., Vega, J. and Scotti de Carolis, A. (1994) Behavioral and electrophysiological correlates of the quinolinic acid rat model of Huntington's disease in rats. Brain Res. Bull. *35*: 329-335.

Pycock, C.J. (1980) Turning behavior in animals. Neurosci. *5*: 461-514.

Pycock, C.J. and Kilpatrick, I.C. (1989) Motor asymmetries and drug effects. Behavioral analyses of receptor activation. In: Psychopharmacology. (Boulton, A., Baker, G. and Greenshaw, A., eds.) Neuromethods, Humana Press, Clifton, pp. 1-93.

Racine, R. (1972) Modification of seizure activity by electrical stimulation: motor seizure. Electroencephalogr. Clin. Neurophysiol. *38*: 281-294.

Rauscher, F., Sambucetti, L., Curran, T., Distel, R. and Spiegelman, B. (1988) Common DNA binding site for Fos protein complexes and transcription factor AP-1. Cell *52*: 471-480.

Reavill, C., Jenner, P., Leigh, N. and Marsden, C. (1981) The role of nigral projections to the thalamus in drug-induced circling behaviour in the rat. Life Sci. *28*: 1457-1466.

Redgrave, P., Mitchell, I. and Dean, P. (1987) Descending projections from the superior colliculus in the rat: a study using orthograde transport of wheatgerm-agglutinin conjugated horseradish peroxidase. Exp. Brain Res. *68*: 147-167.

Redgrave, P., Odekunle, A. and Dean, P. (1986) Tectal cells of origin of predorsal bundle in rat: location and segregation from ipsilateral descending pathway. Exp. Brain Res. *63*: 279-293.

Reynolds, B., Tetzlaff, W. and Weiss, S. (1992) A multipotent EGF-responsive striatal embryonic progenitor cell produces neurons and astrocytes. J. Neurosci. *12*: 4565-4574.

Reynolds, B. and Weiss, S. (1992) Generation of neurons and astrocytes from isolated cells of the adult mammalian central nervous system. Science *255*: 1707-1710.

Richfield, E.K., Maguire-Zeiss, K.A., Vonkeman, H.E. and Voorn, P. (1995) Preferential loss of preproenkephalin versus preprotachykinin neurons from the striatum of Huntington's disease patients. Ann. Neurol. *38*: 852-860.

Robertson, G.S. and Robertson, H.A. (1987) D1 and D2 dopamine agonist synergism: separate sites of action. Trends Pharmacol. Sci. *8*: 295-299.

Robertson, G.S., Tetzlaff, W., Bedard, A.,. St Jean, M., and Wigle, N. (1995) c-*fos* mediates antipsychotic-induced neurotensin gene expression in the rodent striatum. Neurosci. *67*: 325-344.

Robertson, G.S., Vincent, S.R. and Fibiger, H.C. (1992) D1 and D2 dopamine receptors differentially regulate c-*fos* expression in striatonigral and striatopallidal neurons. Neurosci. *49*: 285-296.

Robertson, H.A. (1992) Dopamine receptor interactions: some implications for the treatment of Parkinson's disease. Trends Neurosci. *15*: 201-206.

Robertson, H.A. (1992) Immediate early genes, neuronal plasticity and memory. Biochem. Cell. Biol. *70*: 729-737.

Robertson, H.A., Paul, M.L., Moratalla, R. and Graybiel, A.M. (1991) Expression of the immediate early gene c-*fos* in basal ganglia: induction by dopaminergic drugs. Can. J. Neurol. Sci. *18*: 380-383.

Robertson, H.A., Peterson, M., Murphy, K. and Robertson, G. (1989) D$_1$-dopamine receptor agonists selectively activate striatal c-*fos* independent of rotational behavior. Brain Res. *503*: 346-349.

Robinson, D. (1972) Eye movements evoked by collicular stimulation in the alert monkey. Vision Res. *12*: 1795-1808.

Roth, M. (1980) The diagnosis of dementia in late and middle life. In: The epidemiology of dementia. (J.A. Mortimer, ed.) Oxford: University Press.

Ruffieux, A. and Schultz, W. (1980) Dopaminergic activation of reticulata neurons in the substantia nigra. Nature *285*: 240-241.

Ruigrok,T., van der Burg, H. and Sabel-Goedknegt E. (1996) Locomotion coincides with c-Fos expression in related areas of inferior olive and cerebellar nuclei in the rat. Neurosci. Lett. *214*: 119-122.

Rusak, B., Robertson, H., Wisden, W. and Hunt, S. (1990) Light pulses that shift rhythms induce gene expression in the suprachiasmatic nucleus. Science *248*: 1237-1240.

Ryder, K., Lanahan, A., Perez-Albuerne, E. and Nathans, D. (1989) Jun-D: a third member of the Jun gene family. Proc. Natl. Acad. Sci. (USA) *86*: 1500-1503.

Ryder, K., Lau, L. and Nathans, D. (1988) A gene activated by growth factors is related to the oncogene v-*jun*. Proc. Natl. Acad. Sci. (USA) *85*: 1487-1491.

Sagar, S.M., Sharp, F.R. and Curran, T. (1988) Expression of c-*fos* protein in brain: metabolic mapping at the cellular level. Science *240*: 1328-1331.

Sahibzada, N., Dean, P. and Redgrave, P. (1986) Movements resembling orientation or avoidance elicited by electrical stimulation of the superior colliculus in rats. J. Neurosci. *6*: 723-733.

Sambrook J, Fritsch E, Maniatis T (1989) Molecular Cloning. Nolan C: Cold Spring Harbor Laboratory Press.

Sassone-Corsi, P., Sisson, J. and Verma, I. (1988) Transcriptional autoregulation of the proto-oncogene *fos*. Nature *334*: 314-319.

Scheel-Kruger, J. (1986) Dopamine-GABA interactions: evidence that GABA transmits, modulates and mediates dopaminergic functions in the basal ganglia and the limbic system. Acta. Neurol. Scand. Suppl. *107*: 1-54.

Schiller, P. and Stryker, M. (1972) Single-unit recording and stimulation in the superior colliculus of the alert rhesus monkey. J. Neurophysiol. *35*: 915-924.

Schipper, H.M., Lechan, R.M. and Reichlin, S. (1990) Glial peroxidase activity in the hypothalamic arcuate nucleus: effects of estradiol valerate-induced persistent estrus. Brain Res. *507*: 200-207.

Schuller, J. and Marshall, J. (1995) Intrastriatal DNQX induces rotation and pallidal Fos in the 6-OHDA model of Parkinson's disease. Neuroreport *6*: 2594-2598.

Schwarting, R.K. and Huston, J.P. (1996) The unilateral 6-hydroxydopamine lesion model in behavioral brain research. Analysis of functional deficits, recovery and treatments. Progress Neurobiol. *50*: 275-331.

Shammah-Lagnado, S.J., Negrao, N., Silva, B.A. and Ricardo, J.A. (1987) Afferent connections of the nuclei reticularis pontis oralis and caudalis: a horseradish peroxidase study in the rat. Neurosci. *20*: 961-989.

Sharp, A.H., Loev, S.J., Schilling, G., Li, S.H., Li, X.J., Bao, J., Wagster, M.V., Kotzuk, J.A., Steiner, J.P., Lo, A., et al (1995) Widespread expression of Huntington's disease gene (IT15) protein product. Neuron *14*: 1065-1074.

Sheng, M., Douglas, S.T., McFadden, G. and Greenberg, M.E. (1988) Calcium and growth factor pathways of c-*fos* transcriptional activation require distinct upstream regulatory sequences. Mol. Cell. Biol. *8*: 2787-2796.

Sheng, M., McFadden, G. and Greenberg, M.E. (1990) Membrane depolarization and calcium induce c-*fos* transcription via phosphorylation of transcription factor CREB. Neuron *4*: 571-582.

Sheng, M., Thompson, M. and Greenberg, M. (1991) CREB: a Ca^{2+}-regulated transcription factor phosphorylated by calmodulin-dependent kinases. Science *252*: 1427-1430.

Shevde, N.K., Pike, J.W. (1996) Estrogen modulates the recruitment of myelopoietic cell progenitors in rat through a stromal cell-independent mechanism involving apoptosis. Blood *87*: 2683-2692.

Shibasaki, H., Tsuji, S. and Kuroiwa, Y. (1979) Oculomotor abnormalities in Parkinson's disease. Arch. Neurol. *36*: 360-364.

Shih, C.D., S.H. Chan, and J.Y. Chan (1996) Participation of Fos protein at the nucleus tractus solitarius in inhibitory modulation of baroreceptor reflex response in the rat. Brain Res. *738*: 39-47.

Shih, M. and Malbon, C.C. (1994) Oligodeoxynucleotides antisense to mRNA encoding protein kinase A, protein kinase C and β-adrenergic receptor kinase reveal distinctive cell-type-specific roles in agonist-induced desensitization. Proc. Natl. Acad. Sci. (USA) *91*: 12193-12197.

Shokeir, M.H. (1975) Investigations on Huntington's disease in the Canadian prairies. I. Prevalence. Clin. Genet. *7*: 345-348.

Shoulson, I., Goldblatt, D., Charlton, M. and Joynt, R.J. (1978) Huntington's disease: treatment with muscimol, a GABA-mimetic drug. Ann. Neurol. *4*: 279-284.

Shoulson, I., Odoroff, C., Oakes, D., Behr, J., Goldblatt, D., Caine, E., Kennedy. J., Miller, C., Bamford, K., Rubin, A., et al (1989) A controlled clinical trial of baclofen as protective therapy in early Huntington's disease. Ann. Neurol. *25*: 252-259.

Siegel, J.M. (1979) Behavioral functions of the reticular formation. Brain Res. Rev. *1*: 69-105.

Snyder, S.H. (1982) Neurotransmitters and CNS disease: schizophrenia. Lancet *2*: 970-974.

Sommer, W., Bjelke, B., Ganten, D. and Fuxe, K. (1993) Antisense oligonucleotide to c-*fos* induces ipsilateral rotational behavior to *d*-amphetamine. Neuroreport *5*: 277-280.

Sommer, W., Cui, X., Erdmann, B., Wiklund, L., Bricca, G., Heilig, M. and Fuxe, K. (1998) The spread and uptake pattern of intracerebrally administered oligonucleotides in nerve and glial cell populations of the rat brain. Antisense Nucleic Acid Drug Dev. *8*: 75-85.

Sommer, W., Rimondini, R, O'Connor, W., Hansson, A.C., Ungerstedt, U. and Fuxe, K. (1996) Intrastriatally injected c-*fos* antisense oligonucleotide interferes with striatonigral but not striatopallidal γ-aminobutyric acid transmission in the conscious rat. Proc.Natl. Acad. Sci. (USA) *93*: 14134-14139.

Sparks, D. and Mays, L. (1976) Movement fields of saccade-related burst neurons in the monkey superior colliculus. Brain Res. *113*: 21-34.

Spokes, E.G. (1980) Neurochemical alterations in Huntington's chorea: a study of post-mortem brain tissue. Brain *103*: 179-210.

Starr, M. (1987) Opposing roles of dopamine D1 and D2 receptors in nigral γ-[³H]aminobutyric acid release? J. Neurochem. *49*: 1042-1049.

Stein, C.A. and Cheng, Y.C. (1993) Antisense oligonucleotides as therapeutic agents-is the bullet really magic? Science *261*: 1004-1011.

Stein, C.A. and Cohen, J.S. (1989) Phosphorothioate oligodeoxynucleotide analogues In: Oligodeoxynucleotides: Antisense Inhibitors of Gene Expression (J.Cohen, ed.) pp 97-117.

Stein, C.A., Subasinghe, C., Shinozuka, K. and Cohen, J.S. (1988) Physicochemical properties of phosphorothioate oligodeoxynucleotides. Nucl. Acids Res. *16*: 3209-3221.

Stewart, J.T. (1988) Treatment of Huntington's disease with clonazepam. Southern Med. J. *81*: 102.

Stoof, J.C. and Kebabian, J.W. (1981) Opposing roles for D1 and D2 dopamine receptors in efflux of cyclic AMP from rat neostriatum. Nature *294*: 366-368.

Storey, E. and Beal, M.F. (1993) Neurochemical substrates of rigidity and chorea in Huntington's disease. Brain *116*: 1201-1222.

Strassman, A., and Vos, B. (1993) Somatotopic and laminar organization of Fos-like immunoreactivity in the medullary and upper cervical dorsal horn induced by noxious facial stimulation in the rat. J. Comp. Neurol. *331*: 495-516.

Strong, T.V., Tagle, D.A., Valdes, J.M., Elmer, L.W., Boehm, K., Swaroop, M., Kaatz, K.W., Collins, F.S. and Albin, R.L. (1993) Widespread expression of the human and rat Huntington's disease gene in brain and nonneural tissues. Nature Genet. *5*: 259-265.

Sukhatme, V., Cao, X., Chang, L., Tsai-Morris, C., Stamenkovich, D., Ferreira, P., Cohen, D., Edwards, S., Shows, T., Curran, T., LeBeau, M. and Adamson, E. (1988) A zinc-finger gene coregulated with c-*fos* during growth and differentiation and after depolarization. Cell *53*: 37-43.

Suzuki, S., P. Pilowsky, J. Minson, L. Arnolda, I.J. Llewellyn Smith, and J. Chalmers (1994) c-*fos* antisense in rostral ventral medulla reduces arterial blood pressure. Am. J. Physiol. *266*: R1418-1422.
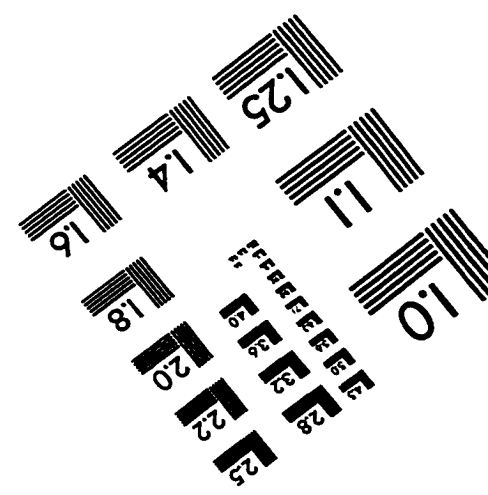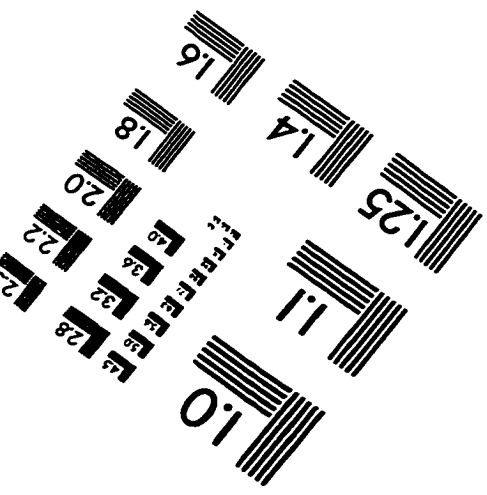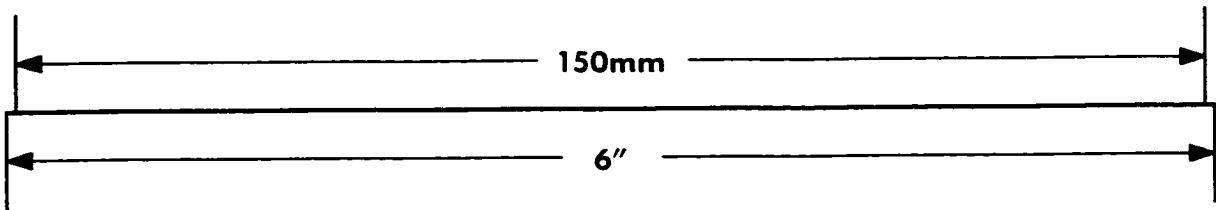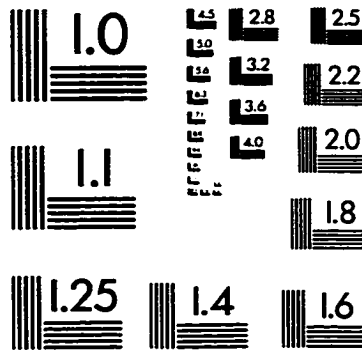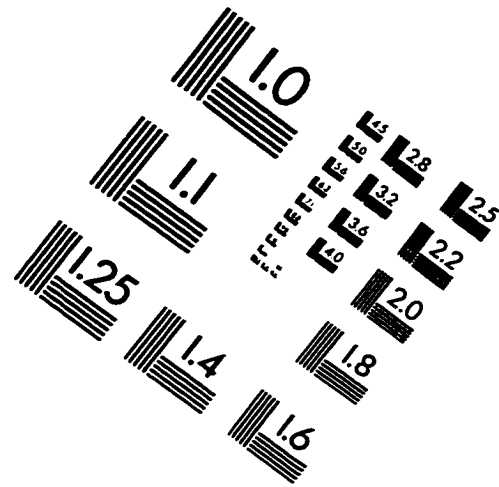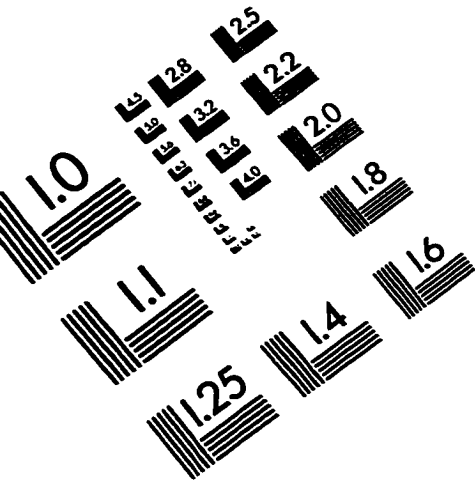
Svenningsson, P., J. Georgieva, E. Kontny, M. Heilig, and B. Fredholm (1997) Involvement of a c-*fos*-dependent mechanism in caffein-induced expression of the prepretachykinin A and neurotensin/neuromedin N genes in rat striatum. Eur. J. Neurosci. *9*: 2135-2141.

Swirnoff, A.H. and Milbrandt, J. (1995) DNA-binding specificity of NGFI-A and related zinc finger transcription factors. Mol. Cell. Biol. *15*: 2275-2287.

Takada, M. and Hattori, T. (1988) Dopaminergic nigrotectal projection in the rat. Brain Res. *457*: 165-168.

Tang, J.Y., Temsamani, J. and Agrawal, S. (1993) Self-stabilized antisense oligonucleotide phosphorothioates: properties and anti-HIV activity. Nuc. Acids Res. *21*: 2729-2735.

Tatter, S.B., Galpern, W.R., Hoogeveen, A.T. and Isacson, O. (1995) Effects of striatal excitotoxicity on huntingtin-like immunoreactivity. Neuroreport *6:* 1125-1129.

Tepper, J.M., Martin, L.P. and Anderson, D.R. (1995) GABAA receptor-mediated inhibition of rat substantia nigra dopaminergic neurons by pars reticulata projection neurons. J. Neurosci. *15*: 3092-3103.

The Huntington's Disease Collaborative Research Group (1993) A novel gene containing a trinucleotide repeat that is expanded and unstable on Huntington's disease chromosomes. Cell *72*: 971-983.

Thompson, R., Ramsay, A. and Yu, J. (1984) A generalized learning deficit in albino rats with early median raphe or pontine reticular formation lesions. Physiol. Behav. *32*: 107-114.

Tischmeyer, W., R. Grimm, H. Schicknick, W. Brysch, and K.H. Schlingensiepen (1994) Sequence-specific impairment of learning by c-*jun* antisense oligonucleotides. Neuroreport *5*: 1501-1504.

Torres-Aleman, I., Rejas, M., Pons, S. and Garcia-Segura, L.M. (1992) Estradiol promotes cell shape changes and glial fibrillary acidic protein redistribution in hypothalamic astrocytes in vitro: a neuronal-mediated effect. Glia *6*: 180-187.

Tranque, P.A., Suarez, I., Olmos, G., Fernandez, B. and Garcia-Segura, L.M. (1987) Estradiol-induced redistribution of glial fibrillary acidic protein immunoreactivity in the rat brain. Brain Res. *406*: 348-351.

Trottier, Y., Devys, D., Imbert, G., Saudou, F., An, I., Lutz, Y., Weber, C., Agid. Y., Hirsch, E.C. and Mandel, J.L. (1995a) Cellular localization of the Huntington's Disease protein and discrimination of the normal and mutated form. Nature Genet. *10*: 104-110.

Trottier, Y., Lutz, Y., Stevanin, G., Imbert, G., Devys, D., Cancel, G., Saudou, F., Weber, C., David, G., Tora, L., Agid, Y., Brice, A. and Mandel, J. (1995b) Polyglutamine expansion as a pathological epitope in Huntington's disease and four dominant cerebellar ataxias. Nature *378*: 403-406.

Umekage, T., M. Namima, K. Fukushima, S. Sugita, and Y. Watanabe (1997) c-*fos* antisense blocks methamphetamine-induced ambulatory activity reversibly. Neuroreport *8*: 407-410.

Ungerstedt, U. (1968) 6-Hydroxydopamine induced degeneration of central monoamine neurons. Eur. J. Pharmacol. *5*: 107-110.

Ungerstedt, U. (1971) Postsynaptic supersensitivity after 6-hydroxydopamine-induced degeneration of the nigro-striatal dopamine system in the rat brain. Acta Physiol. Scand. *82(suppl 376)*: 69-93.

van der Kooy, D. and Carter, D.A. (1981) The organization of the efferent projections and striatal afferents of the entopeduncular nucleus and adjacent areas in the rat. Brain Res. *211*: 15-36.

van der Kooy, D., Coscina, D.V. and Hattori, T. (1981) Is there a non-dopaminergic nigrostriatal pathway? Neurosci. *6*: 345-357.

van Dijk, J.G., vanderVelde, E.A., Roos, R.A. and Bruyn, G.W. (1986) Juvenile Huntington's disease. Hum. Genet. *73*: 235-239.

Vertes, R.P. and Martin, G.F. (1988) Autoradiographic analysis of ascending projections from the pontine and mesencephalic reticular formation and the median raphe nucleus in the rat. J. Comp. Neurol. *275*: 511-541.

Waldron, H.A. and Gwyn, D.G. (1969) Descending nerve tracts in the spinal cord of the rat. I. Fibers from the midbrain. J. Comp. Neurol. *137*: 143-154.

Wang, J.Q., Smith, A.J. and McGinty, J.F. (1995) A single injection of amphetamine or methamphetamine induces dynamic alterations in c-*fos*, *zif*/268 and preprodynorphin messenger RNA expression in rat forebrain. Neurosci. *68*: 83-95.

Wanker, E., Rovira, C., Scherzinger, E., Hasenbank, R., Walter, S., Tait, D., Colicelli, J. and Lehrach, H. (1997) HIP-I: A huntingtin interacting protein isolated by the yeast two-hybrid system. Hum. Mol. Genet. 6: 487-495.

Waszcak, B.L. and Walters, J.R. (1983) Dopamine modulation of the effects of gamma-aminobutyric acid on substantia nigra pars reticulata neurons. Science 220: 218-221.

Waszczak, B.L., Eng, N. and Walters, J.R. (1980) Effects of muscimol and picrotoxin on single unit activity of substantia nigra neurons. Brain Res. 188: 185-197.

Watt, D.C. and Seller, A.S. (1993) A clinico-genetic study of psychiatric disorder in Huntington's chorea. Psychol. Med. (Monograph Suppl.) 23: 1-46.

Weiss, S., Dunne, C., Hewson, J., Wohl, C., Wheatley, M., Peterson, A. and Reynolds, B. (1996) Multipotent CNS stem cells are present in the adult mammalian spinal cord and ventricular neuroaxis. J. Neurosci. 16: 7599-7609.

Westby, G.W., Keay, K.A., Redgrave, P., Dean, P. and Bannister, M. (1990) Output pathways from the rat superior colliculus mediating approach and avoidance have different sensory properties. Exp.Brain Res. 81: 626-638.

White, O.B., Saint-Cyr, J.A., Tomlinson, R.D. and Sharpe, J.A. (1983b) Ocular motor deficits in Parkinson's disease. II. Control of the saccadic and smooth pursuit systems. Brain 106: 571-587.

Wichmann, T. and DeLong, M. (1996) Functional and pathophysiological models of the basal ganglia. Curr. Opin. Neurobiol. 6: 751-758.

Wisden, W., Errington, M., Williams, S., Dunnett, S., Waters, C., Hitchcock, D., Evans, G., Bliss, T. and Hunt, S. (1990) Differential expression of immediate early genes in the hippocampus and spinal cord. Neuron 4: 603-614.

Witkin, J.W., Ferin, M., Popilskis, S.J. and Silverman, A. (1991) Effects of gonadal steroids on the ultrastructure of GnRH neurons in the rhesus monkey: synaptic input and glial apposition. Endocrinol. 129: 1083-1092.

Witkin, J.W. and Silverman, A. (1985) Synaptology of luteinizing hormone-releasing hormone neurons in rat preoptic area. Peptides 6: 263-271.

Wollnik, F., W. Brysch, E. Uhlmann, F. Gillardon, R. Bravo, M. Zimmermann, K.H. Schlingensiepen, and T. Herdegen (1995) Block of c-Fos and JunB expression by antisense oligonucleotides inhibits light-induced phase shifts of the mammalian circadian clock. Eur. J. Neurosci. 7: 388-393.

Wood, J.D., MacMillan, J.C., Harper, P.S., Lowenstein, P.R. and Jones, A.L. (1996) Partial characterisation of murine huntingtin and apparent variations in the subcellular localisation of huntingtin in human, mouse and rat brain. Hum. Mol. Genet. 5: 481-487.

Wurtz, R. (1996) Vision for the control of movement. Inv. Ophthal. Vis. Sci. 37: 2131-2145.

Wurtz, R. and Albano, J. (1980) Visual-motor function of the primate superior colliculus. Annu. Rev. Neurosci. 3: 189-226.

Wurtz, R.H. and Hikosaka, O. (1986) Role of the basal ganglia in the initiation of saccadic eye movements. Progress Brain Res. 64:175-190.

Yakubov, L., Deeva, E., Zarytova, V., Ivanova, E., Ryte, A., Yurchenko, L. and Vlasso, V. (1989) Mechanism of oligonucleotide uptake by cells: Involvement of specific receptors? Proc. Natl. Acad. Sci. (USA) 86: 6454-6458.

Yung, W.H., Hausser, M.A. and Jack, J.J. (1991) Electrophysiology of dopaminergic and non-dopaminergic neurones of the guinea-pig substantia nigra pars compacta in vitro. J. Physiol. 436: 643-667.

Zeitlin S, Liu J, Chapman D, Papaioannou V, Efstratiadis A (1995) Increased apoptosis and early embryonic lethality in mice nullizygous for the Huntington's Disease gene homologue. Nature Genet. 11: 155-163.

Zelphati, O., Imbach, J., Signoret, N., Zon, G., Rayner, B. and Leserman, L. (1994) Antisense oligonucleotides in solution or encapsulated in immunoliposomes inhibit replication of HIV-1 by several different mechanisms. Nuc. Acids Res. 22: 4307-4314.

Zerial, M., Toschi, L., Ryseck, R., Schuermann, M., Muller, R. and Bravo, R. (1989) The product of a novel growth factor activated gene, fosB, interacts with Jun proteins enhancing their DNA binding activity. EMBO J. 8: 805-813.

Zhou, Y., Takiyama, Y., Igarashi, S., Li, Y.F., Zhou, B.Y., Gui, D.C., Endo, K., Tanaka, H., Chen, Z.H., Zhou, L.S., Fan, M.Z., Yang, B.X., Weissenbach, J., Wang, G.X. and Tsuji, S. (1997) Machado-Joseph disease in four Chinese pedigrees: molecular analysis of 15 patients including two juvenile cases and clinical correlations. Neurol. 48: 482-485.

IMAGE EVALUATION
TEST TARGET (QA-3)

150mm

6"